

A Thesis Submitted for the Degree of PhD at the University of Warwick

Permanent WRAP URL:

<http://wrap.warwick.ac.uk/175165>

Copyright and reuse:

This thesis is made available online and is protected by original copyright.

Please scroll down to view the document itself.

Please refer to the repository record for this item for information to help you to cite it.

Our policy information is available from the repository home page.

For more information, please contact the WRAP Team at: wrap@warwick.ac.uk



Self-Assembly of Interlocked Architectures

Stefano Schergna

Submitted for the Degree of Doctor of Philosophy in

Chemistry

University of Warwick

Department of Chemistry

April 2002

1. Introduction	1
2. Objectives	2
3. Methodology	3
4. Results	4
5. Discussion	5
6. Conclusion	6
7. References	7
8. Appendix	8
9. Glossary	9
10. Bibliography	10
11. Index	11
12. Acknowledgements	12
13. Declaration of Interest	13
14. Funding	14
15. Author Contributions	15
16. Ethics Approval	16
17. Data Availability	17
18. Competing Interests	18
19. Copyright	19
20. Reprints and Permissions	20
21. Correspondence	21
22. Additional Information	22
23. Supplementary Material	23
24. References	24
25. Appendix	25
26. Glossary	26
27. Bibliography	27
28. Index	28
29. Acknowledgements	29
30. Declaration of Interest	30
31. Funding	31
32. Author Contributions	32
33. Ethics Approval	33
34. Data Availability	34
35. Competing Interests	35
36. Copyright	36
37. Reprints and Permissions	37
38. Correspondence	38
39. Additional Information	39
40. Supplementary Material	40
41. References	41
42. Appendix	42
43. Glossary	43
44. Bibliography	44
45. Index	45
46. Acknowledgements	46
47. Declaration of Interest	47
48. Funding	48
49. Author Contributions	49
50. Ethics Approval	50
51. Data Availability	51
52. Competing Interests	52
53. Copyright	53
54. Reprints and Permissions	54
55. Correspondence	55
56. Additional Information	56
57. Supplementary Material	57
58. References	58
59. Appendix	59
60. Glossary	60
61. Bibliography	61
62. Index	62
63. Acknowledgements	63
64. Declaration of Interest	64
65. Funding	65
66. Author Contributions	66
67. Ethics Approval	67
68. Data Availability	68
69. Competing Interests	69
70. Copyright	70
71. Reprints and Permissions	71
72. Correspondence	72
73. Additional Information	73
74. Supplementary Material	74
75. References	75
76. Appendix	76
77. Glossary	77
78. Bibliography	78
79. Index	79
80. Acknowledgements	80
81. Declaration of Interest	81
82. Funding	82
83. Author Contributions	83
84. Ethics Approval	84
85. Data Availability	85
86. Competing Interests	86
87. Copyright	87
88. Reprints and Permissions	88
89. Correspondence	89
90. Additional Information	90
91. Supplementary Material	91
92. References	92
93. Appendix	93
94. Glossary	94
95. Bibliography	95
96. Index	96
97. Acknowledgements	97
98. Declaration of Interest	98
99. Funding	99
100. Author Contributions	100
101. Ethics Approval	101
102. Data Availability	102
103. Competing Interests	103
104. Copyright	104
105. Reprints and Permissions	105
106. Correspondence	106
107. Additional Information	107
108. Supplementary Material	108
109. References	109
110. Appendix	110
111. Glossary	111
112. Bibliography	112
113. Index	113
114. Acknowledgements	114
115. Declaration of Interest	115
116. Funding	116
117. Author Contributions	117
118. Ethics Approval	118
119. Data Availability	119
120. Competing Interests	120
121. Copyright	121
122. Reprints and Permissions	122
123. Correspondence	123
124. Additional Information	124
125. Supplementary Material	125
126. References	126
127. Appendix	127
128. Glossary	128
129. Bibliography	129
130. Index	130
131. Acknowledgements	131
132. Declaration of Interest	132
133. Funding	133
134. Author Contributions	134
135. Ethics Approval	135
136. Data Availability	136
137. Competing Interests	137
138. Copyright	138
139. Reprints and Permissions	139
140. Correspondence	140
141. Additional Information	141
142. Supplementary Material	142
143. References	143
144. Appendix	144
145. Glossary	145
146. Bibliography	146
147. Index	147
148. Acknowledgements	148
149. Declaration of Interest	149
150. Funding	150
151. Author Contributions	151
152. Ethics Approval	152
153. Data Availability	153
154. Competing Interests	154
155. Copyright	155
156. Reprints and Permissions	156
157. Correspondence	157
158. Additional Information	158
159. Supplementary Material	159
160. References	160
161. Appendix	161
162. Glossary	162
163. Bibliography	163
164. Index	164
165. Acknowledgements	165
166. Declaration of Interest	166
167. Funding	167
168. Author Contributions	168
169. Ethics Approval	169
170. Data Availability	170
171. Competing Interests	171
172. Copyright	172
173. Reprints and Permissions	173
174. Correspondence	174
175. Additional Information	175
176. Supplementary Material	176
177. References	177
178. Appendix	178
179. Glossary	179
180. Bibliography	180
181. Index	181
182. Acknowledgements	182
183. Declaration of Interest	183
184. Funding	184
185. Author Contributions	185
186. Ethics Approval	186
187. Data Availability	187
188. Competing Interests	188
189. Copyright	189
190. Reprints and Permissions	190
191. Correspondence	191
192. Additional Information	192
193. Supplementary Material	193
194. References	194
195. Appendix	195
196. Glossary	196
197. Bibliography	197
198. Index	198
199. Acknowledgements	199
200. Declaration of Interest	200
201. Funding	201
202. Author Contributions	202
203. Ethics Approval	203
204. Data Availability	204
205. Competing Interests	205
206. Copyright	206
207. Reprints and Permissions	207
208. Correspondence	208
209. Additional Information	209
210. Supplementary Material	210
211. References	211
212. Appendix	212
213. Glossary	213
214. Bibliography	214
215. Index	215
216. Acknowledgements	216
217. Declaration of Interest	217
218. Funding	218
219. Author Contributions	219
220. Ethics Approval	220
221. Data Availability	221
222. Competing Interests	222
223. Copyright	223
224. Reprints and Permissions	224
225. Correspondence	225
226. Additional Information	226
227. Supplementary Material	227
228. References	228
229. Appendix	229
230. Glossary	230
231. Bibliography	231
232. Index	232
233. Acknowledgements	233
234. Declaration of Interest	234
235. Funding	235
236. Author Contributions	236
237. Ethics Approval	237
238. Data Availability	238
239. Competing Interests	239
240. Copyright	240
241. Reprints and Permissions	241
242. Correspondence	242
243. Additional Information	243
244. Supplementary Material	244
245. References	245
246. Appendix	246
247. Glossary	247
248. Bibliography	248
249. Index	249
250. Acknowledgements	250
251. Declaration of Interest	251
252. Funding	252
253. Author Contributions	253
254. Ethics Approval	254
255. Data Availability	255
256. Competing Interests	256
257. Copyright	257
258. Reprints and Permissions	258
259. Correspondence	259
260. Additional Information	260
261. Supplementary Material	261
262. References	262
263. Appendix	263
264. Glossary	264
265. Bibliography	265
266. Index	266
267. Acknowledgements	267
268. Declaration of Interest	268
269. Funding	269
270. Author Contributions	270
271. Ethics Approval	271
272. Data Availability	272
273. Competing Interests	273
274. Copyright	274
275. Reprints and Permissions	275
276. Correspondence	276
277. Additional Information	277
278. Supplementary Material	278
279. References	279
280. Appendix	280
281. Glossary	281
282. Bibliography	282
283. Index	283
284. Acknowledgements	284
285. Declaration of Interest	285
286. Funding	286
287. Author Contributions	287
288. Ethics Approval	288
289. Data Availability	289
290. Competing Interests	290
291. Copyright	291
292. Reprints and Permissions	292
293. Correspondence	293
294. Additional Information	294
295. Supplementary Material	295
296. References	296
297. Appendix	297
298. Glossary	298
299. Bibliography	299
300. Index	300

Contents

Chapter One

1.	Introduction to Catenanes and Rotaxanes	1
1.1	Supramolecular Interactions	1
1.2	Introducing the Interlocked Architectures: Catenanes, Rotaxanes and Knots	2
1.2.1	Catenanes	2
1.2.2	Rotaxanes	3
1.2.3	Molecular Knots	4
1.3	<i>Once upon a time, a long time ago</i> - Early Synthesis of Interlocked Architectures	5
1.3.1	Catenanes	5
1.3.1.1	Statistical Approaches to Catenanes	5
1.3.1.2	Directed Approaches to Catenanes	6
1.3.2	Rotaxanes	7
1.3.2.1	Statistical approaches to rotaxanes	7
1.4	Template-Directed Syntheses of Catenanes and Rotaxanes	8
1.4.1.1	Template-Directed Syntheses of Catenane/Rotaxanes Using Hydrophobic Interactions	9
1.4.1.2	Metal Template-Directed Synthesis of Catenane/Rotaxanes	10
1.4.1.3	Donor/Acceptor Template-Directed Syntheses of Catenane/Rotaxanes	10
1.4.2	Hydrogen Bonding for Catenane/Rotaxane Self-Assembly	12
1.5	Effects of the Macrocyclic Wheel on the Chemical Properties of Functional Groups of the Thread	22
1.5.1.1	Chemical Reactions on the Thread of Rotaxanes - Steric Hindrance by the Macrocycle	22
1.5.1.2	Insulated Molecular Wires	24
1.5.2	Chiral Geometry of Rotaxanes Promoted the Chirality	25
	References	27

Chapter Two

2.	Synthesis of a Novel Class of Rotaxanes with a Diene in the Axle	35
2.1	Abstract	35
2.2	Introduction	35
2.3	Results and discussion	40
2.4	Conclusions	56
2.5	Experimental Part	57
2.6	References	73

Chapter Three

3.	Investigations Into the Effect of Thread Rigidity on Rotaxane Yield Using Muconic Acid Thread Analogues	75
3.1	Abstract	75
3.2	Introduction	75
3.3	Results and discussion	77
3.4	Conclusions	84
3.5	Experimental Part	86
3.6	References	92

Chapter Four

4.	Naphthalene Functionalised Macrocycle	94
4.1	Abstract	94
4.2	Introduction	94
4.3	Results and discussion	95
4.4	Conclusions	111
4.5	Experimental Part	112
4.6	References	140

Chapter Five

5.	Chemical Reactions on the Axle of Rotaxane Containing Dienes	143
5.1	Abstract	143
5.2	Introduction	143
5.3	Results and discussion	145
5.4	Conclusions	155
5.5	Experimental Part	156
5.6	References	163

Chapter Six

6. Self-assembled Monolayers of Heterocircuit [2]Catenanes on Gold	164
6.1 Abstract	164
6.2 Introduction	164
6.3 Results and discussion	165
6.4 Conclusions	177
6.5 Experimental Part	177
6.6 References	203
Appendix : General Experimental Data	206

List of Figures

Chapter One

- Figure 1** A cartoon representation of a [2]catenane **1** and its component macrocycles **2**. 2
- Figure 2** Schematic representation of the simplest among rotaxanes, a [2]rotaxane, made of a ring threaded onto a dumbbell whose stoppers prevent unthreading. 3
- Figure 3** A cartoon representation of a trefoil knot. 4
- Figure 4** From π -electron donor and π -electron acceptor interactions to rotaxanes. 12
- Figure 5** A hydrogen bond formed between an acidic hydrogen atom (hydrogen bond donor **D**) and an appropriator acceptor (**A**). 13
- Figure 6** Solid state structure of the benzylic amide [2]catenane **27** (carbon atoms on one ring are shown as yellow and those of the other light blue, oxygen red, nitrogen dark blue and hydrogen white; the non hydrogen bonding hydrogens have been removed for clarity). 15
- Figure 7** Solid state structure of the amphiphilic [2]catenane **30c** (carbon atoms are on the host macrocycle are shown as yellow and those of the guest macrocycle light blue, oxygen red, nitrogen dark blue and hydrogen white; the non hydrogen bonding hydrogens have been removed for clarity). 18
- Figure 8** Solvent induced switching in the amphiphilic catenane **30c**. 19
- Figure 9** An approach to insulated molecular wires by Anderson. 24
- Figure 10** Cycloenantiomeric [2]rotaxanes **44a** and **44b** (mirror plane the square arrow indicate the sequence of the atoms). 26
- Figure 11** The chiral [2]pseudorotaxanes **45-49** prepared by Stoddart's group. 26

Chapter Two

- Figure 2.1** The postulated mechanistic pathway to hydrogen bond-assembled rotaxane formation illustrating how the template

	50a induces a conformational change in the immediate precursor to ring closure 51a.	36
Figure 2.2	X-ray structure of a fumaric-based rotaxane 52.	37
Figure 2.3	Solid state structure of the C16 rotaxane 53 as determined by X-ray crystallography. For clarity, carbon atoms of the macrocyclic ring are shown in light blue and the carbon atoms of the C16 thread in yellow; oxygen atoms are depicted red, nitrogen atoms dark blue and hydrogen atoms white. Non H-bonding hydrogens have been removed.	39
Figure 2.4	Schematic representations of three new classes of thread templates. <i>E,E</i> , <i>E,Z</i> and <i>Z,Z</i> muconic based systems will be reported in this chapter. <i>E</i> -hydromuconic and glutaconic will be considered in the next chapter (Chapter Three).	41
Figure 2.5	Solid state structure of the <i>cis,cis</i> -muconic rotaxanes 62 as determined by X-ray crystallography. For clarity carbon atoms of the macrocyclic ring are shown in light blue and the carbon atoms of the muconic thread in yellow; oxygen atoms are depicted red, nitrogen atoms dark blue and hydrogen atoms white. Selected interatomic distances [Å]: N2-O40 3.369, N2A-O40A 3.369, N11-O40 3.093, N11A-O40 3.093.	43
Figure 2.6	¹ H-NMR spectra (400 MHz, CDCl ₃ top two spectra) of muconic thread 61 and muconic rotaxane 62.	44
Figure 2.7	¹ H-NMR spectra (400 MHz, CDCl ₃) of muconic thread 63 and muconic rotaxane 64.	46
Figure 2.8		47
Figure 2.9	Solid state structure of the <i>trans,trans</i> -muconic rotaxanes 58. For clarity carbon atoms of the macrocyclic ring are shown in light blue and the carbon atoms of the muconic thread in yellow; oxygen atoms are depicted red, nitrogen atoms dark blue and hydrogen atoms white. Non H-bonding hydrogens have been removed. Selected interatomic distances [Å]: N2-O39 2.969, N2A-O39A 2.969.	48

- Figure 2.10** ^1H -NMR spectra (400 MHz, CDCl_3) of muconic thread **57** and muconic rotaxane **58**. 49
- Figure 2.11** Solid state structure of the *trans,trans*-muconic rotaxanes **67** as determined by X-ray crystallography. For clarity carbon atoms of the macrocyclic ring are shown in light blue and the carbon atoms of the muconic thread in yellow; oxygen atoms are depicted red, nitrogen atoms dark blue and hydrogen atoms white. Non H-bonding hydrogens have been removed. Selected interatomic distances [Å]: N2-O39 2.923, N2A-O39A 2.923. 51
- Figure 2.12** ^1H -NMR spectra (400 MHz, CDCl_3) of muconic thread **66** and muconic rotaxane **67**. 52

Chapter Three

- Figure 3.1** Solid state structure of the C16 rotaxane **53** (for clarity carbon atoms of the macrocyclic ring are shown in light blue and the carbon atoms of the C16 thread in yellow; oxygen atoms are depicted red, nitrogen atoms dark blue and hydrogen atoms white. Non H-bonding hydrogens have been removed for clarity). 76
- Figure 3.2** Solid state structure of the *trans*- β -hydromuconic rotaxane **75**. For clarity carbon atoms of the macrocyclic ring are shown in light blue and the carbon atoms of the hydromuconic thread in yellow; oxygen atoms are depicted red, nitrogen atoms dark blue and hydrogen atoms white. Non H-bonding hydrogens have been removed. Selected interatomic distances [Å]: N2-O40 3.229, N2A-O40 3.229, N11-O40 2.975, N11A-O40 2.975. 78
- Figure 3.3** ^1H -NMR spectra (400 MHz, CDCl_3) of hydromuconic thread **74** and hydromuconic rotaxane **75**. 79
- Figure 3.4** Solid state structure of the glutaconic rotaxane **80**. For clarity carbon atoms of the macrocyclic ring are shown in light blue and the carbon atoms of the glutaconic thread in yellow; oxygen atoms are depicted red, nitrogen atoms

dark blue and hydrogen atoms white. Non H-bonding hydrogens have been removed for clarity. Selected interatomic distances [Å]: N29-O41 3.088, N20-O41 2.980, N2-O45 2.903.

81

Figure 3.5 Solid state structure of the glutaconic thread **79** hydrogen bonding the tetramide macrocycle **27**. It was obtained highlighting the thread from the previous X-ray structure by removal of the macrocycle; (for clarity the carbon atoms of the glutaconic thread are shown in grey; oxygen atoms are depicted red, nitrogen atoms dark blue and hydrogen atoms white. Non H-bonding hydrogens have been removed for clarity).

82

Figure 3.6 ^1H -NMR spectra (400 MHz, CDCl_3) of glutaconic thread **79** and glutaconic rotaxane **80**.

83

Chapter Four

Figure 4.1 Solid state structure of rotaxane **106**. For clarity carbon atoms of the macrocyclic ring are shown in light blue and the carbon atoms of the muconic thread in yellow; oxygen atoms are depicted red, nitrogen atoms dark blue and hydrogen atoms white. Non H-bonding hydrogens have been removed for clarity. Selected interatomic distances [Å]: N1-O3 2.892, N1A-O3A 2.892, N11-O3 2.979, N11A-O3A 2.979.

100

Figure 4.2 ^1H -NMR spectra (400 MHz, CDCl_3) of muconic thread **95** and muconic rotaxane **98** and **96**.

102

Figure 4.3 ^1H -NMR spectra (400 MHz, CDCl_3) of fumaric thread **108** and fumaric rotaxane **110** and **109**.

104

Figure 4.4 ^1H -NMR spectra (400 MHz, $\text{DMSO}-d_6$) of allyl macrocycle **123** and catenanes **125** and **124**.

108

Figure 4.5

109

Figure 4.6

111

Chapter Five

Figure 5.1 152

Chapter Six

Figure 6.1 165

Figure 6.2 ^1H -NMR spectra (400 MHz, CDCl_3 top two spectra and $\text{DMSO}-d_6$ bottom two spectra) of allyl macrocycle **123** and allyl [2]catenane **125**. 168

Figure 6.3 Solid state structure of the Allyl [2]Catenane **125** as determined by X-ray crystallography. For clarity, carbon atoms of the "small" tetramide macrocyclic ring are shown in light blue and the carbon atoms of the allyl amphyphilic "big" macrocycle in yellow; oxygen atoms are depicted red, nitrogen atoms dark blue and hydrogen atoms white. Non H-bonding hydrogens have been removed. Selected interatomic distances [\AA]: N1-O9 2.983; N2-O10 2.912; N4-O2 2.812; N3-O7 2.849. 169

Figure 6.4 Schematic representation of sulfur-containing self-assembled monolayers on gold with the three distinct structural parts and three types of sulfur containing adsorbates. 171

Figure 6.5 175

Figure 6.6 176

List of Schemes

Chapter One

Scheme 1	The first synthesis of a [2]catenane 6 by Wasserman exploiting the statistical <i>threading</i> of a linear chain through a macrocycle.	6
Scheme 2	Synthesis of the first covalently templated [2]catenane <i>via</i> the synthetic methodology proposed by Lüttringhaus and Schill.	7
Scheme 3	The polymer-supported cyclic component was treated with a solution of 11 , 10-decane-diol, followed by treatment with trityl chloride. The resin was washed in order to remove the by-products and the overall procedure was repeated seventy times. The ester linking the rotaxane to the polymeric support was cleaned to obtain the [2]rotaxane 12 in a yield of only 6%.	8
Scheme 4	The template-directed synthesis of a [2]rotaxane using chelation of copper(I) ions by 1, 10-phenanthroline ligands (Gibson and co-workers).	10
Scheme 5	Clipping and threading approaches to the first [2]rotaxane incorporating π -electron rich and π electron deficient components.	11
Scheme 6	The synthesis of the first amide-based [2]-catenane reported by Hunter.	14
Scheme 7	One pot synthesis of a benzylic amide [2]catenane.	15
Scheme 8	Synthesis of amphiphilic benzylic amide [2]catenanes.	17
Scheme 9	A "one pot" preparation of a rotaxane recently proposed by Vögtle and co-workers.	20
Scheme 10	The synthesis of peptido rotaxanes 37 by clipping, a hydrogen bonding directed assembly processes.	21
Scheme 11	High-yielding anionic template synthesis of rotaxanes with bis(phenyl ether) thread where phenolate-macrocycle complexes act as supramolecular nucleophiles for the reaction with semi-thread 40 .	22

Scheme 12	The macrocycle 32 (blue square) acts as a protecting group by sterically hindering the reaction on the thread.	23
------------------	---	----

Chapter Two

Scheme 2.1	38
Scheme 2.2	42
Scheme 2.3	43
Scheme 2.4	45
Scheme 2.5	47
Scheme 2.6	50
Scheme 2.7	54
Scheme 2.8	54

Chapter Three

Scheme 3.1	77
Scheme 3.2	81

Chapter Four

Scheme 4.1	96
Scheme 4.2	97
Scheme 4.3	98
Scheme 4.4	(i) <i>tert</i> -butyl chloride; (ii) sodium dichromate; (iii) 1,3-diamino propane 103 . 98
Scheme 4.5	99
Scheme 4.6	101
Scheme 4.7	106
Scheme 4.8	107
Scheme 4.9	110

Chapter Five

Scheme 5.1	144
Scheme 5.2	141
Scheme 5.3	152
Scheme 5.4	153
Scheme 5.5	154

Chapter Six

Scheme 6.1	168
Scheme 6.2	169
Scheme 6.3	173
Scheme 6.4	175
Scheme 6.5	176

List of Tables and Diagrams

Chapter One

Table 1	Structural tolerance in the benzylic amide catenane synthesis.	16
----------------	--	----

Chapter Three

Table 3.1		85
------------------	--	----

Chapter Five

Diagram 5.1	Isomerization of Z,Z-muconic thread 61 at low (4%) and high (40%) concentration of I ₂ in the presence of light. In red the Z,Z thread 61 and in blue the E,Z thread 63 .	146
Diagram 5.2	Isomerization of Z,Z-muconic rotaxane 62 at low (4%) and high (40%) concentration of I ₂ in the presence of light. In red the Z,Z rotaxane 62 , in blue the E,Z rotaxane 64 and in black the E,E rotaxane 58 .	147
Diagram 5.3	Isomerization of Z,Z-muconic thread 61 at 40% concentration of I ₂ in the absence of light. In red the Z,Z thread 61 and in blue the E,Z thread 63 .	148
Diagram 5.4	Isomerization of Z,Z-muconic rotaxane 62 at a 40% concentration of I ₂ in the presence of light and BHT. In red the Z,Z specie 62 , in blue the E,Z 64 and in black the E,E rotaxane 58 .	150

Acknowledgments

There are no words to describe how much I am grateful to Guy and Angeles for their incredible support in these four years.

Thanks to Sandro, Marisa, Angelo, Thomas, “Bad Boy” Songwei, Céline I and II, Célinette, Francesca, Sergey, Lando, Rocco, Vix, Ricard, Torrente, Marian, Barbara, Panagiota, Bilge, Sergio, John, Beckie, Julie, Steve, the red bricks people and many more.

Then a special thank to Professor Leigh for the fantastic opportunity that gave me and to Professor Prato for ... a lot of things.

Summary

An area of great interest is the synthesis and characterisation of molecules possessing moving parts, with the goal that they can act as “molecular machine” carrying out tasks that molecules with fixed conventional architectures cannot do. Rotaxanes and catenanes (mechanically interlocked architectures) represent one approach toward achieving these aims as their component *wheels* and / or *threads* are connected together but can still move in certain, controlled directions. This thesis focused on the study of structural rigidity and the preorganisation of thread binding sites as factors of major influence on template efficiency in the synthesis of hydrogen bond assembled supramolecular structures (rotaxanes and catenanes).

Chapter One gives a brief outline of the common synthetic approaches to interlocked architectures (catenanes and rotaxanes) that are now being developed to address the problems outlined above.

Chapter Two and **Chapter Three** concerns the synthesis of novel amide-based rotaxanes containing various saturated and unsaturated skeletons in their templating core. These new amide-based rotaxanes (muconic, hydromuconic and glutaconic) were synthesised by a clipping strategy in high yields.

Chapter Four concerns the synthesis of a novel class of rotaxanes containing a naphthalene tetramide macrocycle that has a larger cavity (102). Several rotaxanation experiments based on macrocycle 102 precursors and threads containing several possible templating motifs were examined.

Chapter Five report on the use of rotaxane wheels as a non-covalent protecting group able to influence the chemical behaviour of the functional groups in the central part of the axle.

Chapter Six several heterocircuit [2]catenanes functionalised with various sulphide groups were synthesised and their monolayer forming capability on a gold surface studied. Another approach involving covalent attachment of macrocycles and catenanes on a pre-formed monolayer was also investigated.

Declaration

The work performed in this thesis was carried in the Department of Chemistry, University of Manchester Institute of Science and Technology, between January 1998 and September 1998 and in the Chemistry Department, University of Warwick between September 1998 and May 2001. Unless otherwise stated, it is the work of the author and has not been submitted in whole or in support of an application for another degree of qualification of this or any other University or other institute of learning.

Abbreviations Used in the Text

Ac	Acetyl Group
Ar	Aryl Group
<i>t</i> -Boc	<i>tert</i> -Butoxycarbonyl Group
<i>t</i> -Bu	<i>tert</i> -Butyl Group
CA	Contact Angle Measurements
Calcd	Calculated
DCC	1,3-Dicyclohexylcarbodiimide
DCM	Dichloromethane
DMAP	4-Dimethylaminopyridine
DMF	Dimethylformamide
DMSO	Dimethylsulphoxide
EDCI	1-(3-Dimethylaminopropyl)-3-ethyl-carbodiimide hydrochloride
Et ₃ N	Triethylamine
EtOAc	Ethyl Acetate
EtOH	Ethanol
HCl	Hydrochloric Acid
MeOH	Methanol
mp	Melting Point
m/z	mass/charge
11-MUA	11-Mercaptoundecanoic Acid
NMR	Nuclear Magnetic Resonance
Pd(OAc) ₂	Palladium Acetate
Ph	Phenyl
PPh ₃	Triphenyl Phosphine
ppm	Parts per Million
RT	Room Temperature
SAM	Self Assembled Monolayers
THF	Tetrahydrofuran
TLC	Thin Layer Chromatography
TFA	Trifluoroacetic Acid
VAZO [®]	1,1'-Azobis(cyclohexanecarbonitrile)
XPS	X-ray Photoelectron Spectroscopy

Chapter One

1. Introduction to Catenanes and Rotaxanes

1.1 Supramolecular Interactions

Molecular interactions form the basis of many of the processes that occur in our daily life. In Nature these processes are optimised to a high degree by evolution. Biological and biochemical studies have provided understanding and detailed insight in the molecular design of life.¹ The chemical mechanisms of many crucial process of life are now understood. The processes rely on the interactions between molecules and highly sophisticated molecular assemblies like those of proteins, enzymes, membranes, cells and viruses. Despite the complexity of these systems, the building blocks are relatively simple, such as sugars, amino acids and phospholipids. The three-dimensional assembly of these functions and the interactions are mainly determined by non-covalent interactions.

The field of supramolecular chemistry deals with the understanding and control of the non-covalent intermolecular bond.² Inspired by the achievements of Nature, synthetic systems organised and held together by means of intermolecular binding interactions have been designed using weak forces like hydrogen bonding, Van der Waals interactions, electrostatic and $\pi-\pi$ interactions. A comprehensive understanding of intermolecular forces allows the targeted construction of supramolecular assemblies, which are not limited to the structures and processes found in biological systems. The spontaneous formation of such supramolecular structures is called self-

assembly. This can be exploited to construct assemblies that cannot easily be built via covalent synthesis. Various examples of highly ordered self-assembled systems have been reported,³ like host-guest systems,⁴ hydrogen bonded rosette structures,⁵ nanotubes ⁶ or fascinating interlocked molecules⁷ such as rotaxanes and catenanes.⁸ Current challenges in materials synthesis lie in the development of devices such as molecular wires ⁹ or switches,¹⁰ nano-structured materials,¹¹ modification of the properties of functional groups,¹² light and electrochemically based molecular shuttles ¹³ where supramolecular chemistry may offer some unique opportunities for their design and synthesis.

1.2 Introducing the Interlocked Architectures: Catenanes, Rotaxanes and Knots

1.2.1 Catenanes

Catenane,⁸ from the Latin word "catena" meaning "chain", is used to describe molecules that can be thought of as two or more macrocycles that are mechanically interlocked together and cannot be separated without cleavage of a covalent bond ¹⁴ (Figure 1).



Figure 1 A cartoon representation of a [2]catenane **1** and its component macrocycles **2**.

Interlocked structures belong to a class of topologically non-trivial molecules for which the usual description of structure are not sufficient.^{15,16} Compounds with identical connectivity are said to be topological isomers if they cannot be interconverted by continuous deformation of the bonds between the atoms.¹⁴ Therefore a [2]catenane **1** represented in Figure 1 is a "topological isomer" of the separated component rings **2** as the two rings cannot be separated without breaking a covalent bond in one of the rings.⁸

1.2.2 Rotaxanes

Rotaxane, from the Latin "Rota" meaning "Wheel", and "Axis" meaning "Axle", are molecules comprised of a dumbbell-shaped component encircled by one or more macrocyclic components. The stoppers attached at both ends of the dumbbell-shaped component must be bulky enough to trap mechanically the macrocyclic components, avoiding the possibility of unthreading (Figure 2).

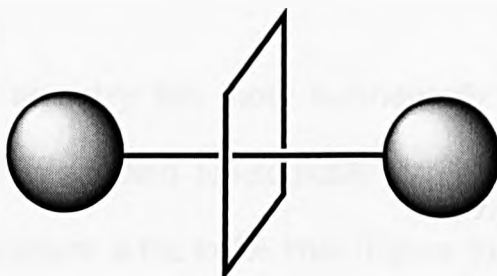


Figure 2 Schematic representation of the simplest among rotaxanes, a [2]rotaxane, made of a ring threaded onto a dumbbell whose stoppers prevent unthreading.

The early syntheses of rotaxanes were mainly based upon statistical threading or directed methodologies involving chemical conversion.^{14,17}

However, with the advent of supramolecular chemistry, a series of host-guest and template-directed approaches ^{2,18} relying on non-covalent interactions between recognition sites incorporated within the macrocycle (or macrocycle precursor) and thread, have been successfully developed. Non covalent interactions such as metal template-directed syntheses,¹⁹ π -electron acceptors and π -electron donors,^{38,39} hydrophobic interactions ²¹ and hydrogen bond self-assembly ²² have all been used to construct rotaxanes. The research described within this thesis is mainly concerned with the hydrogen bonding templated assembly of amide-containing rotaxanes and the effect of rotaxane formation on the properties of the interlocked components.

As has already been stated it is possible to have more than two interlocked components. The number of components in an interlocked architecture is given a prefix e.g. a [3]rotaxane comprises a thread and two macrocycles.

1.2.3 Molecular Knots

Molecular knots ²³ are arguably the most synthetically challenging, and hence most rare, of the interlocked topologically complex structures. The simplest of this type of structure is the trefoil knot (Figure 3).²⁴



Figure 3 A cartoon representation of a trefoil knot

1.3 Once upon a time, a long time ago - Early Synthesis of Interlocked Architectures

1.3.1 Catenanes

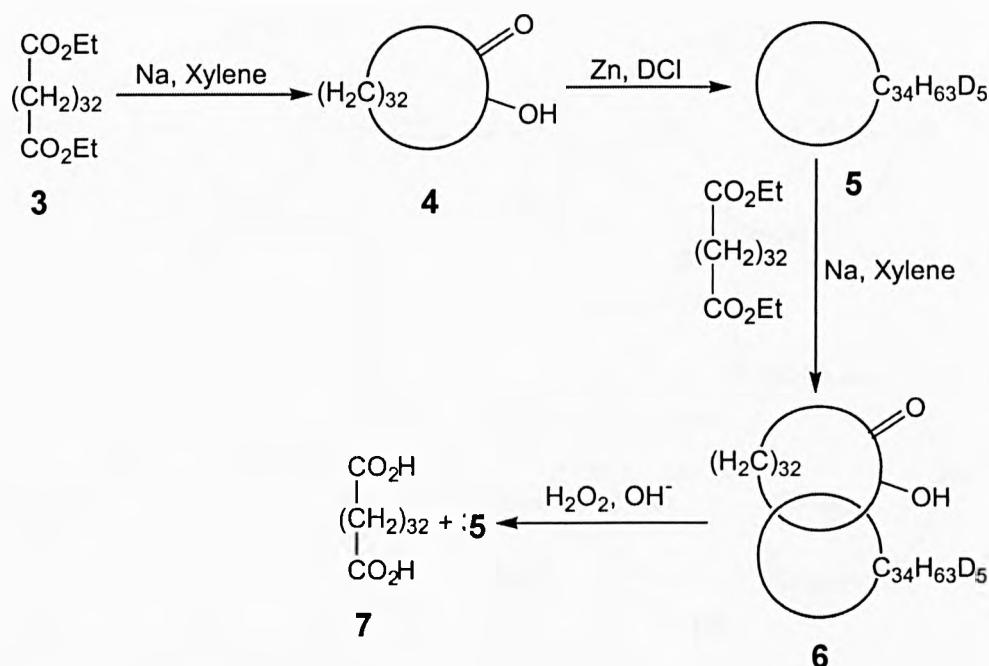
Although the Nobel laureate Willstätter discussed the existence of molecular interlocked rings at the beginning of the 20th century, it was not until the early 1960's that Frisch and Wasserman reported a synthetic method to access these molecules.¹⁴

Catenane synthesis involves the formation of interlocked rings and therefore the major challenge is to promote this interlocking process. Prior to the 1980's chemists considered this to be a standard covalent synthesis and several synthetic approaches were proposed.⁸

1.3.1.1 Statistical Approaches to Catenanes

The first synthesis of a catenane reported in 1960 by Wasserman¹⁴ involved the synthesis of a hydrocarbon macrocycle **5** using acyloin ring closure of **3** to give macrocycle **4** followed by zinc reduction. Exploiting the statistical "threading" of **3** through **5** followed by a second acyloin ring closure resulted in small quantities of the catenane **6**.

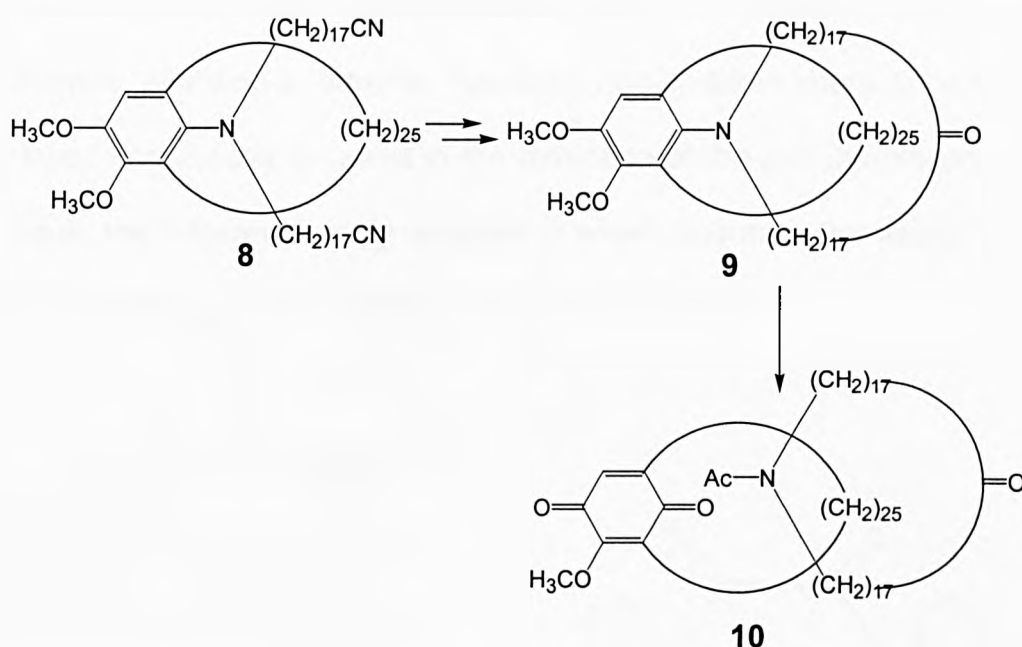
Oxidation of a mixture containing the acyloin fraction resulted in formation of the acid **7**, and isolation of small quantities of **5** proving the compound had been successfully synthesised (Scheme 1).



Scheme 1 The first synthesis of a [2]catenane **6** by Wasserman¹⁴ exploiting the statistical threading of a linear chain through a macrocycle.

1.3.1.2 Directed Approaches to Catenanes

An alternative to the statistical approach makes use of an auxiliary linkage to force the macrocycle precursor into mutual proximity and promote the interlocking. This link would be cleaved in the latter stage of the synthesis to free the rings of the catenane. The auxiliary linkage could conceivably be a covalent bond, a coordinative bond or a non-covalent bond. Lüttringhaus and Schill^{8,29} reported the use of covalent bonds as templates in a catenane synthesis in 1964. Their method involved the synthesis of a pre-catenane **8** and its subsequent ring closure yielding the covalently linked interlocked rings **9**. Cleavage of this covalent link afforded the [2]catenane **10** in a 8% yield (Scheme 2).



Scheme 2 Synthesis of the first covalently templated [2]catenane *via* the synthetic methodology proposed by Lüttringhaus and Schill.⁸

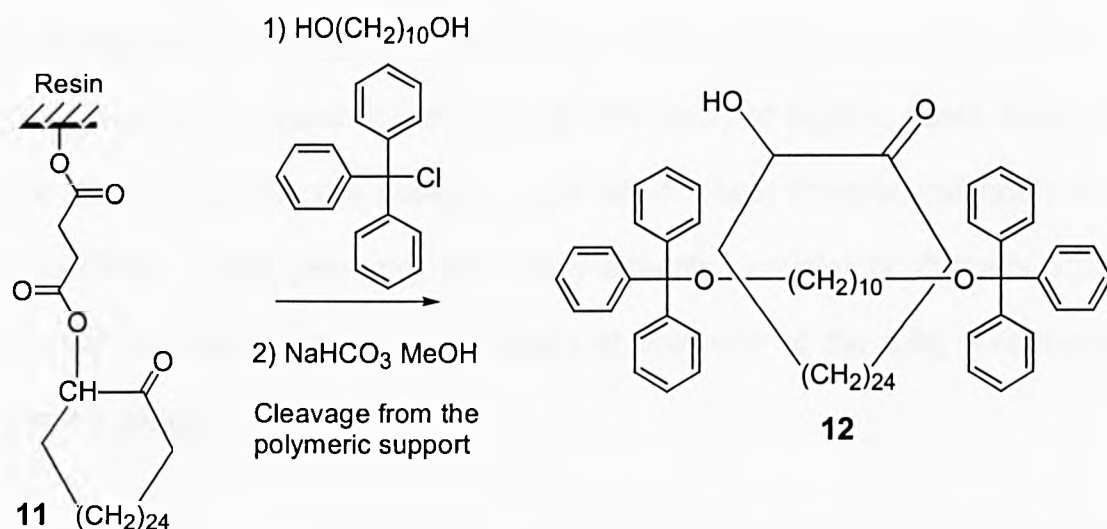
1.3.2 Rotaxanes

The early syntheses of rotaxanes were mainly based on the statistical or directed methods, whose drawbacks were having no particular interaction between thread and macrocycle for the former and numerous chemical steps for the latter. The yield of rotaxane formation was very low using both approaches.

1.3.2.1 Statistical approaches to rotaxanes

The first syntheses of a [2]rotaxane achieved by a statistical approach was reported by Harrison and Harrison ^{17a} in 1967. It was reasoned that, by mixing in solution, an acyclic with a macrocycle molecule, a small portion of the linear species would be inserted through the cavity of the cyclic one as a result of statistical threading. Subsequent covalent attachment of two bulky

groups at the end of the acyclic species provides a mechanical trap for the macrocycle, affording a rotaxane. However, non-covalent interactions are not employed consciously to assist in the formation of the pseudorotaxane, and as result, the rotaxane is only obtained in small amounts after using a large excess of starting cyclic or linear components (Scheme 3).



Scheme 3 The polymer-supported cyclic component was treated with a solution of **11**, 1,10-decane-diol, followed by treatment with trityl chloride. The resin was washed in order to remove the by-products and the overall procedure was repeated seventy times. The ester linking the rotaxane to the polymeric support was cleaved to obtain the [2]rotaxane **12** in a yield of only 6%.

1.4 Template-Directed Syntheses of Catenanes and Rotaxanes

The early syntheses of rotaxanes were mainly based upon the low yielding statistical and directed approaches. With the advent of supramolecular chemistry, numerous efficient and relatively simple synthetic methodologies for the construction of rotaxanes have been developed. Thus, template-directed synthetic approaches to rotaxanes, relying on the stabilisation

provided by noncovalent bonds between the recognition sites incorporated within macrocycles or macrocyclic precursors and threads, have been developed. A wide diversity of macrocyclic host molecules have been investigated during the last twenty years.³⁰

These weak interactions such as [N-H...O] hydrogen bonds, π - π stacking interactions controlling the complexation of π -electron rich guest by π -electron deficient hosts; hydrophobic interactions or metal ligand co-ordination induce the threading of organic guests through the cavity of organic hosts. Many of the resultant complexes possess a so-called *wheel* (macrocycle host) and *axle* (linear guest) geometry. By simply attaching covalently stoppers bulky enough to trap the wheel mechanically at both end of the axle, a rotaxane can be generated.

1.4.1.1 Template-Directed Syntheses of Catenanes and Rotaxanes Using Hydrophobic Interactions

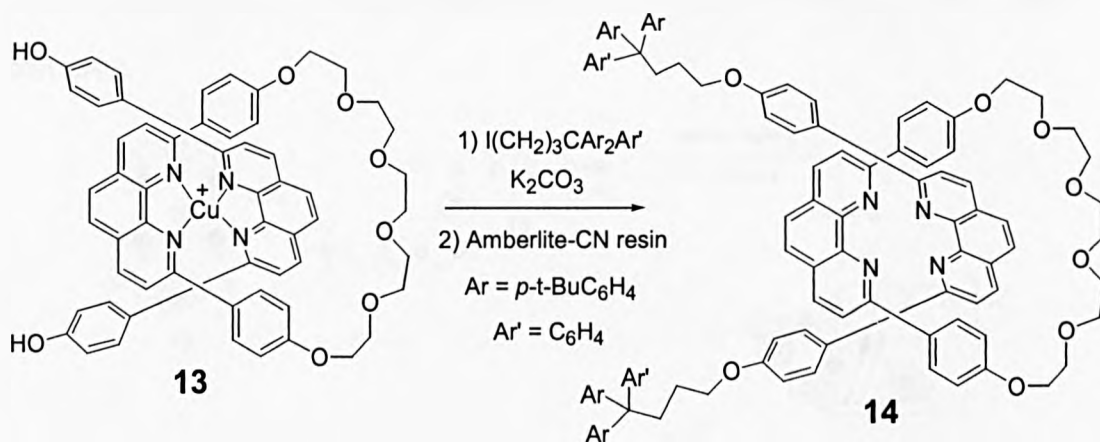
A nice example of rotaxane formation using hydrophobic interactions to induce the threading is provided by cyclodextrins,³¹ which were first reported in 1981 by Ogino.³¹ In a related approach, Anderson recently synthesised water-soluble rotaxanes by threading in water with very good yields.³¹

Fujita has also synthesised catenanes using hydrophobic interactions to induced the threading of organic guests through the cavity of organic hosts in polar media.³²

1.4.1.2 Metal Template-Directed Synthesis of Catenanes and Rotaxanes

The pre-rotaxane/catenane components could also be assembled around a transition metal, which would play the role of a template. A unique feature of this approach is that the template can easily be removed at the end of the synthesis based on organic fragments. The components of the final rotaxane structure will be maintained.

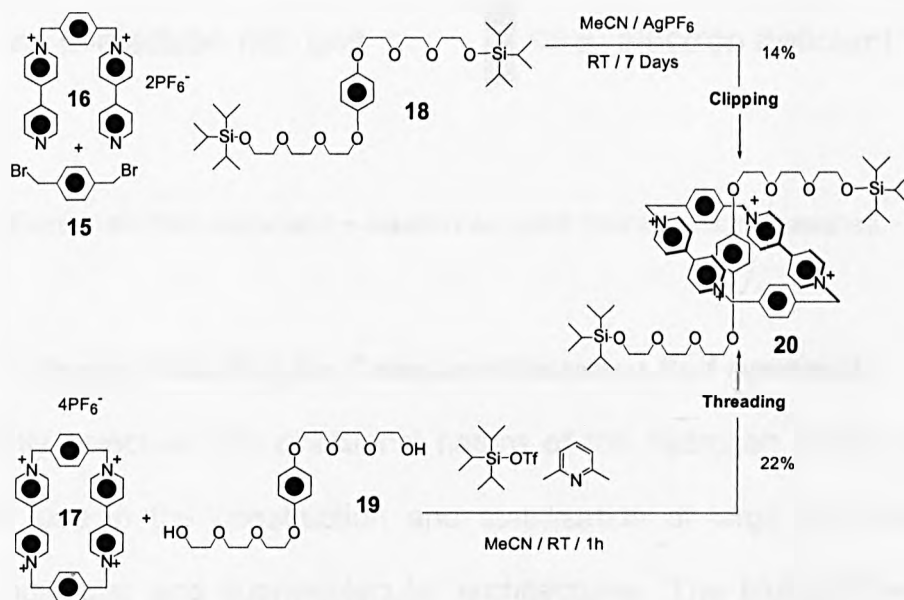
Sauvage and co-workers³³ have pioneered the creation of interlocked molecules, -catenanes,³⁴ by this metal template-directed approach. Gibson also used the above strategy to synthesise a [2]rotaxane in 24% overall yield (Scheme 4).³⁵ Further developments by this approach were also published by Sauvage^{19,36} and Lehn.³⁷



Scheme 4 The template-directed synthesis of a [2]rotaxane using chelation of copper(I) ions by 1, 10-phenanthroline ligands (Gibson and co-workers).^{33a}

1.4.1.3 Donor/Acceptor Template-Directed Syntheses of Catenanes and Rotaxanes

The first [2]rotaxane, incorporating a π -electron rich dumbbell-shaped component, reported by Stoddart,³⁸ was self-assembled by both the clipping and the threading approaches (Scheme 5). Further work detailed the synthesis of the first π -electron donor and π -electron acceptor catenane in a remarkable 70% yield.³⁹ The driving forces for rotaxane formation are (**a**) π - π -stacking between the π -electron deficient bipyridinium rings and the π -electron rich hydroquinone unit, as well as (**b**) hydrogen bonding between some of the polyether oxygen atoms and the acidic hydrogen atoms on the bipyridinium units. In addition to π - π -stacking and hydrogen bonding interactions, (**c**) edge-to-face T-type interactions between the hydrogen atoms attached to the hydroquinone ring are observed in the rotaxane complex.



Scheme 5 Clipping and threading approaches to the first [2]rotaxane incorporating π -electron rich and π electron deficient components.

By reversing the role of the recognition sites, a hydroquinone-based macrocycle is able to bind a bipyridinium thread to generate rotaxanes by simply attaching bulky stoppers at both ends of the thread (Figure 4).

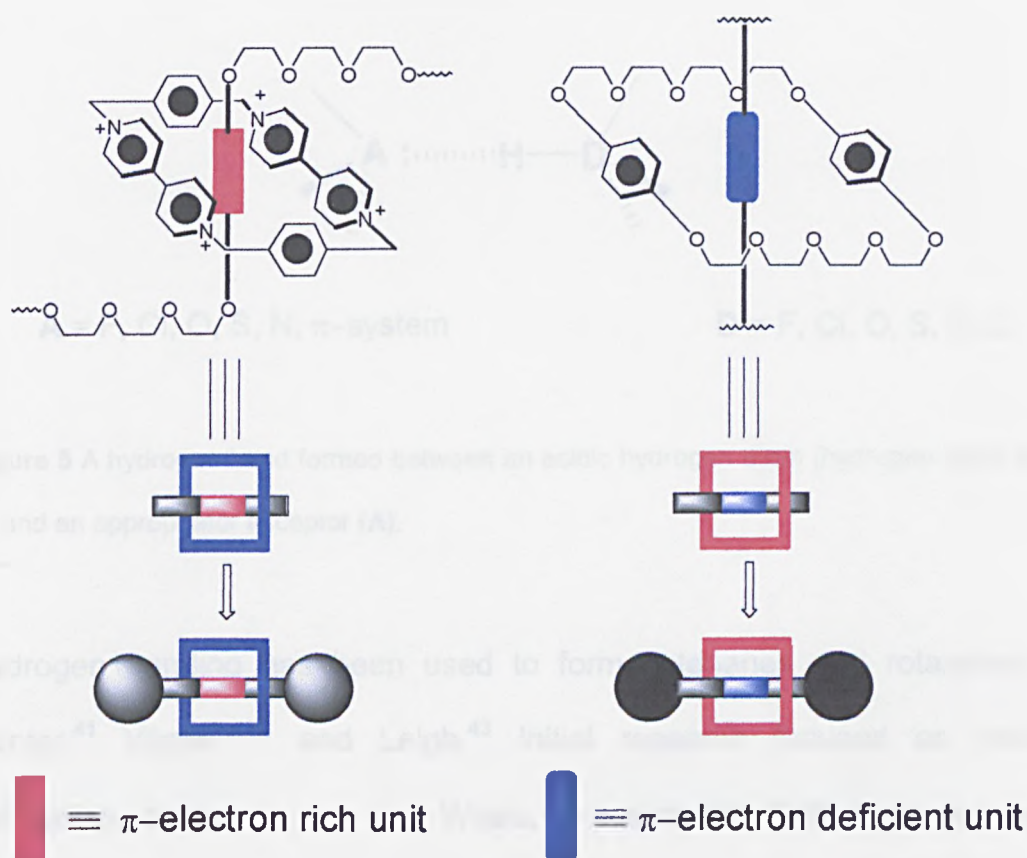
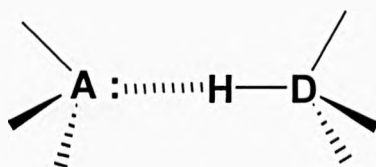


Figure 4 From π -electron donor and π -electron acceptor interactions to rotaxanes.

1.4.2 Hydrogen Bonding for Catenane/Rotaxane Self-Assembly

The highly selective and directional nature of the hydrogen bond makes it ideal for use in the construction and stabilisation of large non-covalently linked molecular and supramolecular architectures. The biological world is replete with examples of such systems: DNA and protein tertiary structures are amongst the most obvious examples.

Hydrogen bonds are formed when a donor (D) with an available acidic hydrogen atom is brought into intimate contact with an acceptor (A) carrying available nonbonding lone pairs of electrons. The strength of the hydrogen bond depends on the precise nature of the system involved.^{40(libro su H-bonding)}

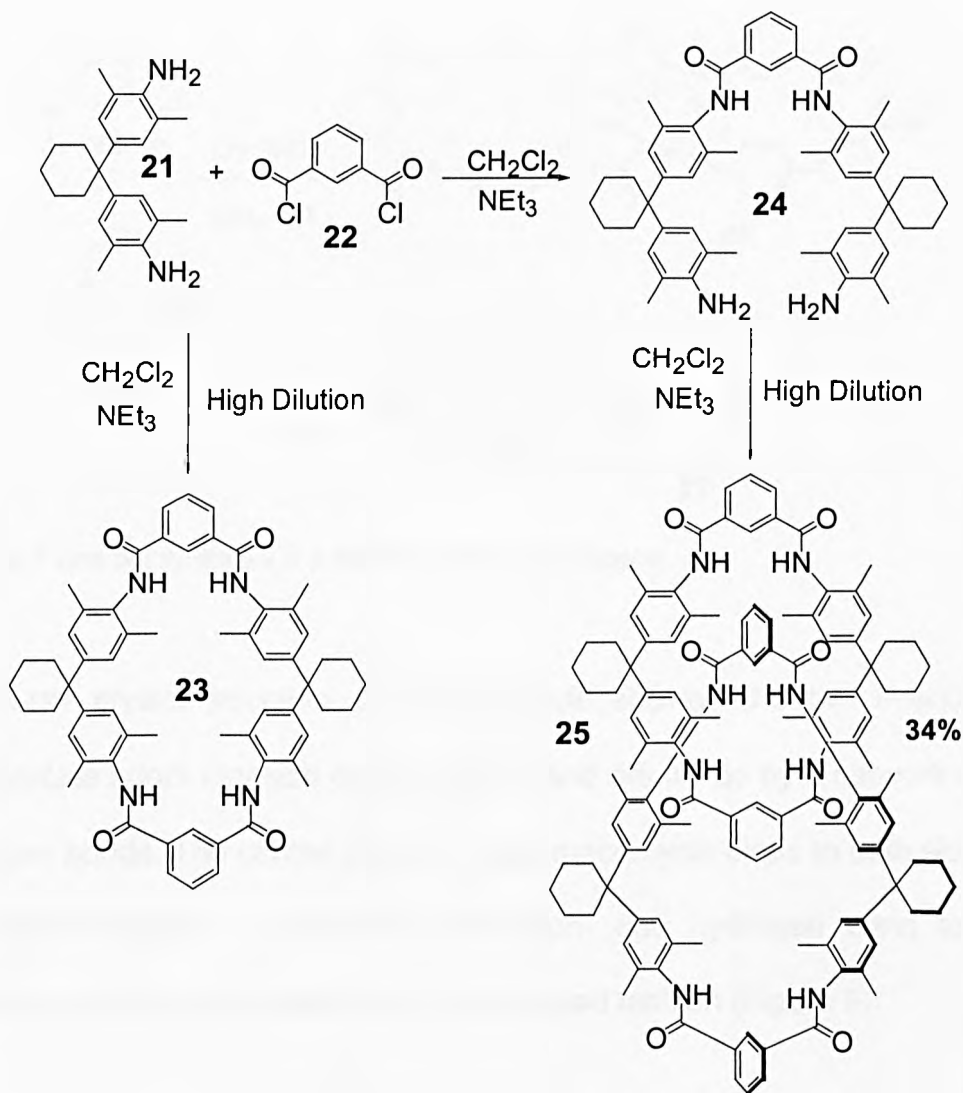


A = F, Cl, O, S, N, π -system

D = F, Cl, O, S, N, C

Figure 5 A hydrogen bond formed between an acidic hydrogen atom (hydrogen bond donor **D**) and an appropriator acceptor (**A**).

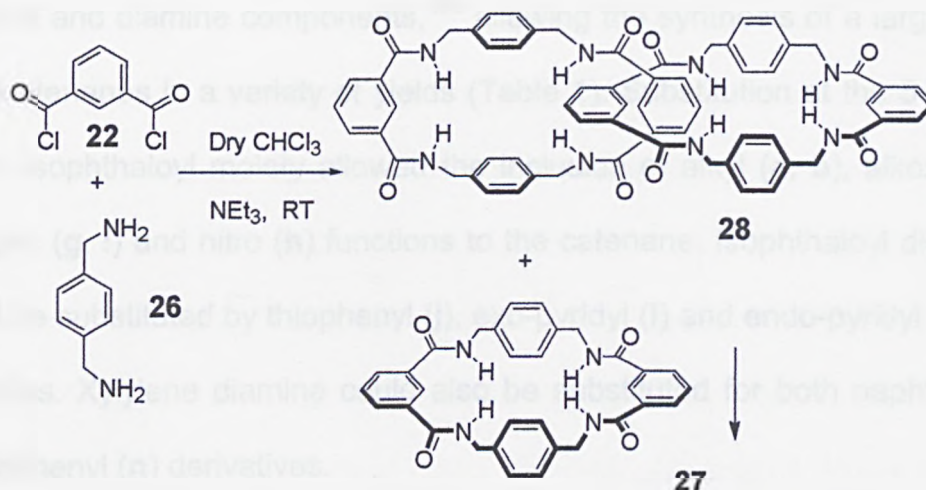
Hydrogen bonding has been used to form catenanes and rotaxanes by Hunter,⁴¹ Vögtle⁴², and Leigh.⁴³ Initial research focused on making catenanes, based on van der Waals, π - π and $\text{NH}\cdots\text{O}=\text{C}$ hydrogen bond interactions between the macrocycle and macrocycle precursor. In 1992, Hunter reported the discovery of a new class of catenanes. The macrocycle **23** had been shown to be a receptor for *p*-benzoquinone. Its original preparation was achieved by the reaction of the bis-amide **21** and isophthaloyl dichloride **22**. An improvement to this synthesis was sought in the form of a stepwise route, in which the bis-amide **24** was prepared, before being reacted with isophthaloyl chloride **22** under high dilution conditions to yield the desired macrocycle **23** in 51% yield. In addition, the [2]catenane **25** was isolated in a remarkable 34% yield (Scheme 6).



Scheme 6 The synthesis of the first amide-based [2]-catenane reported by Hunter.⁴¹

Shortly after Hunter's first report of the hydrogen bonding template synthesis of the [2]catenane, Vögtle and his co-workers described the synthesis of a closely related compound.⁴⁴

The group led by Leigh reported the synthesis of the benzylic amide [2]catenane **28** from commercially available materials.⁴³ A condensation between isophthaloyl dichloride **22** and *p*-xylylene diamine **26** formed the [2]catenane **28** in a yield of 20% (Scheme 7).



Scheme 7 One pot synthesis of a benzylic amide [2]catenane.

The X-ray crystal structure of the molecule showed the two interlocked macrocycles adopt identical conformations and are linked by a network of six hydrogen bonds. The central cavity of each macrocycle binds to both sides of an amide through a three-point interaction- one hydrogen bond to the hydrogen and two to the carbonyl in a bifurcated fashion (Figure 6).

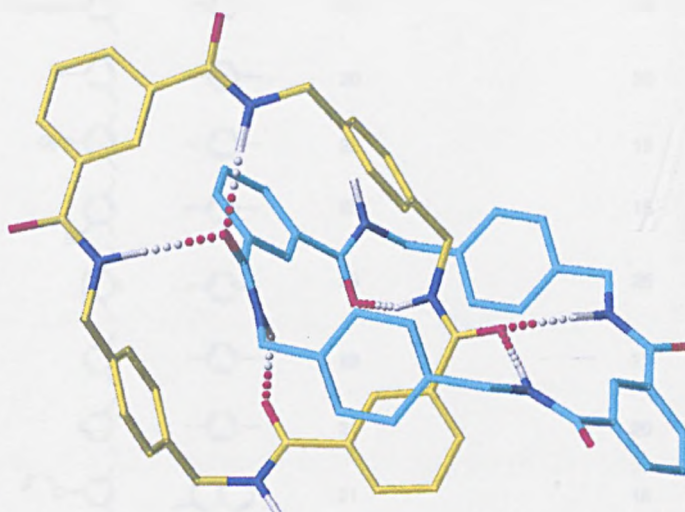
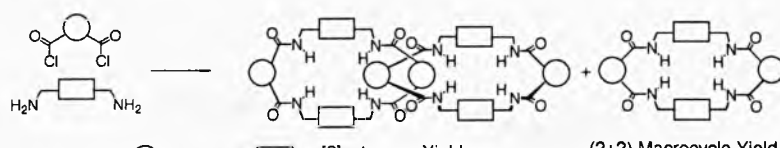


Figure 6 Solid state structure of the benzylic amide [2]catenane **28** (carbon atoms on one ring are shown as yellow and those of the other light blue, oxygen red, nitrogen dark blue and hydrogen white; the non hydrogen bonding hydrogens have been removed for clarity).

The synthesis is remarkably tolerant of structural variation in both the acid chloride and diamine components,^{43b} allowing the synthesis of a large family of [2]catenanes in a variety of yields (Table 1). Substitution at the 5-position of the isophthaloyl moiety allowed the inclusion of alkyl (**a**, **b**), alkoxy (**c-f**), halogen (**g**, **i**) and nitro (**h**) functions to the catenane. Isophthaloyl dichloride could be substituted by thiophenyl (**j**), exo-pyridyl (**l**) and endo-pyridyl (**k**) acid chlorides. Xylylene diamine could also be substituted for both naphthyl (**m**) and biphenyl (**n**) derivatives.



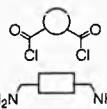



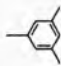

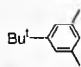

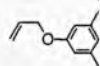

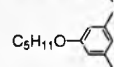

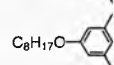

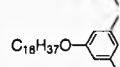

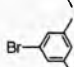

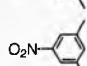

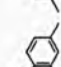

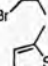



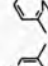
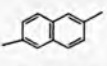
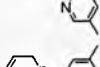
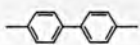
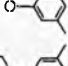
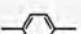
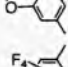
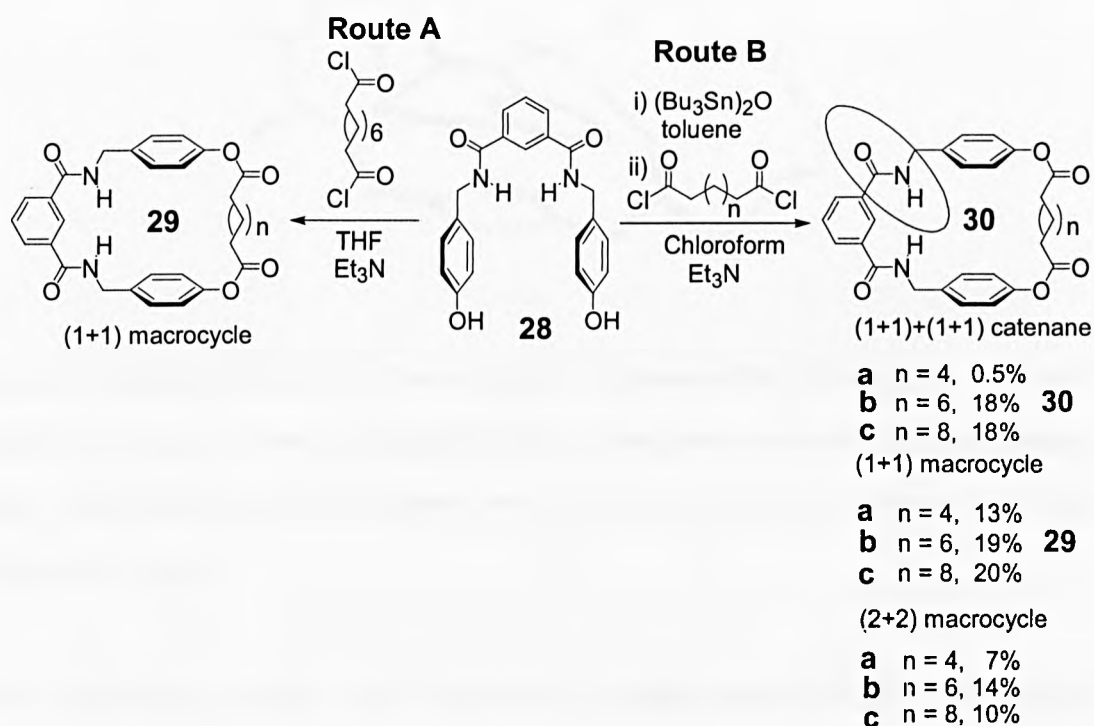
			[2]catenane Yield (%)	(2+2) Macrocycle Yield (%)
			22	20
a)			25	18
b)			20	18
c)			20	21
d)			19	20
e)			22	15
f)			20	20
g)			22	18
h)			25	15
i)			25	25
j)			20	27
k)			21	20
l)			21	18
m)			19	19
n)			0	20
o)				

Table 1 Structural tolerance in the benzylic amide catenane synthesis.

Leigh *et al.* went on to replace some of the amides within the simple benzylic amide catenane with esters.^{45,46} Preliminary attempts at catenane synthesis failed (Scheme 8, route **A**), since the diol **28** only proved soluble in polar solvents which disrupt the hydrogen bond templated catenane assembly. Initial conversion of the diol to a more soluble derivative allowed the reaction to proceed in much less polar media. As a consequence a variety of [2]catenanes could be isolated by simple stannylation of the diol, followed by ring closure with a variety of alkyl diacid chlorides (Scheme 9, Route **B**).



Scheme 8 Synthesis of amphiphilic benzylic amide [2]catenanes.

In the solid state, the [2]catenane **30b** displayed markedly different structural features to the previously reported all amide catenanes (Figure 7). The two component macrocycles adopt differing conformations, one acting as a host and the other a guest. One amide of the guest is held within the central cavity

of the host macrocycle by a total of four hydrogen bonds – two to the amide hydrogen from the ester carbonyls and two to the amide carbonyl from the familiar isophthaloyl diamide.

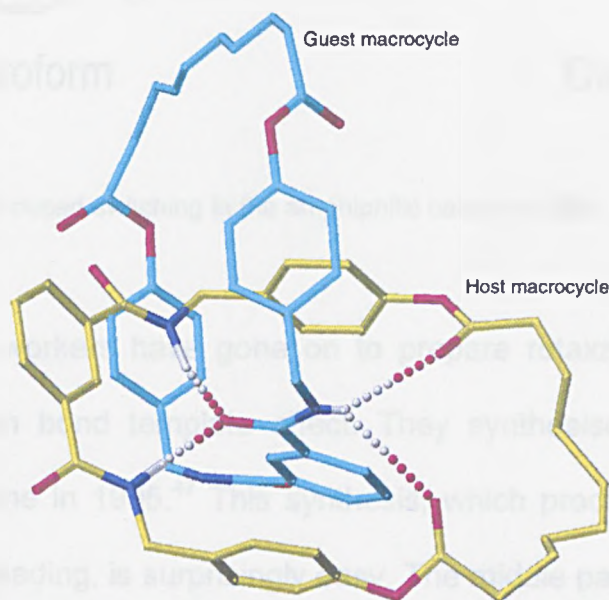


Figure 7 Solid state structure of the amphiphilic [2]catenane **30b** (carbon atoms on the host macrocycle are shown as yellow and those of the guest macrocycle light blue, oxygen red, nitrogen dark blue and hydrogen white. The non H-bonding hydrogens have been removed for clarity).

The interlocked nature of the amphiphilic [2]catenane allows for remarkable changes in the conformation of the molecule dependent on the polarity of the environment (Figure 8). ^1H NMR studies reveal that in non-polar solvents (such as chloroform) the catenane adopts a conformation similar to that found in the solid state. Moving to dimethyl sulfoxide switches the conformation, placing the alkyl chains within the centre of the catenane and minimising unfavourable hydrophobic interactions with the solvent.

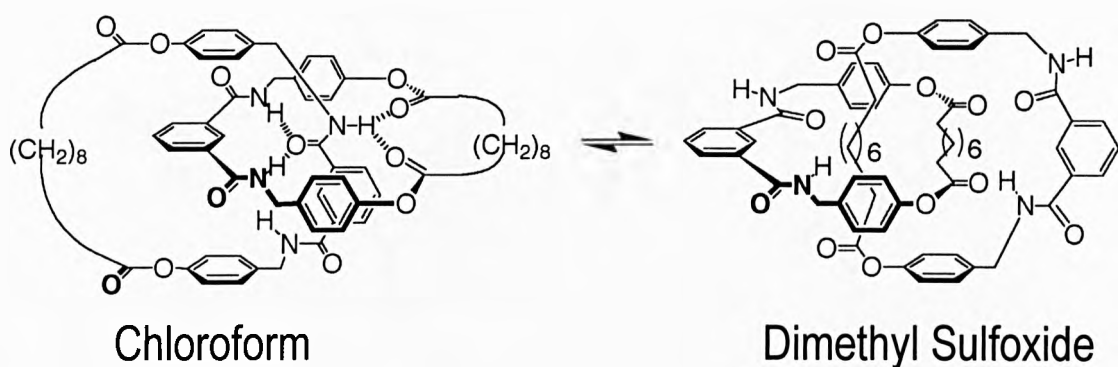
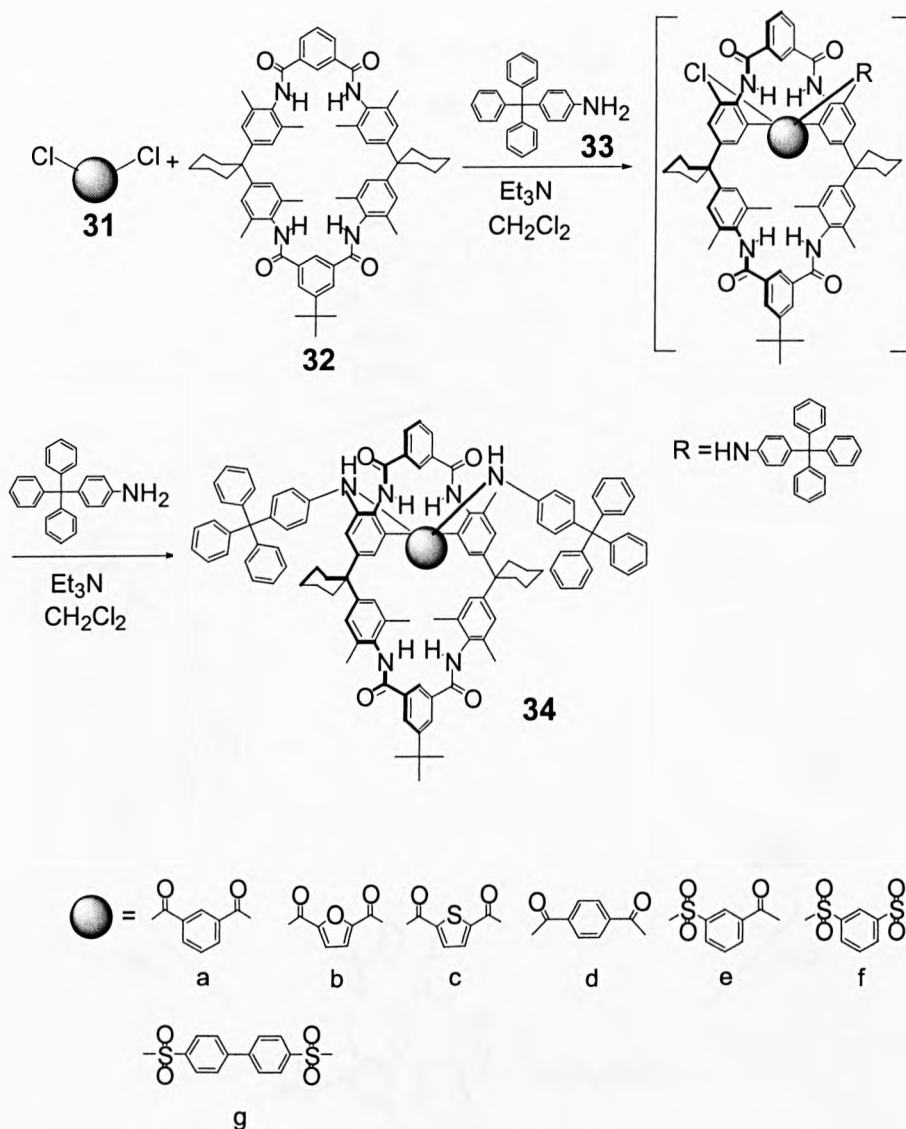


Figure 8 Solvent induced switching in the amphiphilic catenane **30b**.

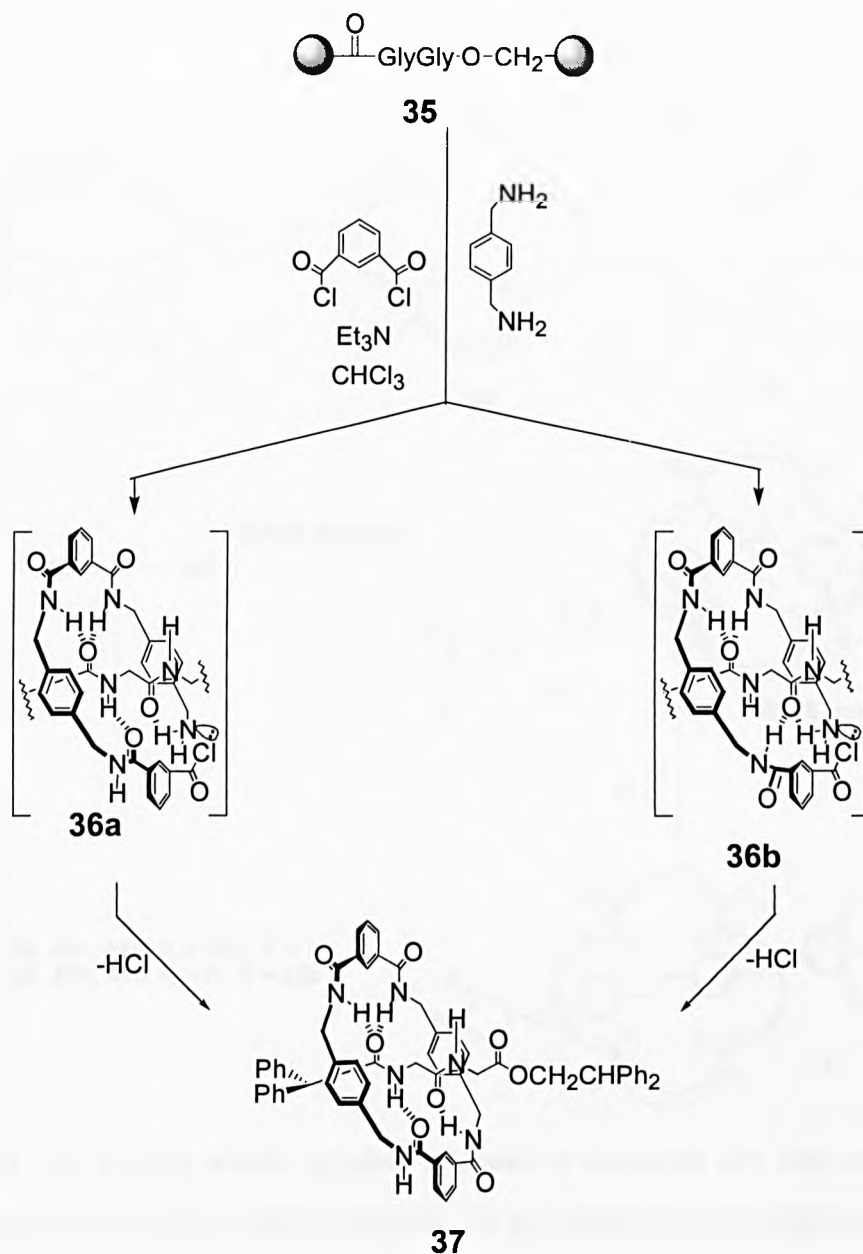
Vögtle and co-workers have gone on to prepare rotaxanes based on this amide hydrogen bond template effect. They synthesised the first amide-linked [2]rotaxane in 1995.⁴⁷ This synthesis, which proceeds with a neutral template by threading, is surprisingly easy. The middle part of the “axle” **31a-g** (guest) was added into the non-polar solution of the “wheel” **32**, which acts as a concave template. The reaction with (4-aminophenyl)triphenylmethane **33**, which acts as blocking group, results in a mechanical bond between “wheel” and axle” to form the [2] rotaxane **34a-g** (Scheme 9).

The exchange of meta- or para-phenylene unit or with five-member heteroarenes led to the synthesis of other [2]rotaxanes with different middle parts within the axle. Even the sulfonyl chlorides were included in the “hospitable” macrocycle **32**, which enabled the first [2]rotaxane with sulfonamide units in yields as high as 41%.



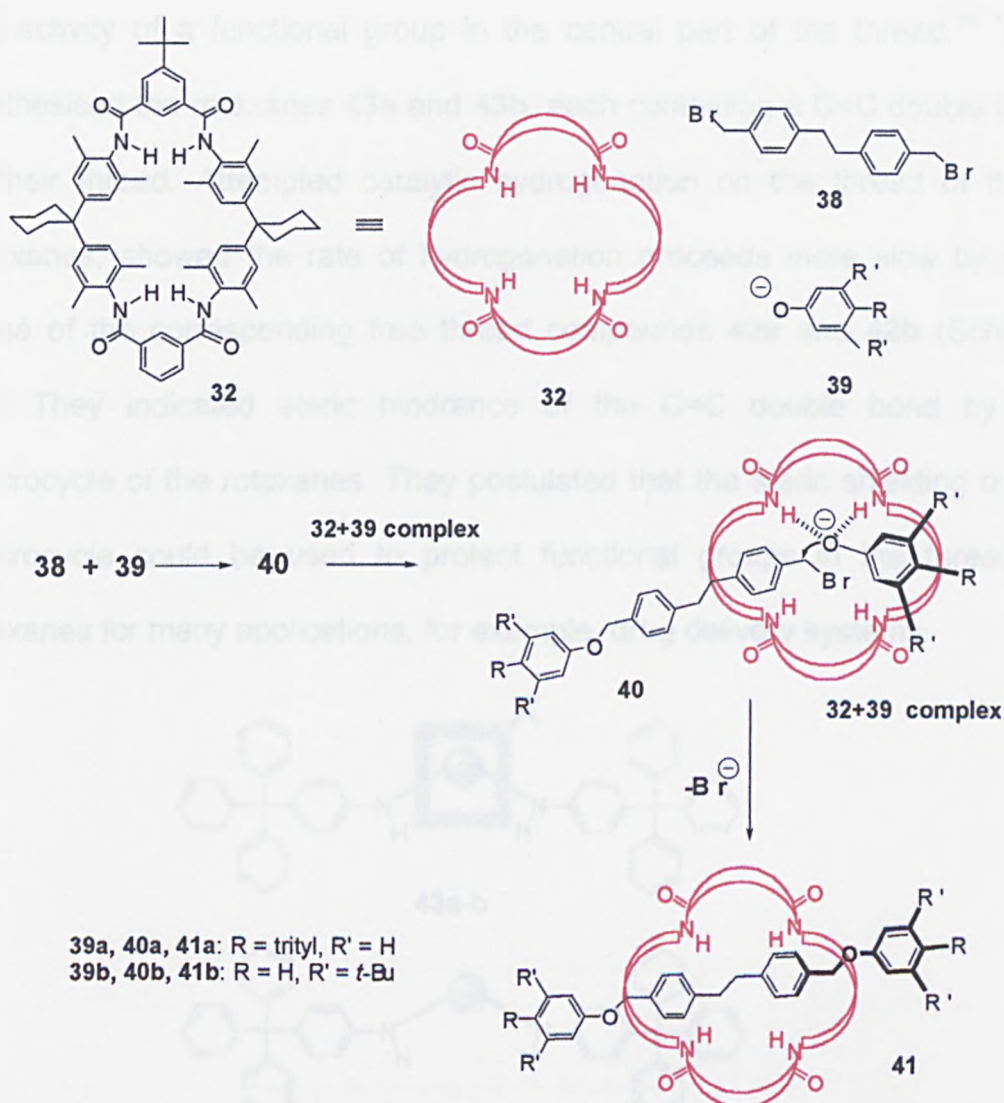
Scheme 9 A "one pot" preparation of a rotaxane recently reported by Vögtle and co-workers.

After the synthesis of the benzylic amide [2]catenanes in 1997, Leigh reported that glycyglycine derivatives could be used as templates for the formation of benzylic amide macrocycles through a five-molecule, hydrogen bond directed "clipping" strategy to give peptido[2]rotaxanes **37** in yields as high as 62%⁴⁸ and have described the principle mechanism of the "clipping" strategy to benzylic rotaxanes (Scheme 10).



Scheme 10 The synthesis of peptido rotaxanes **37** by clipping, a hydrogen bonding directed assembly processes.

In addition to the hydrogen bonding between macrocyclic amide and neutral molecular threads, Vögtle and co-workers recently published a study of the anion binding abilities of macrocyclic tetralactams, which have much larger binding constants than neutral molecular guests, and used this to form a new series of rotaxanes in high yield (Scheme 11).⁴⁹



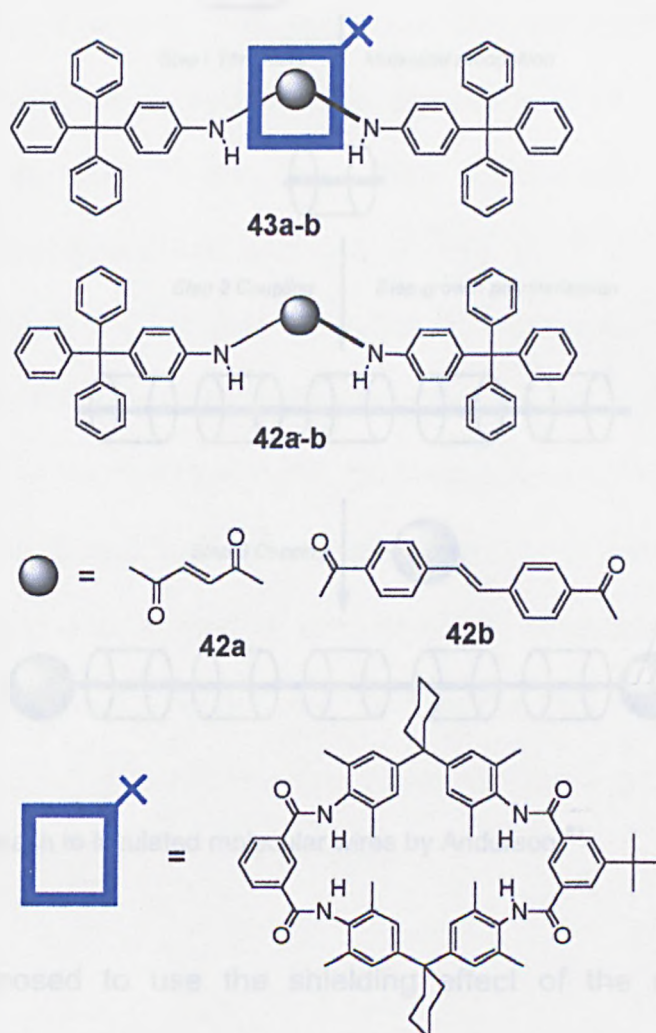
Scheme 11 High-yielding anionic template synthesis of rotaxanes with bis(phenyl ether) thread where phenolate-macrocycle complexes act as supramolecular nucleophiles for the reaction with semi-thread 40.

1.5 Effects of the Macrocyclic Wheel on the Chemical Properties of Functional Groups of the Thread.

1.5.1.1 Chemical Reactions on the Thread of Rotaxanes - Steric Hindrance by the Macrocycle

Recently, Vögtle reported the possibility of using the macrocycle of the rotaxane as a non-covalent protecting group that could significantly decrease

the activity of a functional group in the central part of the thread.⁵⁰ They synthesised the rotaxanes **43a** and **43b**, each containing a C=C double bond in their thread. Attempted catalytic hydrogenation on the thread of these rotaxanes, showed the rate of hydrogenation proceeds more slow by then those of the corresponding free thread compounds **42a** and **42b** (Scheme 12). They indicated steric hindrance of the C=C double bond by the macrocycle of the rotaxanes. They postulated that the steric shielding of the macrocycle could be used to protect functional groups in the thread of rotaxanes for many applications, for example, drug delivery systems.



Scheme 12 The macrocycle **32** (blue square) acts as a protecting group by sterically hindering the reaction on the thread.

1.5.1.2 Insulated Molecular Wires

Organic molecules with a long conjugated π system have many potential applications: in non-linear optics, in organic electron-luminescent display devices, and as organic semiconductors,⁵¹ and could be regarded as "molecular wires" ⁵² because they have mobile electrons. The small HOMO-LUMO energy gaps responsible for their special electronic properties often lead to chemical reactivity and instability, which can limit their usefulness.

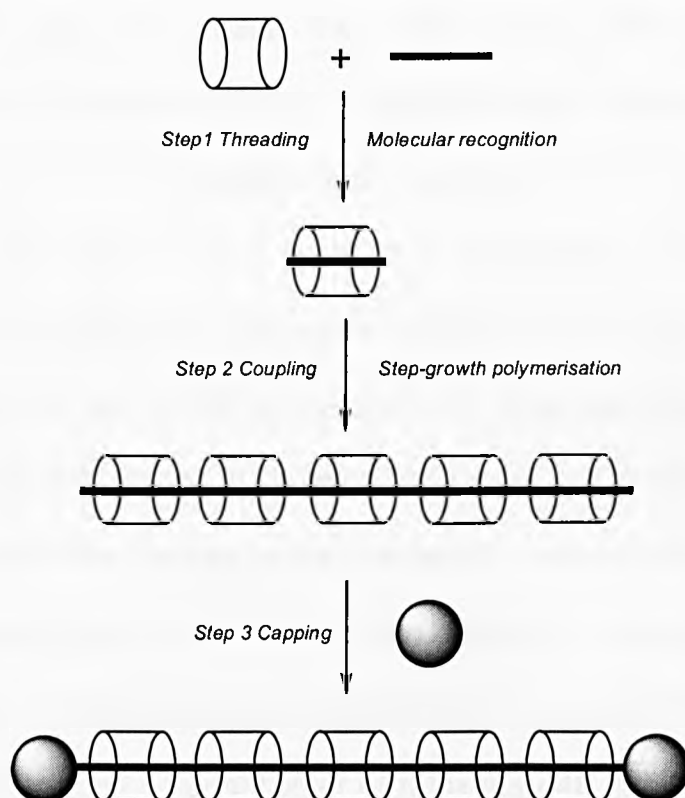


Figure 9 An approach to insulated molecular wires by Anderson.⁵³

Anderson proposed to use the shielding effect of the macrocycle of a rotaxane as an insulator for a conducting thread.

The hydrophobic effect^{21c,21d,53} was used to drive the macrocycle threading in water and reactions like Glaser coupling to form threads with conjugated

backbones generating a molecular necklace under aqueous conditions. The addition of large bulky end-groups, or stoppers, to prevent the insulators - macrocycles, from unthreading yields the poly-rotaxanes (Figure 9). In these rotaxanes, the macrocycles acts as molecular insulators protecting the threads "molecular wires", from chemical reactions.

1.5.2 Chiral Geometry of Interlocked Architectures

In the 80s, Sauvage *et al.* published the first synthesis of a topological chiral catenane,^{23d,54} after five years, the same group achieved the partial separation into the enantiomers in co-operation with Okamoto.⁵⁵ In 1996, Vögtle and co-workers reported the synthesis of a topological chiral sulfonamide catenane⁵⁶ and then they successfully synthesised the [2]rotaxane enantiomers **44a** and **44b** (Figure 10).⁵⁷ These mechanically bonded molecules are the first examples for rotaxane cycloenantiomers, consisting of a dumbbell and a macrocycle that are not in themselves chiral. The object and its mirror image in this case result from different sequences of the sulfonamide group and three amide groups on the macrocycle in rotaxane **44a** and **44b**, around an unsymmetrical dumbbell. They separated the (+)-enantiomer and (-)-enantiomer of rotaxane **44b**, in which the circular dichrogram (CD) of the enantiomeric rotaxanes show pronounced Cotton effects in the aromatic chromophore region.⁵⁸

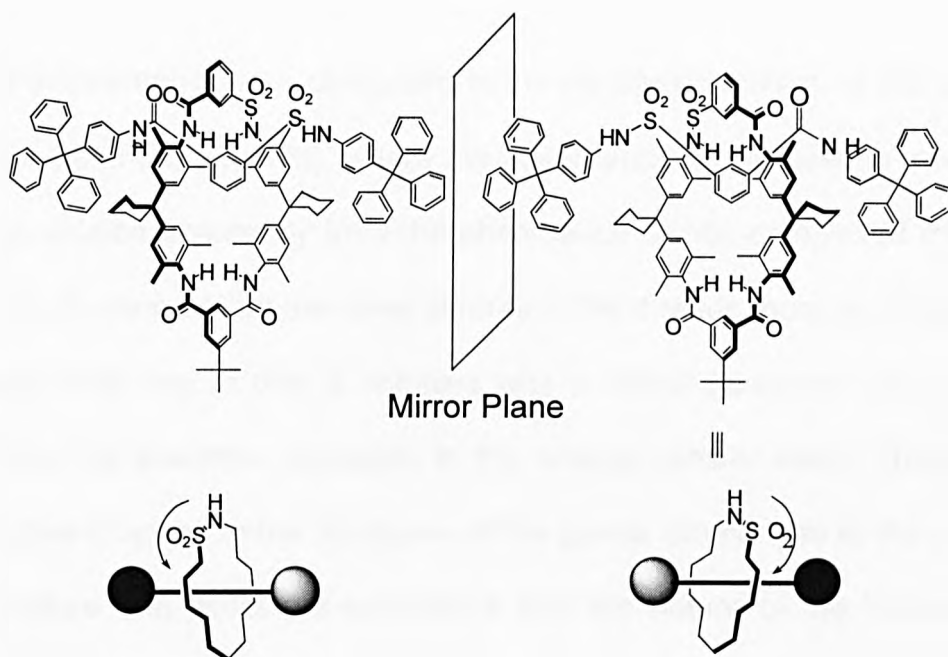


Figure 10 Cycloenantiomeric [2]rotaxanes **44a** and **44b** (the square arrow indicates the sequence of the atoms).

In 1998, Stoddart and co-workers synthesised [2]pseudorotaxanes **45-49** (Figure 11) with chiral threads.⁵⁹

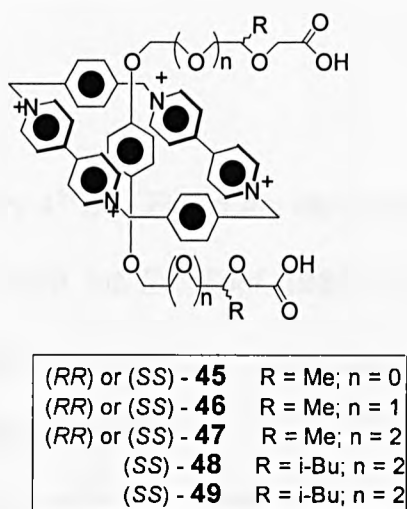


Figure 11 The chiral [2]pseudorotaxanes **45-49** prepared by Stoddart's group.

Circular dichroism measurements of these [2]pseudorotaxanes were performed in order to study the geometry of the pseudorotaxanes in solution.

The measurements were conducted in the wavelength region of the charge-transfer band (400-600nm), where the absorbance of the pseudo-rotaxanes can be studied separately from the absorbance of non-complexed material. The results showed that the chiral centres of the threads must be close to the hydroquinone ring to give a complex with a "chiral geometry" and thus to influence the electronic transition in the charge-transfer band. They found that subtle changes in the structures of the guests or changes in the solution temperature can direct the occurrence and the nature of the induced CD effect in the charge-transfer transition of the complex. The chirality present in the π -electron rich threadlike guest can induce chirality that is associated with the supramolecular structure as a whole. The resultant CD spectra were influenced by the geometry of the chiral threads and macrocycle, as Vögtle predicted, and it may be possible to steer or even alter chiroptical properties in the future.

References:

1. Stryer, L. *Biochemistry* 4th ed., Freeman: New York, **1995**.
2. Lehn, J.M. *Angew. Chem. Int. Ed. Engl.* **1988**, 27, 89.
3. For a review on self-assembly see: Stoddart, J.F.; Philp, D. *Angew. Chem. Int. Ed. Engl.* **1996**, 35, 1155.
4. Reinhoudt, D.N. *J. Coord. Chem.* **1988**, 18, 21.
5. Whitesides, G.M.; Simanek, E.E.; Mathias, J.P.; Seto, C.T.; Chin, D.N.; Mammen, M.; Gordon, D.M. *Acc. Chem. Res.* **1995**, 28, 37.
6. Ghadiri, M.R. *Adv. Mater.* **1995**, 7, 675.

7. For a comprehensive review see Amabilino, D.B.; Stoddart, J.F. *Chem. Rev.* **1995**, 95, 2725.
8. Schill, G. *Catenanes, Rotaxanes and Knots*; Academic Press: New York, **1971**.
9. Gust, D. *Nature* **1994**, 372, 133.
10. Feringa, B.L.; Jager, W.F.; de Lange, B.L. *Tetrahedron* **1993**, 49, 8267.
11. (a) Collins, P.G.; Zettl, A.; Bando, H.; Thess, A.; Smalley, R.E. *Science* **1997**, 278, 100. (b) Stupp, S.I.; Le Bonheur, V.; Walker, K.; Li, L.S.; Huggins, K.E.; Keser, M.; Amstutz, A. *Science* **1997**, 276, 384. (c) Tans, S.J.; Devoret, M.H.; Dai, H.; Thess, A.; Smalley, R.E.; Geerligs, L.J.; Dekker, C. *Nature* **1997**, 386, 474.
12. (a) Anderson, S.; Claridge, T.D.W.; Anderson, H.L. *Angew. Chem. Int. Ed. Engl.* **1997**, 36, 1310. (b) Parham, A.H.; Windisch, B.; Vögtle, F. *Eur. J. Org. Chem.* **1999**, 5, 1233.
13. (a) Bissell, R.A.; Córdova, E.; Kaifer, A.E.; Stoddart, J.F. *Nature* **1994**, 369, 133. (b) Collin, J.P.; Gavina, P.; Sauvage, J.P. *New J. Chem.* **1997**, 21, 525. (c) Sauvage, J.P. *Science* **2001**, 291, 2105. (d) Brouwer, A.M.; Frochot, C.; Gatti, F.G.; Leigh, D.A.; Mottier, L.; Paolucci, F.; Roffia, S.; Würpel, G.W.H. *Science* **2001**, 291, 2124.
14. Wasserman, E.J. *J. Am. Chem. Soc.* **1960**, 82, 4433.
15. Walba, D.M. *Tetrahedron* **1985**, 41, 3161.
16. Frish, H.L.; Wasserman, E.J. *J. Am. Chem. Soc.* **1961**, 83, 3789.
17. (a) Harrison, I.T.; Harrison, S. *J. Am. Chem. Soc.* **1967**, 89, 5723. (b) Harrison, I.T. *J. Chem. Soc. Perkin Trans. 1* **1974**, 301. (c) Agam, G.; Graiver, D.; Zilkha, A. *J. Am. Chem. Soc.* **1967**, 98, 9206.

18. (a) Busch, D.H.; Stephenson, N.A. *Coord. Chem. Rev.* **1990**, *100*, 119. (b) Lindsey, J.S. *New. J. Chem.* **1991**, *15*, 153. (c) Whitesides, G.M.; Mathias, J.P.; Seto, C.T. *Science* **1991**, *254*, 1312. (d) Philp, D.; Stoddart, J.F.; *Synlett.* **1991**, 445. (e) Busch, D.H. *J. Inclusion Phenom.* **1992**, *12*, 389. (f) Anderson, S.; Anderson, H.L.; Sanders, J.K.M. *Acc. Chem. Res.* **1993**, *26*, 469. (g) Cacciapaglia, R.; Mandolini, L. *Chem. Soc. Rev.* **1993**, *22*, 221. (h) Hoss, R.; Vögtle, F. *Angew. Chem. Int. Ed. Engl.* **1994**, *33*, 375. (i) Schneider, J.P.; Kelly, J.W. *Chem. Rev.* **1995**, *95*, 2169. (j) Raymo, F.M.; Stoddart, J.F. *Acc. Chem. Res.* **1997**, *30*, 313. (k) Fyfe, M.C.T., Stoddart, J.F. *Acc. Chem. Res.* **1997**, *30*, 393.
19. (a) Chambron, J.C.; Heitz, V., Sauvage, J.P. *J. Chem. Soc., Chem. Commun.* **1992**, 1131. (b) Chambron, J.C.; Harriman, A.; Heitz, V.; Sauvage J.P. *J. Am. Chem. Soc.* **1993**, *115*, 6106. (c) Chambron, J.C.; Harriman, A.; Heitz, V.; Sauvage, J.P. *J. Am. Chem. Soc.* **1993**, *115*, 7419. (d) Chambron, J.C.; Heitz, V.; Sauvage, J.P. *J. Am. Chem. Soc.* **1993**, *115*, 12378. (e) Chambron, J.C.; Chardon-Noblat, S.; Harriman, A.; Heitz, V.; Sauvage J.P. *Pure Appl. Chem.* **1993**, *65*, 2343. (f) Chambron, J.C.; Dietrich-Buchecker, C.O.; Nierengarten, J.F.; Sauvage, J.P. *Pure Appl. Chem.* **1994**, *66*, 1543. (g) Chambron, J.C.; Dietrich-Buchecker, C.O.; Heitz V.; Nierengarten, J.F.; Sauvage, J.P.; Pascard, C.; Guilhem, J. *Pure Appl. Chem.* **1995**, *67*, 233. (h) Chambron, J.C.; Dietrich-Buchecker, C.O.; Hosseini, M.W.; Sauvage, J.P. *Comprehensive Supramolecular Chemistry* Pergamon: Oxford, **1996**, Vol. 9, pp 43-83.
20. Schill, G.; Henschel, R. *Liebigs Ann. Chem.* **1970**, 731, 113.
21. (a) Ogino, H. *New J. Chem.* **1993**, *17*, 683. (b) Wenz, G.; Wolf, F.;

Wagner, M.; Kubik, S. *New J. Chem.* **1993**, 17, 729. (c) Anderson, S.; Anderson, H.L. *Angew. Chem. Int. Ed. Engl.* **1996**, 35, 1956. (d) Anderson, S.; Clegg, W.; Anderson, H.L. *Chem. Commun.* **1998**, 2379.

22. (a) Hunter, C.A. *J. Am. Chem. Soc.* **1992**, 114, 5303. (b) Lane, A.S.; Leigh, D.A.; Murphy, A. *J. Am. Chem. Soc.* **1997**, 119, 11092. (c) Clegg, W.; Gimenez-Saiz, C.; Leigh, D.A.; Murphy, A.; Slawin, A.M.Z.; Teat, S.J. *J. Am. Chem. Soc.* **1999**, 121, 4124. (d) Gatti, F.G.; Leigh, D.A.; Nepogodiev, S.A.; Slawin, A.M.Z.; Teat, S.J.; Wong, J.K.Y. *J. Am. Chem. Soc.* **2001**, 123, 5983. (e) Parham, A.H.; Schmieder, R.; Vögtle, F. *Synlett.* **1999**, 12, 1887. (f) Seel, C.; Parham, A.H.; Safarowsky, O.; Hübner, G.M.; Vögtle, F. *J. Org. Chem.* **1999**, 64, 7236. (g) Seel, C.; Vögtle, F. *Chem. Eur. J.* **2000**, 6, 21. Also see references: 40, 44, 45, 46, 47, 48, 49, 50, 51 and 52.

23. (a) Dietrich-Buchecker, C.O.; Nierengarten, J.F.; Sauvage, J.P. *Tetrahedron Lett.* **1992**, 33, 3625. (b) Dietrich-Buchecker, C.O.; Nierengarten, J.F.; Sauvage, J.P.; Armaroli, N.; Balzani, V.; De Cola, L. *J. Am. Chem. Soc.* **1993**, 115, 11237. (c) Dietrich-Buchecker, C.O.; Sauvage, J.P.; De Cian, A.; Fischer, J. *J. Chem. Soc., Chem. Commun.* **1994**, 2231. (d) Nierengarten, J.F.; Dietrich-Buchecker, C.O.; Sauvage, J.P. *J. Am. Chem. Soc.* **1994**, 116, 375. (e) Dietrich-Buchecker, C.O.; Leize, E.; Nierengarten, J.F.; Sauvage, J.P.; van Dorsselaer, A. *J. Chem. Soc., Chem. Commun.* **1994**, 2257.

24. Dietrich-Buchecker, C.O.; Sauvage, J.P. *Angew. Chem. Int. Ed. Engl.* **1989**, 28, 189.

25. Schill, G.; Lüttringhaus, A. *Angew. Chem. Int. Ed. Engl.* **1964**, 3, 546.

26. Logeman, E.; Rissler, K.; Schill, G.; Fritz, H. *Ber. Dtsch. Chem. Ges.*

1981, 114, 2245.

27. Logeman, E.; Schill, G.; Vetter, W. *Ber. Dtsch. Chem. Ges.* **1978**, *111*, 2615.

28. Agam, G.; Zilkha, A. *J. Am. Chem. Soc.* **1976**, *98*, 5214.

29. (a) Schill, G.; Zollenkopf, H. *Liebigs Ann. Chem.* **1969**, *721*, 53. (b) Schill, G.; Henschel, R. *Liebigs Ann. Chem.* **1970**, *731*, 113.

30. (a) Stoddart, J.F. *Angew. Chem. Int. Ed. Engl.* **1992**, *31*, 846. (b) Wenz, G. *Angew. Chem. Int. Ed. Engl.* **1994**, *33*, 802.

31. (a) Ogino, H. *J. Am. Chem. Soc.* **1981**, *103*, 1303. (b) Ogino, H.; Ohata, K. *Inorg. Chem.* **1984**, *23*, 3312. (c) Nepogodiev, S.A.; Stoddart, J.F. *Chem. Rev.* **1998**, *98*, 1959. (d) Buston, J.E.H.; Young, J.R.; Anderson, H.L. *Chem. Commun.* **2000**, 905. (e) Taylor, P.N.; O' Connell, M.J.; Mc Neill, L.A.; Hall, M.J.; Aplin, R.T.; Anderson, H.L. *Angew. Chem. Int. Ed. Engl.* **2000**, *39*, 3456. (f) Stanier, C.A.; O' Connell, M.J.; Clegg, W.; Anderson, H.L. *Chem. Commun.* **2001**, 493.

32. (a) Fujita, M.; Ogura, K. *Coord. Chem. Rev.* **1996**, *148*, 249. (b) Fujita, M. *Comprehensive supramolecular chemistry*, Hosseini, M.W.; Sauvage J.P. Eds., Pergamon: Oxford, **1996**, Vol. 9, pp 253-282. (c) Fujita, M. *Chem. Soc. Rev.* **1998**, *27*, 417. (d) Fujita, M. *Acc. Chem. Res.* **1999**, *32*, 53.

33. (a) Wu, C.; Lecavalier, P.R.; Shen, Y.X.; Gibson, H.W. *Chemistry of Materials* **1991**, *3*, 569. (b) Dietrich-Buchecker, C.O.; Sauvage, J.P. *Chem. Rev.* **1987**, *87*, 795. (c) Chambron, J.C.; Dietrich-Buchecker, C.O.; Heitz, V.; Nierengarten, J.F.; Sauvage J.P. *Transition metals in supramolecular chemistry*, Fabbrizzi, L.; Poggi, A. Eds., Kluwer Academic Publishers, Boston, **1994**, 371.

34. (a) Dietrich-Buchecker, C.O.; Sauvage, J.P.; Kintzinger, J.P. *Tetrahedron Lett.* **1983**, 24, 5095. (b) Dietrich-Buchecker, C.O.; Sauvage, J.P.; Kern, J.M. *J. Am. Chem. Soc.* **1984**, 106, 3043.
35. Wu, C.; Lecavalier, P.R.; Shen, Y.X.; Gibson, H.W. *Chem. Mater.* **1991**, 3, 569.
36. Diederich, F.; Dietrich-Buchecker, C.O.; Nierengarten, J.F.; Sauvage, J.P. *J. Chem. Soc., Chem. Commun.* **1995**, 781.
37. Sleiman, H.; Baxter, P.; Lehn, J. M.; Rissanen, K. *J. Chem. Soc., Chem. Commun.* **1995**, 715.
38. Anelli, P.L.; Ashton, P.R.; Ballardini, R.; Balzani, V.; Delgado, M.; Gandolfi, M.T.; Goodnow, T.T.; Kaifer, A.E.; Philp, D.; Pietraszkiewicz, M.; Prodi, L.; Reddington, M.V.; Slawin, A.M.Z.; Spencer, N.; Stoddart, J.F.; Vicent, C.; Williams, D.J. *J. Am. Chem. Soc.* **1992**, 114, 193.
39. Ashton, P.R.; Goodnow, T.T.; Kaifer, A.E.; Reddington, M.V.; Slawin, A.M.Z.; Spencer, N.; Stoddart, J.F.; Vicent C.; Williams D.J. *Angew. Chem. Int. Ed. Engl.* **1989**, 28, 1396.
40. For a comprehensive understanding of hydrogen-bond: Jeffrey, G.A. *An Introduction to Hydrogen Bonding* Oxford University Press, **1997**.
41. Hunter, C.A. *J. Am. Chem. Soc.* **1992**, 114, 5303.
42. (a) Vögtle, F.; Meier, S.; Hoss, R. *Angew. Chem. Int. Ed. Engl.* **1992**, 31, 1619. (b) Meier, S.; Ottens-Hildebrandt, S.; Brodesser, G.; Vögtle, F. in *Chemical Synthesis Vol. E 320* (Eds.: Chatgililoglu, C.; Snieckus, V.) Kluwer, Dordrecht, **1996**, pp 361-379.
43. (a) Johnston A.G.; Leigh, D.A.; Pritchard, R.J.; Deegan, M.D. *Angew. Chem. Int. Ed. Engl.* **1995**, 34, 1209. (b) Johnston A.G.; Leigh, D.A.; Nezhat,

- L.; Smart, J.P.; Deegan, M.D. *Angew. Chem. Int. Ed. Engl.* **1995**, 34, 1212.
44. Vögtle, F.; Meier, S.; Hoss, R. *Angew. Chem. Int. Ed. Engl.* **1992**, 31, 1619.
45. Leigh, D.A.; Murphy, A.; Smart, J.P.; Deleuze, M.S.; Zerbetto, F. *J. Am. Chem. Soc.* **1998**, 120, 6458.
46. Leigh, D.A.; Moody, K.; Smart, J.P.; Watson, K.J.; Slawin, A.M.Z. *Angew. Chem. Int. Ed. Engl.* **1996**, 35, 306.
47. Vögtle, F.; Händel, M.; Meier, S.; Ottens-Hildebrandt, S.; Ott, F.; Schmidt, T. *Liebigs Ann.* **1995**, 739.
48. Leigh, D.A.; Murphy, A.; Smart, J.P.; Slawin, A.M.Z. *Angew. Chem. Int. Ed. Engl.* **1997**, 36, 728.
49. Hübner, G.H.; Gläser, J.; Seel, C.; Vögtle, F. *Angew. Chem. Int. Ed. Engl.* **1999**, 38, 383.
50. Parham, A.H.; Windisch, B.; Vögtle, F. *Eur. J. Org. Chem.* **1999**, 1233.
51. Kraft, A.; Grimsdale, A.C.; Holmes, A.B. *Angew. Chem. Int. Ed. Engl.* **1998**, 37, 402.
52. (a) Ward, M.D. *Chem. Ind. (London)*, **1996**, 15, 568. (b) Grosshenny, V.; Harriman, A.; Ziessel, R. *Angew. Chem. Int. Ed. Engl.* **1995**, 34, 1100.
53. Anderson, S.; Aplin, R.T.; Claridge, T.D.W.; Goodson, T.; Maciel, A.C.; Rumbles, G.; Ryan, J.F.; Anderson, H.L. *J. Chem. Soc., Perkin Trans. 1* **1998**, 2383.
54. (a) Mitchell, D.K.; Sauvage J.P. *Angew. Chem. Int. Ed. Engl.* **1988**, 27, 930. (b) Nierengarten, J.F.; Dietrich-Buchecker, C.O.; Sauvage, J.P. *J. Am. Chem. Soc.*, **1994**, 116, 375.
55. Kaida, Y.; Okamoto, Y.; Chambron, J.C.; Mitchell, D.K.; Sauvage, J.P.

Tetrahedron Lett. **1993**, 34, 1019.

56. Ottens-Hildebrandt, S.; Schmidt, T.; Harren, J.; Vögtle, F. *Liebigs Ann.* **1995**, 1855.

57. Jäger, R.; Händel, M.; Harren, J.; Rissanen, K.; Vögtle, F. *Liebigs Ann.* **1996**, 1201.

58. Yamamoto, C.; Okamoto, Y.; Schmidt, T.; Jäger, R.; Vögtle, F. *J. Am. Chem. Soc.* **1997**, 119, 10547.

59. Asakawa, M.; Ashton, P.R.; Hayes, W.; Janssen, H.M.; Meijer, E.W.; Menzer, S.; Pasini, D.; Stoddart, J.F.; White, A.J.P.; Williams, D.J. *J. Am. Chem. Soc.* **1998**, 120, 920.

Chapter Two

2. Synthesis of a Novel Class of Rotaxanes with a Diene in the Axle

Abstract: Rotaxanes ¹ currently enjoy a great deal of interest due to their unique topological and dynamic properties.² Further to our initial studies on the hydrogen bond-directed synthesis of peptide ³ and fumaric ⁴ based rotaxanes, here we report the synthesis of a new class of rotaxanes based on the geometrical isomers of muconic acid. These new muconic based rotaxanes were synthesised by a clipping strategy in high yields. The *E,E* and *Z,Z* isomers of the muconic axle form rotaxanes in similar yields but the *E,Z* is far superior as a template for rotaxane formation. The crystal structures of the *E,E* and *Z,Z* isomers have been obtained. The importance of rigidity in the thread was addressed by comparison to the analogous all saturated systems.^{2,3}

Introduction: Leigh *et al.* ^{3,6} recently reported the 5-component assembly of rotaxanes from *para*-xylylene diamine and isophthaloyl dichloride with peptide-based threads in good yields (typically 28-62%). It is postulated that the five component clipping reactions (Figure 2.1) produce rotaxanes because of a change in the preferred conformation of the immediate precursor from linear oligomer (**51**) to macrocyclic precursor in the presence of a suitable template **50a**. In the absence of such a template, 1,3-diamide units like **51** preferentially adopt *syn-anti* conformations.⁷ In the presence of template **50a** however, co-operative multi-point hydrogen-

bonding interactions between thread and macrocyclic precursor shift the conformational preference of the 1,3-diamide unit to *syn-syn* as a direct result of bifurcated hydrogen-bonding to a carbonyl of the thread as illustrated in **51a**.

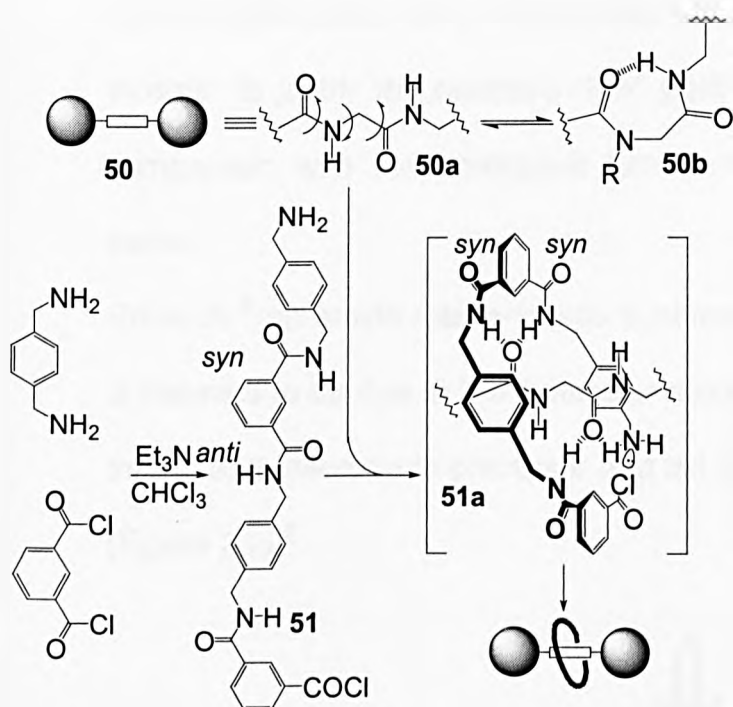


Figure 2.1 The postulated mechanistic pathway to hydrogen bond-assembled rotaxane formation illustrating how the template **50a** induces a conformational change in the immediate precursor to ring closure **51a**.

Additional 'handles' on the template **50a** hold the reactive end groups in mutual proximity such that cyclisation of **51** occurs rapidly around the template **51a** to give the mechanically interlocked product. Such a pathway is also proposed for the synthesis of the benzylic amide catenane **28** - the molecule that inspired these investigations.⁸ Although the gly-gly motif is clearly acting as a good template in such an H-bond based rotaxane formation, the thread **50a** possesses several internal degree of freedom that

are lost in the supramolecular complex **52**. These include torsional freedom around the three bonds of the backbone shown in **50a** (Figure 2.1). Furthermore, the high flexibility of such a backbone means that it can adopt additional conformations (e.g. **50b**). Such a seven-membered-ring conformation based on an intra-molecular hydrogen-bond may be significant in order to justify the relatively "low" yield of the peptide based rotaxane in comparison with the analogous fumaric-amide based template described below.

Recently,⁹ an amide rotaxane was synthesised in 97% yield.⁴ The high yield is believed to be due to the molecular recognition with a "perfect fit" between thread and macrocycle precursor that led to "ideal" templating pre-conditions (Figure 2.2).⁵

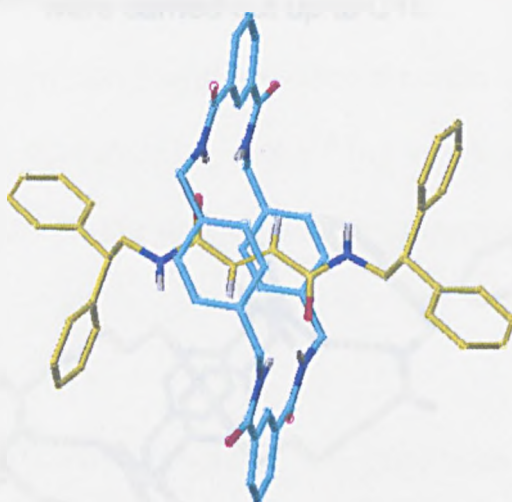


Figure 2.2 X-ray structure of a fumaric-based rotaxane **52**.

The crystal structure (Figure 2.2) of the fumaramide based rotaxane showed four bifurcated intercomponent H-bonds without any distortion in the conjugation of the isophthalamide system while the tetramide macrocycle adopt a favourable chair conformation. Probably, the extraordinary yield of

IMAGING SERVICES NORTH

Boston Spa, Wetherby

West Yorkshire, LS23 7BQ

www.bl.uk

**PAGE MISSING IN
ORIGINAL**

In the succinic motif (C4) the distance between the two amide groups of the thread is virtually identical to the fumaric thread but, because of the absence of a double bond and its associated rigidity, the geometry is probably very different. More internal degrees of freedom are introduced and the thread is now able to fold and form intramolecular H-bonds. The substitution of sp^2 centres by more sterically demanding sp^3 carbons between the two H-bond accepting groups on the thread and the loss of the π - π stacking capability between the thread and aromatic rings of the macrocycle probably also contributes to the lower yields. In the C6, as the distance between the two amides increase, so does the internal degrees of freedom as a direct consequence.

Further lengthening the distance between the H-bond accepting carbonyls by methylene insertion^{10,11,12} were carried out up to C16.

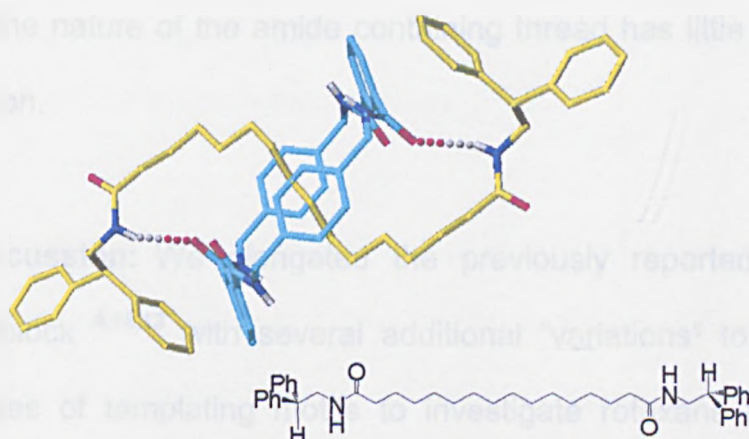


Figure 2.3 Solid state structure of the C16 rotaxane **53** as determined by X-ray crystallography. For clarity, carbon atoms of the macrocyclic ring are shown in light blue and the carbon atoms of the C16 thread in yellow; oxygen atoms are depicted red, nitrogen atoms dark blue and hydrogen atoms white. Non H-bonding hydrogens have been removed.

The crystal structure of the C16 rotaxane **53** (Figure 2.3) containing 14 methylene groups between the templating amide carbonyls revealed that the amide NHs of the macrocycle can still form hydrogen-bonds with the two carbonyls at either end of the thread as the internal atoms between the templating groups bend in order to accommodate these interactions (Figure 2.3).

These results inspired us to investigate the preparation of a series of alkene-based building blocks to determine the tolerance of the macrocycle precursor (host) to further variations of the templating group (guest) and how the presence of rigid conjugated double bonds in the centre of the axle can affect the yield of rotaxane formation. With alkene containing threads the templating group cannot adapt itself so easily to meet the H-bond requirements of the macrocycle amides due to the increased rigidity.

The synthesis of rotaxanes containing two double bonds in the axle based on muconic acid has been published by Vögtle ⁹ but in a low yielding threading strategy where the nature of the amide containing thread has little effect on rotaxane formation.

Results and discussion: We elongated the previously reported fumaric amide building block ^{4,12,13} with several additional “variations” to produce three new classes of templating motifs to investigate rotaxane formation (Figure 2.4).

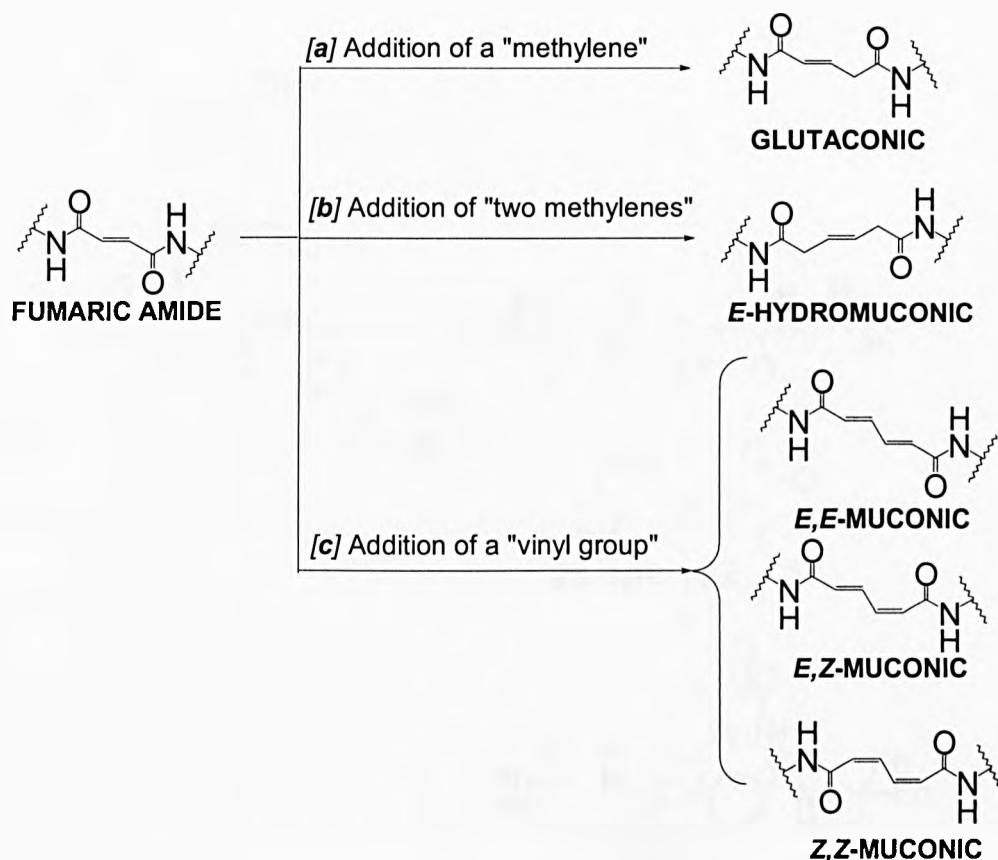
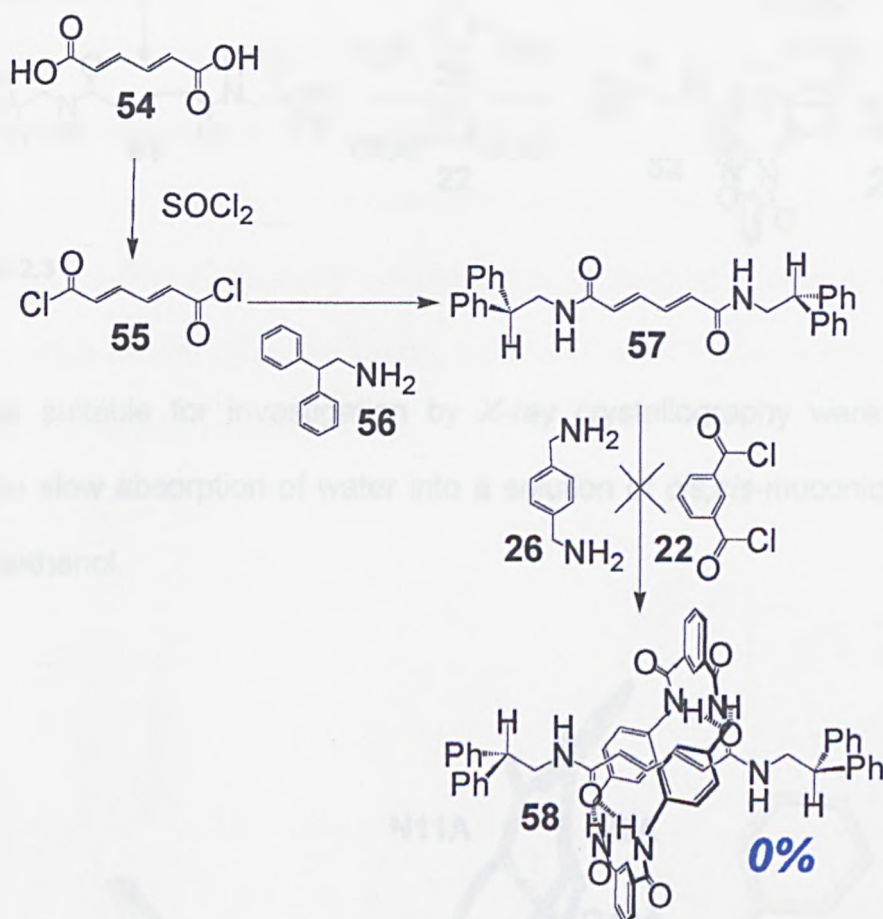


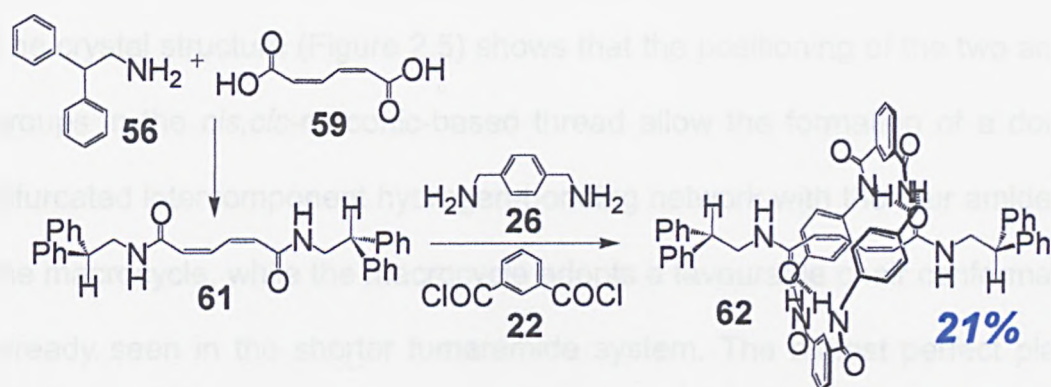
Figure 2.4 Schematic representations of three new classes of thread templates. *E,E*, *E,Z* and *Z,Z* muconic based systems will be reported in this chapter. *E*-hydromuconic and glutaconic will be considered in the next chapter (Chapter Three).

Starting from commercially available *E,E*-muconic acid **54** the *E,E*-muconic thread **57** was obtained in high yield (90%) by condensation of acid chloride **55** with the bulky amine stopper **56**. On addition of *p*-xylene diamine **26** and isophthaloyl dichloride **22**, no rotaxane was obtained following our well-established rotaxane forming strategy because of the poor solubility of thread **57** in non-polar solvents such as CHCl_3 and even mixtures of acetonitrile/ CHCl_3 (Scheme 2.2).



Scheme 2.2

In order to increase the solubility of secondary amide containing threads like **59** in non-polar solvents other preparative strategies were explored. From commercially available Z,Z-muconic acid (**54**), thread **61** was prepared in one step by condensation with 2,2-diphenylethyl amine (**56**). This thread was highly soluble in non-polar solvents and the subsequent rotaxane forming reaction gave the desired rotaxanes **62** in 21% yield (23% crude yield by ^1H -NMR) (Scheme 2.3).



Scheme 2.3

Crystals suitable for investigation by X-ray crystallography were obtained from the slow absorption of water into a solution of *cis,cis*-muconic rotaxane **62** in methanol.

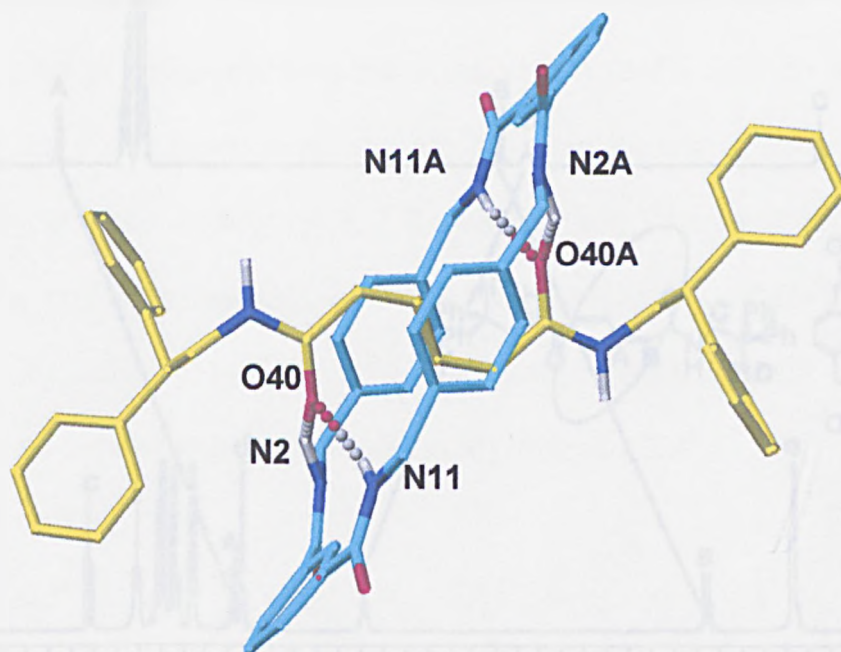


Figure 2.5 Solid state structure of the *cis,cis*-muconic rotaxanes **62** as determined by X-ray crystallography. For clarity carbon atoms of the macrocyclic ring are shown in light blue and the carbon atoms of the muconic thread in yellow; oxygen atoms are depicted red, nitrogen atoms dark blue and hydrogen atoms white. Selected interatomic distances [Å]: N2-O40 3.369, N2A-O40A 3.369, N11-O40 3.093, N11A-O40 3.093.

The crystal structure (Figure 2.5) shows that the positioning of the two amide groups in the *cis,cis*-muconic-based thread allow the formation of a double bifurcated intercomponent hydrogen-bonding network with the four amides of the macrocycle, while the macrocycle adopts a favourable chair conformation already seen in the shorter fumaramide system. The almost perfect planar alignment of the conjugated double bond system of the thread with the xylene rings of the tetramide macrocycle with a 3.73 Å separation, indicate π -stacking between these groups.

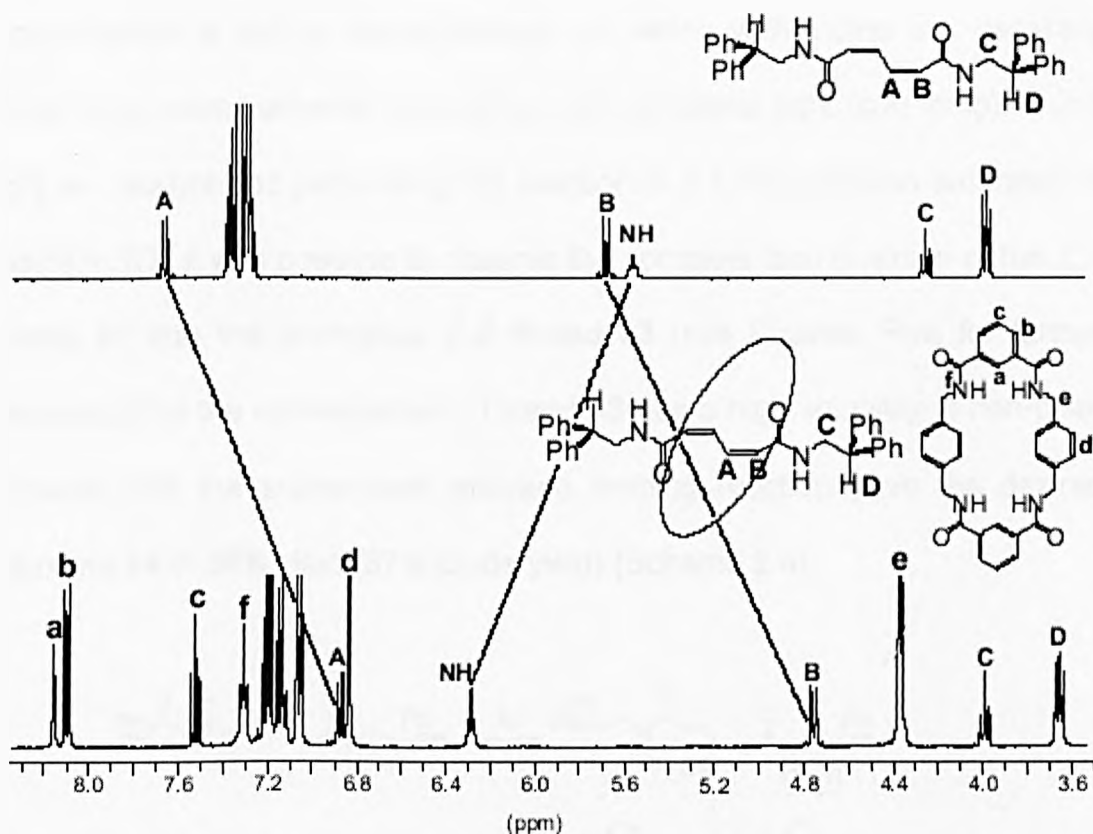
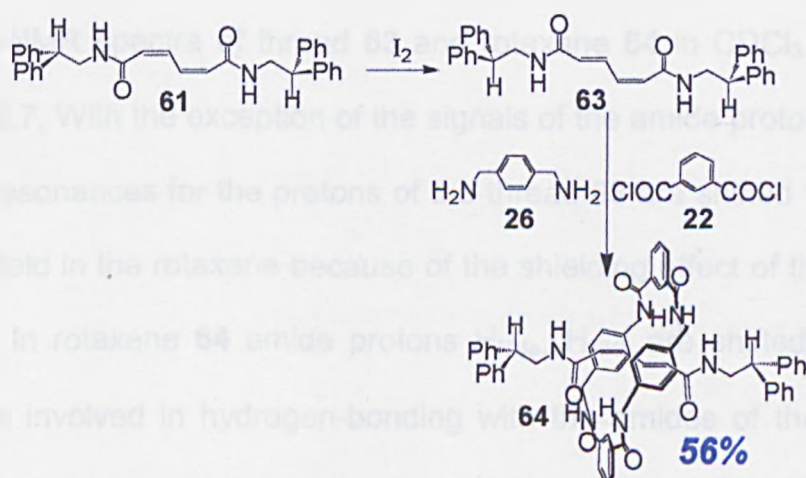


Figure 2.6 ^1H -NMR spectra (400 MHz, CDCl_3) of muconic thread **61** and muconic rotaxane **62**.

Comparison of the ^1H -NMR spectra (Figure 2.6) indicate that the macrocycle is located over the olefins due to the large chemical shift for protons H_A and

H_B in comparison with the protons of the stoppers (H_C and H_D). This is an indication of the shielding effect of the macrocycle sheath on the protons located in the core of the thread. In addition, the large shift for the H_{NH} protons on the rotaxane axle (6.28 ppm, **62**) compared to the free thread (5.54 ppm **61**) suggest hydrogen-bonding between the amides of the macrocycle and the amides of the templating group as seen in the solid state structure (Figure 2.5).

The interconversion of olefinic geometrical isomers is well known.^{14,15} The most common reagent used to promote the internal geometrical isomerisation is iodine. Isomerisations of olefins with iodine are generally done in non-polar solvents sometimes with additional light (sun lamp). Using light as catalyst and performing the reaction in a CHCl₃ solution saturated in iodine at RT, it was possible to observe the complete isomerisation of the *Z,Z* thread **61** into the analogous *E,Z* thread **63** (see Chapter Five for further discussion on the isomerisation). Thread **63** has a high solubility in non-polar solvents and the subsequent rotaxane forming reaction gave the desired rotaxane **64** in 56% yield (57% crude yield) (Scheme 2.4).



Scheme 2.4

The much improved yield over the *cis,cis*-muconic analogue would imply a better fit between templating thread and macrocycle precursor. Unfortunately, it was not possible to obtain crystals of good enough quality to undertake X-ray crystal structure investigations.

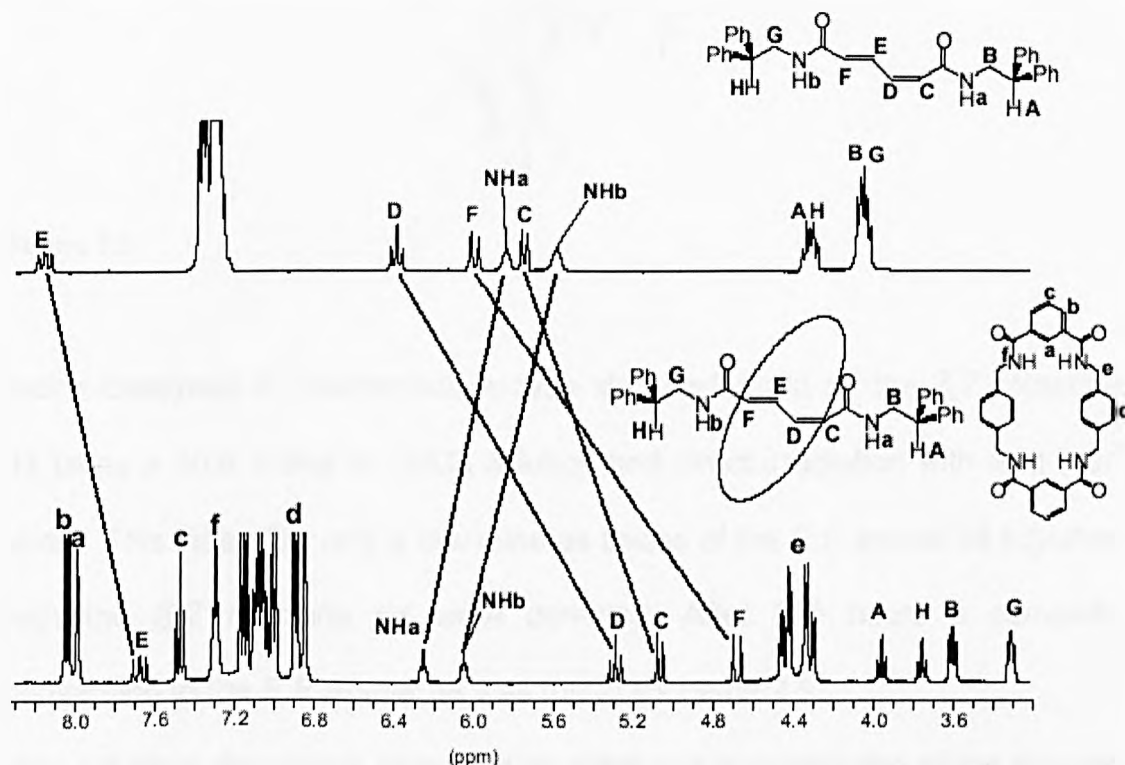


Figure 2.7 ^1H -NMR spectra (400 MHz, CDCl_3) of muconic thread **63** and muconic rotaxane **64**.

The ^1H -NMR spectra of thread **63** and rotaxane **64** in CDCl_3 are shown in Figure 2.7. With the exception of the signals of the amide protons H_{NH_a} , H_{NH_b} , all the resonances for the protons of the thread **63** are shifted to significantly higher field in the rotaxane because of the shielding effect of the macrocycle sheath. In rotaxane **64** amide protons H_{NH_a} , H_{NH_b} are shifted downfield as they are involved in hydrogen-bonding with the amides of the macrocycle. The two protons on the benzyl position of the macrocycle ($e+e'$) are split into

an ABX system as the thread is unsymmetrical (Figure 2.8) rather than the doublet seen for the symmetrical *cis,cis* rotaxane **62**.

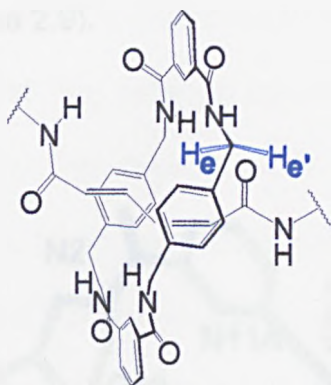
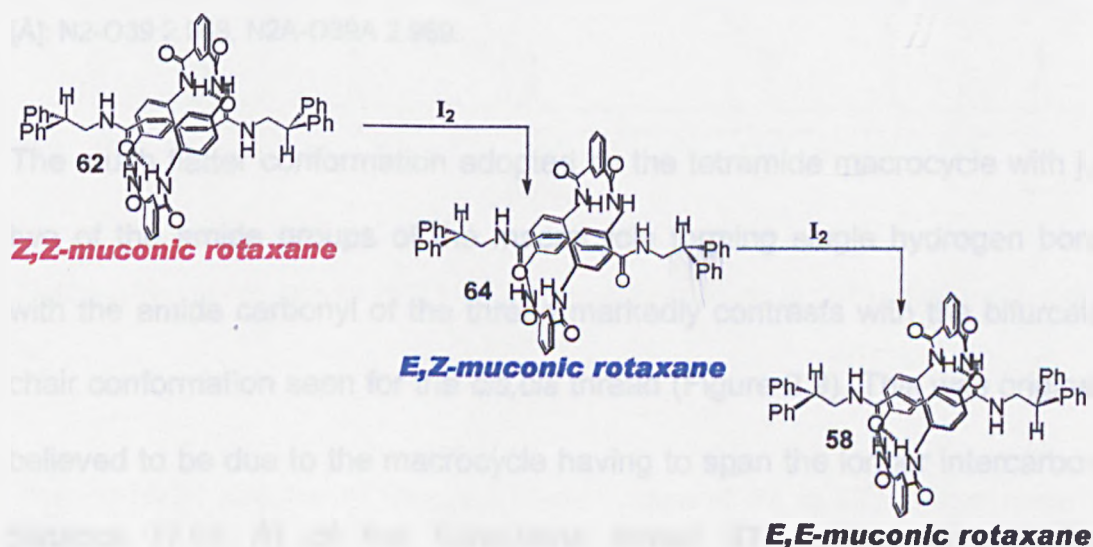


Figure 2.8

Iodine-catalysed *E,Z*-isomerisation was also performed on the *Z,Z* rotaxane **62** using a 40% iodine in CHCl_3 solution and direct irradiation with light (sun lamp). This time after only a few minutes traces of the *E,E* isomer **58** together with the *E,Z* rotaxane **64** were detected. After five hours a complete conversion to the *E,E* isomer **58** was found (Scheme 2.5).

(For a further discussion of the iodine catalysed isomerisation of the threads and rotaxanes, see Chapter Five).



Scheme 2.5

Crystals suitable for investigation by X-ray crystallography were obtained from the slow saturation with water of a solution of the *trans,trans*-muconic rotaxane **58** in DMF (Figure 2.9).

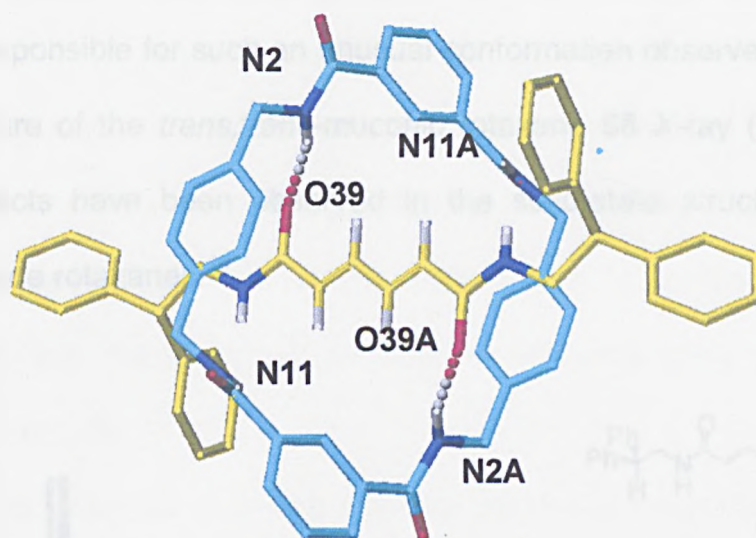


Figure 2.9 Solid state structure of the *trans,trans*-muconic rotaxanes **58**. For clarity carbon atoms of the macrocyclic ring are shown in light blue and the carbon atoms of the muconic thread in yellow; oxygen atoms are depicted red, nitrogen atoms dark blue and hydrogen atoms white. Non H-bonding hydrogens have been removed. Selected interatomic distances [Å]: N2-O39 2.969, N2A-O39A 2.969.

The much flatter conformation adopted by the tetramide macrocycle with just two of the amide groups of the macrocycle forming single hydrogen bonds with the amide carbonyl of the thread markedly contrasts with the bifurcated chair conformation seen for the *cis,cis* thread (Figure 2.9). This was originally believed to be due to the macrocycle having to span the longer intercarbonyl distance (7.04 Å) of the *trans,trans* thread **57**. Further investigations

however, revealed in the next chapter (Figure 3.3), show that the macrocycle is able to adopt the typical bifurcated chair structure over a similarly long intercarbonyl distance of 6.63 Å (hydromuconic-based system) in the solid state despite the longer distance between the carbonyls.

Crystallisation from the strong hydrogen-bond disrupting solvent (DMF), could be responsible for such an unusual conformation observed in the solid state structure of the *trans,trans*-muconic rotaxane **58** X-ray (Figure 2.10). Solvent effects have been observed in the solid-state structure of other benzylic amide rotaxanes.¹⁶

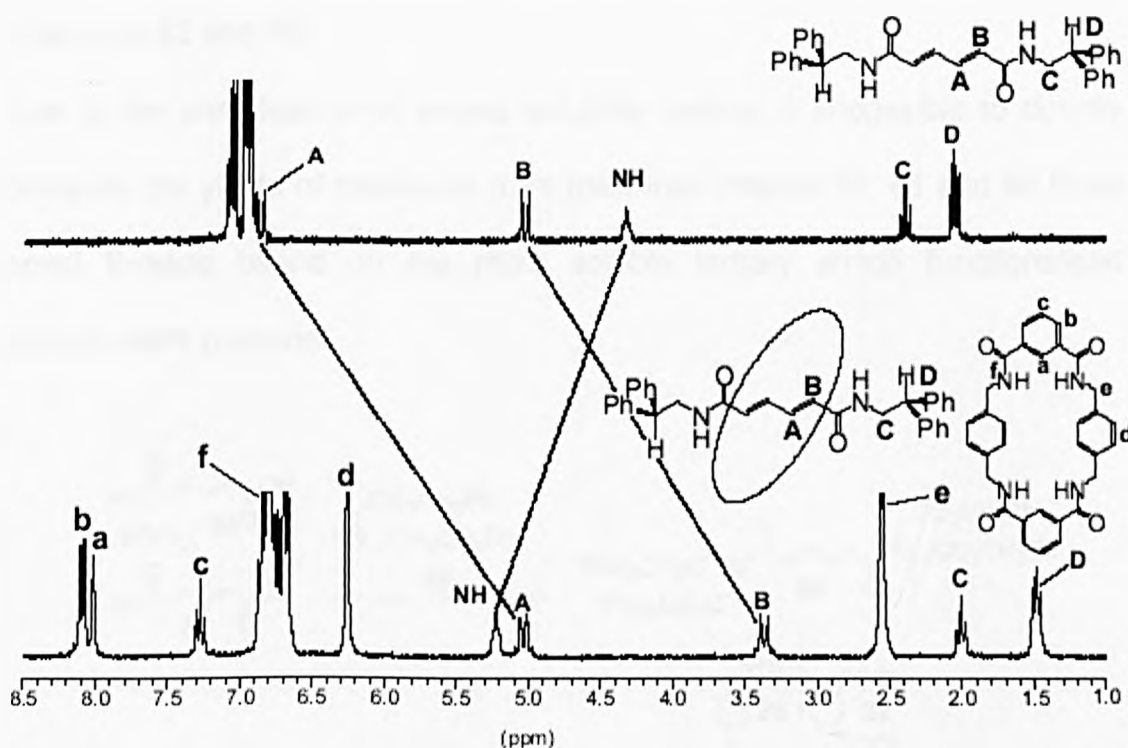


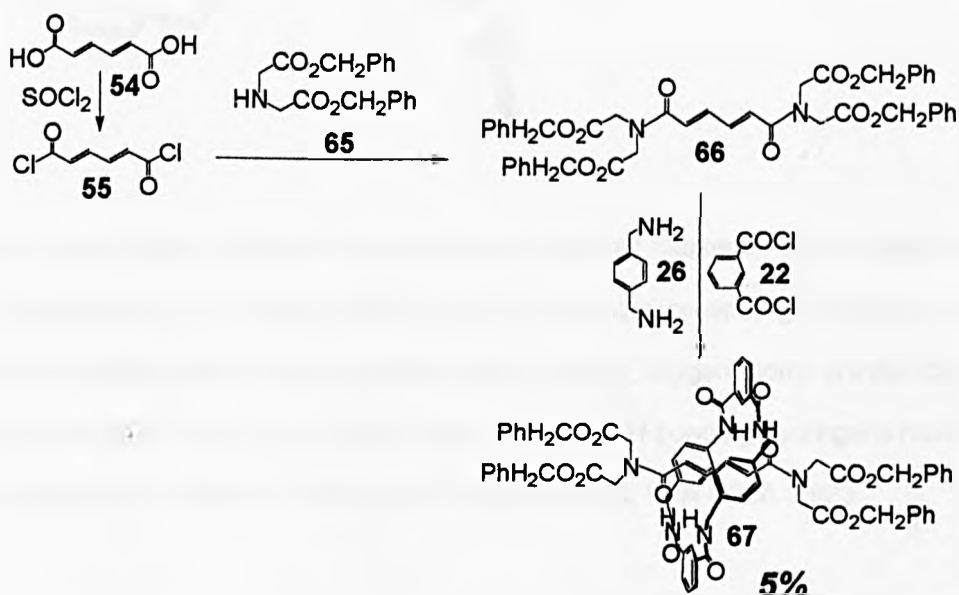
Figure 2.10 ¹H-NMR spectra (400 MHz, CDCl₃) of muconic thread **57** and muconic rotaxane **58**.

The ¹H-NMR spectra of thread **57** and rotaxane **58** in CDCl₃ are shown in Figure 2.10. As in the two previous cases all the resonances for the protons

of the olefinic region are shifted to significantly higher field in the rotaxane because of the shielding effect of the macrocycle with the hydrogen bonding locating the macrocycle over the olefins. Similarly, there is a downfield shift in the rotaxane spectrum for H_{NH} protons due to hydrogen-bonding to the carbonyl of the macrocycle amides.

Comparison of the spectra of threads **57**, **61**, **63** and rotaxanes **58**, **62**, **64** respectively, predominantly show shielding of the central vinyl region of the thread with a much less pronounced effect on the stoppers. The macrocycle spends most of its time around the olefin region in solution, hydrogen-bonding with the thread amides as seen in the solid state structures of rotaxanes **62** and **58**.

Due to the complication of thread solubility making it impossible to directly compare the yields of rotaxanes from the three threads **57**, **61** and **63** three novel threads based on the more soluble tertiary amide functionalised threads were prepared.



Scheme 2.6

The *E,E*-muconic tertiary amide based thread, **66**,^{4,13} was easily prepared and was very soluble in CHCl_3 (Scheme 2.6).

The slow addition of *p*-xylene diamine and isophthaloyl dichloride under high dilution conditions to thread **66** gave the rotaxane **67** in 5% yield after chromatography. The crude yield from $^1\text{H-NMR}$ for rotaxane **67** was actually about 9%.

Crystals of rotaxane **67** suitable for investigation by X-ray crystallography were obtained by slow evaporation of diethyl ether into a solution of rotaxane **67** in DMF (Figure 2.11).

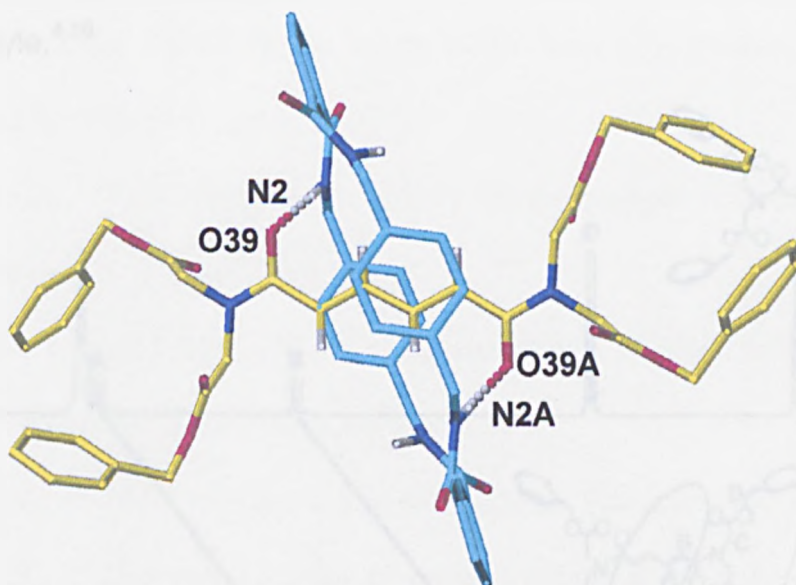


Figure 2.11 Solid state structure of the *trans,trans*-muconic rotaxanes **67** as determined by X-ray crystallography. For clarity carbon atoms of the macrocyclic ring are shown in light blue and the carbon atoms of the muconic thread in yellow; oxygen atoms are depicted red, nitrogen atoms dark blue and hydrogen atoms white. Non H-bonding hydrogens have been removed. Selected interatomic distances [Å]: N2-O39 2.923, N2A-O39A 2.923.

The macrocycle appear almost flat (as for the *trans,trans*-muconic rotaxane **58**) with the two xylene rings aligned parallel with the olefin motif, one ring π -

π stacking with one alkene and one with the other. The twist in the macrocycle is also carried through into the hydrogen-bonding pattern. Only one of the amides of the isophthalic unit of the macrocycle are hydrogen bonded to the thread, the other is hydrogen-bonding with a carbonyl of a neighbouring rotaxane in the crystal. As the thread is relatively rigid with its conjugated π system, it is the macrocycle that has to stretch in order to hydrogen-bond to the amide component of the thread assuming an almost planar conformation. This is the opposite from that observed in the solid state structure of the rotaxane with a saturated C6 thread (Figure 2.11). Here it is the thread that bends to accommodate the chair conformation of the macrocycle.^{4,10}

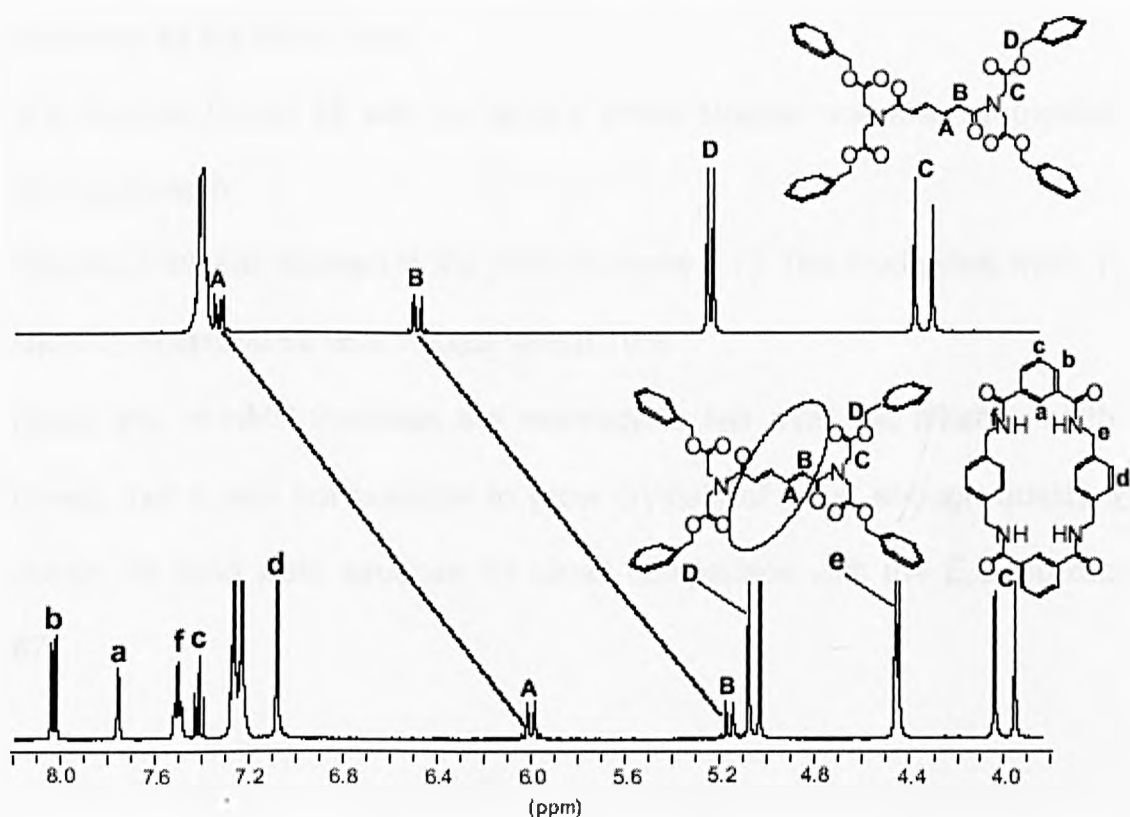


Figure 2.12 ¹H-NMR spectra (400 MHz, CDCl₃) of muconic thread **66** and muconic rotaxane **67**.

The tertiary amide based system has a complex ^1H -NMR spectra because of the slow rotation of the tertiary amides on the ^1H -NMR time scale.

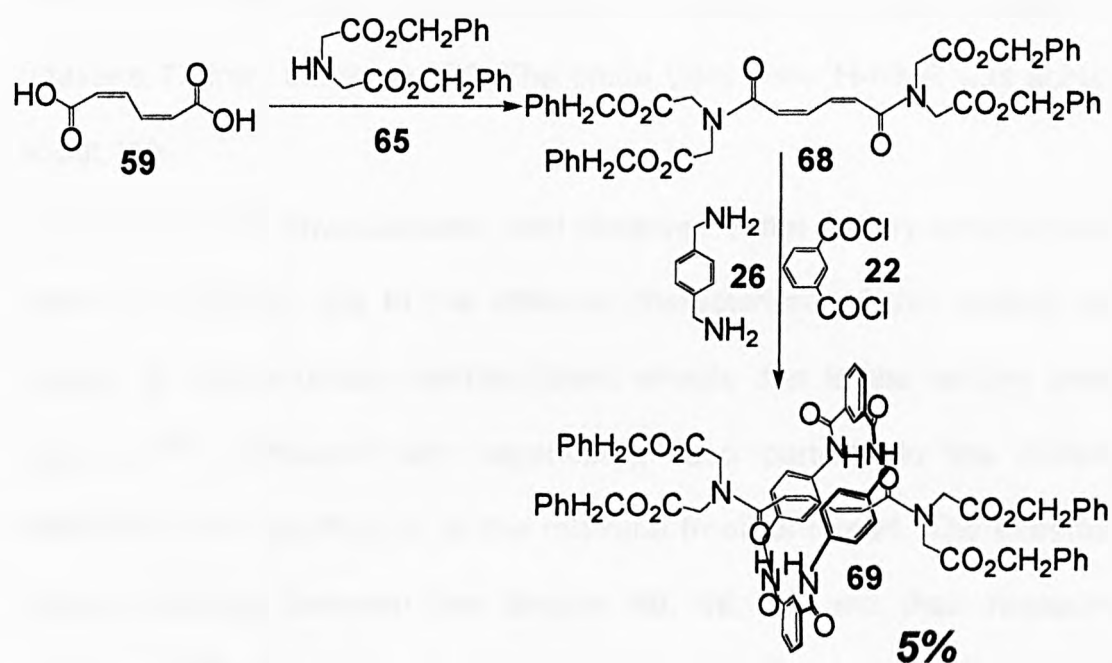
Comparison of thread **66** and rotaxane **67** show shielding of all the signals of the thread (Figure 2.12). The hydrogen bonding locating the macrocycle over the olefins as indicated by the large chemical shift for protons H_A and H_B in comparison with the stoppers (H_C and H_D).

Lower yields have been observed in rotaxane formation with tertiary amide threads in comparison with secondary amide based threads. Using tertiary amide-based groups (slightly stronger hydrogen bond acceptors than secondary amides) in the thread is over compensated by the presence of larger stoppers producing a much more sterically hindered system and accounts for the lower yield.

Z,Z-Muconic thread **68** with the tertiary amide stopper was also synthesised for comparison.

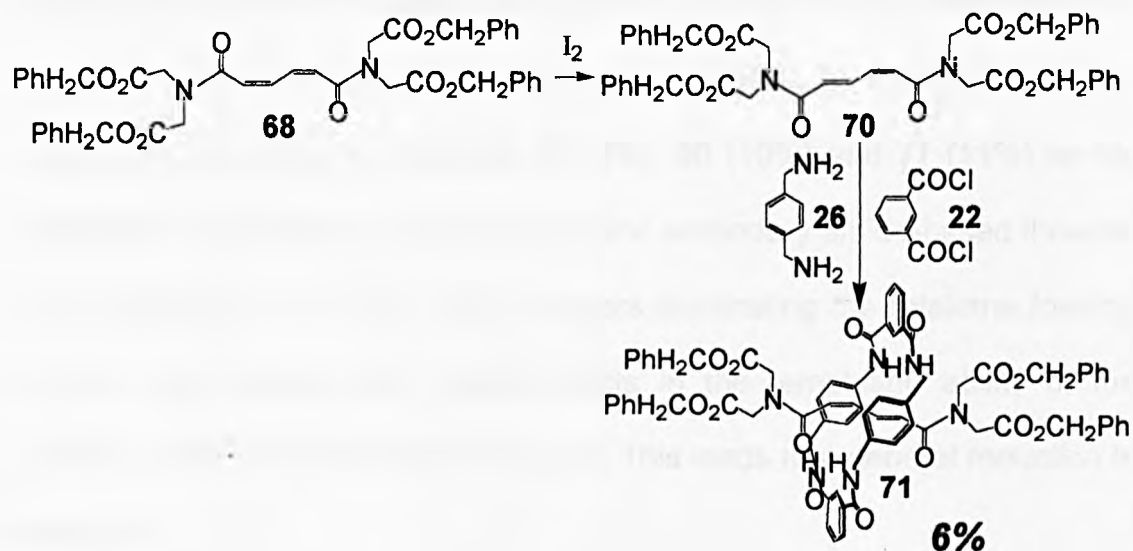
Rotaxane **69** was isolated in 5% yield (Scheme 2.7). The crude yield from ^1H -NMR for rotaxane **69** was actually about 10%.

Again the ^1H -NMR indicates the macrocycle lies over the alkenes of the thread, but it was not possible to grow crystals of good enough quality to obtain the solid state structure for direct comparison with the *E,E*-rotaxane **67**.



Scheme 2.7

By illuminating (sun lamp) a CHCl_3 solution of thread **68** saturated in iodine at RT, it was possible to observe the complete isomerisation of the *Z,Z* isomer **68** into the analogous *E,Z* isomer **70** after a few hours (Scheme 2.8).



Scheme 2.8

Rotaxane formation on thread **70** gave the rotaxane **71** in 6% isolated yield. The low yield was due to the preparative difficulties in order to purify the rotaxane **71** from the thread **70**. The crude yield from $^1\text{H-NMR}$ was actually about 11%.

The considerable lower isolated yield observed in the tertiary amides-based system is partially due to the different characteristic of this system with respect to the secondary amides (steric effects due to the tertiary amide stoppers ^{4,13} compared with secondary),⁴ and partially to the extreme difficulties in the purification of the rotaxane from its thread. The extremely similar R_f -values between the threads **66**, **68**, **70** and their respective rotaxanes **67**, **69**, **71** required several chromatographic columns and preparative TLC in order to obtain the desired rotaxanes pure.

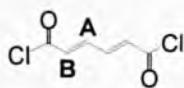
As already seen in the fumaramide based-system,⁴ the introduction of the bis-tertiary stoppers is associated with a considerable lower capability in promoting rotaxane formation of the templating motif (using a fumaric template gives 97% rotaxane formation for bis-secondary amide stoppers and 67% for bis-tertiary amide stoppers). In addition, by comparison of the crude yield for muconic rotaxanes **67** (9%), **69** (10%) and **71** (11%) no big differences are reported in contrast with the secondary amide-based threads. This is probably due to the bulky stoppers dominating the rotaxane forming process and masking any subtle effects in the templating ability of the different isomers of the muconic threads. This leads to a general reduction in the yields.

The new rotaxane structures **58**, **62**, **64**, **67**, **69** and **71** were confirmed by ^1H and ^{13}C spectroscopy, mass spectra, elemental analysis and X-ray crystal structure determination (for **58**, **62** and **67**).

Conclusions: Several new amide-based [2]rotaxanes containing two conjugated double bonds were prepared. By manipulation of the stereochemistry of the axle of the rotaxanes, it was possible to generate rotaxane isomers impossible to synthesise under the clipping protocol. Although it was not possible to compare directly the yield of rotaxane for all the three different isomeric threads with the two types of stoppers because of solubility and purification problems, it appears clear that a huge difference in the templating properties of the *cis,trans* thread **63** with respect to the *cis,cis* analogue **61** occurs (the comparison with the *trans,trans* secondary amide-based system was not possible because of the impossibility of obtaining the rotaxane via direct formation due to the insolubility of the thread **57** in non-polar solvents). By direct comparison of the secondary amide-based system with the tertiary amide-based one, the presence of a bulky stopper has a critical effect on the yields in the rotaxane formation process overshadowing the templating ability of the different muconic acid isomers.

Experimental Part:

***trans,trans*-Muconic acid dichloride (**55**)¹⁷**

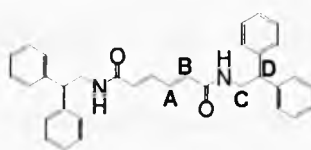


trans,trans-Muconic acid **54** (5.0 g, 35.2 mmol) was dissolved in thionyl chloride (25 mL) in a 100 mL one necked flask equipped with a condenser and heated to 80°C for 24h. Then the thionyl chloride was removed and the muconic chloride was triturated in a mixture of petroleum spirit (60-80°C) (95%) and diethyl ether (5%) in order to afford the muconic chloride **55** as a pale yellow powder (6.1 g, 34.1 mmol, 97%).

Literature reported m.p. 98-99°C.¹⁷

m.p. 98-99°C; ¹H NMR (400 MHz, CDCl₃): δ= 7.48 (dd, 2H, *J*= 14.3 + 3.0 Hz, **A**), 6.56 (dd, 2H, *J*= 14.3 + 3.0 Hz, **B**).

***trans,trans*-Muconic thread (**57**)**

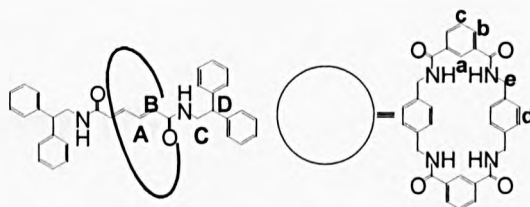


2,2-Diphenylethyl amine **56** (1.6 g, 8.1 mmol) and triethylamine (1.2 mL) were dissolved in chloroform (75 mL) in a 250 mL one necked flask under nitrogen. *trans,trans*-Muconic chloride **55** (700.0 mg, 3.9 mmol) was also dissolved in chloroform (50 mL) and added dropwise at RT over 1h. The solution was stirred at RT over a 5h period. The precipitate was filtered off to

give the product **57**, which was crystallised from ethanol (1.8 g, 3.5 mmol, 90%).

m.p. 220-221°C; ^1H NMR (400 MHz, $\text{DMSO-}d_6$): δ = 8.26 (t, 2H, J = 5.9 Hz, NH), 7.31 (m, 16H, ArH), 7.20 (m, 4H, ArH), 7.03 (dd, 2H, J = 14.3 + 3.0 Hz, **A**), 6.25 (dd, 2H, J = 14.3 Hz + 3.0 Hz, **B**), 4.25 (t, 2H, J = 7.9 Hz, **D**), 3.81 (dd, 4H, J = 7.9 + 5.9 Hz, **C**); ^{13}C NMR (100 MHz, $\text{DMSO-}d_6$): δ = 164.86 (CO), 143.20 (q, ArC), 136.69 (CH), 130.87 (CH), 128.79 (ArCH), 128.20 (ArCH), 126.70 (ArCH), 50.42 (CH), 43.65 (CH_2). FAB MS (*m*BNA matrix) m/z 502 $[\text{M}+\text{H}]^+$. Anal. Calcd. for $\text{C}_{34}\text{H}_{32}\text{N}_2\text{O}_2$ (500.63): C, 81.57; H, 6.44; N, 5.60. Found: C, 81.87; H, 6.51; N, 5.96.

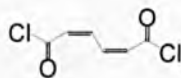
***trans,trans*-Muconic rotaxane (**58**)**



trans,trans-Muconic thread **57** (500.0 mg, 1.0 mmol) and triethylamine (3.5 mL) were dissolved in a hot mixture (250 mL) of chloroform (85%) and acetonitrile (15%) and stirred vigorously whilst solutions of the *p*-xylylene diamine **26** (1.6 g, 12.0 mmol) in chloroform (40 mL) and of the isophthaloyl dichloride **22** (2.4 g, 12.0 mmol) in chloroform (40 mL) were simultaneously added over a period of 2h using motor-driven syringe pumps. The resulting suspension was filtered and concentrated under reduced pressure to afford the crude product. From a preliminary analysis of the crude of both filtrate

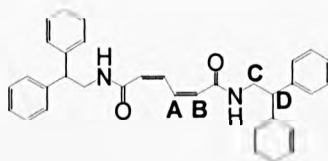
and precipitate was possible to observe that no rotaxane formation had occurred due to the insolubility of the *trans,trans*-muconic thread **57**.

***cis,cis*-Muconic acid dichloride (**60**)**



cis,cis-Muconic acid **59** (5.0 g, 35.2 mmol) was dissolved in thionyl chloride (25 mL) in a 100-mL one necked flask equipped with a condenser and heated to 80°C for 24h. Then the thionyl chloride was removed and the muconic chloride tritiated in a mixture of petroleum spirit (60-80°C) (95%) and diethyl ether (5%). 6.0 g of *trans,trans*-muconic chloride and no *cis,cis*-muconic chloride **60** were recovered.

***cis,cis*-Muconic thread (**61**)**

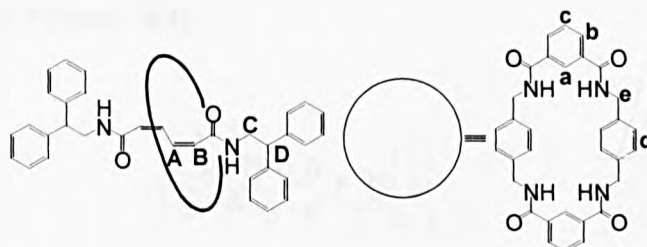


2,2-Diphenylethyl amine **56** (1.5 g, 7.7 mmol), triethylamine (2.0 mL) and *cis,cis*-muconic acid **59** (500.0 mg, 3.5 mmol) were dissolved in THF (125 mL) in a 250 mL one necked flask under nitrogen. The solution was then chilled with ice to 0°C. EDCI (1.5 g, 7.7 mmol) was added slowly over 1h. The solution was stirred at RT overnight. The solvent was then removed and the solution dissolved in CHCl₃ (200 mL) and washed with aqueous NaOH solution (2×150 mL), then with water (3×150 mL) and dried with MgSO₄. A

white solid was obtained after the solvent was eliminated by rotary evaporation. The solid was triturated with diethyl ether to give a white powder (1.5 g) composed of a mixture of *cis,cis* thread **61** (93%) and *cis,trans* thread **63** (7%). After purification by silica gel chromatography (CHCl_3) the *cis,cis* thread **61** was recovered as a white powder (1.4 g, 2.8 mmol, 80%).

m.p. 220-221°C; ^1H NMR (400 MHz, CDCl_3): δ = 7.64 (dd, 2H, J = 10.3 + 2.3 Hz, **A**), 7.40 - 7.20 (m, 20H, ArH), 5.66 (dd, 2H, J = 10.3 + 2.3 Hz, **B**), 5.54 (t, 2H, J = 5.9 Hz, NH), 4.24 (t, 2H, J = 7.9 Hz, **D**), 3.98 (dd, 4H, J = 7.9 + 5.9 Hz, **C**); ^{13}C NMR (100 MHz, CDCl_3): δ = 166.86 (CO), 142.07 (q, ArC), 135.59 (CH), 129.19 (ArCH), 128.43 (ArCH), 127.32 (ArCH), 126.08 (CH), 50.93 (CH), 44.16 (CH_2). FAB MS (*m*BNA matrix) m/z 501 M^+ . Anal. Calcd. for $\text{C}_{34}\text{H}_{32}\text{N}_2\text{O}_2$ (500.63): C, 81.57; H, 6.44; N, 5.60. Found: C, 81.42; H, 6.26; N 5.55.

2,2-Diphenylethylamine *cis,cis*-muconic rotaxane (**62**)

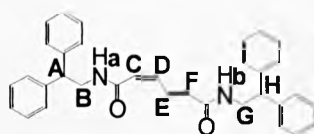


cis,cis-Muconic thread **61** (400.0 mg, 0.8 mmol) was dissolved in chloroform (50 mL) and stirred vigorously whilst solutions of *p*-xylylene diamine **26** (1.3 g, 9.6 mmol) and triethylamine (1.4 mL) in chloroform (40 mL) and of isophthaloyl dichloride **22** (2.0 g, 9.6 mmol) in chloroform (40 mL) were simultaneously added over a period of 4h using motor-driven syringe pumps. The resulting suspension was then filtered and concentrated under reduced

pressure to afford the crude product. After purification by silica gel chromatography (CHCl_3) the rotaxane **62** was isolated as a white powder (173.5 mg, 0.17 mmol, 21%).

m.p. 327-328°C; ^1H NMR (400 MHz, CDCl_3): δ = 8.14 (s, 2H, **a**), 8.08 (dd, 4H, J = 7.8 + 1.4 Hz, **b**), 7.51 (t, 2H, J = 7.8 Hz, **c**), 7.30 (t, 4H, J = 5.0 Hz, NH_{macro}), 7.25 - 7.00 (m, 20H, ArH), 6.86 (dd, 2H, J = 10.3 + 2.3 Hz, **A**), 6.82 (s, 8H, **d**), 6.28 (t, 2H, J = 5.9 Hz, $\text{NH}_{\text{thread}}$), 4.74 (dd, 2H, J = 10.3 + 2.3 Hz, **B**), 4.36 (d, 8H, J = 5.0 Hz, **e**), 3.99 (t, 2H, J = 7.9 Hz, **D**), 3.65 (dd, 4H, J = 7.9 + 5.9 Hz, **C**); ^{13}C NMR (100 MHz, CDCl_3): δ = 166.43 (CO), 166.20 (CO), 141.33 (q, ArC), 137.32 (ArC), 134.43 (CH), 134.03 (q, ArC), 131.49 (ArCH), 131.17 (ArCH), 129.45 (ArCH), 128.87 (ArCH), 128.83 (ArCH), 127.14 (ArCH), 124.17 (ArCH), 123.82 (CH), 50.41 (CH), 44.12 (CH_2), 44.02 (CH_2). FAB MS (*m*BNA matrix) m/z 1034 $[\text{M}+\text{H}]^+$. Anal. Calcd. for $\text{C}_{66}\text{H}_{60}\text{N}_6\text{O}_6$ (1033.22): C, 76.72; H, 5.85; N, 8.13. Found: C, 76.68; H, 5.82; N, 8.11.

***cis,trans*-Muconic thread (63)**

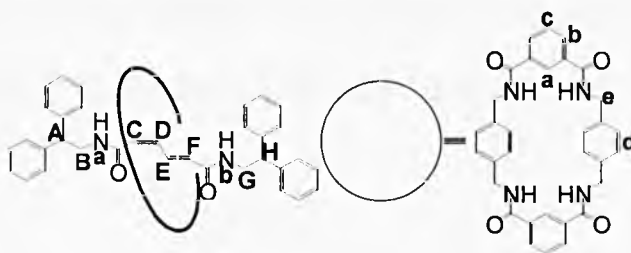


cis,cis-Muconic thread **61** (750.0 mg, 1.5 mmol) was dissolved in CDCl_3 (10 mL) together with iodine (190 mg, 0.75 mmol) in a 50 mL one necked flask under nitrogen. The reaction was stirred at RT and in presence of light (sun lamp) for 24h until the total conversion of the *cis,cis*-muconic thread **61** into the *cis,trans*-muconic thread **63** was observed (^1H -NMR). The solution was then diluted to 200 mL with chloroform and washed with a 10% solution of

sodium bisulphite (2×75 mL) then water (2×125 mL) and dried with MgSO₄ to afford the *cis,trans*-muconic thread **63** as a white powder (735.0 mg, 1.5 mmol, 98%).

m.p. 220-221°C; ¹H NMR (400 MHz, CDCl₃): δ= 8.14 (m, 1H, **E**), 7.40 - 7.20 (m, 20H, ArH), 6.36 (m, 1H, **D**), 5.96 (d, *J*= 15.6 Hz, 1H, **F**), 5.80 (t, *J*= 5.9 Hz, 1H, NH_b), 5.72 (d, *J*= 11.2 Hz, 1H, **C**), 5.55 (t, *J*= 5.9 Hz, 1H, NH_a), 4.30 (t, *J*= 7.9 Hz, 1H, **H**),), 4.25 (t, *J*= 7.9 Hz, 1H, **A**), 4.05 (dd, 2H, *J*= 7.9 + 5.9 Hz, **G**), 4.00 (dd, 2H, *J*= 7.9 + 5.9 Hz, **B**); ¹³C NMR (100 MHz, CDCl₃): δ= 165.57 (CO), 165.51 (CO), 142.20 (q, ArC), 138.20 (q, ArC), 137.76 (CH), 135.13 (CH), 131.07 (CH), 129.68 (ArCH), 129.41 (CH), 129.13 (ArCH), 128.45 (ArCH), 128.17 (ArCH), 126.85 (ArCH), 126.12 (ArCH), 50.98 (CH), 50.75 (CH), 44.60 (CH₂), 44.32 (CH₂). FAB MS (*m*BNA matrix) *m/z* 500 M⁺. Anal. Calcd. for C₃₄H₃₂N₂O₂ (500.63): C, 81.57; H, 6.44; N, 5.60. Found: C, 81.47; H, 6.29; N 5.51.

2,2-Diphenylethylamine *cis,trans*-muconic rotaxane (**64**)

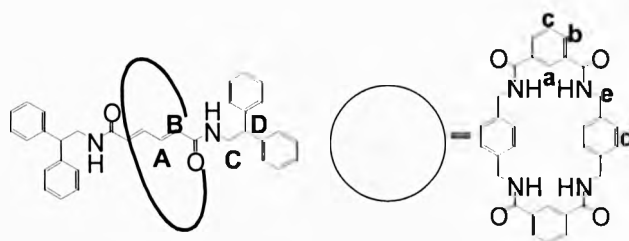


cis,trans-Muconic thread **63** (400 mg, 0.8 mmol) was dissolved in chloroform (50 mL), and stirred vigorously whilst solutions of the *p*-xylylene diamine **26** (1.3 g, 9.6 mmol) and triethylamine (1.4 mL) in chloroform (40 mL) and isophthaloyl dichloride **22** (2.0 g, 9.6 mmol) in chloroform (40 mL) were simultaneously added over a period of 4h using motor-driven syringe pumps.

The resulting suspension was then filtered and concentrated under reduced pressure to afford the crude product. After purification by silica gel chromatography (CHCl_3) the rotaxane **64** was recovered as a white powder (462.9 mg, 0.4 mmol, 56%).

m.p. 327-328°C; ^1H NMR (400 MHz, CDCl_3): δ = 8.06 (dd, 4H, J = 7.8 + 1.4 Hz, **b**), 8.01 (s, 2H, **a**), 7.69 (m, 1H, **E**), 7.49 (t, 2H, J = 7.8 Hz, **c**), 7.31 (t, 4H, J = 5.0 Hz, NH_{macro}), 7.20 - 6.90 (m, 20H, ArH), 6.87 (s, 8H, **d**), 6.26 (t, 1H, J = 5.9 Hz, NH_b), 6.06 (t, 1H, J = 5.9 Hz, NH_a), 5.30 (m, 1H, **D**), 5.06 (d, 1H, J = 11.3 Hz, **C**), 4.67 (d, 1H, J = 15.6 Hz, **F**), 4.50 - 4.25 (m, 8H, **e**), 3.95 (t, 1H, J = 7.9 Hz, **A**), 3.75 (t, 1H, J = 7.9 Hz, **H**), 3.59 (dd, 2H, J = 7.9 + 5.9 Hz, **B**), 3.30 (dd, 2H, J = 7.9 + 5.9 Hz, **G**); ^{13}C NMR (100 MHz, CDCl_3): δ = 167.13 (CO), 166.33 (CO), 165.63 (CO), 142.14 (q, ArC), 141.96 (q, ArC), 137.89 (q, ArC), 137.67 (q, ArC), 134.65 (CH), 134.10 (ArCH), 131.54 (ArCH), 130.69 (ArCH), 129.67 (CH), (ArCH), 129.15 (ArCH), 128.99 (ArCH), 128.70 (ArCH), 128.53 (ArCH), 128.33 (CH), 128.31 (ArCH), 125.70 (CH), 125.15 (ArCH), 50.67 (CH), 50.29 (CH), 44.71 (CH_2), 44.55 (CH_2), 44.38 (CH_2). FAB MS (*m*BNA matrix) m/z 1034 $[\text{M}+\text{H}]^+$. Anal. Calcd. for $\text{C}_{66}\text{H}_{60}\text{N}_6\text{O}_6$ (1033.22): C, 76.72; H, 5.85; N, 8.13. Found: C, 76.68; H, 5.82; N, 8.11.

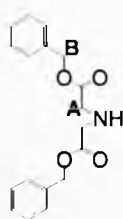
***trans,trans*-Muconic rotaxane (58)**



cis,cis-Muconic rotaxane **62** (100.0 mg, 0.1 mmol) was dissolved in CDCl₃ (5 mL) together with iodine (95 mg, 0.38 mmol) in a 10 mL one necked flask under nitrogen. The reaction was stirred at RT in presence of light (sun lamp) for 3h until the total conversion of the *cis,cis*-muconic rotaxane **62** into the *trans,trans*-muconic rotaxane **58** was observed (¹H-NMR). The solution was then diluted to 25 mL with chloroform and washed with a 10% solution of sodium bisulphite (2×25 mL) then water (2×25 mL) and dried with MgSO₄ to afford the *trans,trans*-muconic rotaxane **58** as a white powder (98.0 mg, 0.1 mmol, 98%).

m.p. 327-328°C; ¹H NMR (400 MHz, DMSO-*d*₆): δ= 8.38 (t, 2H, *J*= 5.9 Hz, NH_{thread}), 8.22 (s, 2H, **a**), 8.03 (dd, 4H, *J*= 7.8 + 1.4 Hz, **b**), 7.63 (t, 4H, *J*= 7.8 Hz, **c**), 7.48 (t, 4H, *J*= 5.0 Hz, NH_{mac}), 7.30 – 7.10 (m, 20H, ArH), 6.88 (s, 8H, **d**), 6.08 (dd, 2H, *J*_{gem}= 14.3 Hz *J*_{vic}= 3.0 Hz, **A**), 5.21 (dd, 2H, *J*_{gem}= 14.3 Hz *J*_{vic}= 3.0 Hz, **B**), 4.32 (d, 8H, *J*= 5.0 Hz, **e**), 4.09 (dd, 2H, *J*= 7.9 + 5.9 Hz, **D**), 3.57 (t, 4H, *J*= 7.9 Hz, **C**); ¹³C NMR (100 MHz, DMSO-*d*₆): δ= 165.00 (CO), 164.31 (CO), 143.20 (q, ArC), 141.86 (q, ArC), 141.01 (q, ArC), 131.48 (CH), 130.45 (ArCH), 129.67 (ArCH), 129.50 (ArCH), 129.47 (ArCH), 129.00 (ArCH), 126.87 (CH), 126.56 (ArCH), 50.38 (CH), 32.78 (CH₂), 30.05 (CH₂). FAB MS (*m*BNA matrix) *m/z* 1034 [M+H]⁺. Anal. Calcd. for C₆₆H₆₀N₆O₆ (1033.22): C, 76.72; H, 5.85; N, 8.13. Found C, 76.74; H, 5.57; N, 8.09.

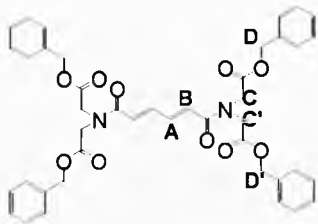
(Phenoxycarbonylmethyl-amino)-acetic acid benzyl ester (65)



Iminodiacetic acid (4.0 g, 30.0 mmol) and *p*-toluenesulphonic acid (6.3 g, 33.0 mmol) were dissolved in toluene (120 mL) in a 500 mL one necked flask equipped with a Dean-Stark apparatus and a condenser and heated to reflux overnight. When all the water was removed benzyl alcohol (20 mL) was added and the solution was refluxed for 72h. The solution was then cooled using an ice bath and the precipitate filtrated, washed with diethyl ether and dissolved in chloroform (300 mL). To the organic solution a second solution of saturated sodium bicarbonate (100 mL) was added. The mixture of the two solutions was alternatively stirred and sonicated for 2h. Then the two phases were separated and the organic phase washed with water (3×75 mL) and dried with MgSO₄. The product **65** was isolated as a colourless oil (8.5 g, 27.2 mmol, 91%).

¹H NMR (400 MHz, CDCl₃): δ= 7.38 (m, 10H, ArH), 5.20 (s, 4H, **B**), 3.81 (s, 4H, **A**), 2.60 (vbs, 1H, NH); ¹³C NMR (100 MHz, CDCl₃): δ= 168.85 (CO), 135.55 (q, ArC), 129.28 (ArCH), 128.98 (ArCH), 128.56 (ArCH), 67.74 (CH₂), 49.12 (CH₂). FAB MS (*m*NBA matrix) *m/z* 314 [M+H]⁺. Anal. calcd for C₁₈H₁₉NO₄ (313.35): C, 68.99; H, 6.11; N, 4.47. Found: C, 68.89; H, 6.21; N, 4.34.

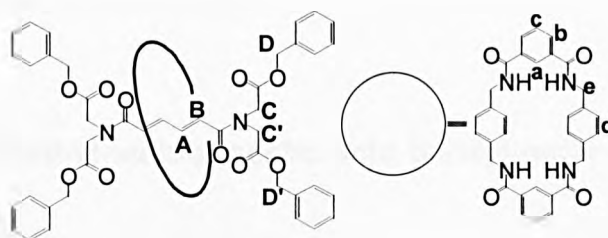
(Phenoxycarbonylmethyl-amino)-acetic acid benzyl ester amide
***trans,trans*-Muconic thread (66)**



(Phenoxycarbonylmethyl-amino)-acetic acid benzyl ester **65** (523.0 mg, 1.7 mmol) and triethylamine (244 μ L) were dissolved in chloroform (75 mL) in a 250-mL one necked flask under nitrogen. *trans,trans*-Muconic chloride **55** (142 mg, 0.8 mmol) dissolved in chloroform (50 mL), was added dropwise at RT over a period of 1h. The solution was then stirred at RT over 5h. The solution was then washed with aqueous NaOH solution (2 \times 150 mL) then with water (3 \times 150 mL) and dried with MgSO₄. A white solid was obtained after the solvent was removed by rotary evaporation. The solid was re-crystallised from ethanol to give the product **66** as a white powder (550.0 mg, 0.75 mmol, 95%).

m.p. 185-186°C; ¹H NMR (400 MHz, CDCl₃): δ = 7.37 (m, 20H, ArH), 7.32 (dd, 2H, J = 14.3 + 3.0 Hz, **A**), 6.47 (dd, 2H, J = 14.3 + 3.0 Hz, **B**), 5.22 (s, 4H, **D**), 5.20 (s, 4H, **D'**), 4.34 (s, 4H, **C**), 4.27 (s, 4H, **C'**); ¹³C NMR (100 MHz, CDCl₃): δ = 169.27 (CO), 168.87 (CO), 166.82 (CO), 141.25 (q, ArC), 141.20 (q, ArC), 135.61 (CH), 135.19 (CH), 129.24 (ArCH), 129.19 (ArCH), 129.04 (ArCH), 128.97 (ArCH), 128.76 (ArCH), 126.31 (ArCH), 68.06 (CH₂), 67.53 (CH₂), 50.70 (CH₂), 48.99 (CH₂). FAB MS (*m*BNA matrix) m/z 733 [M+H]⁺. Anal. Calcd. for C₄₂H₄₀N₂O₁₀ (732.27): C, 68.84; H, 5.50; N, 3.82. Found: C, 68.68; H, 5.45; N, 3.91.

(Phenoxycarbonylmethyl-amino)-acetic acid benzyl ester amide *trans-trans* muconic Rotaxane (67)

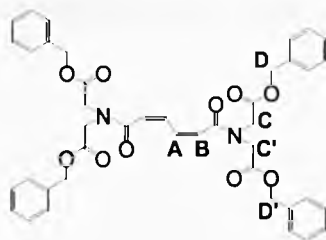


trans,trans-Muconic thread **66** (430.0 mg, 0.6 mmol) and triethylamine (2.0 mL) were dissolved in chloroform (50 mL), and stirred vigorously whilst solutions of *p*-xylylene diamine **26** (960.0 mg, 7.1 mmol) in chloroform (40 mL) and isophthaloyl dichloride **22** (1.4 g, 7.1 mmol) in chloroform (40 mL) were simultaneously added over a period of 4h using motor-driven syringe pumps. The resulting suspension was then filtered and concentrated under reduced pressure to afford the crude product. After purification by silica gel chromatography (CHCl₃) the rotaxane **67** were recovered as a white powder (38.0 mg, 0.03 mmol, 5%).

m.p. 270-271°C; ¹H NMR (400 MHz, CDCl₃): δ= 8.03 (dd, 4H, J= 7.8 + 1.5 Hz, **b**), 7.75 (s, 2H, **a**), 7.50 (t, 4H, J= 5.0 Hz, NH_{macro}), 7.41 (t, 2H, J= 7.8 Hz, **c**), 7.30 - 7.20 (m, 20H, ArH), 7.08 (s, 8H, **d**), 6.00 (dd, 2H, J= 14.3 + 3.0 Hz, **A**), 5.13 (dd, 2H, J= 14.3 + 3.0 Hz, **B**), 5.06 (s, 4H, **D**), 5.02 (s, 4H, **D'**), 4.44 (s, 4H, **e_{ax}**), 4.43 (s, 4H, **e_{eq}**), 4.02 (s, 4H, **C**), 3.93 (s, 4H, **C'**); ¹³C NMR (100 MHz, CDCl₃): δ= 169.35 (CO), 168.96 (CO), 167.30 (CO), 166.83 (CO), 140.49 (q, ArC), 138.49 (q, ArC), 135.34 (CH), 135.12 (CH), 134.56 (q, ArC), 134.50 (q, ArC), 131.78 (ArCH), 129.59 (ArCH), 129.49 (ArCH), 129.16 (ArCH), 129.09 (ArCH), 129.01 (ArCH), 128.75 (ArCH), 128.43 (ArCH), 125.00 (ArCH), 123.90 (ArCH), 68.49 (CH₂), 67.78 (CH₂), 50.94 (CH₂), 49.57

(CH₂), 46.21 (CH₂), 44.22 (CH₂). FAB MS (*m*BNA matrix) *m/z* 1266 [M+H]⁺.
Anal. Calcd. for C₇₄H₆₈N₆O₁₄ (1265.36): C, 70.24; H, 5.42; N, 6.64. Found: C, 69.61; H, 5.43; N, 6.51.

(Phenoxycarbonylmethyl-amino)-acetic acid benzyl ester amide *cis,cis*-Muconic thread (68)



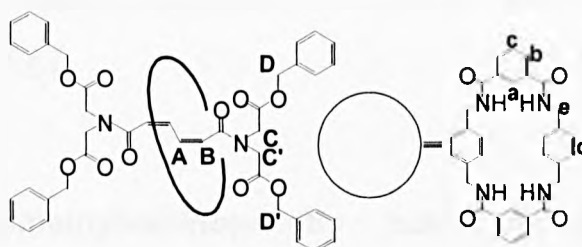
(Phenoxycarbonylmethyl-amino)-acetic acid benzyl ester **65** (523.0 mg, 1.7 mmol), *cis,cis*-muconic diacid **59** (114 mg, 0.8 mmol) and triethyl amine (244 μ L) were dissolved in chloroform (75 mL) in a 250-mL one necked flask under nitrogen. The mixture was cooled using an ice bath and EDCI (326 mg, 1.7 mmol) was slowly added. After 30 mins the ice bath was removed and the solution stirred at RT over a period of 5h.

The solution was then washed with aqueous NaOH solution (2 \times 50 mL) then with water (3 \times 50 mL) and dried with MgSO₄. A dark yellow solid was obtained after the solvent was eliminated by rotary evaporation. The solid was then purified by silica gel chromatography (CHCl₃/MeOH 9.8/0.2) to afford the product **68** as a white powder (440 mg, 0.6 mmol, 75%).

m.p. 185-186°C; ¹H NMR (400 MHz, CDCl₃): δ = 7.39 (m, 20H, ArH), 7.08 (dd, 2H, *J*= 10.3 + 2.3 Hz, **A**), 6.08 (dd, 2H, *J*= 10.3 + 2.3 Hz, **B**), 5.20 (s, 8H, **D** + **D'**), 4.30 (s, 4H, **C**), 4.22 (s, 4H, **C'**); ¹³C NMR (100 MHz, CDCl₃): δ = 169.67 (CO), 168.96 (CO), 168.04 (CO), 157.12 (CH), 134.37 (q, ArC), 133.75 (q,

ArC), 129.16 (ArCH), 128.78 (ArCH), 128.55 (ArCH), 127.64 (ArCH), 126.00 (ArCH), 125.44 (ArCH), 121.95 (CH), 67.55 (CH₂), 67.05 (CH₂), 48.63 (CH₂), 48.07 (CH₂). FAB MS (*m*BNA matrix) *m/z* 734 [M+H]⁺. Anal. Calcd. for C₄₂H₄₀N₂O₁₀ (732.77): C, 68.84; H, 5.50; N, 3.82. Found: C, 68.68; H, 5.45; N, 3.91.

(Phenoxycarbonylmethyl-amino)-acetic acid benzyl ester *cis,cis*-Muconic Rotaxane (69)

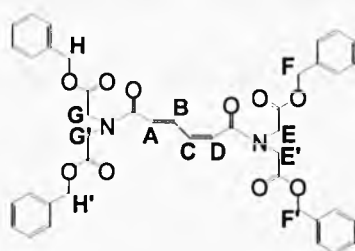


cis,cis-Muconic thread **68** (430.0 mg, 0.6 mmol) and triethylamine (2.0 mL) were dissolved in chloroform (50 mL), and stirred vigorously whilst solutions of *p*-xylylene diamine **26** (960.0 mg, 7.1 mmol) in chloroform (40 mL) and isophthaloyl dichloride **22** (1.4 g, 7.1 mmol) in chloroform (40 mL) were simultaneously added over a period of 4h using motor-driven syringe pumps. The resulting suspension was then filtered and concentrated under reduced pressure to afford the crude product. Purification by silica gel chromatography (CHCl₃) gave the rotaxane **69** as a white powder (38.4 mg, 0.03 mmol, 5%).

m.p. 270-271°C; ¹H NMR (400 MHz, CDCl₃): δ= 8.14 (d, 4H, *J*= 7.8 + 1.5 Hz, **b**), 8.02 (s, 2H, **a**), 7.52 (t, 2H, *J*= 7.8 Hz, **c**), 7.42 (t, 4H, *J*= 5.0 Hz, NH_{macro}), 7.40 - 7.20 (m, 20H, ArH), 7.14 (s, 8H, **d**), 6.28 (dd, 2H, *J*= 10.3 + 2.3 Hz, **A**),

5.09 (dd, 2H, $J = 10.3 + 2.3$ Hz, **B**), 5.11 (s, 4H, **D**), 5.04 (s, 4H, **D'**), 4.53 (s, 4H, **e_{ax}**), 4.51 (s, 4H, **e_{eq}**), 4.05 (s, 4H, **C**), 3.98 (s, 4H, **C'**); ^{13}C NMR (100 MHz, CDCl_3): $\delta = 169.37$ (CO), 168.96 (CO), 168.08 (CO), 166.83 (CO), 140.47 (CH), 138.49 (q, ArC), 135.06 (q, ArC), 134.79 (q, ArC), 134.55 (q, ArC), 131.91 (ArCH), 131.77 (ArCH), 129.63 (ArCH), 129.48 (ArCH), 129.32 (ArCH), 129.20 (ArCH), 129.03 (ArCH), 128.75 (ArCH), 128.53 (ArCH), 123.52 (ArCH), 129.16 (ArCH), 78.08 (CH), 68.34 (CH_2), 67.78 (CH_2), 51.05 (CH_2), 49.10 (CH_2), 44.22 (CH_2). FAB MS (*m*BNA matrix) m/z 1266 $[\text{M}+\text{H}]^+$. Anal. Calcd. for $\text{C}_{74}\text{H}_{68}\text{N}_6\text{O}_{14}$ (1265.36): C, 70.24; H, 5.42; N, 6.64. Found: C, 69.61; H, 5.43; N, 6.51.

**(Phenoxycarbonylmethyl-amino)-acetic acid benzyl ester amide
cis,trans-Muconic thread (70)**

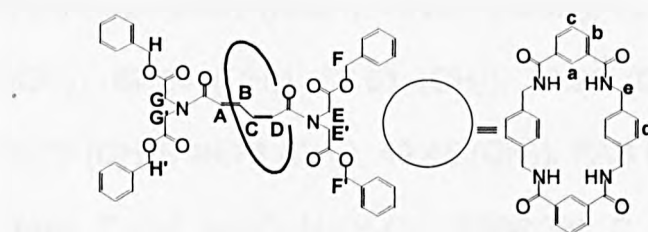


cis,cis-Muconic thread **68** (750 mg, 1.0 mmol) was dissolved in a saturated solution of iodine in CDCl_3 (10 mL) in a 50 mL one necked flask under nitrogen. The reaction was stirred at RT and in presence of light (sun lamp) for 24h until the total conversion of the *cis,cis*-muconic thread **68** into the *cis,trans*-muconic thread **70** was observed (^1H -NMR). The solution was then diluted to 200 mL with chloroform and washed with a 10% solution of sodium bisulphite (2×75 mL) and water (2×125 mL) and dried over MgSO_4 .

Evaporation of the solvent at reduced pressure gave the *cis,trans*-muconic thread **70** as a white powder (720 mg, 1.0 mmol, 96%).

m.p. 185-186°C; ^1H NMR (400 MHz, CDCl_3): δ = 7.67 (m, 1H, **B**), 7.35 - 7.10 (m, 20H, ArH), 6.33 (m, 1H, **C**), 6.22 (d, 1H, J = 15.1 Hz, **A**), 6.01 (d, 1H, J = 11.3 Hz, **D**), 5.11 (s, 2H, **F**), 5.10 (s, 2H, **F'**), 5.08 (s, 2H, **H**), 5.06 (s, 2H, **H'**), 4.22 (s, 2H, **E**), 4.21 (s, 2H, **E'**), 4.17 (s, 2H, **G**), 4.12 (s, 2H, **G'**); ^{13}C NMR (100 MHz, CDCl_3): δ = 171.52 (CO), 171.35 (CO), 170.42 (CO), 169.99 (CO), 167.45 (CO), 166.75 (CO), 138.53 (CH), 136.64 (q, ArC), 136.62 (q, ArC), 134.76 (q, ArC), 133.98 (q, ArC), 131.18 (ArCH), 130.08 (ArCH), 129.19 (ArCH), 129.11 (ArCH), 129.02 (CH), 129.00 (ArCH), 128.96 (ArCH), 128.90 (ArCH), 128.84 (ArCH), 128.76 (ArCH), 128.70 (CH), 128.00 (CH), 127.04 (ArCH), 126.60 (ArCH), 126.10 (ArCH), 67.89 (CH_2), 67.58 (CH_2), 67.45 (CH_2), 67.43 (CH_2), 51.14 (CH_2), 50.84 (CH_2), 50.00 (CH_2), 49.95 (CH_2), 48.77 (CH_2), 47.67 (CH_2), 47.59 (CH_2). FAB MS (*m*BNA matrix) m/z 733 $[\text{M}+\text{H}]^+$. Anal. Calcd. for $\text{C}_{42}\text{H}_{40}\text{N}_2\text{O}_{10}$ (732.77): C, 68.84; H, 5.50; N, 3.82. Found: C, 68.70; H, 5.41; N, 3.87.

(Phenoxycarbonylmethyl-amino)-acetic acid benzyl ester amide
***cis,trans*-Muconic Rotaxane (71)**



cis,trans-Muconic thread **70** (430.0 mg, 0.6 mmol) and triethylamine (2.0 mL) were dissolved in chloroform (50 mL), and stirred vigorously whilst solutions

of the *p*-xylylene diamine **26** (960.0 mg, 7.1 mmol) in chloroform (40 mL) and isophthaloyl dichloride **22** (1.4 g, 7.1 mmol) in chloroform (40 mL) were simultaneously added over a period of 4h using motor-driven syringe pumps. The resulting suspension was filtered and concentrated under reduced pressure to afford the crude product. After purification by silica gel chromatography (CHCl₃) the rotaxane **71** was recovered as a white powder (45.6 mg, 0.04 mmol, 6%).

m.p. 270-271°C; ¹H NMR (400 MHz, CDCl₃): δ= 8.10 (d, 4H, *J*= 7.8 Hz, **b**), 8.02 (s, 2H, **a**), 7.63 (t, 4H, *J*= 5.8 Hz, NH_{macro}), 7.47 (t, 2H, *J*= 7.8 Hz, **c**), 7.40 - 7.25 (m, 20H, ArH), 7.17 (m, 1H, **B**), 7.13 (s, 8H, **d**), 5.36 (d, 1H, *J*= 11.3 Hz, **A**), 5.32 (d, 1H, *J*= 15.1 Hz, **D**), 5.14 (s, 2H, **F**), 5.10 (t, 1H, *J*= 11.3 Hz, **C**), 5.03 (s, 2H, **F'**), 5.01 (s, 2H, **H**), 4.98 (s, 2H, **H'**), 4.65 - 4.35 (m, 8H, **e**), 4.17 (s, 2H, **E**), 3.98 (s, 2H, **G**), 3.93 (s, 2H, **E'**), 3.92 (s, 2H, **H'**); ¹³C NMR (100 MHz, CDCl₃): δ= 171.21 (CO), 169.86 (CO), 168.99 (CO), 168.89 (CO), 168.82 (CO), 167.05 (CO), 166.87 (CO), 137.96 (CH), 137.22 (q, ArC), 135.73 (q, ArC), 135.50 (q, ArC), 134.97 (q, ArC), 132.89 (q, ArC), 132.29 (q, ArC), 131.10 (ArCH), 129.30 (ArCH), 129.11 (ArCH), 129.04 (ArCH), 128.97 (CH), 128.94 (ArCH), 128.83 (ArCH), 128.77 (ArCH), 128.76 (ArCH), 128.72 (ArCH), 128.14 (ArCH), 127.88 (ArCH), 126.53 (CH), 125.98 (CH), 125.17 (ArCH), 125.02 (ArCH), 124.97 (ArCH), 124.27 (ArCH), 124.13 (ArCH), 68.24 (CH₂), 68.03 (CH₂), 67.84 (CH₂), 67.61 (CH₂), 50.98 (CH₂), 50.91 (CH₂), 50.82 (CH₂), 50.79 (CH₂), 49.76 (CH₂), 49.45 (CH₂). FAB MS (*m*BNA matrix) *m/z* 1265 M⁺. Anal. Calcd. for C₇₄H₆₈N₆O₁₄ (1265.36): C, 70.24; H, 5.42; N, 6.64. Found: C, 70.01; H, 5.23; N, 6.57.

References:

1. (a) Amabilino, D.B.; Stoddart, J.F. *Chem. Rev.* **1995**, 2725. (b) Schill, G. *Catenanes, Rotaxanes and Knots*, Academic Press, New York, **1971**.
2. (a) Bermudez, V.; Capron, N.; Gase, T.; Gatti, F.G.; Kajzar, F.; Leigh, D.A.; Zerbetto, F.; Zhang, S. *Nature* **2000**, 406, 608. (b) Armaroli, N.; Balzani, V.; Collin, J.P.; Gavina, P.; Sauvage, J.P.; Ventura, B. *J. Am. Chem. Soc.* **1999**, 121, 4397. (c) Bissel, R.A.; Córdova, E.; Kaiefer, A.E.; Stoddart, J.F. *Nature* **1994**, 369, 133. (d) Fujita, M.; Ibukuro, F.; Hagihara, H.; Ogura, K. *Nature* **1994**, 367, 720.
3. Leigh, D.A.; Murphy, A.; Smart, J.P.; Slawin, A.M.Z. *Angew. Chem. Int. Ed. Engl.* **1997**, 36, 728.
4. Gatti, F.G.; Leigh, D.A.; Napogodiev, S.A.; Slawin, A.M.Z.; Teat, S.J.; Wong, J.K.Y. *J. Am. Chem. Soc.* **2001**, 123, 5983.
5. For accounts referring to self-assembly and template directed synthesis see: (a) Philp, D.; Stoddart, J.F. *Angew. Chem. Int. Ed. Engl.* **1996**, 35, 1154. (b) Lawrence D.S.; Jing, T.; Levett, M. *Chem. Rev.* **1995**, 2229. (c) Lehn, J.M. *Angew. Chem. Int. Ed. Engl.* **1990**, 29, 1304.
6. Johnston, A.G.; Leigh, D.A.; Murphy, A.; Smart, J.P.; Deegan, M.D. *J. Am. Chem. Soc.* **1996**, 118, 10662.
7. (a) Johnston, A.G.; Leigh, D.A.; Nezhat, L.; Smart, J.P.; Deegan, M.D. *Angew. Chem. Int. Ed. Engl.* **1995**, 34, 1212. (b) Carver, F.J.; Hunter, C.A.; Shannon, R.J. *J. Chem. Soc., Chem. Commun.* **1994**, 4124. (c) C.A. Geib, C.A.; Vincent, C.; Fan, E.; Hamilton, A.D. *Angew. Chem. Int. Engl.* **1993**, 32, 119. (d) Hunter, C.A.; Purvis, D.H. *Angew. Chem. Int. Ed. Engl.* **1992**, 31, 792.

8. Johnston, A.G.; Leigh, D.A.; Pritchard, R.J.; Deegan, M.D. *Angew. Chem. Int. Ed. Engl.* **1995**, 34, 1209.
9. Dünwald, T.; Parham, A.H.; Vögtle, F. *Synthesis* **1998**, 339.
10. Wong, J.K.Y.; Leigh, D.A. unpublished results.
11. (a) Jeon, K.S.; Choi, J.S.; Chang, S.Y.; Chang, H.Y. *Angew. Chem. Int. Ed. Engl.* **2000**, 39, 1692. (b) Chang, S.Y.; Choi, J.S.; Jeon, K.S. *Chem. Eur. J.* **2001**, 7, 2687.
12. Jäger, R.; Baumann, S.; Fisher, M.; Safarowsky, O.; Nieger, M.; Vögtle, F. *Liebig. Ann. Recueil.* **1997**, 2269.
13. Hübner, G.M.; Nachtsheim, G.; Li, Q.Y.; Seel, C.; Vögtle, F. *Angew. Chem. Int. Ed.* **2000**, 39, 1269.
14. Sonnet, P.E. *Tetrahedron* **1980**, 36, 557.
15. Ideses, R.; Shani, A. *J. Am. Oil Chem. Soc.* **1989**, 66, 948.
16. Biscarini, F.; Cavallini, M.; Leigh, D.A.; León, S.; Teat, S.J.; Wong, J.K.Y.; Zerbetto, F. *J. Am. Chem. Soc.* **2002**, 124, 225.
17. Milas, N.A.; Fleš, D. *J. Am. Chem. Soc.* **1956**, 78, 5903.

Chapter Three

3. Investigations Into the Effect of Thread Rigidity on Rotaxane Yield Using Muconic Acid Thread Analogues.

Abstract: Here we report the synthesis of novel amide-based rotaxanes containing various saturated and unsaturated skeletons in their templating core. The effect of chain length and the introduction of a double bond and its stereochemistry will be discussed in the context of rotaxane yield.

Introduction: We recently described the rotaxane formation around threads based on a four carbon motif of either fumaric or succinic bis-amides¹ with benzylic tetramide macrocycles using a five molecule, hydrogen bond-directed clipping strategy that gave rotaxane with an outstanding yield of 97% for the fumaric-based thread and 56% for the succinic analogue.¹ Structural rigidity and pre-organisation of the thread binding sites are shown to have a major influence on template efficiency in the synthesis of hydrogen bond-assembled rotaxanes.¹ Elongation of the succinic motif through insertion of additional carbons has also been investigated ^{2,3,4,5} to further probe the structural requirements for rotaxane formation. Yields fall rapidly from 56% for the succinyl based system to around 10% with up to twelve carbons between the templating amides. The drop in yield from the fumaric to succinic motif is because the rigidity and stereochemistry that holds the templating carbonyl groups in the ideal trans orientation is lost in the substitution of the vinyl for two methylenes. Further methylene insertion

increases both the distance and degrees of freedom between the two carbonyl groups and has an even more pronounced effect on the rotaxane yield.

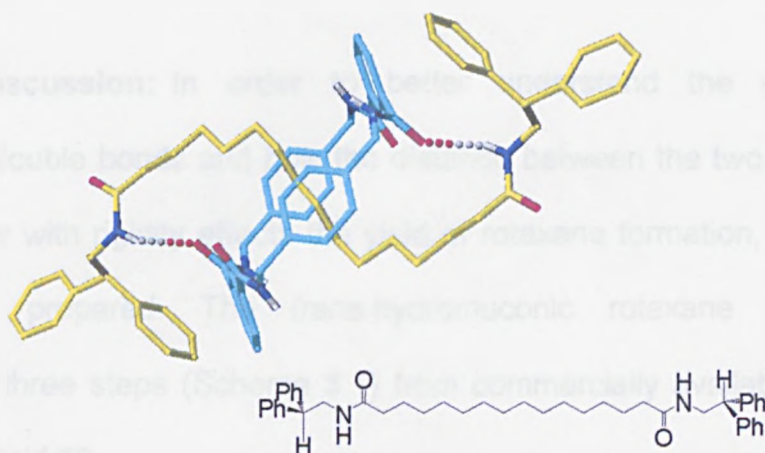
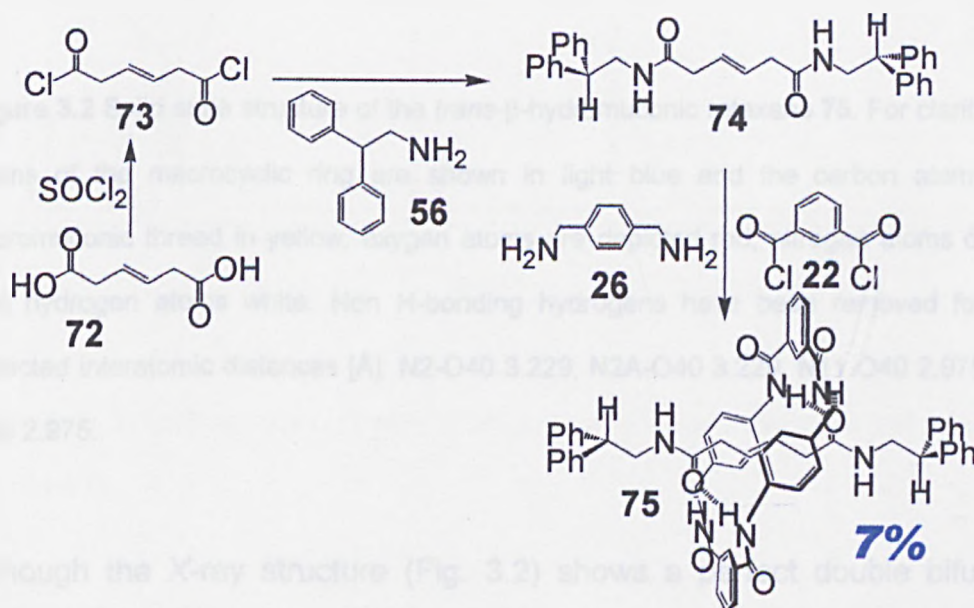


Figure 3.1 Solid state structure of the C16 rotaxane **53**. For clarity carbon atoms of the macrocyclic ring are shown in light blue and the carbon atoms of the C16 thread in yellow; oxygen atoms are depicted red, nitrogen atoms dark blue and hydrogen atoms white. Non H-bonding hydrogens have been removed.

Crystal structure analysis of rotaxanes with between four and fourteen carbon atoms between the templating amide carbonyls (see Figure 3.1) show that the alkyl chain adopts an orientation so that both the terminal amide carbonyls of the thread can still hydrogen bond with the NHs of the macrocycle amides. In the previous chapter (chapter two) a full rigid six carbon templating motif (muconic) was shown to be a more efficient templating unit under the rotaxane-forming conditions with respect to the all saturated analogue. In this chapter to better understand how rigidity and length between the templating amides are effecting rotaxane formation, just a

single double bond will be introduced into these longer threads to see how it affects rotaxane yields and their solid state structures. Additionally the effect of encapsulation on the chemistry of these double bonds by the macrocycle will also be investigated.

Results and discussion: In order to better understand the effect of introducing of double bonds and how the distance between the two carbonyl groups together with rigidity affects the yield of rotaxane formation, two new threads were prepared. The *trans*-hydromuconic rotaxane **75** was synthesised in three steps (Scheme 3.1) from commercially available *trans*-hydromuconic acid **72**.



Scheme 3.1

The rather low isolated yield (7%) of rotaxane **75** was due to the difficulty in separating the rotaxane from the thread (as previously reported for the tertiary amide-based species **67**, **69**, **71**). ^1H -NMR analysis on the reaction mixture of thread and rotaxane showed the crude yield to be 12%.

Crystals of rotaxane **75** suitable for investigation by X-ray crystallography were obtained from the slow evaporation of methanol into a solution of rotaxane **75** in chloroform.

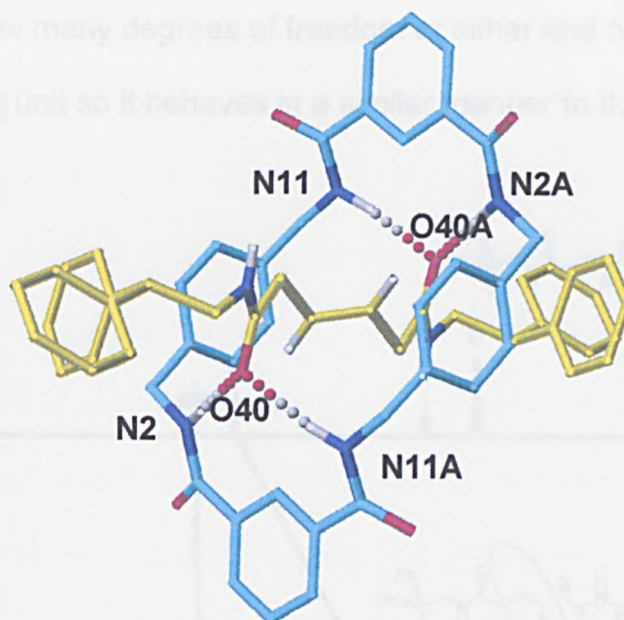


Figure 3.2 Solid state structure of the *trans*- β -hydromuconic rotaxane **75**. For clarity carbon atoms of the macrocyclic ring are shown in light blue and the carbon atoms of the hydromuconic thread in yellow; oxygen atoms are depicted red, nitrogen atoms dark blue and hydrogen atoms white. Non H-bonding hydrogens have been removed for clarity. Selected interatomic distances [Å]: N2-O40 3.229, N2A-O40 3.229, N11-O40 2.975, N11A-O40 2.975.

Although the X-ray structure (Fig. 3.2) shows a perfect double bifurcated-chair orientation of the macrocycle in a similar manner to the solid-state structure of the fumaric rotaxane (yield 97%); the low yield of rotaxanation with thread **74** suggested a poor propensity of the *trans*-hydromuconic motif to act as a template.

Making a comparison with the all saturated C6 rotaxane analogue (10% yield), the hydromuconic system contains less sterically demanding sp^2

centres, an olefin for possible π - π stacking interactions with the xylylene units of the macrocycle and less degrees of freedom in the core of the axle yet still has a similar yield to the all saturated analogue. The two methylenes in the core still allow many degrees of freedom at either end of the olefinic bond of the templating unit so it behaves in a similar manner to the all saturated C6 template.

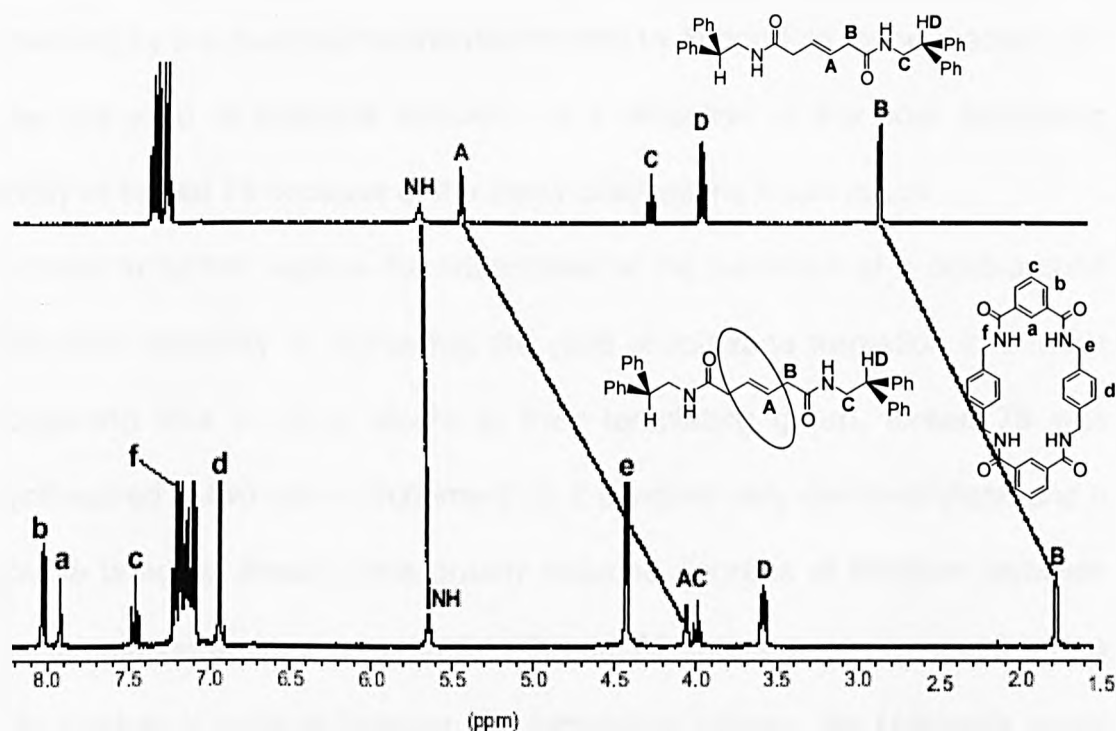
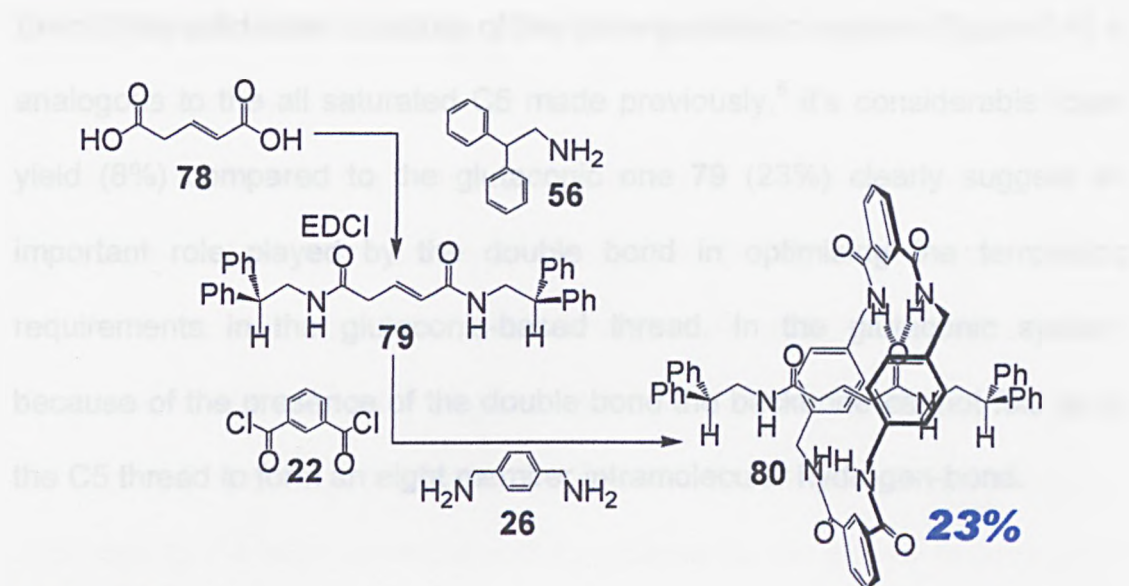


Figure 3.3 ^1H -NMR spectra (400 MHz, CDCl_3) of hydromuconic thread **74** and hydromuconic rotaxane **75**.

The ^1H -NMR spectra of hydromuconic thread **74** and rotaxane **75** in CDCl_3 show that the signals of the phenyl stoppers and amide protons (NH) are virtually unchanged in the two spectra, the resonances for the protons belonging to the core are shifted to significantly higher field in the rotaxane because of the shielding effects of the wheel.

Interestingly there is little deshielding effect observed on the shift of the NH protons of the axle and would seem to indicate little H-bonding interaction with the carbonyls of the thread. This would be backed up by the low yield of rotaxane but contradicts the H-bond interactions observed between the macrocycle and thread in the solid state (Figure 3.4) and probably means that the position of the axle NHs in the ^1H NMR spectra is a balance between shielding by the macrocycle and deshielding by H-bonding to the macrocycle. The low yield of rotaxane formation is a reflection of the poor templating ability of thread **74** because of the many orientations it can adopt.

In order to further explore the importance of the presence of a double bond and their capability of increasing the yield of rotaxane formation in threads containing four or more atoms in their templating group, thread **79** was synthesised in two steps (Scheme 3.2). It contains only one methylene and a double bond so should have greatly reduced degrees of freedom between the templating amides compared to thread **74**. Interestingly, because of the odd number of carbons between the templating amides, the carbonyls would adopt a *cis* orientation if the thread was drawn in an all zig-zag conformation. Fascinatingly, thread **79** gave rotaxane **80** in a 23% yield.



Scheme 3.2

Crystals of rotaxane **80** suitable for investigation by X-ray crystallography were obtained from the slow absorption of water into a solution of rotaxane **80** in methanol (Figure 3.4).

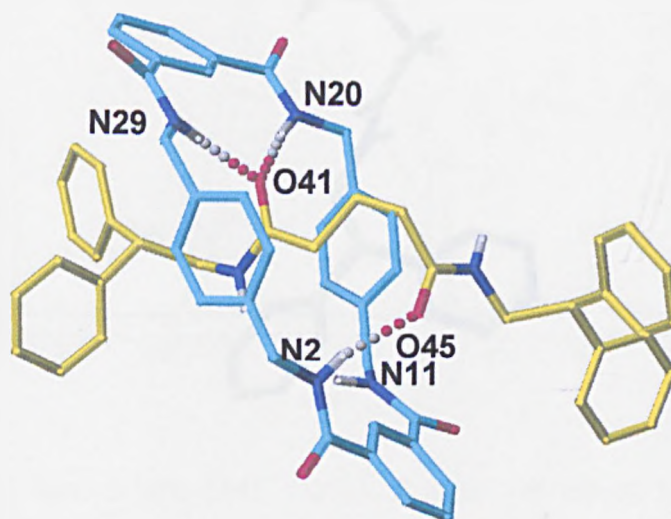


Figure 3.4 Solid state structure of the glutamic rotaxane **80**. For clarity carbon atoms of the macrocyclic ring are shown in light blue and the carbon atoms of the glutamic thread in yellow; oxygen atoms are depicted red, nitrogen atoms dark blue and hydrogen atoms white. Non H-bonding hydrogens have been removed for clarity. Selected interatomic distances [Å]: N29-O41 3.088, N20-O41 2.980, N2-O45 2.903.

Even if the solid-state structure of the *trans*-glutaconic system (Figure 3.4) is analogous to the all saturated C5 made previously,⁵ it's considerable lower yield (8%) compared to the glutaconic one **79** (23%) clearly suggest an important role played by the double bond in optimising the templating requirements in the glutaconic-based thread. In the glutaconic system, because of the presence of the double bond the backbone cannot fold as in the C5 thread to form an eight member intramolecular hydrogen-bond.

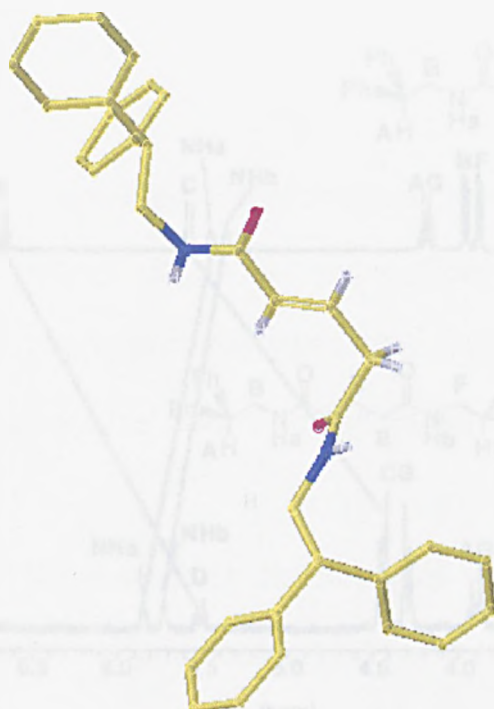


Figure 3.5 Solid state structure of the glutaconic thread **79** hydrogen bonding the tetramide macrocycle **27**. It was obtained highlighting the thread from the previous X-ray structure by removal of the macrocycle; (for clarity the carbon atoms of the glutaconic thread are shown in yellow; oxygen atoms are depicted red, nitrogen atoms dark blue and hydrogen atoms white. Non H-bonding hydrogens have been removed for clarity.

Highlighting the structure of the glutaconic thread **79** (Figure 3.5) by removal of the tetramide macrocycle **27** from the X-ray structure of glutaconic rotaxane **80** shows the significant bending of the templating unit when encompassed by the macrocycle in order to full fill its hydrogen bonding requirements (e.g. the *trans* disposition of the two carbonyls of the thread). Comparison of the spectra of glutaconic thread **79** and glutaconic rotaxane **80** (Figure 3.6) show the macrocycle laying over the central part of the axle as indicated by the large chemical shift for protons H_D, H_C and H_E in comparison with the stoppers (H_A, H_B, H_G and H_F).

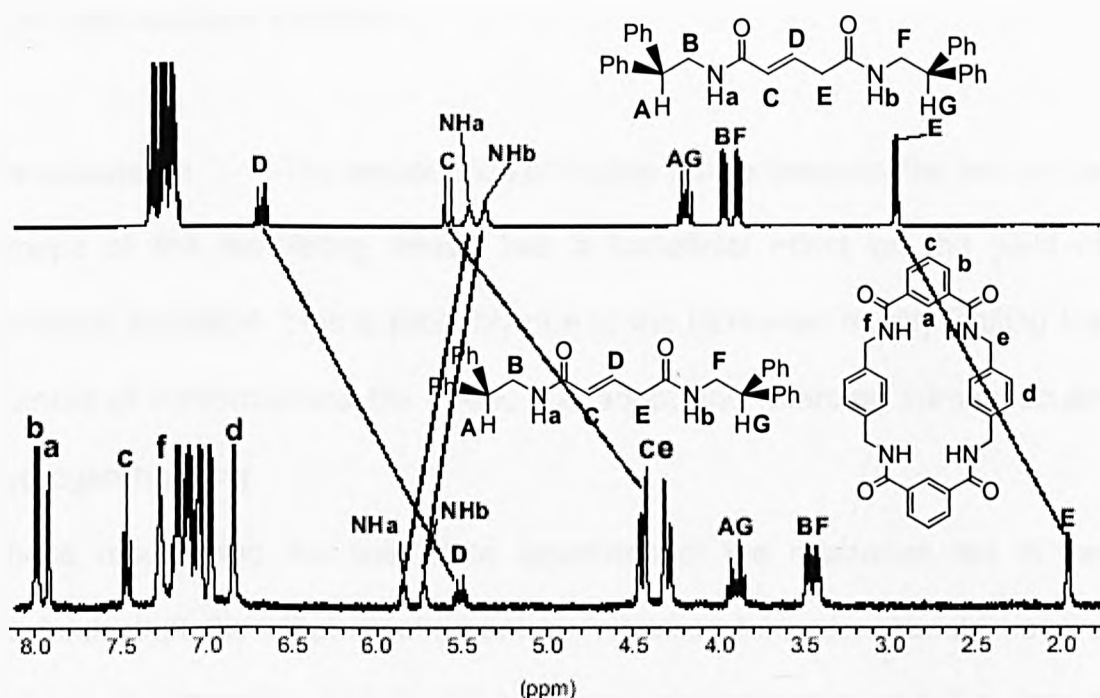


Figure 3.6 ¹H-NMR spectra (400 MHz, CDCl₃) of glutaconic thread **79** and glutaconic rotaxane **80**.

The amide protons of the thread are also deshielded in the rotaxane by hydrogen bonding with the macrocycle amides. The different signals for the amides and stoppers are a consequence of the asymmetry of the thread.

The yield of rotaxane formation (23%) is similar to that obtained for the *cis,cis*-muconic based system (21%) but quite different from the hydromuconic templating unit (7%). This last comparison seem to indicate that for the glutaconic system the relative lack of rigidity (compared to the muconic based system) is compensated by a shorter distance between the two carbonyls of the template in accord with previous results; in addition it highlights the limitations of one double bond promoting rotaxane formation when it is in the middle of a six carbon atom templating unit (hydromuconic motif) and is not enough to promote those geometrical factors responsible for high yield rotaxane formation.

Conclusions: The introduction of double bonds between the two amide groups of the templating thread has a beneficial effect on the yield of rotaxane formation. This is probably due to the increased rigidity limiting the number of conformations the thread can adopt and retarding intramolecular hydrogen-bonding.

These results and the solid-state structures of the rotaxanes led to the postulate that the ideal requirement for rotaxane formation should have a multi-point interaction between the macrocycle precursor and the thread where the two carbonyls are held at a certain distance which occurs in the *trans* orientation. However, when the distance between these amide carbonyls is changed by the introduction of additional carbon atoms, at least one of these essential factor (distance) is modified, and for systems such as the glutaconic and hydromuconic motifs, so the rigidity, an essential precondition for rotaxane formation, is also altered.

As highlighted earlier, a direct comparison of the isolated yields of all the rotaxanes is not possible due to difficulties encountered in their purification. The crude yields, based on ^1H NMRs were therefore used (Table 3.1).

However, using its crude yield (12% by ^1H -NMR), the comparison with the all unsaturated C6 system ($\sim 10\%$)³ suggest that the introduction of just one double bond in the middle of the axle has only a small effect on the yield of the rotaxane forming process. On the contrary, the relatively high yields for the muconic system, Z,Z-muconic rotaxane **62** (23% - crude yield) and E,Z-muconic rotaxane **64** (56%) (a direct comparison is not possible with the E,E-muconic rotaxane **58**) seem to confirm the importance of the two conjugated double bonds leading to an optimisation of the geometry of the templating amides which partially compensate for the longer distance between them.

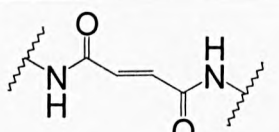
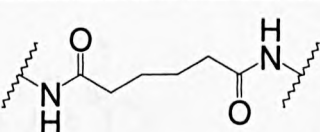
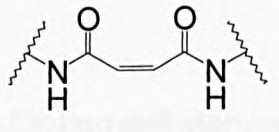
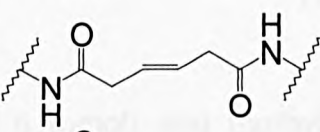
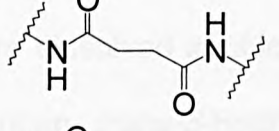
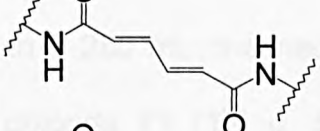
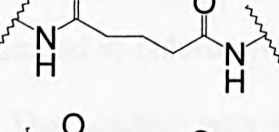
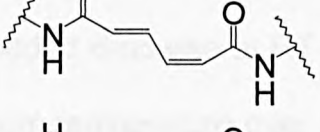
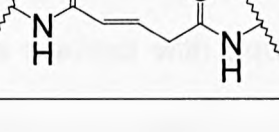
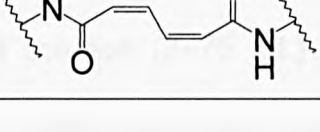
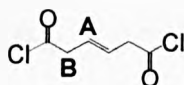
THREADS	CRUDE YIELD	THREADS	CRUDE YIELD
	97%		10%
	0%		12%
	56%		NOT POSSIBLE
	8%		56%
	23%		23%

Table 3.1

Experimental Part:

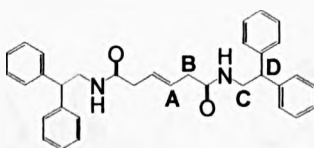
Hydromuconic diacid chloride (**73**)⁸



β -*trans*-Hydromuconic acid **72** (5.0 g, 34.7 mmol) was dissolved in thionyl chloride (25 mL) in a 250 mL one necked flask equipped with a condenser and heated to 80°C for 24h. Then the thionyl chloride was removed under reduced pressure and the hydromuconic chloride precipitated in a mixture of petroleum spirit (60-80°C) (95%) and diethyl ether (5%) to afford the hydromuconic chloride **73** as a white powder (6.0 g, 33.0 mmol, 95%).

m.p. 193-194°C (Lit. m.p. 193-194°C.⁸); ¹H NMR (400 MHz, CDCl₃): δ = 5.80 (t, 2H, J = 5.6 Hz, **A**), 3.68 (d, 4H, J = 5.6 Hz, **B**).

trans- β -Hydromuconic thread (**74**)



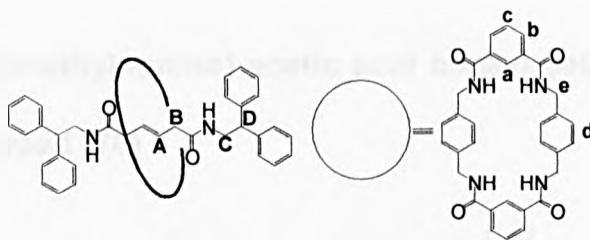
2,2-Diphenylethylamine **56** (2.3 g, 11.6 mmol) and triethylamine (1.7 mL) were dissolved in chloroform (75 mL) in a 250 mL one necked flask under nitrogen. *trans*- β -Hydromuconic acid chloride **73** (1.0 g, 5.5 mmol), also dissolved in chloroform (50 mL), was added dropwise at RT over a period of 1h. The solution was then stirred at room temperature over 5h. The solution was washed with aqueous 1M NaOH solution (2×75 mL) then with water (3×75 mL) and dried with MgSO₄. A white solid was obtained after the solvent was eliminated by rotary evaporation. Thread **74** was isolated as a

white powder after washing (2×15 mL) with hot diethyl ether (2.1 g, 4.2 mmol, 76%).

m.p. 175-176°C; ^1H NMR (400 MHz, CDCl_3): δ = 7.40 - 7.20 (m, 20H, ArH), 5.67 (t, J = 5.9 Hz, 2H, NH), 5.40 (t, 2H, J = 5.6 Hz, A), 4.22 (t, 2H, J = 7.9 Hz, D), 3.91 (dd, 4H, J = 7.9 + 5.9 Hz, C), 2.80 (d, 4H, J = 5.6 Hz, B); ^{13}C NMR (100 MHz, CDCl_3): δ = 170.91 (CO), 142.25 (q, ArC), 129.12 (ArCH), 128.49 (ArCH), 128.33 (ArCH), 127.25 (CH), 50.86 (CH), 44.30 (CH_2), 40.28 (CH_2). FAB MS (*m*BNA matrix) m/z 503 [M^+]. Anal. Calcd for $\text{C}_{34}\text{H}_{34}\text{N}_2\text{O}_2$ (502.65): C 81.24, H 6.82, N 5.57. Found: C 80.81, H 6.17, N 5.47.

The incorrect value obtained for C and H in the elemental analysis was due to the persistent presence of solvent in the sample even after high-vacuum treatment overnight.

***trans*- β -Hydromuconic rotaxane (75)**

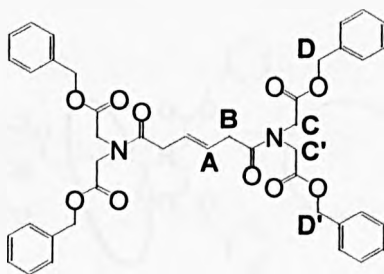


trans- β -Hydromuconic thread **74** (500.0 mg, 1.0 mmol) and triethylamine (3.5 mL) were dissolved in chloroform (50 mL), and stirred vigorously whilst solutions of the *p*-xylylene diamine **26** (1.6 g, 12.0 mmol) in chloroform (40 mL) and isophthaloyl dichloride **22** (2.4 g, 12.0 mmol) in chloroform (40 mL) were simultaneously added over a period of 4h using motor-driven syringe pumps. The resulting suspension was filtered and concentrated under

reduced pressure to afford the crude product. After purification by silica gel chromatography (chloroform) the rotaxane **75** was recovered as a white powder (72.4 mg, 0.07 mmol, 7%).

m.p. 230-231°C; ^1H NMR (400 MHz, CDCl_3): δ = 8.06 (dd, 4H, J = 7.8 + 1.4 Hz, **b**), 7.95 (s, 2H, **a**), 7.49 (t, 2H, J = 7.8 Hz, **c**), 7.24 (t, 4H, J = 5.0 Hz, NH_{macro}), 7.24 - 7.10 (m, 20H, ArH), 6.95 (s, 8H, **d**), 5.65 (t, J = 5.9 Hz, 2H, $\text{NH}_{\text{thread}}$), 4.41 (d, 8H, J = 5.0 Hz, **e**), 4.04 (t, J = 5.6 Hz, 2H, **A**), 3.97 (t, J = 7.9 Hz, 2H, **D**), 3.56 (dd, 4H, J = 7.9 + 5.9 Hz, **C**), 1.73 (d, J = 5.6 Hz, 4H, **B**); ^{13}C NMR (100 MHz, CDCl_3): δ = 171.89 (CO), 166.78 (CO), 143.55 (q, ArC), 143.13 (q, ArC), 142.80 (q, ArC), 132.65 (ArCH), 131.65 (ArCH), 129.47 (ArCH), 129.22 (ArCH), 128.37 (ArCH), 127.97 (ArCH), 125.92 (CH), 125.53 (ArCH), 49.77 (CH), 44.30 (CH_2), 43.28 (CH_2), 38.84 (CH_2). FAB MS (*m*BNA matrix) m/z 1036 $[\text{M}+\text{H}]^+$. Anal. Calcd for $\text{C}_{66}\text{H}_{62}\text{N}_6\text{O}_6$ (1035.24): C 76.57, H 6.04, N 8.12. Found: C 76.41, H 6.00, N 8.07.

(Phenoxycarbonylmethyl-amino)-acetic acid benzyl ester amide *trans*- β -hydromuconic thread (76)

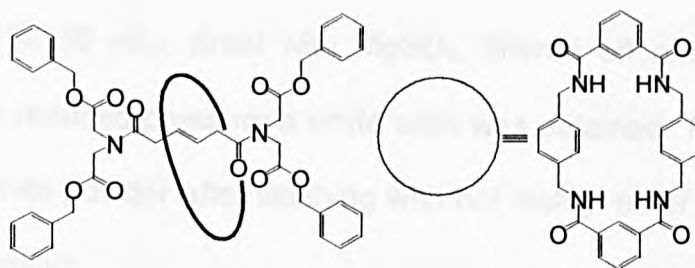


Tertiary amide stopper **65** (670 mg, 2.1 mmol) and triethylamine (312.0 μL) were dissolved in chloroform (75 mL) in a 250 mL one necked flask under nitrogen. *trans*- β -Hydro muconic acid chloride **73** (184 mg, 1.0 mmol), also

dissolved in chloroform (50 mL), was added dropwise at RT over 1h. The solution was stirred at room temperature over 5h. The solution was then washed with aqueous 1M NaOH solution (2×75 mL), with water (3×75 mL) and dried with MgSO₄. A white solid was obtained after the solvent was removed at reduced pressure. Thread **76** (735 mg, 1.0 mmol, 98%) was isolated as a white powder after washing (2×15 mL) with hot diethyl ether.

m.p. 157-158°C; ¹H NMR (400 MHz, CDCl₃): δ= 7.45 - 7.35 (m, 20H, ArH), 5.69 (t, 2H, *J*= 5.6 Hz, **A**), 5.21 (s, 4H, **D**), 5.16 (s, 4H, **D'**), 4.26 (s, 4H, **C**), 4.21 (s, 4H, **C'**), 3.11 (d, 4H, *J*= 5.6 Hz, **B**); ¹³C NMR (100 MHz, CDCl₃): δ= 172.43 (CO), 166.07 (CO), 136.08 (q, ArC), 135.75 (q, ArC), 130.84 (ArCH), 129.07 (ArCH), 128.79 (ArCH), 128.48 (ArCH), 127.83 (CH), 127.42 (ArCH), 124.98 (ArCH), 70.09 (CH₂), 69.09 (CH₂), 52.02 (CH₂), 49.43 (CH₂), 37.02 (CH₂). FAB MS (*m*BNA matrix) *m/z* 735 [*M*⁺]. Anal. Calcd for C₄₂H₄₂N₂O₁₀ (734.79): C, 68.65; H, 5.76; N, 3.81. Found: C, 69.01; H, 6.03; N, 4.01.

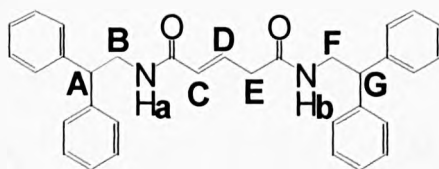
(Phenoxycarbonylmethyl-amino)-acetic acid benzyl ester amide *trans*-β-hydromuconic rotaxane (77**)**



trans-β-Hydromuconic thread **76** (400.0 mg, 0.5 mmol) and triethylamine (1.9 mL) were dissolved in chloroform (50 mL), and stirred vigorously whilst solutions of the *p*-xylylene diamine **26** (890.0 mg, 6.5 mmol) in chloroform (40

mL) and the isophthaloyl dichloride **22** (1.3 g, 6.5 mmol) in chloroform (40 mL) were simultaneously added over a period of 4h using motor-driven syringe pumps. The resulting suspension was filtered and concentrated under reduced pressure to afford the crude product. From a preliminary analysis of the crude of both filtrate and precipitate it was possible to observe that no rotaxane formation had occurred.

Glutaconic thread (**79**)

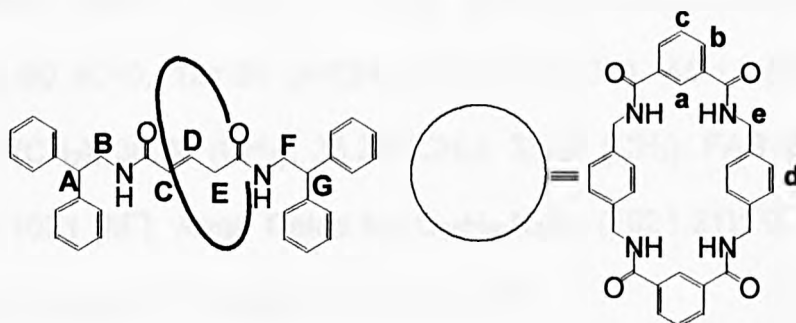


2,2- Diphenylethylamine **56** (7.2 g, 36.8 mmol) and glutaconic acid **78** (2.0 g, 17.5 mmol) were dissolved in THF (250 mL) in a 500 mL one necked flask under nitrogen. The solution was then chilled to 0°C (ice bath) and EDCI (4.9 g, 25.4 mmol) was added slowly over 1h. The solution was then stirred at RT overnight. The solvent was removed and the solution was dissolved in chloroform (200 mL) and washed with aqueous 1M NaOH solution (2×150 mL) then with water (3×150 mL), dried with MgSO₄, filtered off and after removing the solvent at reduced pressure a white solid was obtained. Thread **79** was isolated as a white powder after washing with hot diethyl ether (2×15 mL) (7.3 g, 14.9 mmol, 85%).

m.p. 175-176°C; ¹H NMR (400 MHz, CDCl₃): δ= 7.40 - 7.20 (m, 20H, ArH), 6.71 (m, 1H, **D**), 5.61 (d, 1H, *J*= 15.3 Hz, **C**), 5.48 (t, 1H, *J*= 5.9 Hz, NH_a), 5.39 (t, 1H, *J*= 5.9 Hz, NH_b), 4.23 (t, 1H, *J*= 7.9 Hz, **A**), 4.19 (t, 1H, *J*= 7.9 Hz,

G), 3.98 (dd, 2H, $J = 7.9 + 5.9$ Hz, **B**), 3.91 (dd, 2H, $J = 7.9 + 5.9$ Hz, **F**), 2.98 (d, 2H, $J = 7.0$ Hz, **E**); ^{13}C NMR (100 MHz, CDCl_3): $\delta =$ 169.30 (CO), 165.27 (CO), 142.14 (q, ArC), 142.01 (q, ArC), 136.30 (CH), 129.21 (ArCH), 129.15 (ArCH), 129.43 (ArCH), 128.86 (ArCH), 127.63 (CH), 127.34 (ArCH), 127.27 (ArCH), 50.97 (CH), 50.86 (CH), 44.25 (CH_2), 39.77 (CH_2), 34.66 (CH_2). FAB MS (*m*BNA matrix) m/z 489 [M^+]. Anal. Calcd for $\text{C}_{33}\text{H}_{32}\text{N}_2\text{O}_2$ (488.62): C, 81.12; H, 6.60; N, 5.73. Found: C, 80.24; H, 7.01; N, 5.70.

Glutaconic rotaxane (**80**)



Glutaconic thread **79** (500 mg, 1.0 mmol) was dissolved in chloroform (50 mL), and stirred vigorously whilst solutions of the *p*-xylylene diamine **26** (1.7 g, 12.0 mmol) and triethyl amine (3.6 mL) in chloroform (40 mL) and isophthaloyl dichloride **22** (2.5 g, 12.0 mmol) in chloroform (40 mL) were simultaneously added over a period of 4h using motor-driven syringe pumps. The resulting suspension was then filtered and concentrated under reduced pressure to afford the crude product. After purification by silica gel chromatography (chloroform) rotaxane **80** was isolated as a white powder (235.0 mg, 0.23 mmol, 23%).

m.p. 267-268°C; ^1H NMR (400 MHz, $\text{DMSO}-d_6$): δ = 8.77 (t, 4H, J = 5.0 Hz, NH_{macro}), 8.11 (s, 2H, a), 8.03 (dd, 4H, J = 7.8 + 1.4 Hz, b), 7.64 (t, 2H, J = 7.8 Hz, c), 7.38 (t, 1H, J = 5.9 Hz, NH_a), 7.33 (t, 1H, J = 5.9 Hz, NH_b), 7.30 - 7.10 (m, 20H, ArH), 6.84 (s, 8H, d), 5.73 (m, 1H, D), 4.66 (t, 1H, J = 15.3 Hz, C), 4.30 (d, 8H, J = 5.0 Hz, e), 3.96 (t, 1H, J = 7.9 Hz, A), 3.89 (t, 1H, J = 7.9 Hz, G), 3.46 (dd, 2H, J = 7.9 + 5.9 Hz, B), 3.40 (dd, 2H, J = 7.9 + 5.9 Hz, F), 1.77 (d, 2H, J = 7.0 Hz, E); ^{13}C NMR (100 MHz, $\text{DMSO}-d_6$): δ = 164.84 (CO), 161.92 (CO), 161.12 (CO), 137.28 (q, ArC), 137.20 (q, ArC), 132.32 (q, ArC), 129.72 (q, ArC), 125.73 (ArCH), 123.76 (CH), 123.67 (ArCH), 123.54 (ArCH), 122.90 (ArCH), 122.87 (ArCH), 122.85 (ArCH), 122.80 (ArCH), 122.12 (ArCH), 121.60 (CH), 121.56 (ArCH), 120.13 (ArCH), 45.13 (CH), 44.67 (CH), 37.03 (CH_2), 36.80 (CH_2), 35.24 (CH_2), 33.53 (CH_2). FAB MS (*m*BNA matrix) m/z 1021 [M^+]. Anal. Calcd for $\text{C}_{65}\text{H}_{60}\text{N}_6\text{O}_6$ (1021.21): C, 76.45; H, 5.92; N, 8.23. Found: C, 76.24; H, 6.01; N, 8.00.

References

1. Gatti, F.G.; Leigh, D.A.; Nepogodiev, S.A.; Slawin, A.M.Z.; Teat, S.J.; Wong, J.K.Y. *J. Am. Chem. Soc.* **2001**, *123*, 5983.
2. (a) Jeon, K.S.; Choi, J.S.; Chang, S.Y.; Chang, H.Y. *Angew. Chem. Int. Ed. Engl.* **2000**, *39*, 1692; (b) Chang, S.Y.; Choi, J.S.; Jeon, K.S. *Chem. Eur. J.* **2001**, *12*, 2687.
3. Wong, J.K.Y.; Leigh, D.A. unpublished results.
4. Schergna, S.; Leigh, D.A. paper in preparation.
5. Gatti, F.G. PhD Thesis, University of Warwick, **2001**.

6. a) Brouwer, A.M.; Frochot, C.; Gatti, F.G.; Leigh, D.A.; Mottier, L.; Paolucci, F.; Roffia, S.; Wurpel, G.W.H. *Science* **2001**, 291, 2124. (b) Sauvage, J.P. *Science* **2001**, 291, 2105.
7. Frochot, C.; Brouwer, A.M. unpublished results.
8. Ahmad, R.; Sondheimer, F.; Weedon, B.C.L.; Woods, R.J. *J. Chem. Soc.* **1952**, 4089.

Chapter Four

4. Naphthalene Functionalised Macrocycle.

Abstract: Rotaxanes currently enjoy a great deal of interest due to their unique topological and dynamic properties.¹ Further to our initial studies on the hydrogen bond-directed rotaxane synthesis based on threads containing different templating amide groups and the benzylic tetramide macrocycle **27**,² here we report the synthesis of a novel class of rotaxanes containing a naphthalene tetramide macrocycle which has a larger cavity (**97**). Several rotaxanation experiments based on macrocycle **97** precursors and threads containing several possible templating motifs were examined. The success of rotaxane formation using threads containing the fumaric or muconic templates opens up new possibilities in the development of these supramolecular systems and in particular for photochemical switching applications ¹⁰ due to the presence of a potential sensitising group in the macrocyclic wheel.

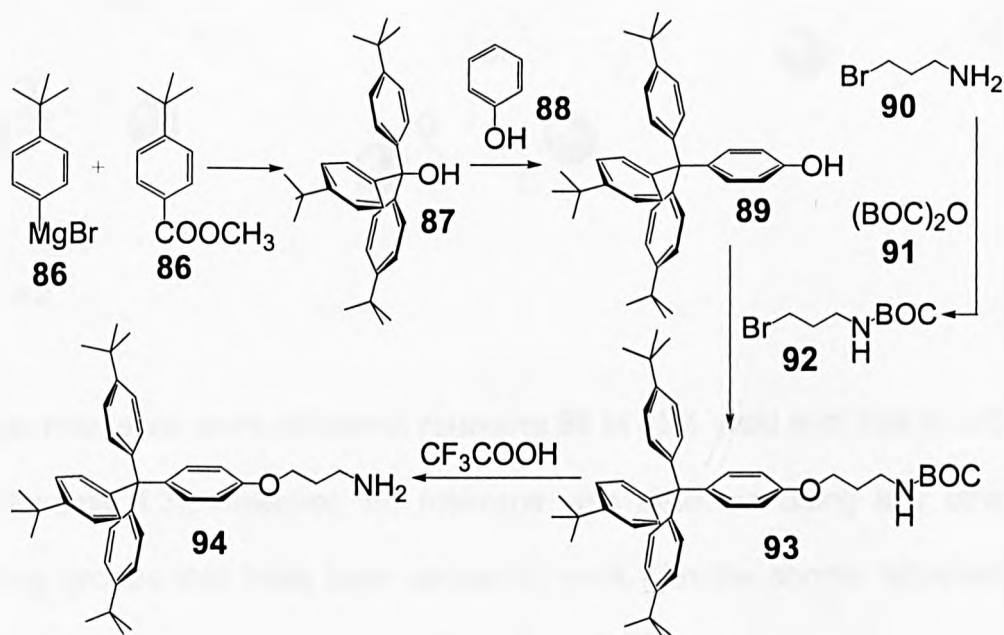
Introduction: In recent years supramolecular ³ chemistry has evolved from being nothing more than an interesting "anomaly" into an important field of research with a constantly increasing variety of applications in modern chemistry such as in chemical synthesis and catalysis, in material science and in life sciences.⁴ Realising that supramolecular interactions affect important process (both natural and artificial),⁵ supramolecular chemistry has given a fresh impetus to modern organic chemistry.⁶ Mechanically interlocked

molecules such as catenanes, knots and rotaxanes can offer the intricate architectures associated with templated assembly together with the robustness of traditional covalent architecture. Perhaps the most versatile interlocked architecture is found in the rotaxane. A rotaxane is a mechanically interlocked molecule constituted by two, or more species - a central linear thread and one or more macrocyclic rings - connected through weak interactions like hydrogen-bonding, π -stacking, electrostatic and van der Waal interactions according to Emil Fisher's key/lock principle.⁷

There are many comparative studies between a single macrocycle (host) and several threads (guests) reported,^{8,14} but relatively few examples between a single thread (guest) and several macrocycles (hosts) have been studied.⁹ This is mainly due to the precise requirement of the macrocyclic host to fit a specific functional group type via a key supramolecular interaction. In the two previous chapters (Chapter Two and Chapter Three) the multi-point binding process that act as the basis of rotaxane formation was studied as a function of the characteristics of the threads (rigidity, geometry, distances, use of different hydrogen donor groups etc.). Here, instead, it will be studied as a function of the distance between the two isophthaloyl bis-amide receptors of a tetramide macrocycle by varying the cavity size.⁹

Results and discussion: In order to evaluate the interactions that are at the heart of the rotaxane forming process two variables were considered: [**a**] the thread and [**b**] the macrocycle. The effects induced using the thread as a variable and the macrocyclic wheel as a constant were highlighted in the previous chapters (Chapters Two and Three). On the contrary, we now plan

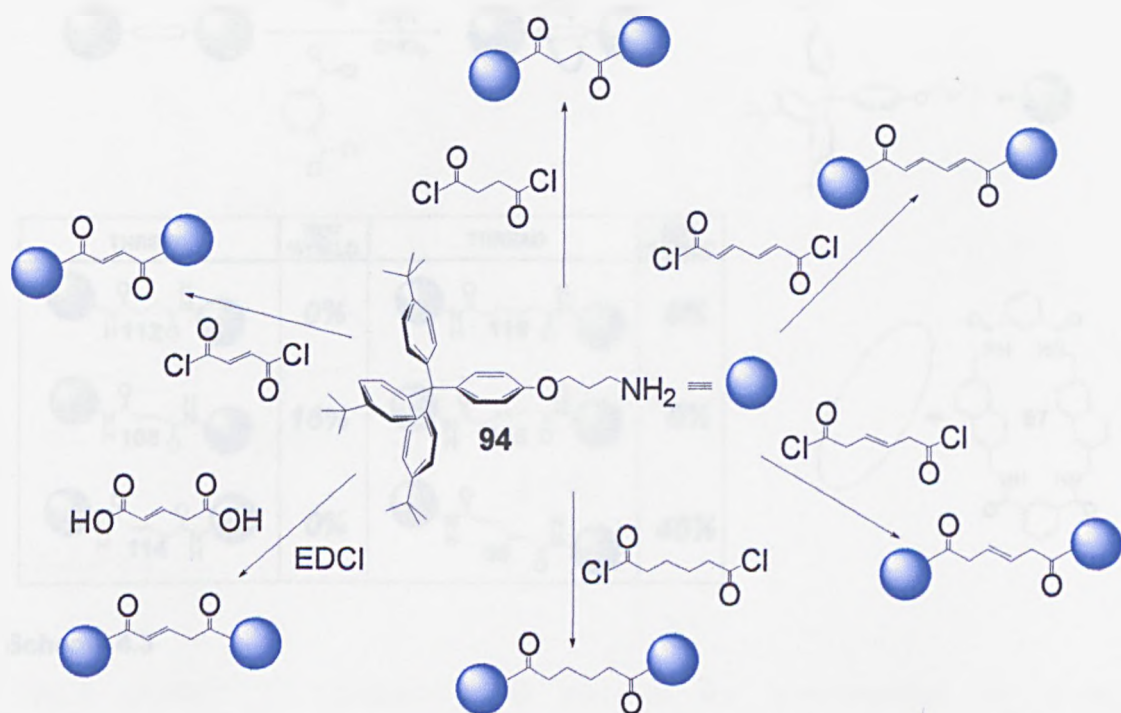
to use the thread as a constant and the macrocycle as a variable by using a naphthalene diamide instead of *p*-xylenediamine. The larger dimension of the cavity of the macrocyclic wheel **97**, require the development of new, bigger stoppers. The new stopper should not only be able to block a larger macrocycle by its considerable bigger size, but also should be able to increase the very low solubility of the muconic-based threads in non-polar solvents (see Chapter Two). The amino functionalised stopper **94** was prepared in a four step synthetic route from commercially available compounds,¹⁰ (Scheme 4.1).



Scheme 4.1

The threads were easily accessed by coupling of the amine stoppers with the required diacid chloride or activating the diacid with EDCI. The required amine, 2,6-bis(aminomethyl)naphthalene was prepared in a two step synthesis from commercially available 2,6-naphthalene-dicarboxylic acid.¹³ It was then used

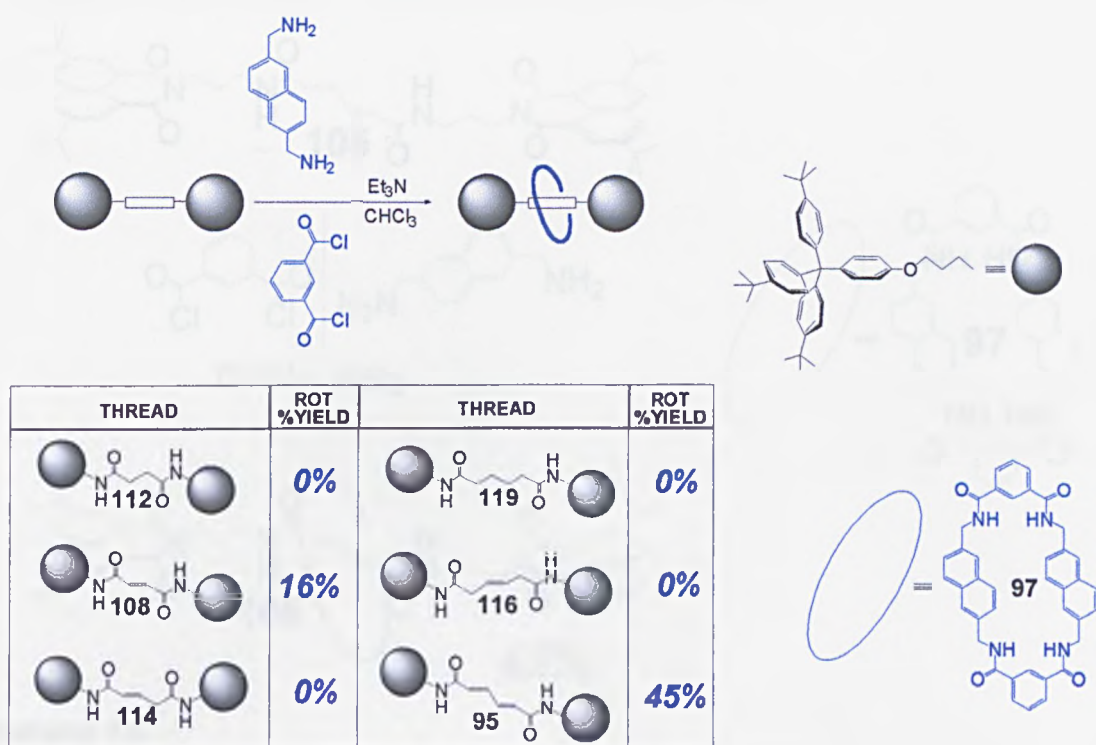
in an identical manner to p-xylenediamine by condensation with isophthaloyl dichloride **22** in a chloroform solution of the thread (Scheme 4.2).¹⁷



Scheme 4.2

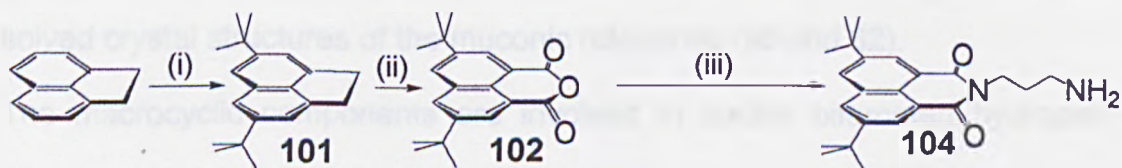
Two new rotaxanes were obtained: rotaxane **96** in 45% yield and **109** in 16% yield (Scheme 4.3); however, no rotaxane was detected using any other templating groups that have been shown to work with the shorter tetramide macrocycle **27** (Table 3.1 – Chapter Three).

In the naphthalenic-based rotaxane formation process, rigidity would seem to be an even more important factor than in the templating of the small macrocycle **27**. No flexibility between the carbonyls of the threads are tolerated at all with only the fumaric and muconic threads **108** and **95** able to act as templates.

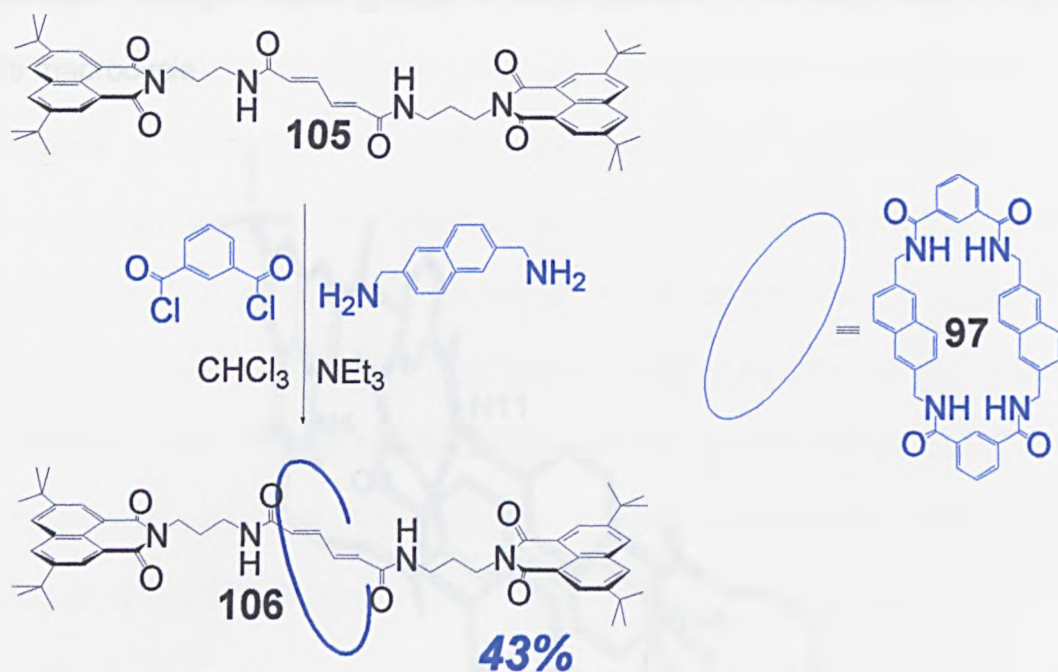


Scheme 4.3

Inspired by the photoinduced molecular shuttle based on a hydrogen-bonded based rotaxane containing a naphthalimide unit as one of the two stoppers and published by *Leigh et al.*¹² a new stopper (**104**) was prepared in a three synthetic step route (scheme 4.4).^{10,11}

Scheme 4.4 (i) *tert*-butyl chloride; (ii) sodium dichromate; (iii) 1,3-diaminopropane **103**.

Rotaxane **106** was obtained in 43% yield (Scheme 4.5).



Scheme 4.5

Single crystals of rotaxane **106** suitable for investigation by X-ray crystallography using a synchrotron source were obtained from the slow evaporation of methanol into a solution of rotaxane **106** in chloroform (Figure 4.1).

The newly solved structure of rotaxane **106** allows the comparison with the crystal structure of the original fumaramide rotaxane and with the previously solved crystal structures of the muconic rotaxanes (**58** and **62**).

The macrocyclic components are involved in doubly bifurcated hydrogen-bonding to the muconicamide. The templating group is close to planar with the aromatic rings while the naphthalene macrocycle adopts a favourable chair conformation. The planarity between olefins of the thread and naphthalene units of the macrocycle is probably due to π - π stacking interactions between the double bonds of the thread and the naphthalene units of the macrocycle. Additional π - π stacking interactions are formed

between the naphthalene groups of the stoppers and the isophthaloyl rings of the macrocycle.

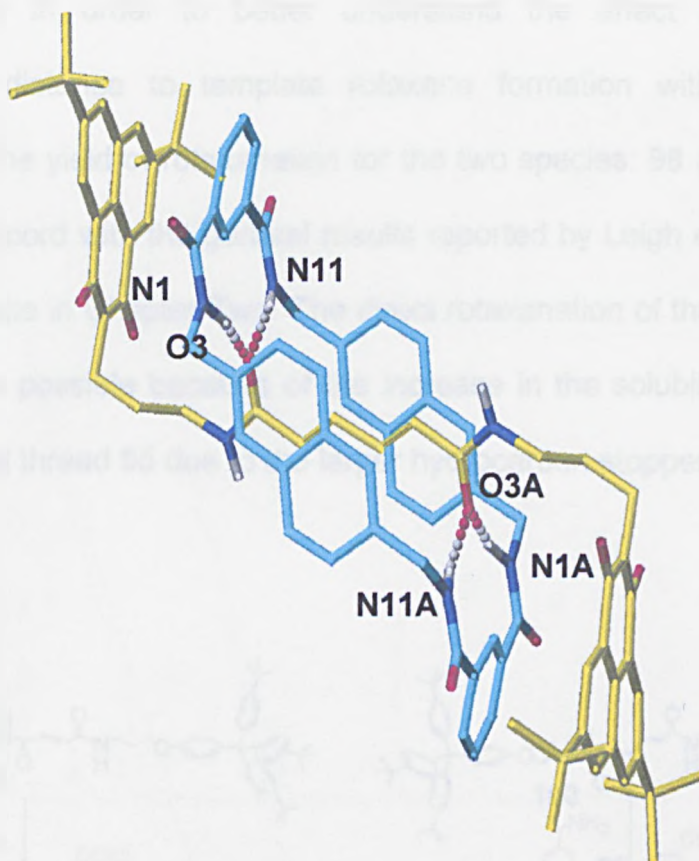
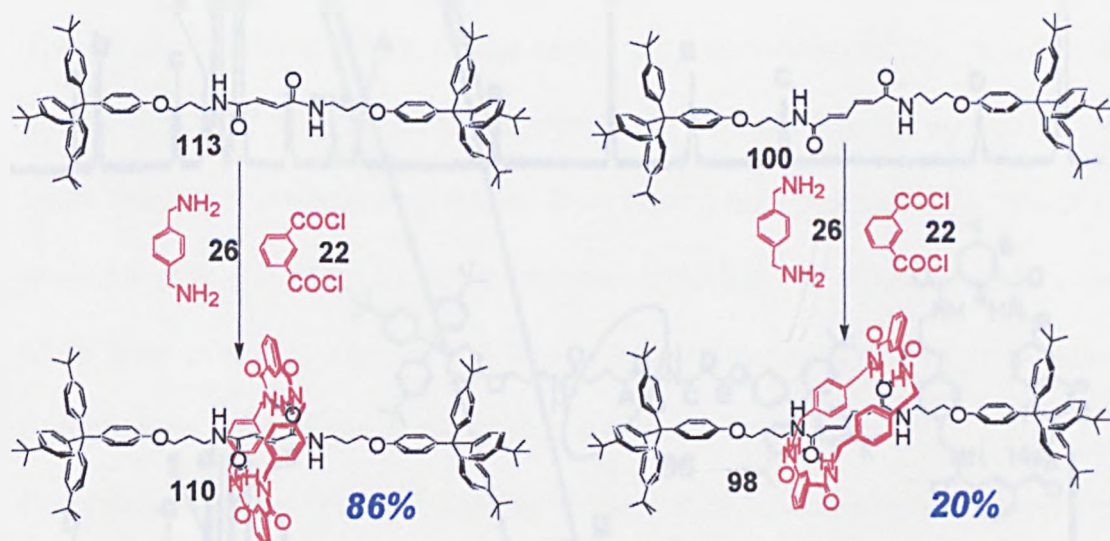


Figure 4.1 Solid state structure of rotaxane **106**. For clarity carbon atoms of the macrocyclic ring are shown in light blue and the carbon atoms of the muconic thread in yellow; oxygen atoms are depicted red, nitrogen atoms dark blue and hydrogen atoms white. Non H-bonding hydrogens have been removed for clarity. Selected interatomic distances [Å]: N1-O3 2.892, N1A-O3A 2.892,, N11-O3 2.979, N11A-O3A 2.979.

The high yield of rotaxane **96** and **106** achieved by combining the muconicamide based templating group (**95**, **105**) with the macrocycle containing the larger cavity contrasts with the lower yield of the rotaxane (**109**) for the fumaric based thread (**108**) with the much shorter distance between the templating amides. As a test, rotaxane formation using *p*-

xylylene diamine instead of 2,6-bis(aminomethyl) naphthalene was also performed on a fumaric thread (**108**) and a *trans,trans* muconic thread (**95**) (Scheme 4.6) in order to better understand the effect of the longer intercarbonyl distance to template rotaxane formation with the smaller macrocycle. The yield of rotaxanation for the two species: **98** (20%) and **110** (86%), is in accord with the general results reported by Leigh *et al.*¹⁴ and the additional results in Chapter Two. The direct rotaxanation of the *E,E*-muconic thread **95** was possible because of the increase in the solubility of the *E,E*-muconic based thread **95** due to the larger hydrocarbon stoppers.



Scheme 4.6

The results indicate that the best yields are obtained when there is a match between the macrocycle component and the templating thread. The larger naphthalene macrocycle best templated by muconic based threads and the smaller xylylene macrocycle best templated by fumaric based threads.

The ^1H -NMR spectra of thread **95** and rotaxanes **96** and **98** in CDCl_3 are shown in Figure 4.2.

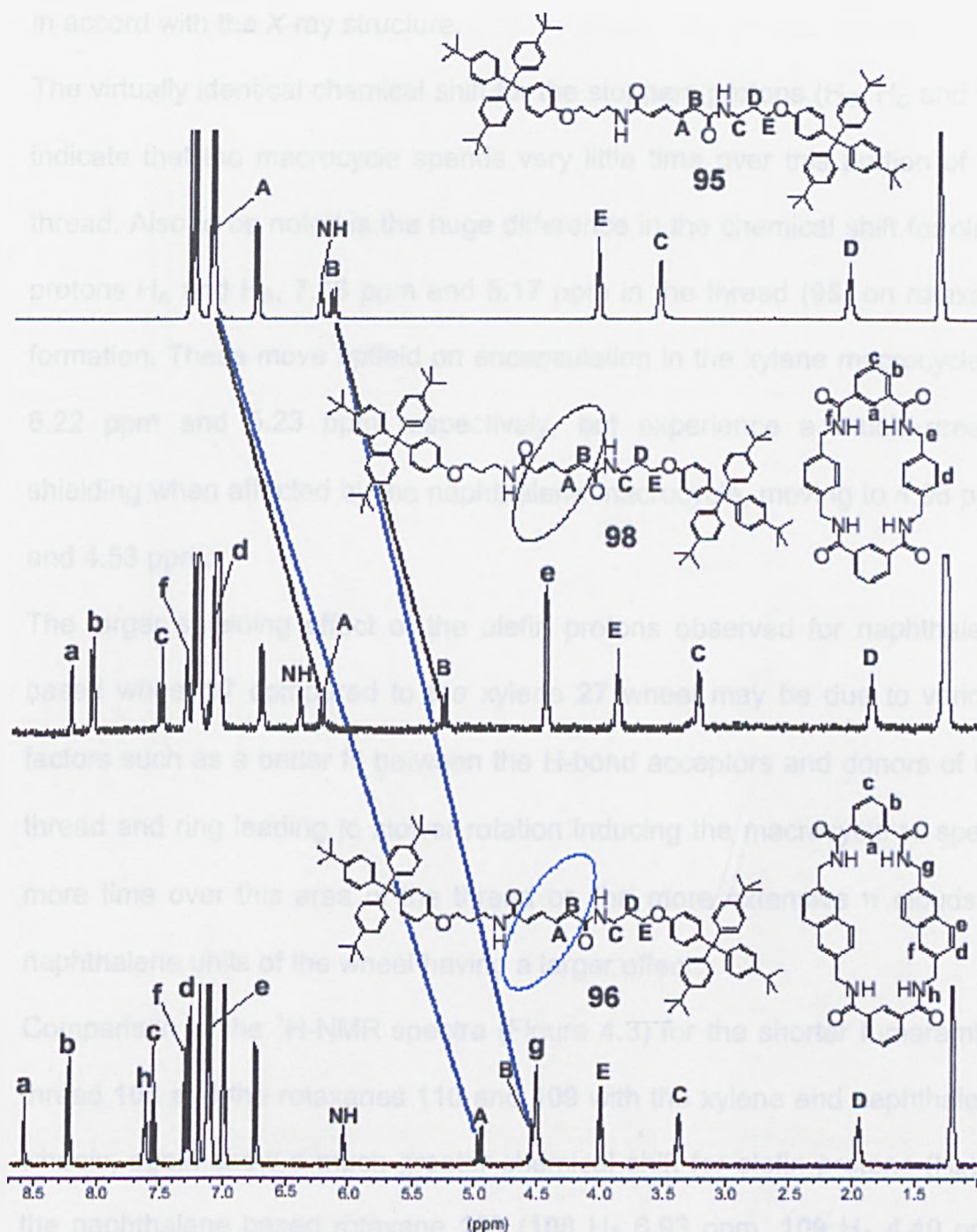


Figure 4.2 ^1H -NMR spectra (400 MHz, CDCl_3) of muconic thread **95** and muconic rotaxane **98** and **96**.

Comparison of the spectra shows that the predominant conformations adopted in solution by the interlocked components is similar for the two

rotaxanes. The central vinyl part of the thread is shielded because hydrogen bonding locates the encompassing macrocycle over the olefins which is also in accord with the X-ray structure.

The virtually identical chemical shift for the stoppers protons (H_C , H_D and H_E) indicate that the macrocycle spends very little time over this portion of the thread. Also to be noted is the huge difference in the chemical shift for olefin protons H_A and H_B , 7.23 ppm and 6.17 ppm in the thread (**95**) on rotaxane formation. These move upfield on encapsulation in the xylene macrocycle to 6.22 ppm and 5.23 ppm respectively, but experience a much greater shielding when affected by the naphthalene macrocycle, moving to 4.96 ppm and 4.53 ppm.

The larger shielding effect of the olefin protons observed for naphthalene based wheel **97** compared to the xylene **27** wheel may be due to various factors such as a better fit between the H-bond acceptors and donors of the thread and ring leading to slower rotation inducing the macrocycle to spend more time over this area of the thread or, the more extensive π clouds of naphthalene units of the wheel having a larger effect.

Comparison of the ^1H -NMR spectra (Figure 4.3) for the shorter fumaramide thread **108** and the rotaxanes **110** and **109** with the xylene and naphthalene wheels; again show a much greater chemical shift for olefin protons (H_A) in the naphthalene based rotaxane **109** (**108** H_A 6.93 ppm, **109** H_A 4.49 ppm and **110** H_A 5.71 ppm).

On the contrary the strength of the hydrogen bonding in the naphthalene rotaxane (**109**) is now much weaker due to the poor fit between the short fumaramide thread (**108**) and the naphthalene wheel. As the shielding effect

of the olefin protons cannot be justified by a better hydrogen-bond network between thread and macrocycle, more extended π clouds in the naphthalene units (π - π stacking with the olefins of the thread and a high electronic ring current) seems to be responsible for this high shielding effect.

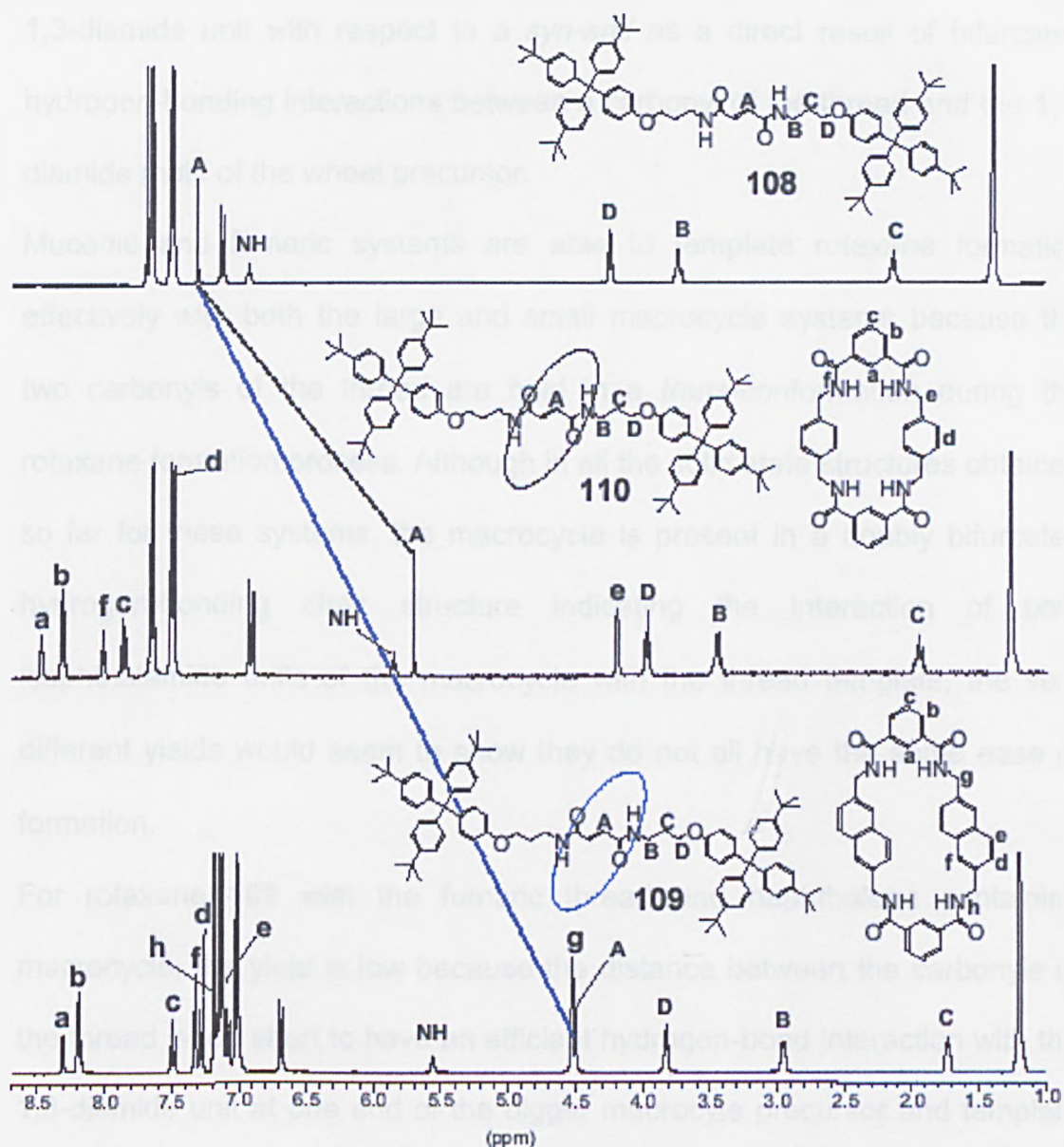


Figure 4.3 ^1H -NMR spectra (400 MHz, CDCl_3) of fumaric thread **108** and fumaric rotaxane **110** and **109**.

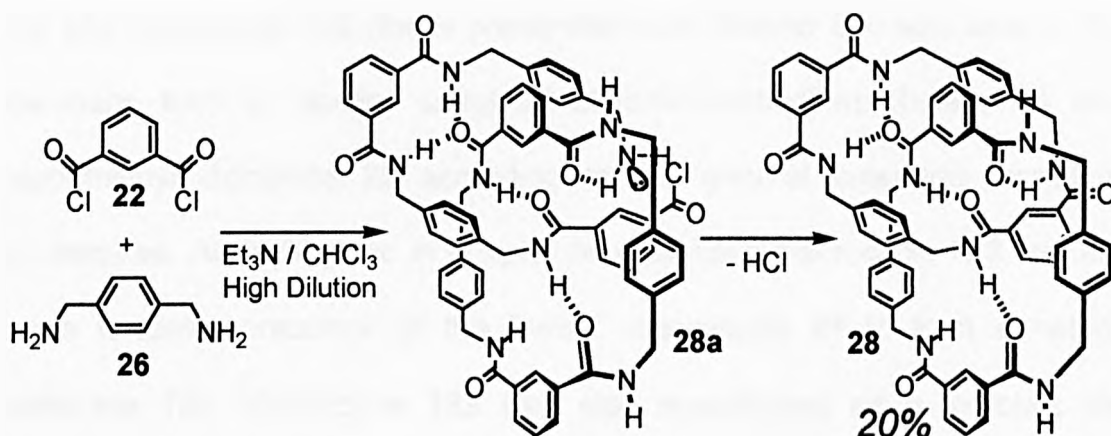
Assuming that rotaxane formation is a five-component clipping assembly process from macrocycle precursors and thread,^{2,15,16} the distance and the

geometry of the five amide groups (two on the thread and three in the macrocyclic precursor) involved in this co-operative multi-point hydrogen-bonding interaction process play a key role in producing a rotaxane. The presence of such templating effects lead to a *syn-syn* conformation of the 1,3-diamide unit with respect to a *syn-anti* as a direct result of bifurcated hydrogen-bonding interactions between a carbonyl of the thread and the 1,3-diamide motif of the wheel precursor.

Muconic and fumaric systems are able to template rotaxane formation effectively with both the large and small macrocycle systems because the two carbonyls of the thread are held in a *trans*-conformation during the rotaxane formation process. Although in all the solid state structures obtained so far for these systems, the macrocycle is present in a doubly bifurcated hydrogen-bonding chair structure indicating the interaction of both isophthalamide units of the macrocycle with the thread template; the very different yields would seem to show they do not all have the same ease of formation.

For rotaxane **109** with the fumaric thread and naphthalene containing macrocycle, the yield is low because the distance between the carbonyls of the thread is too short to have an efficient hydrogen-bond interaction with the 1,3-diamide unit at one end of the bigger macrocycle precursor and template the ring closing at the other end. On the contrary, the relatively low yield for the rotaxane **98** is due to the excessive distance between the carbonyls of the muconic thread to template the formation of the smaller macrocycle.

The high yields of rotaxanation for compounds **96** and **110** is a direct consequence of the match of thread and macrocycle (lock & key) that leads to better hydrogen-bonding interactions to template rotaxane formation.



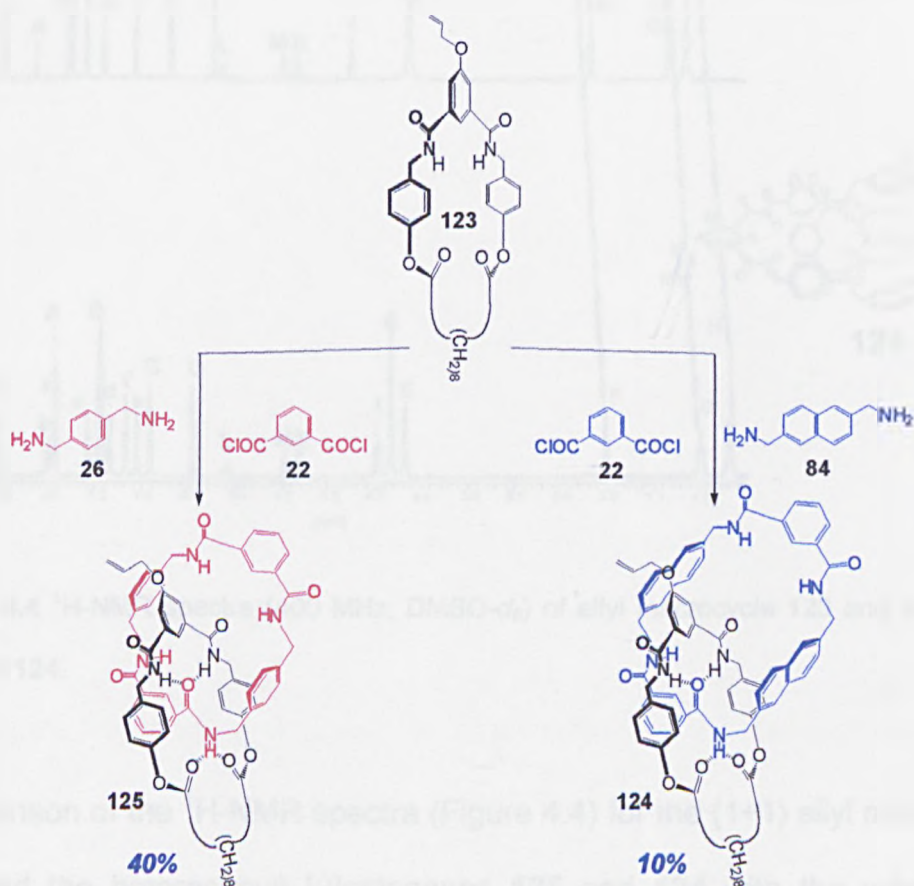
Scheme 4.7

Leigh and co-workers reported the synthesis of a benzylic amide catenane **28** in 20% yield¹⁷ from the reaction of *para*-xylylenediamine and isophthaloyl dichloride with NEt_3 in CHCl_3 at high dilution (Scheme 4.7). The catenane **28** was the only product left in solution at the end of the reaction as all the other products including the [2+2] macrocycle precipitated out of solution. The catenane **28** remains due to the fact that its hydrogen bonding requirements are satisfied intramolecularly. It is believed that this process occurs because one macrocycle acts as a template for the other *via* an intermediate such as **28a**. The synthesis proved to be remarkably tolerant to the use of a range of diacid chlorides and diamines in the synthesis of hydrogen bond-assembled catenanes.¹⁵

The low yield of homo catenane formation (**97a**)¹⁵ with 2,6-bis (aminomethyl) naphthalene **84** and isophthaloyl dichloride **22** with respect to the original

catenane **28** seems to indicate that the macrocycle **97** doesn't have the right dimensions or cannot adopt the appropriate conformation to act as a strong template for self replication.

To confirm this hypothesis two more experiments were attempted. In the first, the allyl macrocycle **123** (for its preparation see Chapter Six) was used in the catenane forming reaction using 2,6-bis(aminomethyl)naphthalene **84** and isophthaloyl dichloride **22** according to the general catenane formation procedures. As highlighted in chapter two, aliphatic macrocycle **123** can act as a template precursor of the "small" macrocycle **27** to form a hetero catenane **125**. Macrocycle **123** was also investigated as a template for catenane formation with the longer bis amine (Scheme 4.8).



Scheme 4.8

Reaction of macrocycle **123** with isophthaloyl dichloride **22** and 2,6-bis (aminomethyl)naphthalene **84** gave the heterocircuit [2]catenane **124** after column chromatography. The yield (10%) was low compared to the analogous catenane based on **123** and the smaller macrocycle **27** (40%).

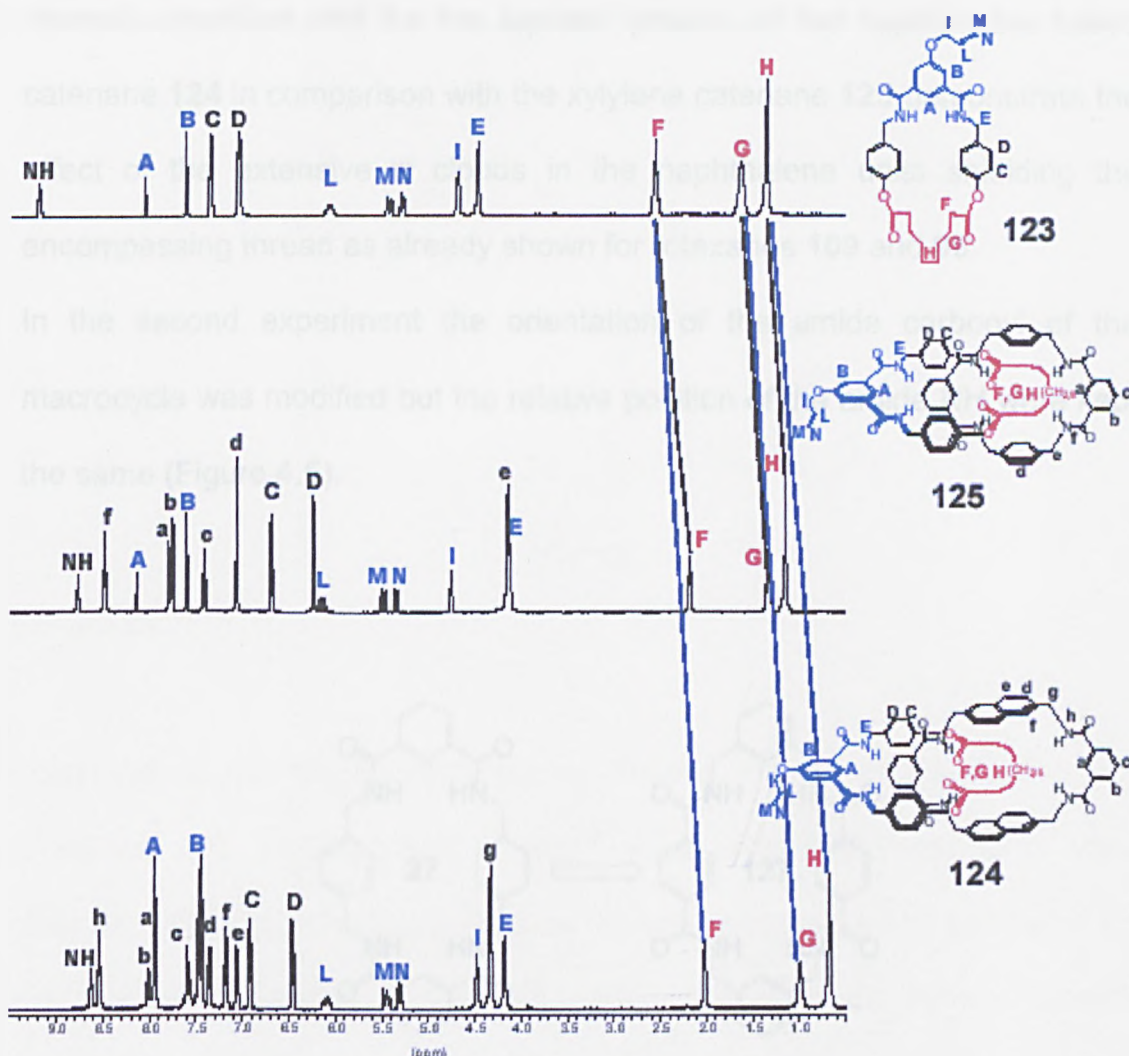


Figure 4.4 ^1H -NMR spectra (400 MHz, $\text{DMSO}-d_6$) of allyl macrocycle **123** and catenanes **125** and **124**.

Comparison of the ^1H -NMR spectra (Figure 4.4) for the (1+1) allyl macrocycle **123** and the heterocircuit [2]catenanes **125** and **124** with the xylene and naphthalene wheels in $\text{DMSO}-d_6$, a hydrogen-bond accepting solvent, show that the protons H_A , H_B and $\text{H}_{\text{NHamphiphilic macro}}$ occur at similar chemical shift in

the macrocycle and hetero [2]catenanes; however, the protons of the sebacoyl chain of the catenanes are heavily shielded with respect to those of the analogous macrocycle (Figure 4.4) indicating the location of the wheel on the aliphatic portion of the amphiphilic macrocycle **123**. However, the more dramatic chemical shift for the aliphatic protons of the naphthalene based catenane **124** in comparison with the xylene catenane **125** demonstrate the effect of the extensive π clouds in the naphthalene units shielding the encompassing thread as already shown for rotaxanes **109** and **96**.

In the second experiment the orientation of the amide carbonyl of the macrocycle was modified but the relative position of the amide NH were kept the same (Figure 4.5).

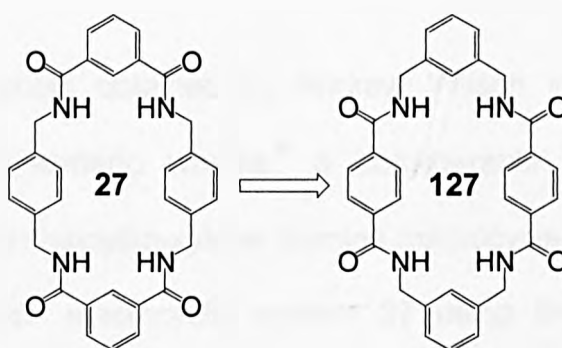
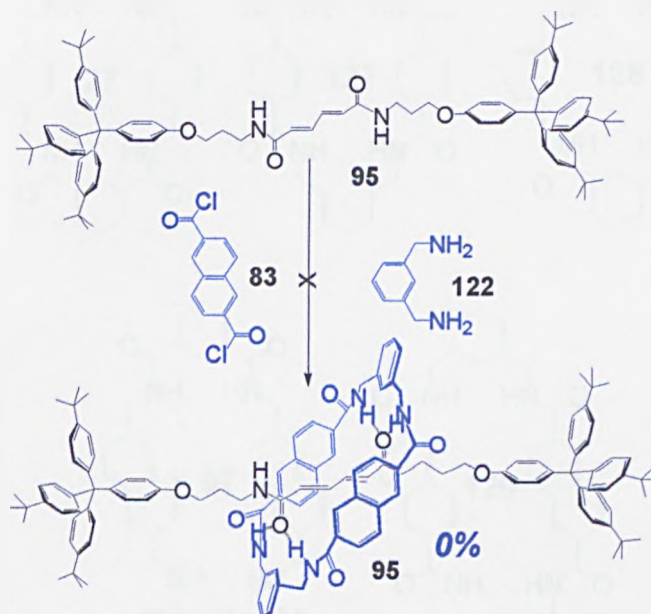


Figure 4.5

Investigations applying this sort of modification to the "small" macrocycle system and using m-xylylenediamine (**121**) and terephthaloyl dichloride (**126**) still gave rotaxane formation but in greatly reduced yield.⁹

No rotaxane formation was detected using thread **95**, *m*-xylylenediamine and 2,6-naphthalenedicarboxyl dichloride (**83**) as precursors following the usual rotaxation procedure (Scheme 4.9).



Scheme 4.9

According to the results obtained by Andrew Wilson in his studies on rotaxanes with regioisomeric wheels,⁹ a considerable lower yield was obtained for the terephthaloyl/*m*-xylene diamine macrocycle **127** compared to the "normal" tetramide macrocyclic system **27** using the fumaric based template. Nevertheless, rotaxane formation was observed for the small macrocycle system. Additionally using *m*-xylylene diamine and 2,6-naphthalenedicarboxyl dichloride as precursors, no catenane was isolated implying that the macrocycle does not self-template to yield catenane either. This poor capability of the macrocycle **97** to act as a template for catenane formation may also be an important factor in the high yield obtained for

rotaxane **96** where the side reaction of catenane formation does not complete.

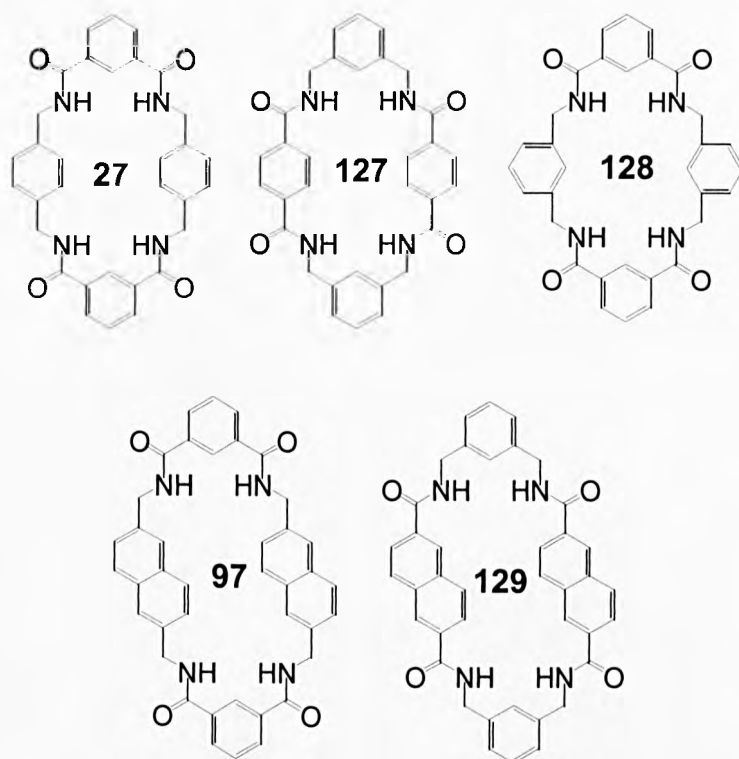


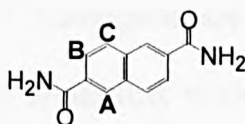
Figure 4.6

Conclusions: Rotaxanes containing a new macrocycle based on 2,6-bis (aminomethyl)naphthalene have been synthesised. Variation of the thread component has been investigated and the best yield of rotaxanation was achieved with the larger *E,E*-muconic system. A comparison of rotaxane yields with different macrocycles was also conducted. In the previous chapters, increasing the distance between the carbonyl groups with respect to the fumaric-based model was an important limitation in promoting rotaxane formation. Using a naphthalene precursor instead of the analogous xylene macrocycle, the bigger dimensions (larger cavity) give a better fit with the muconic based system to extend the hydrogen-bond motif, demonstrating

once more that the rotaxane formation process is a lock & key mechanism where the distances and geometries of the species involved in the non covalent interaction play a key role. Rotaxanes containing the new naphthalene macrocycle are expected to have novel chemical and photochemical properties.

Experimental Part:

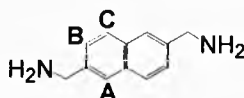
2,6-Naphthalenedicarboxamide (**83**)¹⁴



2,6-Naphthalene dicarboxylic acid **81** (10.0g, 46.0 mmol), thionyl chloride (80 mL) and DMF (2 mL) were stirred and heated to reflux overnight in a 250 mL one-necked flask equipped with a condenser. After cooling to RT, the volatiles were removed by rotary evaporation under reduced pressure. Dry chloroform (200 mL) was added to the residue and stirred. Ammonia gas was bubbled into the solution with the immediate formation of a white precipitate. After the addition the mixture was stirred at RT for 1h and then filtered, washed with hot water (500 mL) and dried to give compound **83** as a white powder (9.0 g, 42.1 mmol, 91 %).

m.p. 338-340°C (Lit. m.p. 339-340°C.¹⁴); ¹H NMR (400 MHz, DMSO-*d*₆): δ = 8.51 (s, 2H, ArH_A), 8.19 (s, 2H, *syn*-CONH), 8.06 (AB q, 2H, *J* = 8.5 Hz, ArH_B), 8.00 (AB q, 2H, *J* = 8.5 Hz, ArH_C), 7.54 (s, 2H, *anti*-CONH).

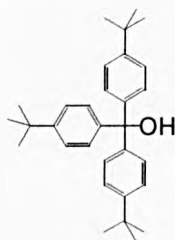
2,6-Bis(aminomethyl)naphthalene (**84**)¹⁴



2,6-Naphthalenedicarboxamide **83** (2.4g, 11.0 mmol) was placed in a 250 mL one-necked flask and borane-THF solution (1M, 110 mL) was added via a graduated additional funnel under nitrogen. The slurry was heated to reflux with stirring for 48h resulting in a clear solution. The solution was cooled using an ice bath and the excess of borane decomposed by a slow addition of conc. HCl (80 mL). The homogeneous milky suspension was then transferred to a 1 L flask, the apparatus rinsed with 4M HCl and the water was removed by rotary evaporation at 75°C. The residue was diluted with water (250 mL), and the solution made alkaline (pH~14) by addition of NaOH pellets. The mixture was extracted with chloroform (2×100 mL) and the combined organic layer dried over magnesium sulphate, filtered and the solvent removed by rotary evaporation to afford 2,6-bis (amino methyl)naphthalene **84** as a white powder (1.8 g, 9.7 mmol, 88%).

m.p. 139-141°C (Lit. m.p. 139-141°C.¹⁴); ¹H NMR (400 MHz, DMSO-*d*₆): δ= 7.76 (d, *J*= 8.0 Hz, 2H, ArH_B), 7.70 (s, 2H, ArH_A), 7.40 (dd, 2H, *J*= 8.0 + 2.1 Hz, ArH_C), 4.00 (s, 4H, CH₂), 1.64 (bs, 4H, NH₂).

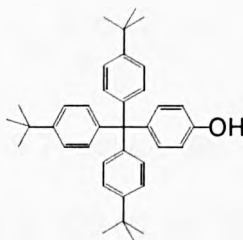
Tris(*p*-*tert*-butylphenyl) methanol (87**)**¹¹



In an oven-dried 2 L three-necked flask equipped with a condenser, dropping funnel, mechanical stirrer, and nitrogen system were placed magnesium turnings (12.2g, 500.0 mmol) with dry THF (75 mL). A catalytic amount of dibromo ethane was added and *p*-*tert*-butylbromobenzene **85** (100.0g, 469.0 mmol) in dry THF (600 mL) was added dropwise with gentle heating; when the reaction started the heated was removed and the *p*-*tert*-butylbromobenzene **85** was added dropwise over 1h. The reaction was stirred for a further 2h. The immediate formation of a brown colour was observed. 4-*tert*-Butylbenzoate **86** (30g, 220 mmol) was then added dropwise over 1h. The mixture was stirred overnight at reflux under nitrogen. The solution was cooled using an ice bath and neutralised with 10% HCl. The product was then extracted with n-hexane (2×350 mL) and the combined organic phases were washed with water (3×500 mL) and dried with MgSO₄. A yellow solid was obtained after removal of the solvent by rotary evaporation. The solid was subjected to re-crystallisation twice from methanol to afford the product **87** as a white powder (59.1g, 333.0 mmol, 71%).

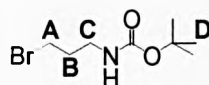
m.p. 214-215°C (Lit. m.p. 214-215°C.¹¹); ¹H NMR (400 MHz, CDCl₃): δ= 7.34 (dd, 12H, *J*= 16.8 + 8.7 Hz, ArH), 3.08 (s, 1H, OH), 1.35 (s, 27H, C(CH₃)₃).

Tris (*p*-*tert*-butylphenyl)(4-hydroxyphenyl) methane (89) ¹¹



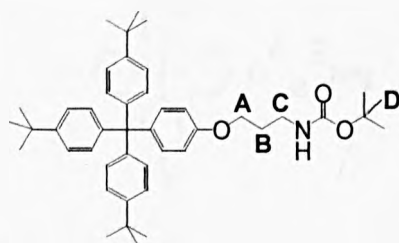
Tris(*p*-*tert*-butylphenyl) methanol **87** (13.0g, 30.3 mmol) was dissolved in phenol **88** (50.0g) by warming at 95°C in a 250 mL two necked flask equipped with a condenser and nitrogen system. HCl (36%, 1.5 mL) was added as a catalyst. A deep reddish-blue colour was observed immediately. After 3h the solution solidified spontaneously. The system was then cooled to room temperature and the product extracted with toluene (3×150 mL). The combined organic phases were washed in 1N NaOH solution (3×250 mL) then with water (3×250 mL) and dried with MgSO₄. The solution was decolorized with activated carbon and the solvent was removed on a rotary evaporator. The solid was boiled in n-hexane for 1h, filtered and recrystallised from a toluene-hexane mixture to obtain compound **89** as a white powder (11.5g, 22.8 mmol, 75 %).

m.p. 304-306°C (Lit. m.p. 304-306°C.¹¹); ¹H NMR (400 MHz, CDCl₃): δ= 7.27 (d, 6H, *J*= 8.8 Hz, ArH), 7.11 (d, 6H, *J*= 8.8 Hz, ArH), 7.08, (d, 2H, *J*= 8.8 Hz, ArH), 6.72 (d, 2H, *J*= 8.8 Hz, ArH), 1.34 (s, 27H, C(CH₃)₃).

(3-bromo-propyl)-carbamic acid *tert*-butyl ester (92)¹⁹

3-bromo-propylamine (10g, 45.7 mmol) **90** and di-*tert*-butylcarbonate **91** (11g, 50.2 mmol) were slurred in 500 mL of THF and chilled with ice/water to 5°C. To this solution was added 1N NaOH (60 mL), over approximately 30 mins. The solution was stirred overnight and allowed to warm to RT. To the reaction was added ethyl acetate (250 mL). The resulting layers were separated and the aqueous one was extracted again with ethyl acetate (100 mL). The combined organic extracts were washed with water (2×250 mL), dried with MgSO₄, filtered and removed at reduced pressure to give an oil that slowly crystallised (13.12g, 41.1 mmol, 90%).

m.p. 185-186°C (Lit. m.p. 185-186°C.¹⁹); ¹H NMR (400 MHz, CDCl₃): δ= 4.96 (bs, 1H, NH), 3.37 (t, *J*= 6.3 Hz, 2H, **A**), 3.19 (m, 2H, **C**), 1.98 (m, 2H, **B**), 1.37 (s, 27H, **D**).

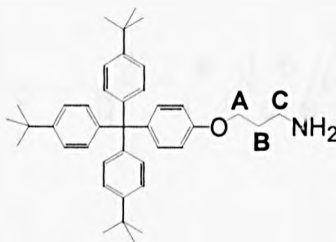
(3-{4-[Bis-(4-*tert*-butyl-phenyl)-(4-isopropyl-phenyl)-methyl]-phenoxy}-propyl)-carbamic acid *tert*-butyl ester (93)

Tris (*p-tert*-butylphenyl)(4-hydroxyphenyl) methane **89** (7.0g, 13.9 mmol) and bromide **92** (4.9g, 15.3 mmol) were dissolved in DMF (100 mL) in a 250-mL one necked flask equipped with a condenser. An excess of potassium carbonate was added and the mixture was allowed to stir at 100°C overnight.

The solution was then cooled to RT and 100 mL of water was added with the immediate formation of a white precipitate that was filtered, washed with water and dried under vacuum to give the product **93** as a white powder (7.7 g, 11.6 mmol, 84 %).

m.p. 298-300°C; ^1H NMR (400 MHz, CDCl_3): δ = 7.27 (d, 6H, J = 8.8 Hz, ArH), 7.12 (d, 6H, J = 8.8 Hz, ArH), 7.11, (d, 2H, J = 8.8 Hz, ArH), 6.78 (d, 2H, J = 8.8 Hz, ArH), 4.85 (bs, 1H, NH), 4.03 (t, J = 6.3 Hz, 2H, **A**), 3.36 (m, 2H, **C**), 1.99 (m, 2H, **B**), 1.47 (s, 9H, **D**), 1.34 (s, 27H, $\text{C}(\text{CH}_3)_3$); ^{13}C NMR (100 MHz, CDCl_3): δ = 163.01 (CO), 148.71 (q, ArC), 144.64 (q, ArC), 144.54 (q, ArC), 140.19 (q, ArC), 132.79 (ArCH), 132.68 (ArCH), 131.14 (ArCH), 124.45 (ArCH), 69.64 (q, C), 66.14 (q, C), 63.46 (q, C), 38.59 (CH_2), 36.92 (CH_2), 34.69 (CH_2), 31.80 (CH_3), 28.84 (CH_3). FAB MS (*m*BNA matrix) m/z 661 [$\text{M}-\text{H}$] $^+$. Anal. Calcd for $\text{C}_{45}\text{H}_{59}\text{NO}_3$ (661.95): C, 81.65; H, 8.98; N, 2.12. Found: C, 81.52; H, 8.91; N 1.99.

3-{4-[Bis-(4-*tert*-butyl-phenyl)-(4-isopropyl-phenyl)-methyl]-phenoxy}-propylamine (94)

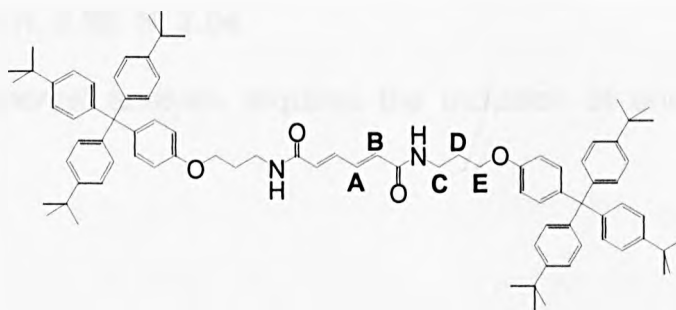


(3-{4-[Bis-(4-*tert*-butyl-phenyl)-(4-isopropyl-phenyl)-methyl]-phenoxy}-propyl)-carbamic acid *tert*-butyl ester **93** (7.5 g, 11.3 mmol) was dissolved in a mixture DCM (30 mL) and trifluoroacetic acid (30 mL) in a 250 mL one necked flask. The solution was stirred at RT over night. A white solid was

obtained after the solvent and the acid were eliminated by rotary evaporation. The white powder was then dissolved in chloroform (100 mL) and washed with potassium bicarbonate (2×75 mL), water (2×75 mL), dried with MgSO₄, filtered and the solvent removed by rotary evaporation. The product **94** was isolated as a white powder (6.2 g, 11.0 mmol, 98 %).

m.p. 210-211°C; ¹H NMR (400 MHz, CDCl₃): δ= 7.26 (d, 6H, *J*= 8.8 Hz, ArH), 7.11 (d, 6H, *J*= 8.8 Hz, ArH), 7.09 (d, 2H, *J*= 8.8 Hz, ArH), 6.78 (d, 2H, *J*= 8.8 Hz, ArH), 4.06 (t, *J*= 6.3 Hz, 2H, **A**), 2.99 (m, 2H, **C**), 2.49 (vbs, 2H, NH), 1.98 (m, 2H, **B**), 1.34 (s, 27H, C(CH₃)₃); ¹³C NMR (100 MHz, CDCl₃): δ= 157.05 (q, ArC), 148.70 (q, ArC), 144.61 (q, ArC), 140.10 (q, ArC), 132.67 (ArCH), 131.13 (ArCH), 124.44 (ArCH), 113.33 (ArCH), 66.14 (q, C), 63.45 (q, C), 36.85 (CH₂), 34.69 (CH₂), 34.10 (CH₂), 31.79 (CH₃). FAB MS (*m*BNA matrix) *m/z* 562 [M⁺]. Anal. Calcd for C₄₀H₅₁NO (561.84): C 85.51; H 9.15; N 2.49. Found: C, 85.43; H, 9.16; N, 2.35.

***E,E*-Muconic thread (95)**

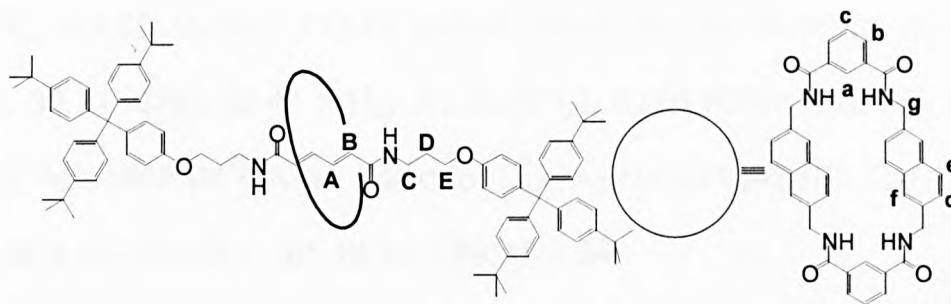


3-{ 4- [Bis- (4- tert- butyl- phenyl) - (4 – isopropyl - phenyl)- methyl]- phenoxy} propylamine **94** (1.0 g, 1.8 mmol) and triethylamine (189.0 mg, 1.9 mmol) were dissolved in chloroform (75 mL) in a 250 mL one necked flask under nitrogen. *E,E*-muconic acid dichloride (152.0 mg, 0.9 mmol) dissolved in

chloroform (50 mL) was added dropwise at RT over 1h. The solution was stirred at RT for 5h. The solution was washed with 1N aqueous NaOH solution (2×75 mL) then with water (3×75 mL) and dried with MgSO₄. A white solid was obtained after the solvent was eliminated by rotary evaporation. Thread **95** was isolated as a white powder after crystallisation from ethanol (952.0 mg, 0.8 mmol, 86%).

m.p. 174-175°C; ¹H NMR (400 MHz, CDCl₃): δ= 7.24 (d, 12H, *J*= 8.8 Hz, ArH), 7.23 (dd, 2H, *J*= 14.3 + 3.0 Hz, **A**), 7.12 (d, 4H, *J*= 8.8 Hz, ArH), 7.10 (d, 12H, *J*= 8.8 Hz, ArH), 6.77 (d, 4H, *J*= 8.8 Hz, ArH), 6.25 (t, 2H, *J*= 5.6 Hz, NH), 6.17 (dd, 2H, *J*= 14.3 + 3.0 Hz, **B**), 4.04 (t, 4H, *J*= 6.3 Hz, **E**), 3.55 (m, 4H, **C**), 2.04 (m, 4H, **D**), 1.33 (s, 54H, C(CH₃)₃); ¹³C NMR (100 MHz, CDCl₃): δ= 165.55 (CO), 156.73 (q, ArC), 148.75 (q, ArC), 144.49 (q, ArC), 140.41 (q, ArC), 138.12 (CH), 132.75 (ArCH), 131.11 (ArCH), 130.38 (CH), 124.58 (ArCH), 113.31 (ArCH), 66.41 (q, C), 63.45 (q, C), 38.81 (CH₂), 38.41 (CH₂), 34.75 (CH₂), 31.87 (CH₃). FAB MS (*m*BNA matrix) *m/z* 1229 [M-H]⁺. Anal. Calcd for C₈₆H₁₀₄N₂O₄.C₂H₅OH (1274.83): C, 82.84; H, 8.69; N, 2.20. Found: C, 82.92; H, 8.89; N, 2.04.

The correct elemental analysis requires the inclusion of one molecule of ethanol.

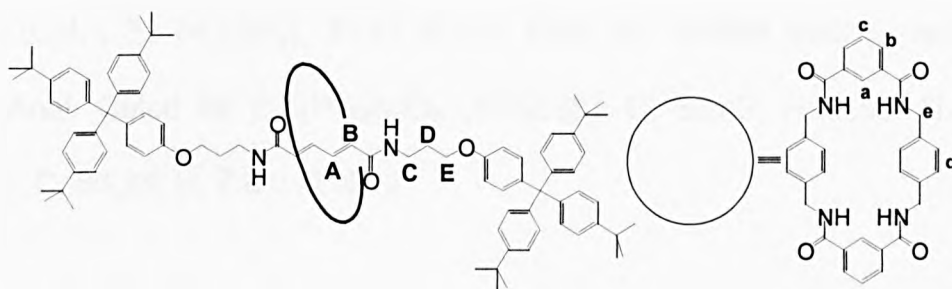
***E,E*-Muconic rotaxane (naphthalene macrocycle) (96)**

E,E-Muconic thread **95** (400.0 mg, 0.3 mmol) and triethylamine (1.1 mL) were dissolved in chloroform (50 mL), and stirred vigorously whilst solutions of the *p*-naphthalene diamine **84** (727.0 mg, 3.6 mmol) in chloroform (50 mL) and isophthaloyl dichloride **22** (792.0 mg, 3.6 mmol) in chloroform (50 mL) were simultaneously added over a period of 4h using motor-driven syringe pumps. The resulting suspension was filtered and concentrated under reduced pressure to afford the crude product. This mixture was then purified using silica gel chromatography (petroleum spirit/chloroform 3/2) to afford rotaxane **96** (252.0 mg, 0.14 mmol, 45%).

m.p. 323-324°C; ^1H NMR (400 MHz, CDCl_3): δ = 8.58 (s, 2H, **a**), 8.23 (dd, 4H, J = 7.9 + 1.4 Hz, **b**), 7.61 (t, 4H, J = 5.8 Hz, NH_{mac}), 7.55 (t, 2H, J = 7.9 Hz, **c**), 7.29 (s, 4H, **f**), 7.26 (d, 4H, J = 7.8 Hz, **d**), 7.13 (dd, 4H, J = 7.8 + 2.1 Hz, **e**), 7.12 (d, 12H, J = 8.8 Hz, $\text{ArH}_{\text{stopper}}$), 7.11 (d, 4H, J = 8.8 Hz, $\text{ArH}_{\text{stopper}}$), 6.99 (d, 12H, J = 8.8 Hz, $\text{ArH}_{\text{stopper}}$), 6.74 (d, 4H, J = 8.8 Hz, $\text{ArH}_{\text{stopper}}$), 6.04 (t, 2H, J = 5.6 Hz, $\text{NH}_{\text{thread}}$), 4.96 (dd, 2H, J = 14.3 + 3.0 Hz, **A**), 4.53 (dd, 2H, J = 14.3 + 3.0 Hz, **B**), 4.51 (d, 8H, J = 5.8 Hz, **g**), 4.00 (t, 4H, J = 6.3 Hz, **E**), 3.37 (m, 4H, **C**), 1.94 (m, 4H, **D**), 1.20 (s, 54H, $\text{C}(\text{CH}_3)_3$); ^{13}C NMR (100 MHz, CDCl_3): δ = 166.58 (CO), 166.44 (CO), 148.84 (q, ArC), 144.31 (q, ArC), 140.98 (q, ArC), 140.01 (q, ArC), 148.84 (q, ArC), 144.31 (q, ArC), 140.98 (q, ArC), 136.61 (ArCH), 135.87 (ArCH), 134.05 (CH), 133.01 (ArCH), 132.21

(ArCH), 131.05 (ArCH), 129.73 (ArCH), 128.46 (CH), 127.62 (ArCH), 124.51 (ArCH), 124.23 (ArCH), 113.29 (ArCH), 67.11 (q, C), 62.98 (q, C), 44.85 (CH₂), 39.21 (CH₂), 32.41 (CH₂), 31.75 (CH₂), 28.96 (CH₃). FAB MS (*m*BNA matrix) *m/z* 1862 [M⁺]. Anal. Calcd for C₁₂₆H₁₃₆N₆O₈ (1862.46): C, 81.26; H, 7.36; N, 4.51. Found: C, 81.12; H, 7.09; N, 4.34.

***E,E*-muconic rotaxane (benzylic macrocycle) (98)**

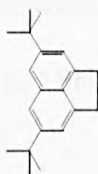


E,E-Muconic thread **95** (500.0 mg, 0.4 mmol) and triethylamine (1.4 mL) were dissolved in chloroform (50 mL), and stirred vigorously whilst solutions of the *p*-xylylene diamine **26** (665.0 mg, 4.8 mmol) in chloroform (40 mL) and isophthaloyl dichloride **22** (990 mg, 4.8 mmol) in chloroform (40 mL) were simultaneously added over a period of 4h using motor-driven syringe pumps. The resulting suspension was filtered and concentrated under reduced pressure to afford the crude product. The rotaxane was then isolated by silica gel chromatography (CHCl₃) to afford rotaxane **98** as a white powder (136.5 mg, 7.9·10⁻² mmol, 20%).

m.p. 317-318°C; ¹H NMR (400 MHz, DMSO-*d*₆): δ= 8.79 (t, 4H, *J* = 5.8 Hz, NH_{mac}), 8.23 (s, 2H, **a**), 7.93 (dd, 4H, *J*= 7.9 + 1.4 Hz, **b**), 7.74 (t, 2H, *J* = 5.6 Hz, NH_{thread}), 7.46 (t, 2H, *J* = 7.9 Hz, **c**), 7.30 (d, 12H, *J*= 8.8 Hz, ArH_{stopper}), 7.06 (d, 12H, *J*= 8.8 Hz, ArH_{stopper}), 7.04 (s, 8H, **d**), 6.93 (d, 4H, *J* = 8.8 Hz, ArH_{stopper}), 5.86 (dd, 2H, *J*= 14.3 + 3.0 Hz, **A**), 6.56 (d, 4H, *J* = 8.8 Hz,

ArH_{stopper}), 4.53 (dd, 2H, $J = 14.3 + 3.0$ Hz, **B**), 4.35 (d, 8H, $J = 5.8$ Hz, **e**), 3.55 (t, 4H, $J = 6.3$ Hz, **E**), 2.90 (m, 4H, **C**), 1.51 (m, 4H, **D**), 1.30 (s, 54H, C(CH₃)₃); ¹³C NMR (100 MHz, DMSO-*d*₆): $\delta =$ 166.21 (CO), 165.07 (CO), 155.32 (q, ArC), 147.87 (q, ArC), 147.08 (q, ArC), 144.56 (q, ArC), 141.12 (q, ArC), 139.99 (q, ArC), 137.55 (CH), 132.87 (ArCH), 131.51 (ArCH), 130.35 (ArCH), 130.08 (ArCH), 128.43 (CH), 127.37 (ArCH), 124.57 (ArCH), 123.86 (ArCH), 113.87 (ArCH), 70.98 (q, C), 66.59 (q, C), 42.69 (CH₂), 41.59 (CH₂), 38.35 (CH₂), 32.14 (CH₂), 31.47 (CH₃). FAB MS (*m*BNA matrix) m/z 1762 [M⁺]. Anal. Calcd for C₁₁₈H₁₃₂N₆O₈ (1762.35): C, 80.42; H, 7.55; N, 4.77. Found: C, 80.28; H, 7.61; N, 4.72.

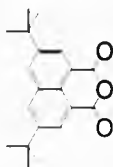
2,5-Di-*tert*-butylacenaphthene (**101**)¹²



Anhydrous aluminum chloride (53.3 g, 0.4 mol) was added during 1h to a stirred solution of acenaphthene **99** (30 g, 0.2 mol) and *tert*-butyl chloride **100** (39.6 g, 0.4 mol) in dry DCM (60 mL). The mixture was refluxed for 2h and then stirred at RT for 24h. The solution was washed in water (3×100 mL) and dried with MgSO₄. The organic phase was then filtered and concentrated at low pressure. The crude product was recrystallised from EtOH in colourless needles to afford 2,5-di-*tert*-butylacenaphthene **101** (38.0 g, 0.14 mol, 71%). Literature reported m.p. 164-165°C.¹²

m.p. 164-165°C; ¹H NMR (400 MHz, CDCl₃): $\delta =$ 7.63 (d, 2H, $J = 1.8$ Hz, ArH), 7.43 (d, 2H, $J = 1.7$ Hz, ArH), 3.47 (s, 4H, CH₂), 1.51 (s, 18H, C(CH₃)₃).

2,5-Di-*tert*-butylacenaphthylic anhydride (**102**)¹²

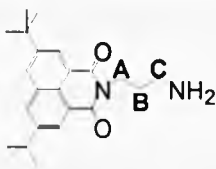


Sodium dichromate (40.0 g, 0.15 mol), was added to a solution of 2,5-di-*tert*-butylacenaphthene **101** (10.0 g, 37.5 mmol) in AcOH (300 mL) at 100°C and refluxed for 1h. After the starting material was completely consumed the reaction mixture was quenched by addition of ice water (500 g). The pale yellow precipitate was then filtrated and crystallized from EtOH as yellow needles to afford 2,5-di-*tert*-butylacenaphthylic anhydride **102** (7.6 g, 24.5 mmol, 65%).

Literature reported m.p. 186-187°C.¹²

m.p. 186-187°C; ¹H NMR (400 MHz, CDCl₃): δ= 8.25 (d, 2H, *J* = 1.8 Hz, ArH), 7.63 (d, 2H, *J*= 1.8 Hz, ArH), 1.51 (s, 18H, C(CH₃)₃).

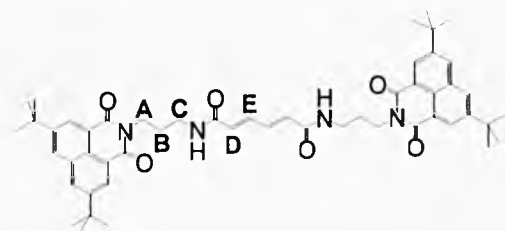
N-(3-propylamino)-2,5-Di-*tert*-butylacenaphthalimide (**104**)



2,5-Di-*tert*-butylacenaphthylic anhydride **102** (1.0 g, 3.2 mmol) was slowly added (dropping funnel) to a suspension of 1,3-diaminopropane **103** (716.0 mg, 9.9 mmol) in EtOH (100 mL) over a period of 1h. The reaction was then stirred at RT for 30 mins. The excess of 1,3-diaminopropane was eliminated by high vacuum distillation to leave the product **104** as a white powder (1.1 g, 3.2 mmol, 100%).

m.p. 209-210°C; ^1H NMR (400 MHz, CDCl_3): δ = 8.61 (d, 2H, J = 1.8 Hz, ArH), 8.11 (d, 2H, J = 1.8 Hz, ArH), 4.27 (t, 2H, J = 6.5 Hz, **A**), 2.75 (m, 2H, **C**), 1.85 (m, 2H, **B**), 1.45 (s, 18H, $\text{C}(\text{CH}_3)_3$); ^{13}C NMR (100 MHz, CDCl_3): δ = 165.13 (CO), 150.61 (q, ArC), 132.37 (q, ArC), 129.66 (q, ArC), 129.63 (q, ArC), 125.24 (ArCH), 122.32 (ArCH), 46.18 (q, C), 39.68 (CH_2), 37.96 (CH_2), 32.47 (CH_2), 31.56 (CH_3). FAB MS (*m*BNA matrix) m/z 367 [M^+]. Anal. Calcd for $\text{C}_{23}\text{H}_{30}\text{N}_2\text{O}_2$ (366.50): C, 75.37; H, 8.25; N, 7.64. Found: C, 75.22; H, 8.54; N, 6.72.

***trans,trans*-Muconic thread (105)**

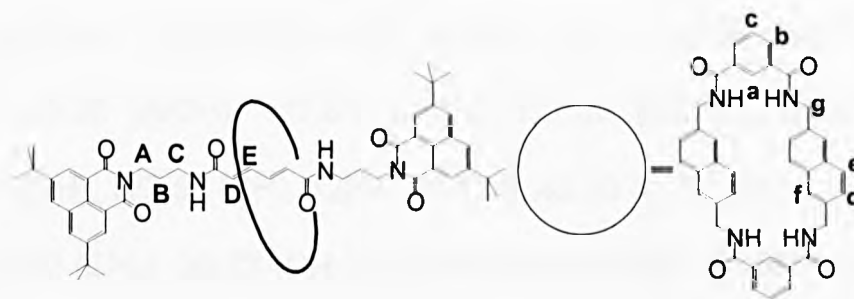


N-(3-propylamino)-2,5-di-*tert*-butylacenaphthalimide **104** (2.0 g, 4.9 mmol) and triethylamine (5.7 mL) were dissolved in chloroform (75 mL) in a 250 mL one necked flask under nitrogen. *trans,trans*-Muconic acid dichloride **55** (472.0 mg, 2.6 mmol) dissolved in chloroform (50 mL) was added dropwise at RT over 1h. The solution was stirred at RT over 5h. The solution was washed in NaOH solution (2×75 mL) then with water (3×75 mL) and dried with MgSO_4 . A white solid was obtained after the solvent was eliminated by rotary evaporation. Thread **105** was crystallised from ethanol as a white powder (2.0 g, 2.4 mmol, 92%).

m.p. 252-253°C; ^1H NMR (400 MHz, CDCl_3): δ = 8.58 (d, 2H, J = 1.8 Hz, ArH), 8.08 (d, 2H, J = 1.8 Hz, ArH), 7.27 (dd, 2H, J = 14.3 + 3.0 Hz, **E**), 6.83 (t, 2H,

$J = 6.1$ Hz, NH), 6.23 (dd, 2H, $J = 14.3 + 3.0$ Hz, **D**), 4.21 (t, 4H, $J = 6.5$ Hz, **A**), 3.32 (m, 4H, **C**), 1.93 (m, 4H, **B**), 1.41 (s, 18H, $\text{C}(\text{CH}_3)_3$); ^{13}C NMR (100 MHz, CDCl_3): $\delta = 165.61$ (CO), 165.53 (CO), 150.44 (q, ArC), 132.37 (q, ArC), 132.06 (CH), 129.64 (q, ArC), 129.60 (q, ArC), 125.24 (ArCH), 124.91 (CH), 121.70 (ArCH), 37.42 (q, C), 36.11 (CH_2), 35.33 (CH_2), 33.34 (CH_2), 31.23 (CH_3). FAB MS (*m*BNA matrix) m/z 839 [M^+]. Anal. Calcd for $\text{C}_{52}\text{H}_{62}\text{N}_4\text{O}_6$ (839.07): C, 74.43; H, 7.45; N, 6.68. Found: C 74.02; H, 7.54; N, 6.82.

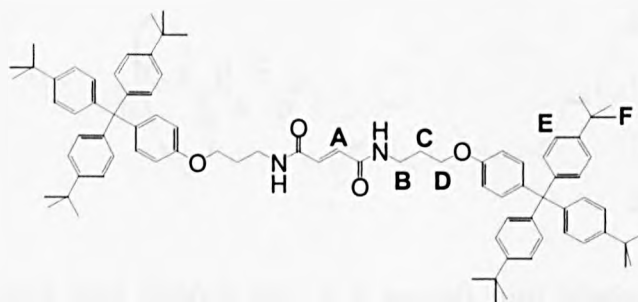
***trans,trans*-Muconic rotaxane (**106**)**



trans,trans-Muconic thread **104** (300.0 mg, 0.4 mmol) and triethylamine (649 μL) were dissolved in chloroform (50 mL), and stirred vigorously whilst solutions of the 2,6-(diaminomethyl)-naphthalene diamine **84** (400.0 mg, 2.2 mmol) in chloroform (50 mL) and isophthloyl dichloride **22** (436.0 mg, 2.2 mmol) in chloroform (50 mL) were simultaneously added over a period of 4h using motor-driven syringe pumps. The resulting suspension was then filtered and concentrated under reduced pressure to afford the crude product. This mixture was passed through a pad of silica gel (CHCl_3) to remove polar impurities to afford a mixture of thread **105** and rotaxane **106**. The mixture was then isolated by titration in hot diethyl ether to afford the rotaxane **106** as a white powder (253.0 mg, $17.2 \cdot 10^{-2}$ mmol, 43%).

m.p. 347-348°C; ^1H NMR (400 MHz, CDCl_3): δ = 8.60 (d, 2H, J = 1.8 Hz, $\text{ArH}_{\text{stopper}}$), 8.22 (dd, 4H, J = 7.9 + 1.4 Hz, **b**), 8.11 (d, 2H, J = 1.8 Hz, $\text{ArH}_{\text{stopper}}$), 7.69 (t, 4H, J = 5.8 Hz, NH_{mac}), 7.55 (t, 2H, J = 7.9 Hz, **c**), 7.43 (d, 4H, J = 7.8 Hz, **d**), 7.34 (s, 4H, **f**), 7.19 (s, 2H, **a**), 7.15 (dd, 4H, J = 7.8 + 2.1 Hz, **e**), 7.00 (t, 2H, J = 6.0 Hz, $\text{NH}_{\text{thread}}$), 5.20 (dd, 2H, J = 14.3 + 3.0 Hz, **E**), 4.90 (dd, 2H, J = 14.3 + 3.0 Hz, **D**), 4.51 (d, 8H, J = 5.8 Hz, **g**), 4.20 (t, 4H, J = 6.5 Hz, **A**), 3.14 (m, 4H, **C**), 1.80 (m, 4H, **B**), 1.41 (s, 18H, $\text{C}(\text{CH}_3)_3$); ^{13}C NMR (100 MHz, CDCl_3): δ = 166.66 (CO), 165.67 (CO), 165.43 (CO), 150.74 (q, ArC), 142.74 (q, ArC), 136.52 (q, ArC), 135.55 (q, ArC), 134.48 (q, ArC), 132.19 (q, ArC), 131.28 (q, ArC), 129.94 (CH), 129.88 (ArCH), 129.68 (ArCH), 129.20 (ArCH), 127.61 (ArCH), 127.36 (ArCH), 127.26 (ArCH), 124.22 (ArCH), 123.52 (CH), 122.13 (ArCH), 45.30 (q, C), 38.14 (CH_2) 37.60 (CH_2), 37.00 (CH_2), 35.73 (CH_2), 31.60 (CH_3). FAB MS (*m*BNA matrix) m/z 1472 [M^+]. Anal. Calcd for $\text{C}_{92}\text{H}_{94}\text{N}_8\text{O}_{10}$ (1471.78): C, 75.08; H, 6.44; N, 7.61. Found: C 74.92; H, 6.31; N, 7.48.

Fumaric thread (108)

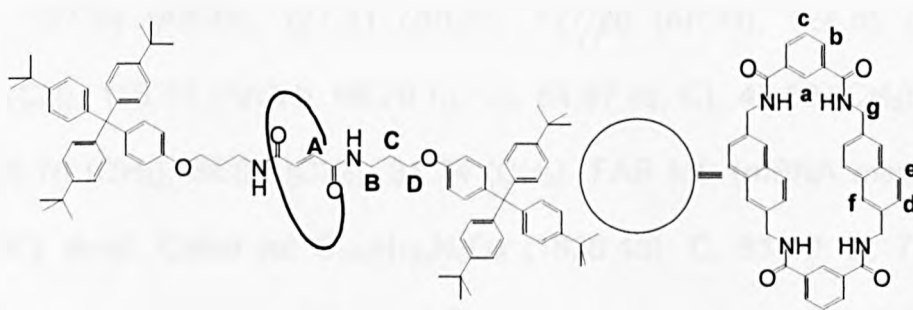


Propyl amine **94** (1.0 g, 1.8 mmol) and triethyl amine (193 μL) were dissolved in chloroform (75 mL) in a 250 mL one necked flask under nitrogen. Fumaryl chloride **107** (0.13 g, 0.9 mmol) dissolved in chloroform (50 mL) was added dropwise at RT over 1h. The solution was stirred at RT over 5h. The solution

was washed with 1N aqueous NaOH solution (2×75 mL) then with water (3×75 mL) and dried with MgSO₄. A white solid was obtained after the solvent was eliminated by rotary evaporation. Thread **108** was crystallised from ethanol as a white powder (1.7 g, 1.4 mmol, 78%).

m.p. 241-242°C; ¹H NMR (400 MHz, CDCl₃): δ= 7.26 (d, 12H, *J*= 8.8 Hz, ArH), 7.13 (d, 12H, *J*= 8.8 Hz, ArH), 7.11, (d, 8H, *J*= 8.8 Hz, ArH), 6.93 (s, 2H, **A**), 6.78 (d, 4H, *J*= 8.8 Hz, ArH), 6.56 (t, 2H, *J*= 5.8 Hz, NH), 4.04 (t, 4H, *J*= 6.3 Hz, **D**), 2.99 (m, 4H, **B**), 1.98 (m, 4H, **C**), 1.34 (s, 54H, C(CH₃)₃); ¹³C NMR (100 MHz, CDCl₃): δ= 164.66 (CO), 156.69 (q, ArC), 148.72 (q, ArC), 144.49 (q, ArC), 140.47 (q, ArC), 133.45 (CH), 132.74 (ArCH), 131.11 (ArCH), 124.47 (ArCH), 113.34 (ArCH), 66.42 (q, C), 63.48 (q, C), 38.26 (CH₂) 34.69 (CH₂), 33.12 (CH₂), 31.79 (CH₃). FAB MS (*m*BNA matrix) *m/z* 1203 [M-H]⁺. Anal. Calcd for C₈₄H₁₀₂N₂O₄ (1203.72): C, 83.82; H, 8.54; N, 2.33. Found: C, 82.42; H, 9.07; N, 1.88.

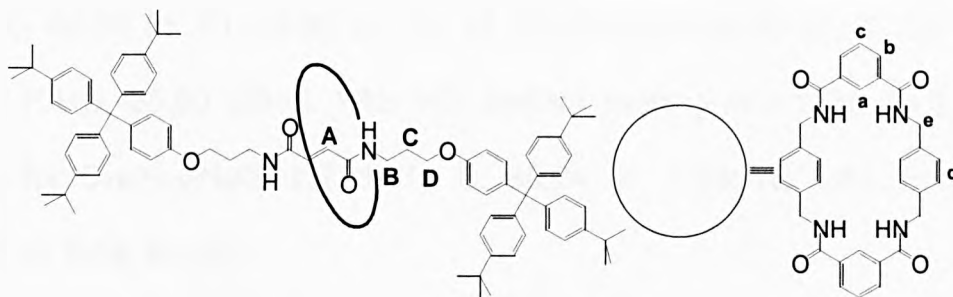
Fumaric rotaxane (naphthalene macrocycle) (**109**)



The fumaric thread **108** (350.0 mg, 0.3 mmol) and triethylamine (1.0 mL) were dissolved in chloroform (50 mL), and stirred vigorously whilst solutions of the *p*-naphthalene diamine **84** (650.0 mg, 3.6 mmol) in chloroform (50 mL) and isophthaloyl dichloride **22** (708.0 mg, 3.6 mmol) in chloroform (50 mL)

were simultaneously added over a period of 4h using motor-driven syringe pumps. The resulting suspension was then filtered and concentrated under reduced pressure to afford the crude product. This mixture was purified using silica gel chromatography (petroleum ether/chloroform 3/2) to remove polar impurities and afford rotaxane **109** as a white powder (86.0 mg, $4.7 \cdot 10^{-2}$ mmol, 16%).

m.p. 348-349°C; ^1H NMR (400 MHz, CDCl_3): δ = 8.31 (s, 2H, **a**), 8.19 (dd, 4H, J = 7.9 + 1.4 Hz, **b**), 7.49 (t, 2H, J = 7.9 Hz, **c**), 7.32 (s, 4H, **f**), 7.29 (d, 4H, J = 7.8 Hz, **d**), 7.14 (d, 4H, J = 7.8 + 2.1 Hz, **e**), 7.12 (t, 4H, J = 5.8 Hz, NH_{mac}), 7.11 (d, 12H, J = 8.8 Hz, $\text{ArH}_{\text{stopper}}$), 7.07 (d, 4H, J = 8.8 Hz, $\text{ArH}_{\text{stopper}}$), 7.02 (d, 12H, J = 8.8 Hz, $\text{ArH}_{\text{stopper}}$), 7.69 (d, 4H, J = 8.8 Hz, $\text{ArH}_{\text{stopper}}$), 5.55 (t, 2H, J = 5.8 Hz, $\text{NH}_{\text{thread}}$), 4.53 (d, 8H, J = 5.8 Hz, **g**), 4.49 (s, 2H, **A**), 3.82 (t, 4H, J = 6.5 Hz, **D**), 2.95 (m, 4H, **B**), 1.73 (m, 4H, **C**), 1.19 (s, 54H, $\text{C}(\text{CH}_3)_3$); ^{13}C NMR (100 MHz, CDCl_3): δ = 164.55 (CO), 163.67 (CO), 148.87 (q, ArC), 144.32 (q, ArC), 142.32 (q, ArC), 134.79 (q, ArC), 133.87 (q, ArC), 132.98 (q, ArC), 132.42 (q, ArC), 131.04 (CH), 129.92 (ArCH), 129.77 (ArCH), 128.21 (ArCH), 127.64 (ArCH), 127.31 (ArCH), 127.26 (ArCH), 124.55 (ArCH), 123.57 (CH), 113.31 (ArCH), 66.76 (q, C), 64.87 (q, C), 45.50 (CH_2), 39.05 (CH_2), 35.76 (CH_2), 34.69 (CH_2), 31.74 (CH_3). FAB MS (*m*BNA matrix) m/z 1836 [M^+]. Anal. Calcd for $\text{C}_{124}\text{H}_{134}\text{N}_6\text{O}_8$ (1836.43): C, 81.10; H, 7.35; N, 4.58. Found: C, 81.00; H, 7.19; N, 4.47.

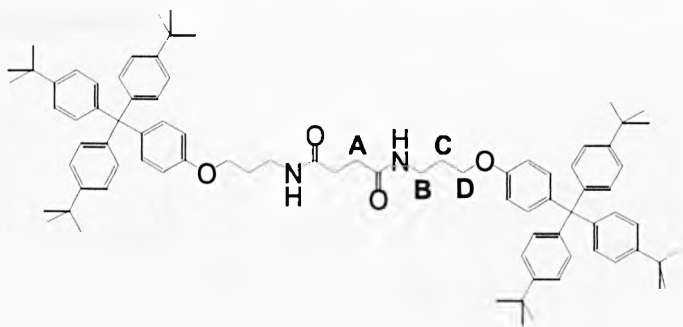
Fumaric rotaxane (benzyl macrocycle) (110)

The fumaric thread **108** (400.0 mg, 0.3 mmol) and triethylamine (1.2 mL) were dissolved in chloroform (50 mL), and stirred vigorously whilst solutions of the *p*-xylylene diamine **26** (542.0 mg, 3.6 mmol) in chloroform (40 mL) and of isophthaloyl dichloride **22** (810.0 mg, 3.6 mmol) in chloroform (40 mL) were simultaneously added over a period of 4h using motor-driven syringe pumps. The resulting suspension was then filtered and concentrated under reduced pressure to afford the crude product. This mixture was passed through a pad of silica gel (CHCl₃) to remove polar impurities to afford a mixture of thread **104** and rotaxane **110**. Rotaxane **110** was then isolated by silica gel column chromatography (chloroform) as a white powder (447.9 mg, 0.3 mmol, 86%).

m.p. 310-311°C; ¹H NMR (400 MHz, DMSO-*d*₆): 8.27 (s, 2H, **a**), 8.08 (dd, 4H, *J* = 7.9 + 1.4 Hz, **b**), 7.59 (t, 4H, *J* = 7.9 Hz, **c**), 7.30 (t, 4H, *J* = 5.8 Hz, NH_{mac}), 7.24 (d, 6H, *J* = 8.8 Hz, ArH_{stopper}), 7.12 (d, 2H, *J* = 8.8 Hz, ArH_{stopper}), 7.08 (t, 2H, *J* = 5.0 Hz, NH_{thread}), 7.05 (d, 6H, *J* = 8.8 Hz, ArH_{stopper}), 6.98 (s, 8H, **d**), 6.75 (d, 2H, *J* = 8.8 Hz, ArH_{stopper}), 5.90 (s, 2H, **A**), 4.31 (d, 8H, *J* = 5.0 Hz, **e**), 3.88 (t, *J* = 6.5 Hz, 4H, **D**), 3.16 (m, 4H, **B**), 1.80 (m, 4H, **C**), 1.23 (s, 54H, C(CH₃)₃); ¹³C NMR (100 MHz, DMSO-*d*₆): δ = 166.03 (CO), 165.06 (CO), 156.77 (q, ArC), 148.27 (q, ArC), 147.99 (q, ArC), 144.26 (q, ArC), 137.13 (q, ArC), 134.60 (q, ArC), 131.80 (ArCH), 130.98 (ArCH), 130.37 (ArCH), 128.88

(CH), 127.68 (ArCH), 125.40 (ArCH), 124.70 (ArCH), 121.03 (ArCH), 113.54 (ArCH), 66.06 (q, C), 62.86 (q, C), 45.30 (CH₂) 38.14 (CH₂), 37.59 (CH₂), 35.72 (CH₂), 31.60 (CH₃). FAB MS (*m*BNA matrix) *m/z* 1736 [M⁺]. Anal. Calcd for C₁₁₆H₁₃₀N₆O₈ (1736.31): C, 80.24; H, 7.55; N, 4.84. Found C, 80.20; H, 8.04; N 4.82.

Succinic thread (112)

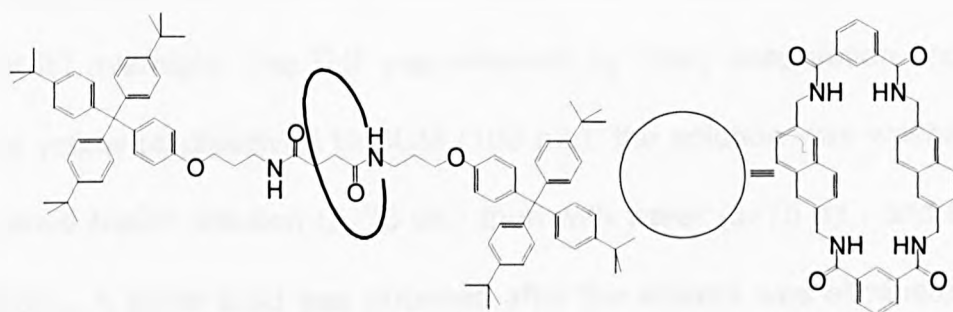


Propylamine **94** (1.0 g, 1.8 mmol) and triethylamine (193 μ L) were dissolved in chloroform (75 mL) in a 250 mL one necked flask under nitrogen. Succinyl chloride **111** (0.13 g, 0.9 mmol) dissolved in chloroform (50 mL) was added dropwise at RT over 1h. The solution was stirred at room temperature over 4h. The solution was washed with aqueous NaOH solution (2 \times 75 mL) then with water (3 \times 75 mL) and dried with MgSO₄. A white solid was obtained after the solvent was eliminated by rotary evaporation. Product **112** was crystallised from ethanol as a white powder (950.0 mg, 0.8 mmol, 93%).

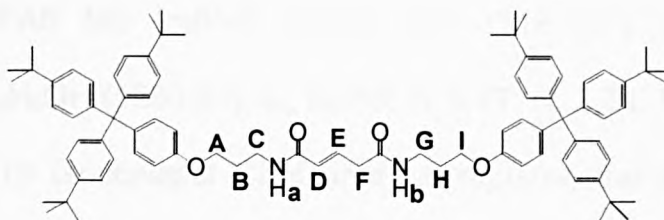
m.p. 183-184°C; ¹H NMR (400 MHz, CDCl₃): δ = 7.26 (d, 12H, *J*= 8.8 Hz, ArH), 7.24 (d, 4H, *J*= 8.8 Hz, ArH), 7.11 (d, 12H, *J*= 8.8 Hz, ArH), 6.76 (d, 4H, *J*= 8.8 Hz, ArH), 6.31 (t, 2H, *J*= 5.8 Hz, NH), 4.00 (t, *J*= 6.3 Hz, 4H, **D**), 3.46 (m, 4H, **B**), 2.52 (s, 4H, **A**), 1.97 (m, 4H, **C**), 1.33 (s, 54H, C(CH₃)₃); ¹³C NMR (100 MHz, CDCl₃): δ = 172.64 (CO), 156.80 (q, ArC), 148.72 (q, ArC), 144.49

(q, ArC), 140.29 (q, ArC), 132.71 (ArCH), 131.11 (ArCH), 124.55 (ArCH), 113.32 (ArCH), 66.33 (q, C), 63.45 (q, C), 37.84 (CH₂) 34.69 (CH₂), 33.30 (CH₂), 32.27 (CH₂), 31.79 (CH₃). FAB MS (*m*BNA matrix) *m/z* 1206 [M]⁺. Anal. Calcd for C₈₄H₁₀₄N₂O₄ (1205.74): C, 83.67; H, 8.69; N, 2.32. Found: C, 83.57; H, 8.61; N, 2.28.

Attempted rotaxane formation with succinic thread **112** and the naphthalene diamine **84**



Succinic thread **112** (250.0 mg, 0.2 mmol) and triethyl amine (733 μ L) were dissolved in chloroform (50 mL) and stirred vigorously whilst solutions of the *p*-naphthalene diamine **84** (464.0 mg, 2.5 mmol) in chloroform (50 mL) and the isophthoyl dichloride **22** (506.0 mg, 2.5 mmol) in chloroform (50 mL) were simultaneously added over a period of 4h using motor-driven syringe pumps. The resulting suspension was filtered and concentrated under reduced pressure to afford the crude product. Purification by silica gel chromatography (petroleum ether/chloroform 3/2) gave recovered thread **112** (240.0 mg, 0.2 mmol, 100%) but no rotaxane **113**.

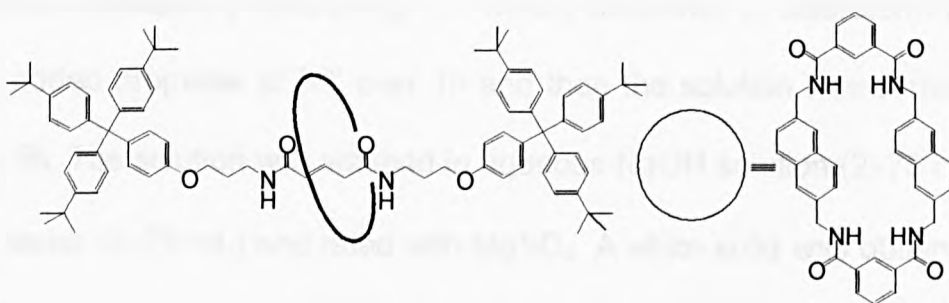
Glutaconic thread (114)

Propylamine **94** (1.0 g, 1.8 mmol) and glutaconic acid **78** (106.0 mg, 0.8 mmol) were dissolved in THF (100 mL) in a 250 mL one necked flask under nitrogen. The solution was then chilled to 0°C with ice. EDCI (157.0 mg, 0.8 mmol) was added slowly over 1h. The ice bath was removed and the solution stirred at RT overnight. The THF was removed by rotary evaporation and the resultant yellow oil dissolved in DCM (100 mL); the solution was washed in 1N aqueous NaOH solution (2×75 mL) then with water (3×75 mL) and dried with MgSO₄. A white solid was obtained after the solvent was eliminated by rotary evaporation. Thread **114** was isolated as a white powder after crystallisation from ethanol (848.0 mg, 0.7 mmol, 87%).

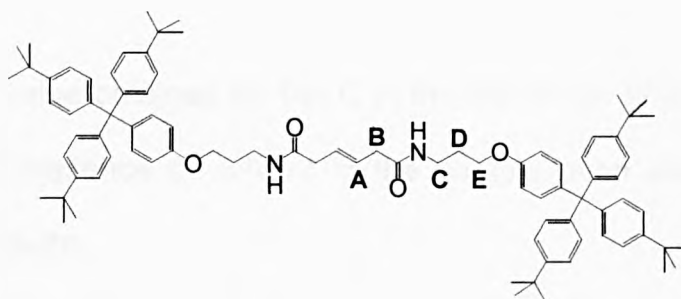
m.p. 198-199°C; ¹H NMR (400 MHz, CDCl₃): δ= 7.21 (d, 12H, *J*= 8.8 Hz, ArH), 7.20 (d, 4H, *J*= 8.8 Hz, ArH), 7.06 (d, 12H, *J*= 8.8 Hz, ArH), 6.83 (m, 1H, E), 6.70 (d, 4H, *J*= 8.8 Hz, ArH), 6.13 (t, 1H, *J*= 7.8 Hz, NH_a), 6.07 (t, 1H, *J*= 7.8 Hz, NH_b), 5.87 (d, 1H, *J*= 15.3 Hz, D), 3.95 (t, 4H, *J*= 6.3 Hz, A and I), 3.44 (m, 2H, C), 3.40 (m, 2H, G), 3.05 (dd, 2H, *J*= 7.8 + 5.6 Hz, F), 1.94 (m, 4H, B and H), 1.28 (s, 54H, C(CH₃)₃); ¹³C NMR (100 MHz, CDCl₃): δ= 169.21 (CO), 165.17 (CO), 156.32 (q, ArC), 156.31 (q, ArC), 148.30 (q, ArC), 148.08 (q, ArC), 144.23 (q, ArC), 144.07 (q, ArC), 143.86 (q, ArC), 139.95 (q, ArC), 135.71 (CH), 132.29 (ArCH), 131.94 (ArCH), 131.09 (ArCH), 130.35 (ArCH), 128.66 (ArCH), 127.82 (CH), 124.45 (ArCH), 124.33 (ArCH), 112.90 (ArCH), 66.15 (q, C), 65.84 (q, C), 63.03 (q, C), 63.00 (q, C), 40.10 (CH₂), 39.64

(CH₂), 37.78 (CH₂), 37.47 (CH₂), 34.27 (CH₂), 34.21 (CH₂), 31.54 (CH₂), 31.38 (CH₃). FAB MS (*m*BNA matrix) *m/z* 1218 [M⁺]. Anal. Calcd for C₈₅H₁₀₄N₂O₄.C₂H₅OH (1263.81): C, 82.68; H, 8.77; N, 2.21. Found: C, 82.72; H, 8.58; N, 2.10 (successful CHN analysis required the inclusion of one molecule of ethanol).

Attempted rotaxane formation with glutaconic thread **114** and naphthalene diamine **84**



Glutaconic thread **114** (250.0 mg, 0.2 mmol) and triethylamine (733 μ L) were dissolved in chloroform (25 mL), and stirred vigorously whilst solutions of the *p*-naphthalene diamine **84** (464.0 mg, 2.5 mmol) in chloroform (30 mL) and isophthoyl dichloride **22** (506.0 mg, 2.5 mmol) in chloroform (30 mL) were simultaneously added over a period of 3h using motor-driven syringe pumps. The resulting suspension was filtered and concentrated under reduced pressure to afford the crude material. After purification by silica gel chromatography (petroleum ether/chloroform 3/2) thread **114** (242.0 mg, 0.2 mmol, 100%) but no rotaxane **115** were recovered.

***trans*- β -Hydro muconic thread (116)**

Propylamine **94** (2.0 g, 3.6 mmol) and triethylamine (510 μ L) were dissolved in chloroform (75 mL) in a 250-mL one necked flask under nitrogen. *trans*- β -Muconic chloride **73** (300.0 mg, 1.7 mmol) dissolved in chloroform (50 mL) was added dropwise at RT over 1h and then the solution was stirred at RT over 5h. The solution was washed in aqueous NaOH solution (2 \times 75 mL) then with water (3 \times 75 mL) and dried with MgSO₄. A white solid was obtained after the solvent was eliminated by rotary evaporation. Thread **116** was isolated as a white powder after silica gel column chromatography (chloroform) (1.5 g, 1.2 mmol, 73%).

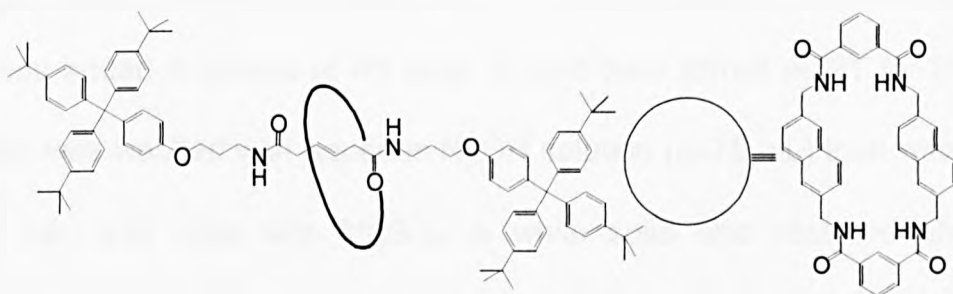
m.p. 220-221 $^{\circ}$ C; ¹H NMR (400 MHz, CDCl₃): δ = 7.25 (d, 12H, J = 8.8 Hz, ArH), 7.24 (d, 4H, J = 8.8 Hz, ArH), 7.10 (d, 12H, J = 8.8 Hz, ArH), 6.76 (d, 4H, J = 8.8 Hz, ArH), 6.16 (t, 2H, J = 7.8 Hz, NH), 5.69 (t, J = 5.6 Hz, 2H, A), 4.00 (t, 4H, J = 6.3 Hz, E), 3.45 (m, 4H, C), 2.97 (d, 4H, J = 5.6 Hz, B), 1.98 (m, 4H, D), 1.33 (s, 54H, C(CH₃)₃); ¹³C NMR (100 MHz, CDCl₃): δ = 171.12 (CO), 156.81 (q, ArC), 148.75 (q, ArC), 144.48 (q, ArC), 140.33 (q, ArC), 132.72 (ArCH), 131.11 (ArCH), 128.67 (CH), 124.55 (ArCH), 113.33 (ArCH), 66.51 (q, C), 63.45 (q, C), 40.41 (CH₂), 38.01 (CH₂), 34.69 (CH₂), 33.48 (CH₂), 31.79 (CH₃). FAB MS (*m*BNA matrix) m/z 1231 [M-H]⁺. Anal. Calcd for

C₈₆H₁₀₆N₂O₄ (1231.77): C, 83.86; H, 8.67; N, 2.27. Found: C, 84.42; H, 9.24; N, 2.21.

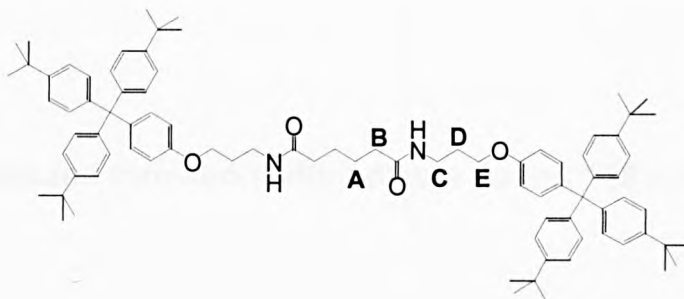
The incorrect value obtained for the C in the elemental analysis was due to the persistent presence of solvent in the sample even after high-vacuum treatment overnight.

Attempted rotaxane formation with thread **116** and naphthalene diamine

84



trans- β -Hydro muconic thread **116** (400.0 mg, 0.3 mmol) and triethylamine (1.1 mL, 8.0 mmol) were dissolved in chloroform (30 mL), and stirred vigorously whilst solutions of the *p*-naphthalene diamine **84** (726.0 mg, 3.6 mmol) in chloroform (40 mL) and isophthaloyl dichloride **22** (791 mg, 3.6 mmol) in chloroform (40 mL) were simultaneously added over a period of 4h using motor-driven syringe pumps. The resulting suspension was filtered and concentrated under reduced pressure to afford the crude material. After purification by silica gel chromatography (petroleum spirit/chloroform 3/2) only thread **116** (387.0 mg, 0.3 mmol, 100%) but no rotaxane **117** was recovered.

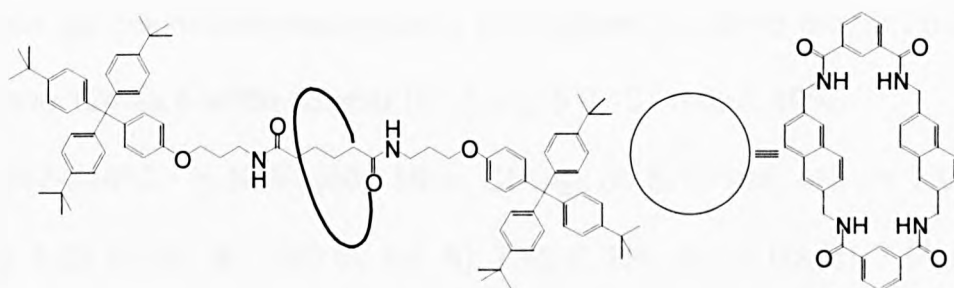
Adipoyl thread (119)

Propane amine **94** (2.0 g, 3.6 mmol) and triethylamine (510 μ L) were dissolved in chloroform (75 mL) in a 250-mL one necked flask under nitrogen. Adipoyl dichloride **118** (0.3 g, 1.7 mmol) dissolved in chloroform (50 mL) was added dropwise at RT over 1h and then stirred at RT for 5h. The solution was washed with aqueous NaOH solution (2 \times 75 mL) then with water (3 \times 75 mL) and dried with MgSO₄. A white solid was obtained after the solvent was eliminated by rotary evaporation. Thread **119** was isolated as a white powder after silica gel column chromatography (chloroform) (1.8 g, 1.5 mmol, 86%).

m.p. 215-217 $^{\circ}$ C; ^1H NMR (400 MHz, CDCl₃): δ = 7.21 (d, 12H, J = 8.8 Hz, ArH), 7.13 (d, 4H, J = 8.8 Hz, ArH), 7.11 (d, 12H, J = 8.8 Hz, ArH), 6.77 (d, 4H, J = 8.8 Hz, ArH), 5.96 (t, 2H, J = 5.9 Hz, NH), 4.03 (t, 4H, J = 6.3 Hz, **E**), 3.46 (m, 4H, **C**), 2.44 (t, 4H, J = 6.0 Hz, **B**), 2.02 (m, 4H, **D**), 1.79 (t, 4H, J = 6.0 Hz, **A**), 1.33 (s, 54H, C(CH₃)₃); ^{13}C NMR (100 MHz, CDCl₃): δ = 172.16 (CO), 156.76 (q, ArC), 148.87 (q, ArC), 144.11 (q, ArC), 140.32 (q, ArC), 132.58 (ArCH), 131.54 (ArCH), 124.55 (ArCH), 113.29 (ArCH), 66.69 (q, C), 63.76 (q, C), 38.29 (CH₂), 36.70 (CH₂), 34.70 (CH₂), 34.41 (CH₂), 38.29 (CH₂), 31.78 (CH₃). FAB MS (*m*BNA matrix) m/z 1233 [M-H]⁺. Anal. Calcd for

$C_{86}H_{108}N_2O_4$ (1233.79): C, 83.72; H, 8.82; N, 2.27. Found: C, 83.67; H, 8.77; N, 2.23.

Attempted rotaxane formation with adipoyl thread **119 and naphthalene diamine **84****

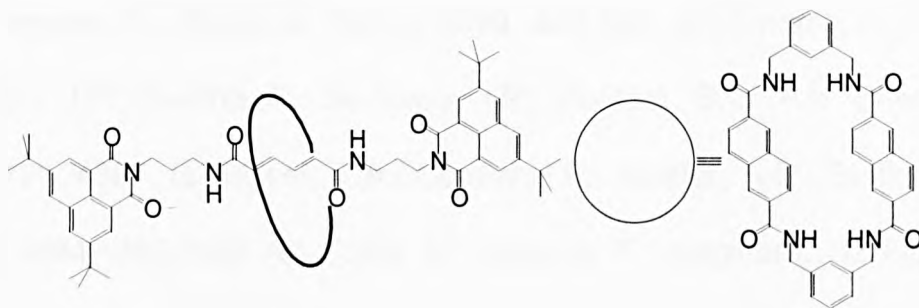


Adipoyl thread **119** (400.0 mg, 0.3 mmol) and triethylamine (1.1 mL) were dissolved in chloroform (30 mL), and stirred vigorously whilst solutions of the *p*-naphthalene diamine **84** (726.0 mg, 3.6 mmol) in chloroform (40 mL) and isophthaloyl dichloride **22** (791.0 mg, 3.6 mmol) in chloroform (40 mL) were simultaneously added over a period of 4h using motor-driven syringe pumps. The resulting suspension was then filtered and concentrated under reduced pressure to afford the crude material. After purification by silica gel chromatography (petroleum spirit/chloroform 3/2) only thread **119** (379.0 mg, 0.3 mmol, 100%) but no rotaxane **120** were recovered.

mmol) in chloroform (50 mL) were added, *via* syringe pumps to a stirring solution of the allyl-macrocycle **123** (0.3 g, 0.5 mmol) and triethyl amine (1.7 mL) in chloroform (300 mL). The reaction mixture was allowed to stir overnight before being filtered, washed with water (6×100 mL), dried over MgSO₄, filtered and concentrated under reduced pressure and finally purified by silica gel column chromatography (chloroform) to afford the vinylbenzoic-catenane **124** as a white powder (61.6 mg, $5.0 \cdot 10^{-2}$ mmol, 10%).

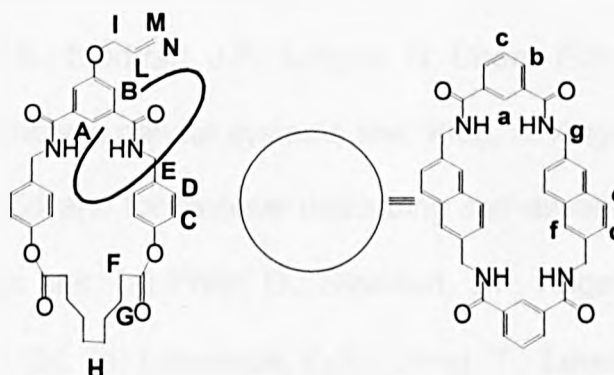
m.p. 347-348°C; ¹H NMR (400 MHz, CDCl₃): δ= 8.10 (dd, 4H, *J*= 7.9 + 1.4 Hz, **b**), 8.03 (s, 2H, **a**), 7.80 (s, 1H, **A**), 7.59 (t, 2H, *J*= 7.9 Hz, **c**), 7.55 (s, 2H, **B**), 7.35 (4H, t, *J*= 5.8 Hz, NH_{naphmac}), 7.30 (t, 2H, *J*= 6.0 Hz, NH_{amphmac}), 7.12 (d, 4H, *J*= 7.8 Hz, **d**), 7.07 (s, 4H, **f**), 6.87 (AA' part of AA'BB' system, 4H, *J*= 8.5 Hz, **C**), 6.83 (dd, 4H, *J*= 7.8 + 2.1 Hz, **e**), 6.59 (BB' part of AA'BB' system, 4H, *J*= 8.5 Hz, **D**), 6.04 (m, 1H, **L**), 5.47 (dd, 1H, *J*_{vic}= 16.0 Hz, *J*_{gem}= 1.0 Hz, **M**), 5.33 (dd, 1H, *J*_{vic}= 9.0 Hz, *J*_{gem}= 1.0 Hz, **N**), 4.58 (d, 2H, *J*= 5.3 Hz, **I**), 4.41 (d, 8H, *J*= 5.8 Hz, **g**), 4.12 (d, 4H, *J*= 6.0 Hz, **E**), 2.44 (t, 4H, *J*= 6.5 Hz, **F**), 1.69 (bs, 4H, **G**), 1.37 (bs, 8H, **H**); ¹³C NMR (100 MHz, CDCl₃): δ= 173.41 (CO), 168.98 (CO), 167.32 (CO), 156.98 (q, ArC), 150.16 (q, ArC), 138.32 (q, ArC), 137.08 (q, ArC), 135.88 (q, ArC), 135.65 (q, ArC), 134.75 (q, ArC), 134.61 (q, ArC), 134.09 (CH), 134.01 (ArCH), 133.87 (ArCH), 131.94 (ArCH), 131.46 (ArCH), 131.00 (ArCH), 128.08 (ArCH), 125.67 (CH₂), 118.56 (ArCH), 118.03 (ArCH), 117.67 (ArCH), 116.02 (ArCH), 68.50 (CH₂), 44.72 (CH₂), 34.45 (CH₂), 31.98 (CH₂), 30.34 (CH₂), 28.87 (CH₂), 28.03 (CH₂). FAB MS (*m*BNA matrix) *m/z* 1231 [M⁺]. Anal. Calcd for C₇₅H₇₀N₆O₁₁ (1231.39): C, 73.15; H, 5.73; N, 6.82. Found: C, 72.56; H, 5.81; N, 6.77.

Attempted rotaxane formation with thread **105**, 2,6-naphthalene di carbonyl chloride and *m*-xylenediamine **121**



E,E-Muconic thread **105** (290.0 mg, 0.4 mmol) and triethylamine (1.2 mL) were dissolved in chloroform (25 mL), and stirred vigorously whilst solutions of *m*-xylylene diamine **121** (565.0 mg, 4.2 mmol) in chloroform (40 mL) and the naphthalene dichloride **82** (1.0 g mg, 4.2 mmol) in chloroform (40 mL) were simultaneously added over a period of 4h using motor-driven syringe pumps. The resulting suspension was filtered and concentrated under reduced pressure to afford the crude material. This mixture was passed through a pad of silica gel (chloroform) to remove polar impurities to afford only thread **105** (275.0 mg, 0.4 mmol, 100%) but no rotaxane **122**.

Naphthalene-based etherocircuit [2]catenane (**124**)



Under an atmosphere of argon, solutions of isophthaloyl dichloride **22** (1.2 g, 6.0 mmol) in chloroform (50 mL) and naphthalene diamine **84** (1.1 g, 6.0

References:

1. (a) Bermudez, V.; Capron, N.; Gase, T.; Gatti, F.G.; Kajzar, F.; Leigh, D.A.; Zerbetto, F.; Zhang, S. *Nature* **2000**, *406*, 608. (b) Amaroli, N.; Balzani, V.; Collin, J.P.; Gavina, P.; Sauvage, J.P.; Ventura, B. *J. Am. Chem. Soc.* **1999**, *121*, 4397. (c) Bissel, R.A.; Córdova, E.; Kaiefer, A.E.; Stoddart, J.F. *Nature* **1994**, *369*, 133. (d) Fujita, M.; Ibukuro, F.; Hagihara, H.; Ogura, K. *Nature* **1994**, *367*, 720.
2. (a) Lane, A.S.; Leigh, D.A.; Murphy, A. *J. Am. Chem. Soc.* **1997**, *119*, 11092. (b) Leigh, D.A.; Murphy A.; Smart, J.P.; Slawin, A.M.Z. *Angew. Chem. Int. Ed. Engl.* **1997**, *36*, 728. (c) Johnson, A.G.; Leigh, D.A.; Murphy, A.; Smart, J.P.; Deegan, M.D. *J. Am. Chem. Soc.* **1996**, *118*, 10662. (d) Clegg, W.; Gimenez-Saiz, C.; Leigh, D.A.; Murphy, A.; Slawin, A.M.Z.; Teat, S.J. *J. Am. Chem. Soc.* **1999**, *121*, 4124.
3. For reviews of supramolecular chemistry see: (a) Mann, S. *Nature* **1993**, *365*, 499. (b) Whitesides, G.M.; Mathias, J.P.; Seto, C.T. *Science* **1991**, *254*, 1312. (c) Lehn, J.M. *Angew. Chem. Int. Ed. Engl.* **1988**, *27*, 89. (d) Cram, D.J. *Angew. Chem. Int. Ed. Engl.* **1988**, *27*, 1009. (e) Pedersen, C.J. *Angew. Chem. Int. Ed. Engl.* **1988**, *27*, 1021.
4. Reinhoudt, D.N.; Stoddart, J.F.; Ungaro, R. *Chem. Eur. J.* **1998**, *8*, 1349.
5. For self-assembly in natural systems see: Klug, A. *Angew. Chem. Int. Ed. Engl.* **1983**, *22*, 565 and for reviews describing self-assembly in natural and unnatural systems see: (a) Philp, D.; Stoddart, J.F. *Angew. Chem. Int. Ed. Engl.* **1996**, *35*, 1154. (b) Lawrence, D.S.; Jiang, T.; Levett, M. *Chem. Rev.* **1995**, *95*, 2229.
6. Fyfe, M.C.T.; Stoddart, J.F. *Acc. Chem. Res.* **1997**, *30*, 393.

7. (a) Fisher, E. *Deut. Chem. Ges.* **1894**, 27, 2987. (b) Lichtenthaler, F.W. *Angew. Chem. Int. Ed. Engl.* **1994**, 33, 2364.
8. Chapters 2 and 3 of this thesis.
9. Wilson, A.; PhD Thesis, University of Warwick, 2000.
10. Gibson, H.W.; Lee, S.H.; Engen, P.T.; Lecavalier, P.; Sze, J.; Shen, Y.X.; Bheda, M. *J. Org. Chem.* **1993**, 58, 3748.
11. (a) Peters, A.T. *J. Am. Chem. Soc.* **1942**, 562. (b) Nürsten, H.E.; Peters, A.T. *J. Am. Chem. Soc.* **1950**, 729. (c) Illingworth, E.; Peters, A.T. *J. Am. Chem. Soc.* **1951**, 2730.
12. (a) Brouwer, A.M.; Frochot, C.; Gatti, F.G.; Leigh, D.A.; Mottier, L.; Paolucci, F.; Roffia, S.; Wurpel, G.W.H. *Science* **2001**, 291, 2124. (b) Sauvage, J.P. *Science* **2001**, 291, 2105.
13. Bruice, T.; Yip, Y.C.; Blaskó, A.; Lightstone, F.C.; Browne, K.A.; Petyak, M.E.; Luo, J. *Tetrahedron* **1997**, 53, 8105.
14. Gatti, F.; Leigh, D.A.; Nepogodiev, S.A.; Slawin, A.M.Z.; Teat, S.J.; Wong, J.K.Y. *J. Am. Chem. Soc.* **2001**, 123, 5983.
15. Johnston, A.G.; Leigh, D.A.; Nezhat, L.; Smart, J.P.; Deegan, M.D. *Angew. Chem. Int. Ed. Engl.* **1995**, 34, 1212.
16. (a) Carver, F.J.; Hunter, C.A.; Shannon, R.J. *J. Chem. Soc., Chem. Commun.* **1994**, 4124. (b) Hunter, C.A.; Purvis, D.H. *Angew. Chem. Int. Ed. Engl.* **1992**, 31, 792. (c) Geib, S.G.; Vincent, C.; Fan, E.; Hamilton, A.D. *Angew. Chem. Int. Ed. Engl.* **1993**, 33, 119.
17. Johnston, A.G.; Leigh, D.A.; Pritchard, R.J.; Deegan, M.D. *Angew. Chem. Int. Ed. Engl.* **1995**, 34, 1209.

18. Brouwer, A.J.; Mulders, S.J.E.; Liskamp, R.M.J. *Eur. J. Org. Chem.* **2001**, 10, 1903.

19. Lee, B.H.; Miller, M.J. *J. Org. Chem.* **1983**, 1, 24.

Chapter Five

5. Chemical Reactions on the Axle of Rotaxane Containing Dienes.

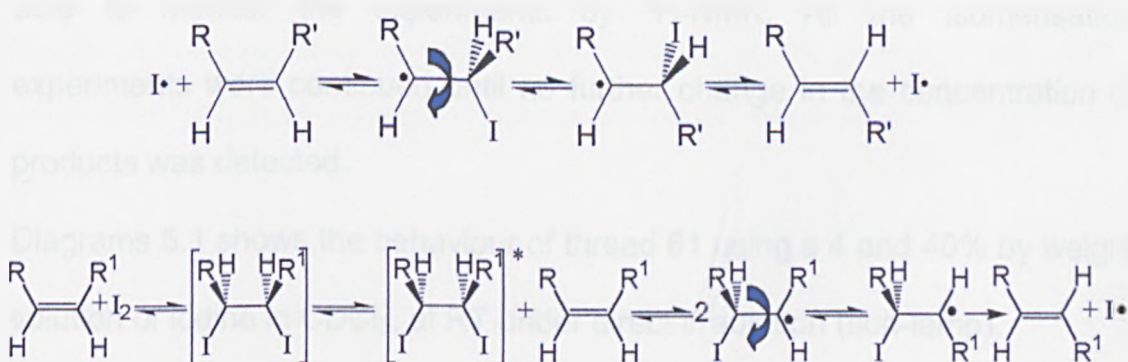
Abstract: Here we report on the use of rotaxane wheels as a non-covalent protecting group able to influence the chemical behaviour of the functional groups in the central part of the axle. Through steric effects and/or by offering an alternative H-bonding motif, the macrocycle is able to suppress the internal H-bonding of the thread and so influence the base or light catalysed isomerisation of the encapsulated thread. The iodine-catalysed Z/E-isomerism of conjugated diene threads was found to proceed via a radical as well as a nucleophilic-electrophilic process. The dienes of the rotaxane show pronounced chemical differences from those of the free thread due to the encircling macrocycle.

Introduction: In recent years, considerable progresses have been made in the synthesis of rotaxanes.¹ This incredible development in the supramolecular synthetic field has allowed target functional groups to be incorporated into previously inaccessible systems and their properties studied. Some limited investigations have probed the effect of the macrocycle on the physical and chemical-physical properties of functional groups in the thread of such classes of molecules.² Effects of chemical reactions on the axle of rotaxanes containing double bonds have already been studied ³ by Vögtle *et al.* In these and other reports the effect induced by using rotaxane wheels as a non-covalent protecting group significantly decrease the activity

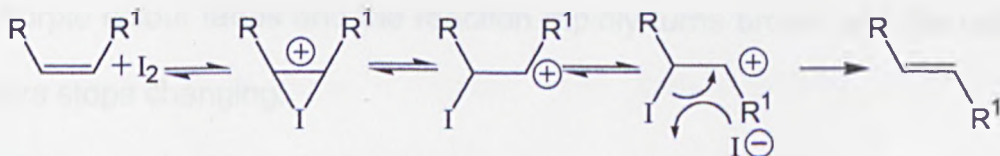
of the functional group in the central part of the axle as a direct consequence of the steric hindrance provided by the wheel. In this work we examine the effect of the macrocycle on the chemistry of the double bonds in the encapsulated threads of the glutaconic and muconic motifs.

Three mechanisms have been suggested for the isomerisation of double bonds in the presence of iodine. Light also aids iodine catalysed isomerisation by generating iodine radicals either by cleavage of the I-I bond or of a C-I bond (Scheme 5.1).^{4,5,6} An electrophilic mechanism has also been proposed which does not require light.

Light conditions



Electrophilic mechanism



Scheme 5.1

It has been suggested that the isomerisation process itself involves rotation around the σ -bond, after reaction of I^{\bullet} or I^+ onto the π -bond (Scheme 5.1).⁷ The rate-determining step is believed to be either the addition step or the rotation around the σ -carbon-carbon bond. *Z/E*-isomerisation of conjugated diene systems induced by iodine also takes place in the dark, albeit much slower than in the light.⁸

5.2 Results and discussion: In order to investigate the effect caused by the macrocyclic wheel on encapsulated olefins, experiments were performed in parallel on both *Z,Z* muconic thread **61** and *Z,Z* rotaxane **62** under analogous experimental conditions. Two different sets of solutions of thread **61** and rotaxane **62** were prepared using deuterated solvents in order to be able to monitor the experiments by ^1H -NMR. All the isomerisation experiments were continued until no further change in the concentration of products was detected.

Diagram 5.1 shows the behaviour of thread **61** using a 4 and 40% by weight solution of iodine in CDCl_3 , at RT under direct irradiation (sun-lamp).

Only a partial isomerisation from *Z,Z* to *E,Z* occurs for the thread **61** (Diagram 5.1). Increasing the amount of iodine to 40% just affects the initial rate of the conversion but not the general characteristics of the reaction.

The purple colour fades and the reaction rapidly turns brown and the ratio of isomers stops changing.

The iodine catalyst appears to be consumed though addition of fresh iodine does not have much effect on the ratio of the isomers.

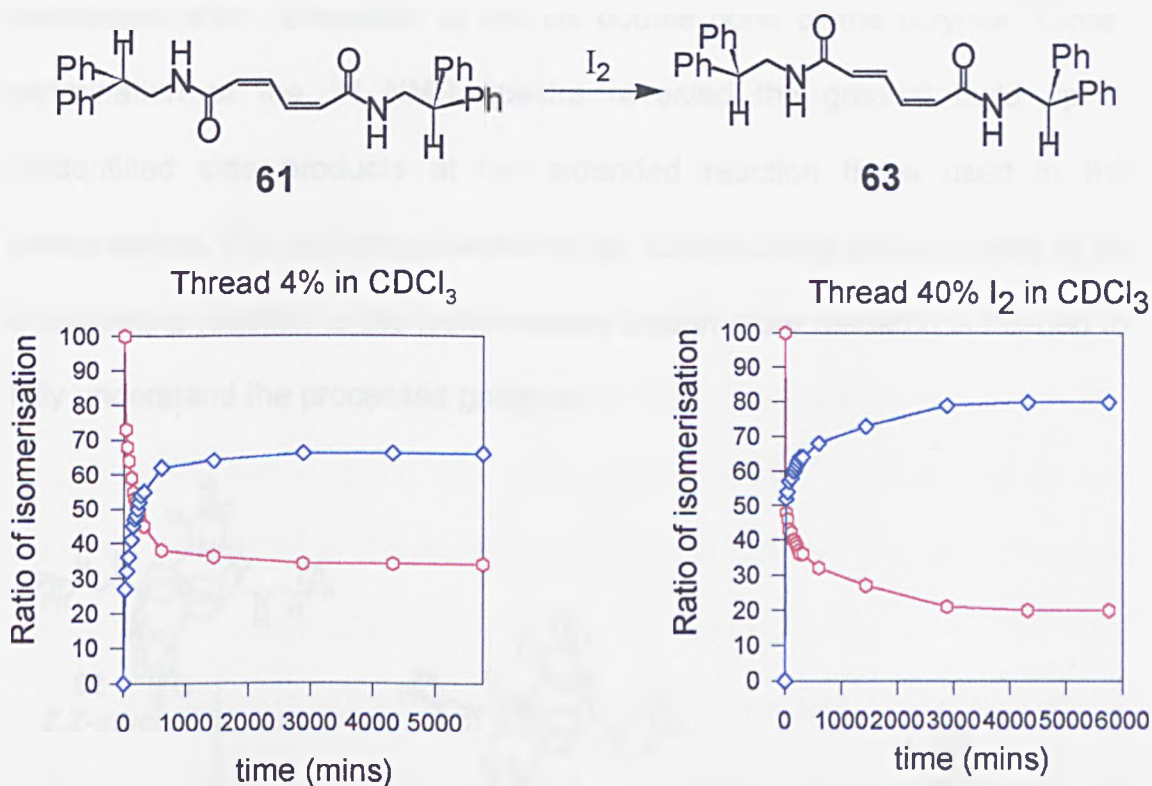


Diagram 5.1 Isomerisation of *Z,Z*-muconic thread **61** at low (4%) and high (40%) concentration of I_2 in the presence of light. In red the *Z,Z* thread **61** and in blue the *E,Z* thread **63**.

The isomerisation of the thread seems to be somehow retarded before the complete isomerisation of the *Z,Z* thread **61** to the *E,Z* thread **63** at these concentrations of iodine.

According to the studies of Benesi and Hildebrand⁹ on the interaction of iodine with aromatic hydrocarbons there is a change of colour of the iodine-based solution from violet to brown. The brown colour observed in isomerisation of the thread **61** may be an indication of the π -addition mechanism proposed by Benesi and Hildebrand.⁹ Additionally, in work carried out on the iodine induced conjugation of *cis*-1,4-polybutadiene this

colour change was also observed.¹⁴ In this case the colour change was associated with 1,2-addition to the *cis* double bond of the polymer. Closer examination of the ¹H NMR spectra revealed the gradual build up of unidentified side products at the extended reaction times used in the isomerisation. The addition of iodine to the double bonds would appear to be a competing reaction to the isomerisation though more research is needed to fully understand the processes going on.

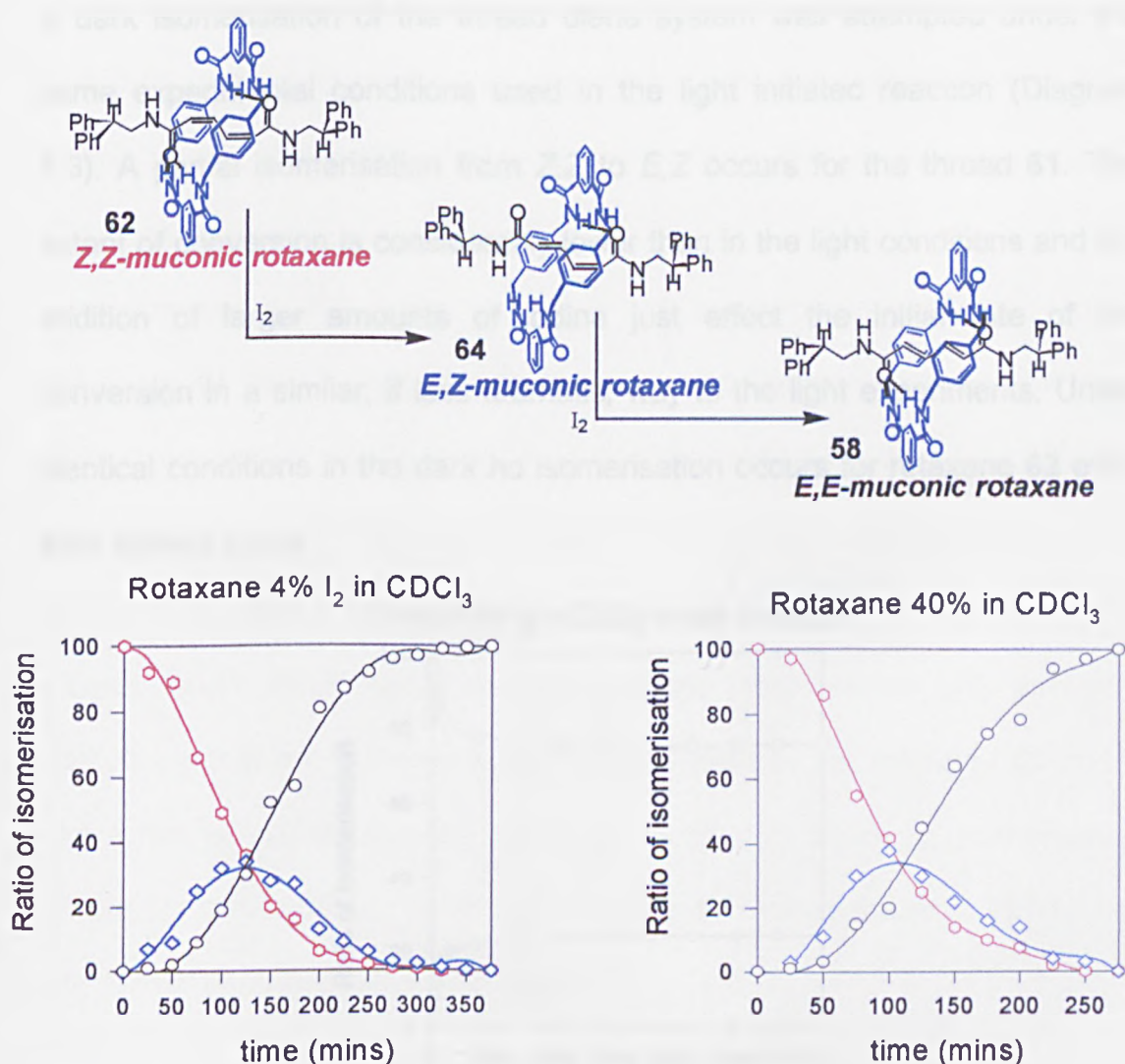


Diagram 5.2 Isomerisation of *Z,Z*-muconic rotaxane **62** at low (4%) and high (40%) concentration of I₂ in the presence of light. In red the *Z,Z* rotaxane **62**, in blue the *E,Z* rotaxane **64** and in black the *E,E* rotaxane **58**.

In contrast, there is a much more rapid isomerisation of the double bonds of the *Z,Z* rotaxane **62** all the way to the *E,E* rotaxane **58**. Diagram 5.2 shows the behaviour of rotaxane **62** using 4 and 40% by weight solution of iodine in CDCl_3 at analogous experimental conditions described for the isomerisation of the thread **61**. A complete isomerisation of the *Z,Z* to the *E,E* rotaxane occurs via the *E,Z* rotaxane **64**. No change of colour of the solution was observed which remains purple and there is no inhibition of the reaction.

A dark isomerisation of the thread diene system was attempted under the same experimental conditions used in the light initiated reaction (Diagram 5.3). A partial isomerisation from *Z,Z* to *E,Z* occurs for the thread **61**. The extent of conversion is considerably lower than in the light conditions and the addition of larger amounts of iodine just effect the initial rate of the conversion in a similar, if less dramatic, way to the light experiments. Under identical conditions in the dark no isomerisation occurs for rotaxane **62** even after several hours.

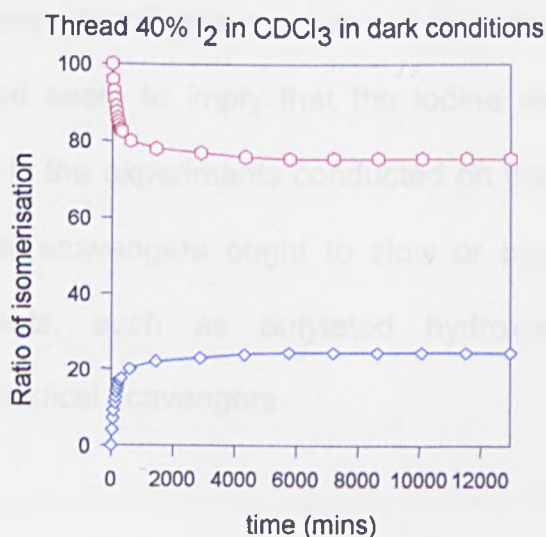


Diagram 5.3 Isomerisation of *Z,Z*-muconic thread **61** at 40% concentration of I_2 in the absence of light. In red the *Z,Z* thread **61** and in blue the *E,Z* thread **63**.

The results would seem to show the existence of two possible mechanisms for iodine-catalysed Z/E-isomerisation in light of the thread **61** and the absence of any π -complex formation of the iodine with the olefin system that is sterically shielded by the macrocyclic wheel in the rotaxane **62**. Thermal dissociation of the iodine molecule into two iodine radicals can take place at room temperature because of the relatively low energy of the I-I bond (37 kcal/mol).¹¹ The total lack of isomerisation for the rotaxane **62** in the dark indicates that the iodide radical may have to be present in considerable amounts in order to produce an observable rate of the isomerisation of the rotaxane **62** through the effect of temperature on the isomerisation was not explored.

The absence of the brown colour in the experiments conducted on the rotaxane **62** both in light and in the dark also indicate that the change of colour observed in the reaction of I_2 with the thread **61** cannot be justified by an addition to the π aromatic system^{11,12,13} but just to the olefin one as the rotaxane contains several aromatic moieties but does not change colour.

These results would seem to imply that the iodine reacts only through a radical mechanism in the experiments conducted on the rotaxane **62** and so the effect of radical scavengers ought to slow or block its isomerization. Phenolic antioxidants, such as butylated hydroxytoluene (BHT) are commonly used as radical scavengers.

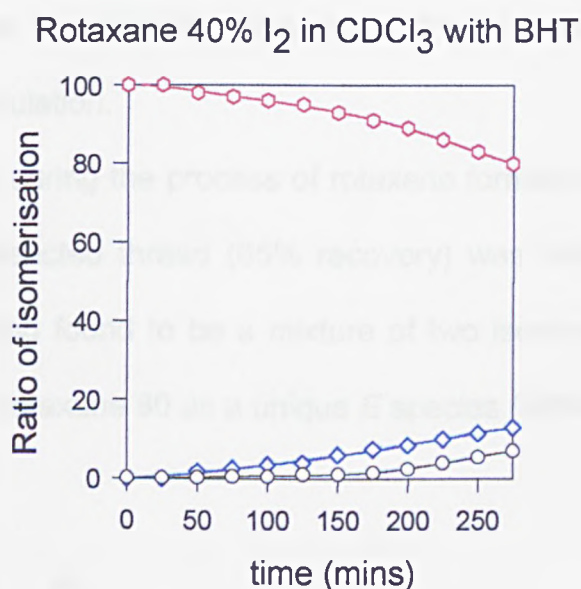
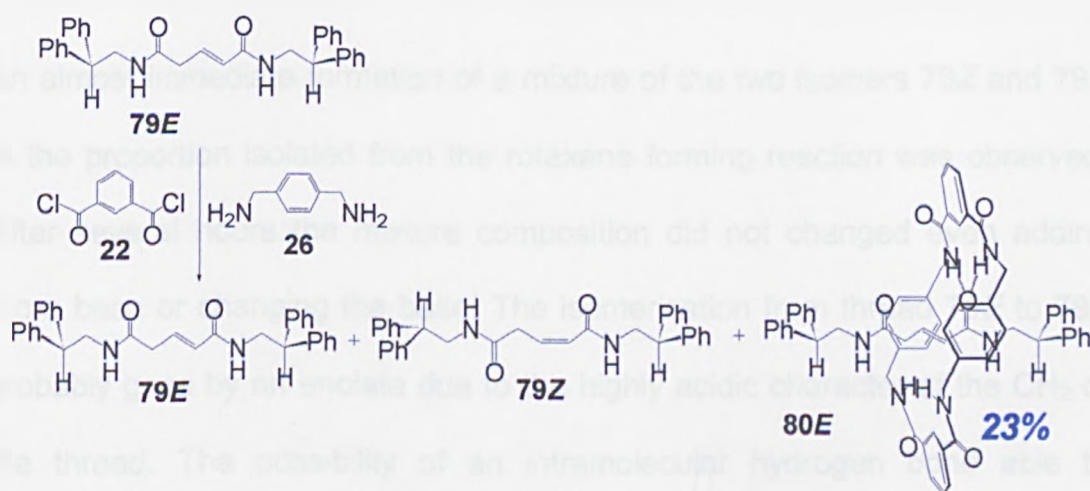


Diagram 5.4 Isomerisation of *Z,Z*-muconic rotaxane **62** at a 40% concentration of I₂ in the presence of light and BHT. In red the *Z,Z* specie **62**, in blue the *E,Z* **64** and in black the *E,E* rotaxane **58**.

Using 40% I₂ in CHCl₃ in the presence of BHT (Diagram 5.4) show the retarding effect of radical scavengers on the rate of isomerisation of the rotaxane **62**. Along with the negligible extent of isomerisation in the dark, this result also indicates a radical reaction as the process for the isomerisation of rotaxane **62**. That the electrophilic mechanism does not seem to operate in the rotaxane **62** is presumably because the macrocyclic wheel screening it from the approach of I₂ shields the olefin. On the contrary, in the absence of this shielding effect, both mechanisms operate in the thread **61**. Using BHT with the thread under light conditions there is an isomerisation rate similar to the one monitored in the dark conditions (20% of conversion from *Z,Z* to *E,Z* in 40% I₂ in CDCl₃ solution).

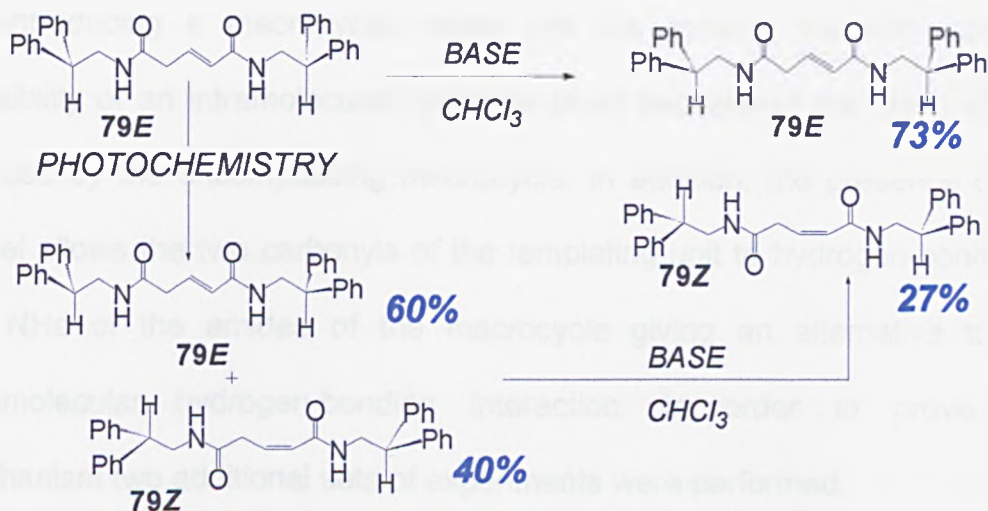
Research was also conducted on the glutaconic rotaxane **76E** (Chapter Three) to see how the reactivity of a single double bond was affected by macrocycle encapsulation.

It was noticed that during the process of rotaxane formation of the glutaconic thread **79**, the unreacted thread (65% recovery) was isolated after column chromatography, and found to be a mixture of two isomers, **79E** (73%) and **79Z** (27%) but the rotaxane **80** as a unique *E* species (Scheme 5.2).



Scheme 5.2

In order to investigate this rather interesting result, several experiments were performed on both the glutaconic-based rotaxane **80** and thread **79**. To a solution of **79E** in CHCl_3 was added an excess of base (NEt_3 , *p*-xylylene diamine or a mixture of the two), to mimic the conditions of rotaxane formation (Scheme 5.3).



Scheme 5.3

An almost immediate formation of a mixture of the two isomers **79Z** and **79E** in the proportion isolated from the rotaxane forming reaction was observed. After several hours the mixture composition did not change even adding more base or changing the base. The isomerisation from thread **79E** to **79Z** probably goes by an enolate due to the highly acidic character of the CH_2 of the thread. The possibility of an intramolecular hydrogen bond able to stabilise the Z-form of the thread may account for the position of the equilibrium (Figure 5.1). This is exhibited in the low field shift of the NH of the *cis* thread **79Z** in chloroform (NH_a 5.48 ppm for **79E** and 7.38 ppm for **79Z** and NH_b 5.38 ppm for **79E** and 7.25 ppm for **79Z**).

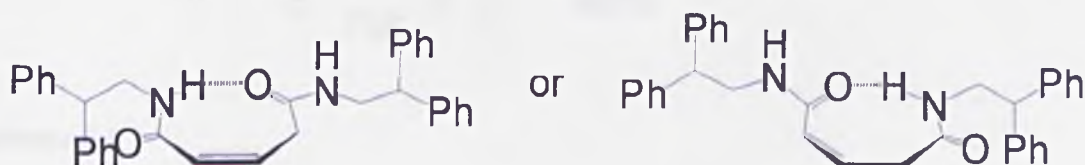
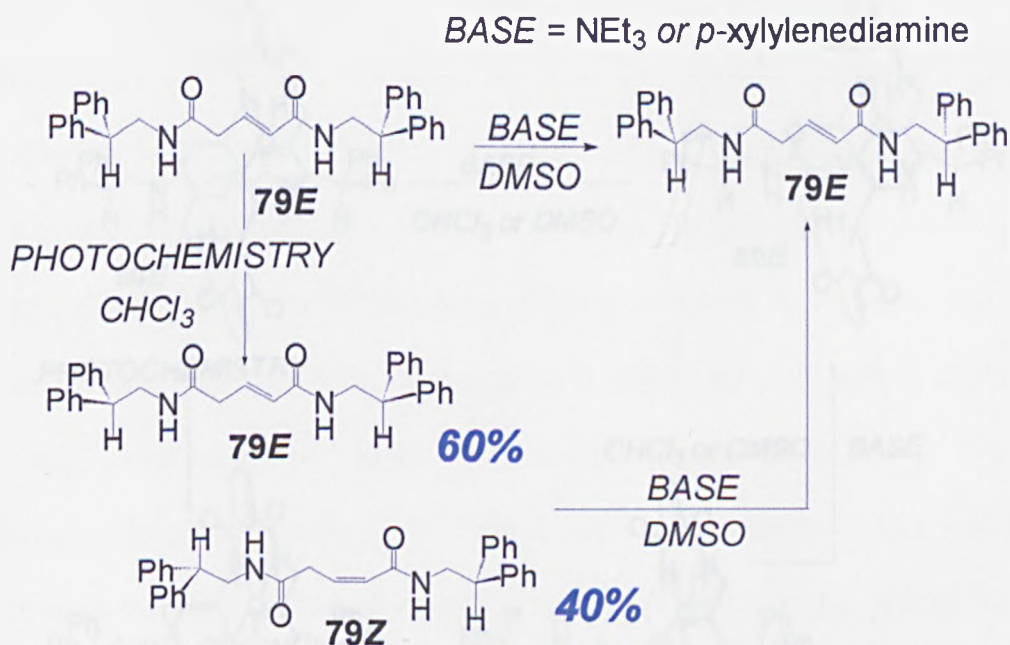


Figure 5.1

By introducing a macrocyclic wheel into the system, we eliminate the possibility of an intramolecular hydrogen bond because of the steric effects induced by the encompassing macrocycle. In addition, the presence of the wheel allows the two carbonyls of the templating unit to hydrogen-bond with the NHs of the amides of the macrocycle giving an alternative to the intramolecular hydrogen-bonding interaction. In order to prove this mechanism two additional sets of experiments were performed.

In the first set of experiments, shown in Scheme 5.4, the same experiments as before were performed under the same experimental conditions but in DMSO. Because of the disruption of the internal hydrogen bond due to the high polarity of the medium, thread **79E** did not isomerise to the Z form under basic conditions.

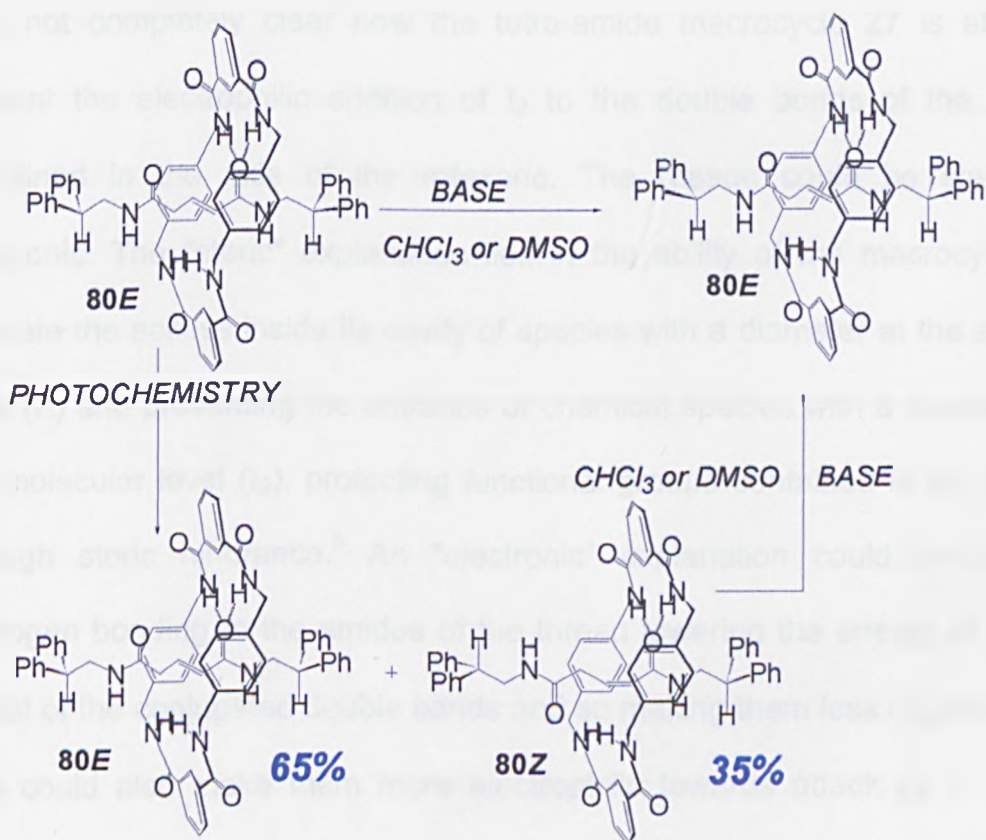


Scheme 5.4

Light can also be used to isomerise the double bond. The light isomerised *Z/E* ratio for thread **79** in CHCl_3 is different from that obtained by the base catalysed route. Again this returns to the all *E* product after treatment with base in DMSO (Scheme 5.4).

The second set of experiments was performed on rotaxane **80E** both in chloroform and DMSO. Both in CHCl_3 and in DMSO (Scheme 5.5) under the usual base catalysed experimental conditions the rotaxane **80E** did not isomerise.

As the rotaxane **80E** could not be isomerised chemically, it was isomerised by direct irradiation at 254 nm^{6,7} in CHCl_3 to give a mixture of the *E+Z* rotaxane (¹H-NMR) in a ratio 65/35. On treatment with base we observed a total conversion of the *Z* isomer into the *E* both in CHCl_3 and in DMSO.



Scheme 5.5

Attempted chromatographic separation of the *E+Z* rotaxane also failed due to the isomerisation of the mixture back to the *E* rotaxane.

Conclusions: The encapsulation of the thread within the macrocycle has a large effect on the chemistry of the thread. Chemical or photochemical isomerisation of the double bond is greatly altered by the presence of the macrocycle. The presence of a macrocycle proves to be an extraordinary "variable", able to change the physical and chemical properties of another molecular species (thread) in the glutamic rotaxane **80**, through steric effects and/or by offering an alternative H-bonding motif, the macrocycle is able to suppress the internal H-bonding of the thread and so influence the base catalysed isomerisation of the encapsulated thread.

It is not completely clear how the tetra-amide macrocycle **27** is able to prevent the electrophilic addition of I_2 to the double bonds of the diene contained in the axle of the rotaxane. The reason could be steric or electronic. The "steric" explanation lies in the ability of the macrocycle to regulate the access inside its cavity of species with a diameter at the atomic level (I^\bullet) and preventing the entrance of chemical species with a diameter at the molecular level (I_2), protecting functional groups contained in the cavity through steric hindrance.³ An "electronic" explanation could be in the hydrogen bonding to the amides of the thread lowering the energy of the π orbital of the conjugated double bonds and so making them less nucleophilic. This could also make them more electrophilic towards attack by I^\bullet . More experiments have to be done in order to understand how the presence of the macrocycle affects the chemistry of the conjugated diene system.

Nevertheless what is really remarkable is the capability of the tetra-amide macrocycle **27** to affect the chemistry of the olefins contained in the supramolecular system not simply slowing down the conversion as previously reported,³ but completely altering the conversion through the promotion/suppression of one or more of the chemical mechanisms involved. Because this remarkable effect is due to the presence of the macrocyclic wheel, here we report for the first time the complete iodine-catalysed *Z/E*-isomerisation of internal conjugated dienes obtained using just a catalytic amount of iodine instead of the large excess necessary for the free thread. These results demonstrate how interlocked molecules can show properties different from the sum of their parts.

Experimental Part:

All threads and rotaxanes were fully characterised by melting point, mass spectroscopy, elemental analysis and ¹H and ¹³C-NMRs and compared with the data obtained for the compounds presented in Chapters Two and Three. Isomerisation was followed by 300 MHz ¹H-NMR and the relative ratio of the isomers were obtained by comparison of the integrals.

Isomerisation of the *cis,cis*-muconic thread **61 under light condition**

Bis (2,2-diphenylethyl)-*N,N'*-*cis,cis*-muconamide **61 (4%)**

Thread **61** (5.0 mg, 0.01 mmol) was dissolved in a solution of 0.1 mg of iodine in 1.0 mL of CDCl₃. (4%) At RT and at constant condition of light (sun lamp) the isomerisation was followed by ¹H-NMR. A 66% isomerization of the

cis,cis isomer **61** into the *cis,trans* **63** was observed after 72h but no further isomerisation was detected even after several days.

Bis (2,2-diphenylethyl)-*N,N'*-*cis,cis*-muconamide **61 (40%)**

Thread **61** (5.0 mg, 0.01 mmol) was dissolved in a solution of 1.0 mg of iodine in 1.0 mL of CDCl₃ (40%). At RT and at constant condition of light (sun lamp) the isomerisation was followed by ¹H-NMR. An 80% isomerization of the *cis,cis* isomer **61** into the *cis,trans* **63** was observed after 48h but no further isomerisation was detected even after several days.

Bis (2,2-diphenylethyl)-*N,N'*-*cis,cis*-muconamide **61 (40%) with BHT**

Thread **61** (5.0 mg, 0.01 mmol) was dissolved in a solution of 1.0 mg of iodine in 1.0 mL of CDCl₃ (40%) and BHT (0.044 mg, 2.0·10⁻⁴ mmol). At RT and at constant condition of light (sun lamp) the isomerisation was followed by ¹H-NMR. A partial isomerization of the *cis,cis* isomer **61** into the *cis,trans* **63** was observed but no further isomerisation was detected even after several days.

Isomerisation of the thread under dark condition (40%) at RT

Thread **61** (5.0 mg, 0.01 mmol) was dissolved in a solution of 1.0 mg of iodine in 1.0 mL of CDCl₃ (40%) in the total absence of light (dark conditions and protection of the sample from light with aluminium foil). At RT and in the total absence of light the isomerisation was followed by ¹H-NMR. A partial isomerization of the *cis,cis* isomer **61** into the *cis,trans* **63** (24.5%) was observed after 72h. No further isomerisation was observed while the sample

was deprived from light. When the sample was placed in light (sun-lamp) isomerisation was observed in a similar manner to the same experiment conducted only in light.

Isomerisation of the thread **61 under dark condition (40%) at 40°C**

Performing the experiment at the same experimental conditions of the previous one but at a constant temperature of 40°C it is possible to observe an increase in the rate of isomerisation even if also in this case the extent isomerisation comparable to the one in light conditions was not achieved (35%).

Isomerisation of the *cis,cis*-muconic rotaxane **62 under light condition**

Bis (2,2-diphenylethyl)-*N,N'*-*cis,cis*-muconamide rotaxane **62 (4%)**

Rotaxane **62** (10.3 mg, 0.01 mmol) was dissolved in a solution of 0.1 mg of iodine in 1.0 mL of CDCl₃ (4%). At RT and at constant condition of light (sun lamp) the isomerisation was followed by ¹H-NMR. A complete isomerization of the *cis,cis* isomer **62** into the *trans,trans* **58** was observed after 375 mins.

Bis (2,2-diphenylethyl)-*N,N'*-*cis,cis*-muconamide rotaxane **62 (40%)**

Rotaxane **62** (10.3 mg, 0.01 mmol) was dissolved in a solution of 1.0 mg of iodine in 1.0 mL of CDCl₃ (40%). At RT and at constant condition of light (sun lamp) the isomerisation was followed by ¹H-NMR. A complete isomerization of the *cis,cis* isomer **62** into the *trans,trans* **58** was observed after 275 mins.

Bis (2,2-diphenylethyl)-*N,N'*-cis,cis-muconamide rotaxane 62 (40%) with BHT

Rotaxane **62** (10.3 mg, 0.01 mmol) was dissolved in a solution of iodine in 1.0 mL of CDCl₃ (40%) and BHT (0.044 mg, 0.0002 mmol). At RT and at constant condition of light (sun lamp) the isomerisation was followed by ¹H-NMR. After 275 mins just a 20% conversion (13% *cis,trans* **64** and 7% of *trans,trans* **58**) was observed. A complete conversion was detected after 24 hours.

Isomerisation of the rotaxane 62 under dark condition (40%) at RT

Rotaxane **62** (10.3 mg, 0.01 mmol) was dissolved in a solution of 1.0 mg of iodine in 1.0 mL of CDCl₃ (40%) in total absence of light. At RT and in total absence of light the isomerisation was followed by ¹H-NMR. No isomerisation was observed even after several hours. When the sample was placed in light (sun-lamp) isomerisation was observed in a similar manner to the same experiment conducted only in light.

Glutaconic Thread 79 Isomerisation Experiments

Chemical Isomerisation of the Glutaconic Thread 79 in CHCl₃ (*p*-xylylene diamine or triethylamine)

Glutaconic thread **79E** (7.5 mg, $1.5 \cdot 10^{-2}$ mmol) was dissolved in 1.0 mL of CDCl₃ and *p*-xylylene diamine (24.5 mg, 0.18 mmol) or triethylamine (18.2 mg, 0.18 mmol) was added. The isomerisation was followed by ¹H-NMR. The *E/Z* isomerization is very fast and after just a few seconds it is possible to

observe a 27% of conversion of the E isomer **79E** into the Z one **79Z**. Then a plateau is reached.

Photochemical Isomerisation of the Glutaconic Thread 79 in CHCl₃

Glutaconic thread **79E** (75.0 mg, 0.15 mmol) was dissolved in 10.0 mL of degassed CDCl₃. Under direct-irradiation (254 nm) the *E/Z* isomerisation is quite fast and occurs in the first 45 mins with a 40% conversion of the *E* isomer **79E** into the *Z* one **79Z**. Then degradation start to occurs. The isomerisation was followed by ¹H-NMR.

Chemical Isomerisation of the Mixture 79E, 79Z in CHCl₃ (*p*-xylylene diamine or triethylamine)

The isomeric mixture of isomers 2,2-diphenylamino glutaconic thread **79E** (60%) and **79Z** (40%) (7.5 mg, $1.5 \cdot 10^{-2}$ mmol) was dissolved in 1.0 mL of CDCl₃ and *p*-xylylene diamine (24.5 mg, 0.18 mmol) or triethylamine (18.2 mg, 0.18 mmol) was added. The isomerisation was followed by ¹H-NMR. The *E/Z* isomerization is very fast and after just a few seconds it is possible to observe a new ratio of the *E* isomer **79E** into the *Z* one **79Z** (73% **79E**, 27% **79Z**); then a plateau is reached.

Chemical Isomerisation of the Glutaconic Thread 79 in DMSO (*p*-xylylene diamine or triethyl amine)

Glutaconic thread **79E** (7.5 mg, $1.5 \cdot 10^{-2}$ mmol) was dissolved in 1.0 mL of DMSO-*d*₆ and *p*-xylylene diamine (24.5 mg, 0.18 mmol) or triethyl amine

(18.2 mg, 0.18 mmol) was added. The isomerisation was followed by ^1H -NMR. No *E/Z* isomerization was observed even after several hours.

Chemical Isomerisation of the Mixture **79E, **79Z** in DMSO (*p*-xylylene diamine or triethyl amine)**

The isomeric mixture of glutaconic thread **79E** (60%) and **79Z** (40%) (7.5 mg, $1.5 \cdot 10^{-2}$ mmol) was dissolved in 1.0 mL of DMSO- d_6 and *p*-xylylene diamine (24.5 mg, 0.18 mmol) or triethyl amine (18.2 mg, 0.18 mmol) was added. The isomerisation was followed by ^1H -NMR. The *E/Z* isomerization occurs in 2h to give a complete isomerisation to the *E* one.

Experiments with Glutaconic Rotaxane **80**

Chemical Isomerisation of the Glutaconic Rotaxane **80 in CHCl_3 (*p*-xylylene diamine or triethylamine)**

Glutaconic rotaxane **80E** (15.3 mg, $1.5 \cdot 10^{-2}$ mmol) was dissolved in 1.0 mL of CDCl_3 and *p*-xylylene diamine (24.5 mg, 0.18 mmol) or triethylamine (18.2 mg, 0.18 mmol) was added. The isomerisation was followed by ^1H -NMR. No *E/Z* isomerization was observed even after several hours.

Photochemical Isomerisation of the Glutaconic Rotaxane **80 in CHCl_3**

Glutaconic rotaxane **80E** (153.0 mg, 0.15 mmol) was dissolved in 10.0 mL of degassed CDCl_3 . Under direct-irradiation (254 nm) the *E/Z* isomerisation is quite fast and occurs in the first 75 mins (65% **80E**, 35% **80Z**); then degradation start to occurs. The isomerisation was followed by ^1H -NMR.

Chemical Isomerisation of the Mixture *80E*, *80Z* in CHCl_3 (*p*-xylylene diamine or triethylamine)

The isomeric mixture of glutaconic rotaxane ***80E*** (65%) and ***80Z*** (35%) (15.3 mg, $1.5 \cdot 10^{-2}$ mmol) was dissolved in 1.0 mL of CDCl_3 and *p*-xylylene diamine (24.5 mg, 0.18 mmol) or triethylamine (18.2 mg, 0.18 mmol) was added. The isomerisation was followed by $^1\text{H-NMR}$. The *E/Z* isomerization is quite slow but after 7 hours it is possible to observe a complete isomerisation to the *E* one.

Chemical Isomerisation of the Glutaconic Rotaxane *80* in DMSO (*p*-xylylene diamine or triethyl amine)

Glutaconic rotaxane ***80E*** (15.3 mg, $1.5 \cdot 10^{-2}$ mmol) was dissolved in 1.0 mL of $\text{DMSO-}d_6$ and *p*-xylylene diamine (24.5 mg, 0.18 mmol) or triethyl amine (18.2 mg, 0.18 mmol) was added. The isomerisation was followed by $^1\text{H-NMR}$. No *E/Z* isomerization was observed even after several hours.

Chemical Isomerisation of the Rotaxane Mixture *80E*, *80Z* in DMSO (*p*-xylylene diamine or triethyl amine)

The isomeric mixture of glutaconic rotaxane ***80E*** (65%) and ***80Z*** (35%) (15.3 mg, $1.5 \cdot 10^{-2}$ mmol) was dissolved in 1.0 mL of $\text{DMSO-}d_6$ and *p*-xylylene diamine (24.5 mg, 0.18 mmol) or triethyl amine (18.2 mg, 0.18 mmol) was added. The isomerisation was followed by $^1\text{H-NMR}$. The *E/Z* isomerization is quite slow but after 12 hours it is possible to observe a complete isomerisation of the *Z* species into the *E* one.

References:

1. (a) Amabilino, D.B.; Stoddart, J.F. *Chem. Rev.* **1995**, 2725. (b) Schill, G. *Catenanes, Rotaxanes and Knots*; Academic Press: New York, **1971**.
2. (a) Anderson, S.; Anderson, H.L. *Angew. Chem. Int. Ed. Engl.* **1996**, 35, 1956. (b) Anderson, S.; Aplin, R.T.; Claridge, T.D.W.; Goodson, T.; Maciel, A.C.; Rumbles, G.; Ryan, J.F.; Anderson, H.L. *J. Chem. Soc. Perkin Trans. 1* **1998**, 15, 2383. (c) Johnston, A.G.; Leigh, D.A.; Murphy, A.; Smart, J.P.; Deegan, M.D. *J. Am. Chem. Soc.* **1996**, 118, 10662.
3. Parham, A.H.; Windish, B.; Vögtle, F. *Eur.J.Org.Chem.* **1999**, 1233.
4. Sonnet, P.E. *Tetrahedron* **1980**, 36, 557.
5. Roelofs, W.; Comeau, A.; Milicevic, G. *Science* **1971**, 174, 297.
6. (a) The Chemistry of Alkenes, edited by S. Patai, Interscience, New York, **1964**. (b) The Chemistry of Alkenes, Vol.2, edited by J. Zabicky, Interscience, New York, **1968**.
7. (a) Egger, K.W.; Benson, S.W. *J. Am. Chem. Soc.* **1965**, 87, 3311. (b) Egger, K.W.; Benson, S.W. *J. Am. Chem. Soc.* **1965**, 87, 3314.
8. Ideses, R.; Shani, A. *J. Am. Oil Chem. Soc.* **1989**, 66, 948.
9. Benesi, H.A.; Hildebrand, J.H. *J. Am. Chem. Soc.* **1949**, 71, 2703.
10. March, J. *Advanced Organic Chemistry: Reactions, Mechanisms and Structure*, 2nd ed., Mc Graw Hill Kogakusha; Tokyo, **1977**, pp 28 and 635.
11. Beckmann, Z. *Physic. Chem.* **1889**, 5, 76.
12. Lachman, A. *J. Am. Chem. Soc.* **1903**, 25, 50.
13. Hildebrand, J.H.; Glascock, B.L. *J. Am. Chem. Soc.* **1909**, 31, 26.
14. Dai, L.; Mau, A.W.H.; Griesser, H.J.; Wink, D. *Macromolecules* **1994**, 27, 6728.

Chapter Six

6. Self-assembled Monolayers of Heterocircuit [2]Catenanes on Gold.

Abstract: Several heterocircuit [2]catenanes functionalised with various sulphide groups were synthesised and their monolayer forming capability on a gold surface studied. Another approach involving covalent attachment of macrocycles and catenanes on a pre-formed monolayer was also investigated.

Introduction: Alkanethiols chemisorb spontaneously from solution onto gold, silver, platinum or copper surfaces with the formation of a stable metal-sulphur bond. Gold is the most frequently used metal because it doesn't form a stable oxide under atmospheric conditions and because it produces a stronger interaction with the sulphur compared to the other metals. The intermolecular interactions between the alkyl chains determine the stability and the order of the Self-Assembled Monolayer (SAM). SAMs with 10 to 16 carbon atoms on the chain are more ordered than those with shorter chains. The recent scientific interest in these films is due to several reasons: the simplicity of the experimental procedure to prepare the films, their reproducibility, easy access to a wide range of surfaces via the incorporation of different groups into the alkyl-chains or on the tail of the chain. These properties allowed the application of the SAMs in many areas of science,

such as microelectronics, materials science, chemical and biochemical sensing, and molecular recognition.

The most common approach to functionalise a Self-Assembled Monolayer involves the chemical modification via covalent bonding between a molecule and the SAM.

Results and discussion: The aim of this research is to synthesised an alkanethiol functionalised heterocircuit [2]catenane, use it to form SAMs on a gold surface and investigate if it still retains the switchable characteristics observed in solution (Figure 6.1).

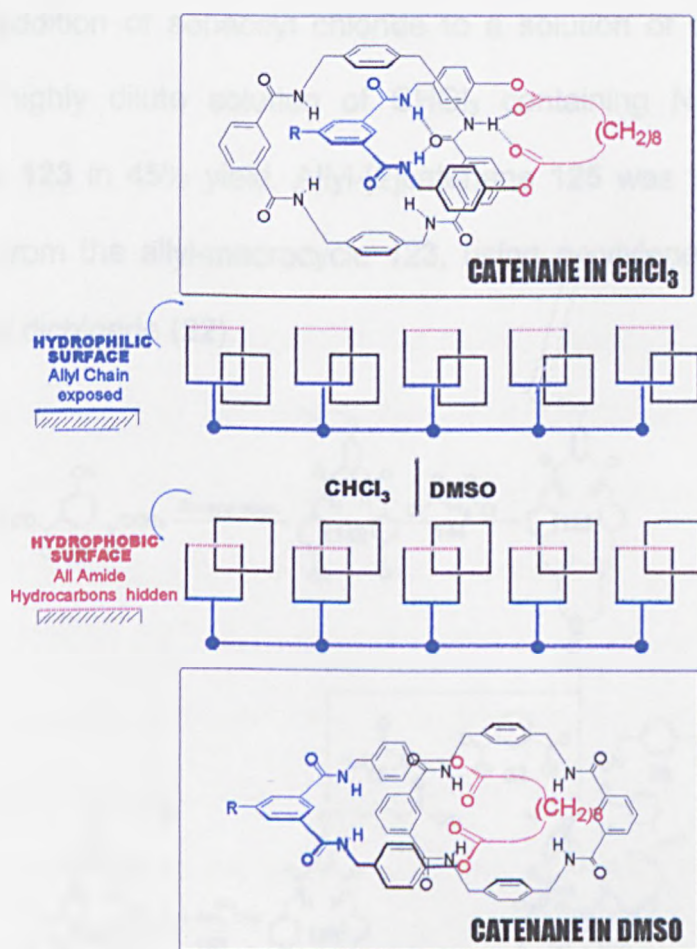
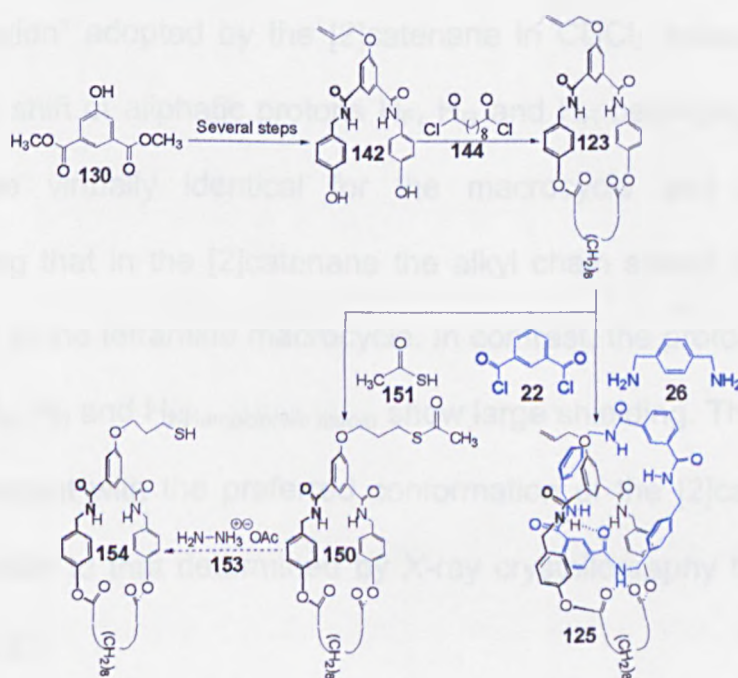


Figure 6.1

As the two rings are different in heterocircuit [2]catenanes composed of an amphiphilic macrocycle (**123**) and tetramide macrocycle (**27**), this allows the mono-functionalisation of only one of the rings and still retains the solvent switchable ability (Figure 6.1).¹

Various synthetic strategies were investigated for the preparation of an alkanethiol containing a catenane as a terminal head group (Scheme 6.1). The preparation of the catenane thiol **154** is a ten step synthetic route starting from commercially available 5-hydroxyisophthalic acid.

The synthesis began with a six step route to the hydroxy-benzyl isophthalamide **142**, (Scheme 6.2), based on other work in the group.¹ Dropwise addition of sebacoyl chloride to a solution of diphenol precursor **142** in a highly dilute solution of CHCl_3 containing NEt_3 afforded allyl-macrocycle **123** in 45% yield. Allyl-[2]catenane **125** was then prepared in a 40% yield from the allyl-macrocycle **123**, using *p*-xylylene diamine (**26**) and isophthaloyl dichloride (**22**).



Scheme 6.1

An allyl group was chosen because of its dual role as a robust protecting group for the phenol during the catenane synthesis and/or it can be used as a handle for further synthetic elaboration.²

Addition of thioacetic acid onto the allyl group of macrocycle **123** mediated by a catalytic amount of VAZO^{®3} dissolved in toluene previously degassed and heated to 90°C, gave the protected thiol **150** in quantitative yield.

These heterocircuit (the two rings are different) [2]catenanes show interesting solvent switching properties. The large macrocycle is composed of polar amide and non-polar alkyl chain domains. The “smaller” interlocked tetramide macrocycle sits preferentially over the amide domain in non-polar solvents where inter ring hydrogen bonding dominates. In polar solvents, inter-ring hydrogen bonding is broken and the tetramide macrocycle lies over the alkyl chain shielding it from the hydrophilic medium.

A comparison of the ¹H-NMR spectra (Figure 6.2) of the (1+1) macrocycle **123** and the [2]catenane **125** allows the determination of the “supramolecular conformation” adopted by the [2]catenane in CDCl₃ solution. In CDCl₃ the chemical shift of aliphatic protons H_F, H_G and H_H belonging to the sebacoyl chain are virtually identical for the macrocycle and the [2]catenane, suggesting that in the [2]catenane the alkyl chain spend little time in close proximity to the tetramide macrocycle. In contrast, the protons of the benzylic spacer H_A, H_B and H_{NH}*amphiphilic macro* show large shielding. These observations are consistent with the preferred conformation of the [2]catenane in CDCl₃ being similar to that determined by X-ray crystallography for the solid state (Figure 6.3).

In DMSO- d_6 , a hydrogen-bond accepting solvent, the protons H_A , H_B and H_{NH} amphiphilic macro occur at similar chemical shift in the macrocycle and hetero [2]catenane; however, the protons of the sebacoyl chain of the [2]catenane are heavily shielded with respect to those of the analogous macrocycle (Figure 6.2).

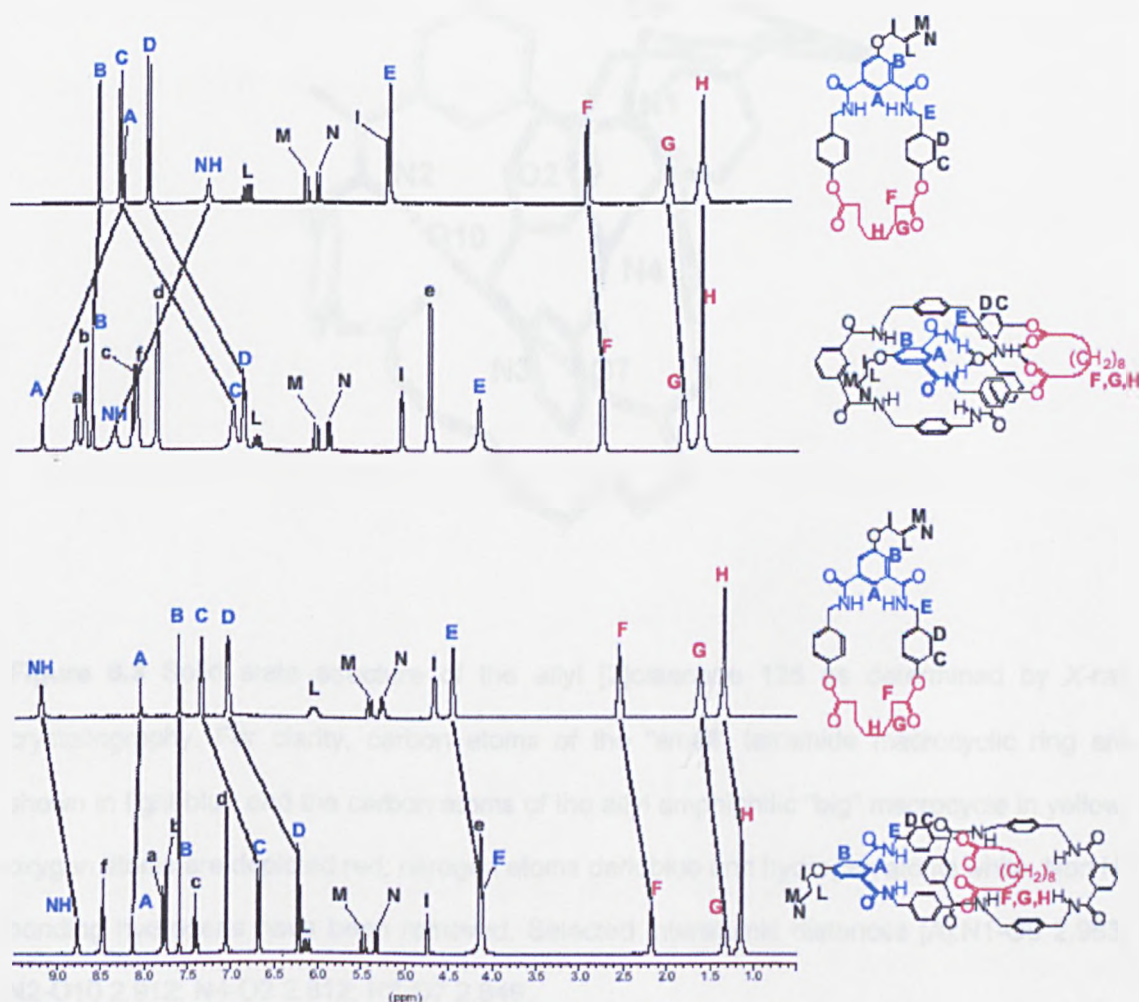


Figure 6.2 ^1H -NMR spectra (400 MHz, CDCl_3 top two spectra and $\text{DMSO}-d_6$ bottom two spectra) of allyl macrocycle **123** and ally [2]catenane **125**.

Single crystals of catenane **125** suitable for investigation by X-ray diffraction were obtained from a CHCl_3 /methanol mixture by slow evaporation. The crystal structure analysis (Figure 6.3) shows that the small macrocycle lies

over the isophthalamide portion of the mixed amide/ester macrocycle (big macrocycle) **123** held by a network of inter ring hydrogen bonds.

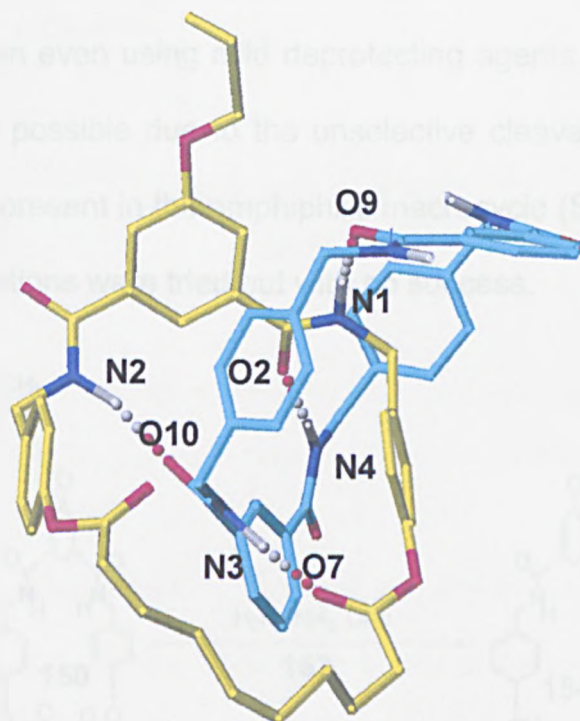
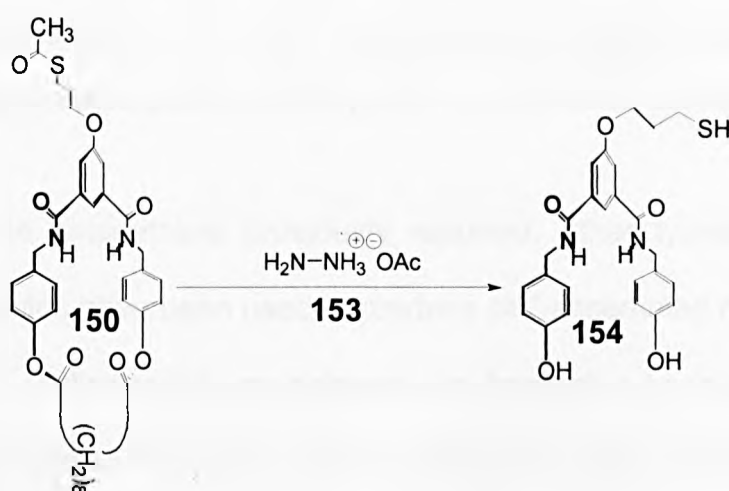


Figure 6.3 Solid state structure of the allyl [2]catenane **125** as determined by X-ray crystallography. For clarity, carbon atoms of the "small" tetramide macrocyclic ring are shown in light blue and the carbon atoms of the allyl amphiphilic "big" macrocycle in yellow; oxygen atoms are depicted red, nitrogen atoms dark blue and hydrogen atoms white. Non H-bonding hydrogens have been removed. Selected interatomic distances [Å]: N1-O9 2.983; N2-O10 2.912; N4-O2 2.812; N3-O7 2.849.

The isophthaloyl 1,3-diamide group of the larger macrocycle adopt a *syn-anti* conformation that orients one amide NH towards the central cavity where it participates in a hydrogen bond with a carbonyl of the tetramide macrocycle (**27**). There is a reciprocal arrangement with the isophthalamides of the small macrocycle.

Additionally, macrocycle **27** adopts a boat-like conformation in contrast to the chair-like form more usual in the solid state structures of the rotaxanes.

Despite the successful preparation of this target molecule, the deprotection of the sulphur function even using mild deprotecting agents such as hydrazine acetate ⁴ was not possible due to the unselective cleavage of the phenolic ester functionality present in the amphiphilic macrocycle (Scheme 6.2). Other experimental conditions were tried but with no success.



Scheme 6.2

Because of the difficulties encountered in attempting to prepare a [2]catenane containing a free thiol function, **155**, a new strategy was developed in order to attach the supramolecular species via a thio-ether functional group.⁵

In order to attach a molecule to a gold layer three distinct parts of the molecule have to be taken into account: [**a**] the sulfur for the interaction with the gold surface, [**b**] the orientation and order of the alkyl chain ⁶ and [**c**] the terminal head-group (fig. 6.4).

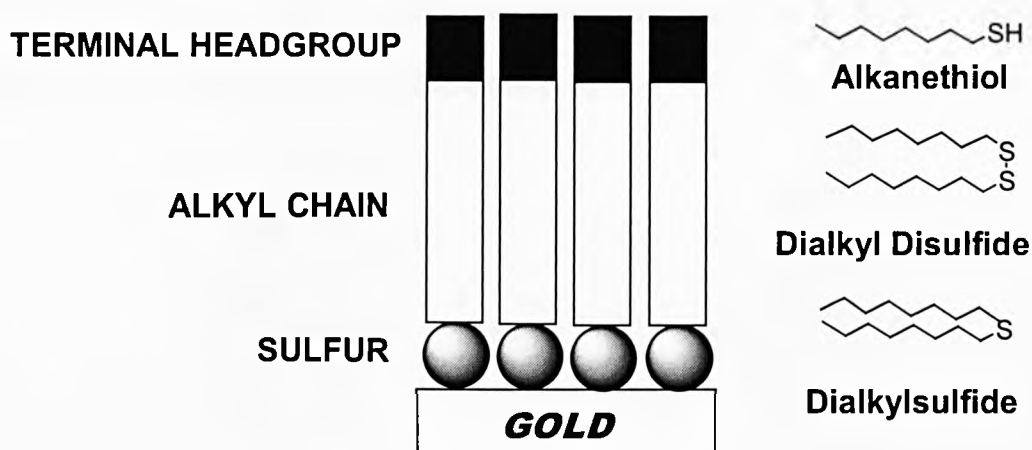
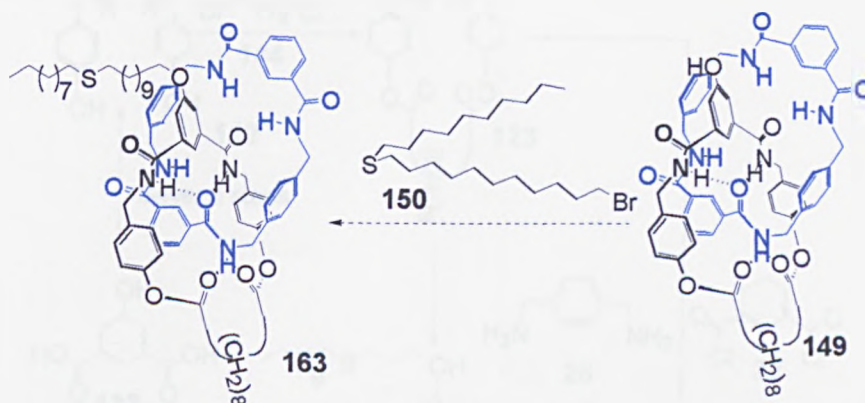


Figure 6.4 Schematic representation of sulfur-containing self-assembled monolayers on gold with the three distinct structural parts and three types of sulfur containing adsorbates.

In addition to the alkanethiols previously reported, other types of sulfur-containing molecules have been used to produce self-assembled monolayers (SAMs) on gold. Dialkyl sulfide monolayers are beginning to receive some attention as opposed to the more common alkanethiol and dialkyl disulfide derived SAMs. Thio-ethers bind to the gold film with a very strong coordinative sulfide bond in contrast to the covalent bonds formed between gold and alkyl thiols or dialkyl disulfides. The monolayer forming ability of thio-ethers have been pioneered by Reinhoudt and co-workers. Thio ethers have been used to make monolayers on gold of systems containing calixarenes,⁷ dendrimers,⁸ β -cyclodextrins,⁹ and pseudo-rotaxanes based on the host-guest interactions of cyclodextrin containing self-assembled monolayers on gold.¹⁰

Two different synthetic strategies were developed. According to the first synthetic strategy the [2]catenane **125** was deprotected (87% yield) and the

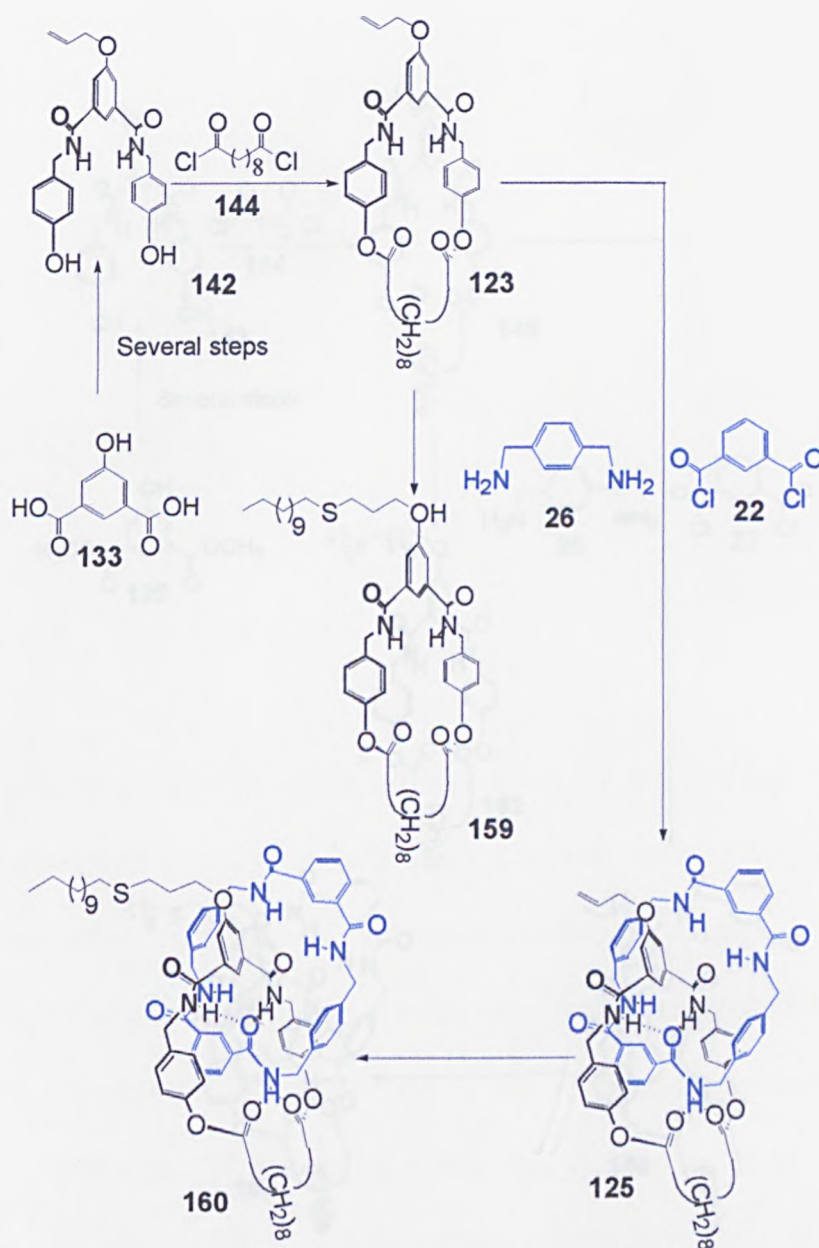
resulting molecule functionalised by alkylation of the phenol substituted heterocircuit [2]catenane **149** (Scheme 6.3).



Scheme 6.3

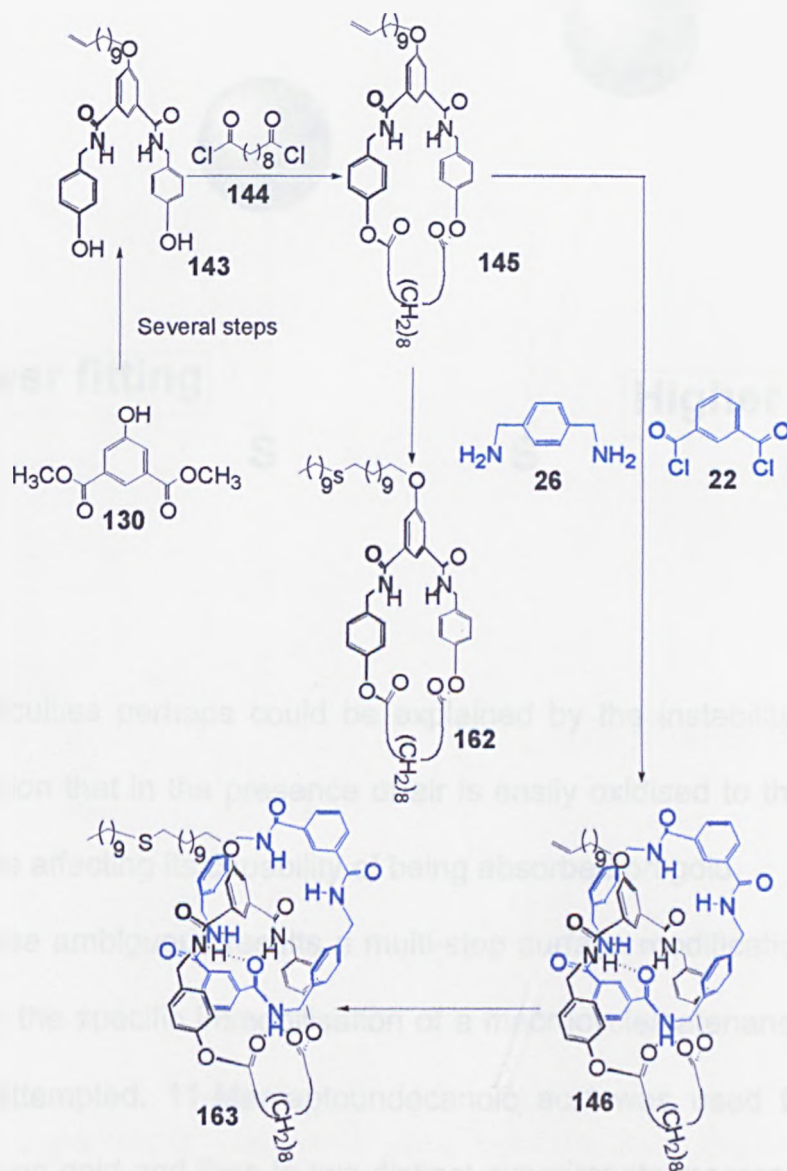
Unfortunately this approach was not very successful due to the very low reactivity of the phenol group of the amphiphilic catenane **149**.

In a second approach a series of longer chains were attached to the starting macrocycle in order to produce a new series of macrocycles and catenanes suitable for the attachment of the sulfide unit (Scheme 6.4) following the synthetic methodology developed by the Reinhoudt group for calixarene-based systems.⁵ Longer chains facilitate well-ordered film formation on the gold surface.⁶ Macrocycles and catenanes functionalised with pendent alkene groups were transformed into thio-ethers by radical addition of sulfides to the double bond. Macrocycle **123** and catenane **125** functionalised with the short allyl chain were used for model studies of thiol addition to catenanes and macrocycles because they were already available. AIBN catalysed addition of thiols to the allyl group proved problematic but the use of VAZO[®]³ gave quantitative addition to yield the thio-ether macrocycles and catenanes.



Scheme 6.4

Macrocycle **159** and catenane **160** with a three-carbon atoms chain between the sulphur and the macrocycle did not form layers on gold. Lengthening the size of the chain on the other side of the thiol had no effect on these materials' film forming ability of these materials. It is known that better aligned and regular films of similar thio-ethers are obtained by having a chain of at least 10 atoms long and a complementary shorter chain (Scheme 6.5).⁵



Scheme 6.5

The presence of a considerable longer chain could allow a better fitting of this secondary chain under the terminal heading group, with a consequent more organised tertiary structure and so with a better stability of the SAM. But even in this case no clear experimental evidence could be obtained to prove unequivocally film formation on gold (Figure 6.5).

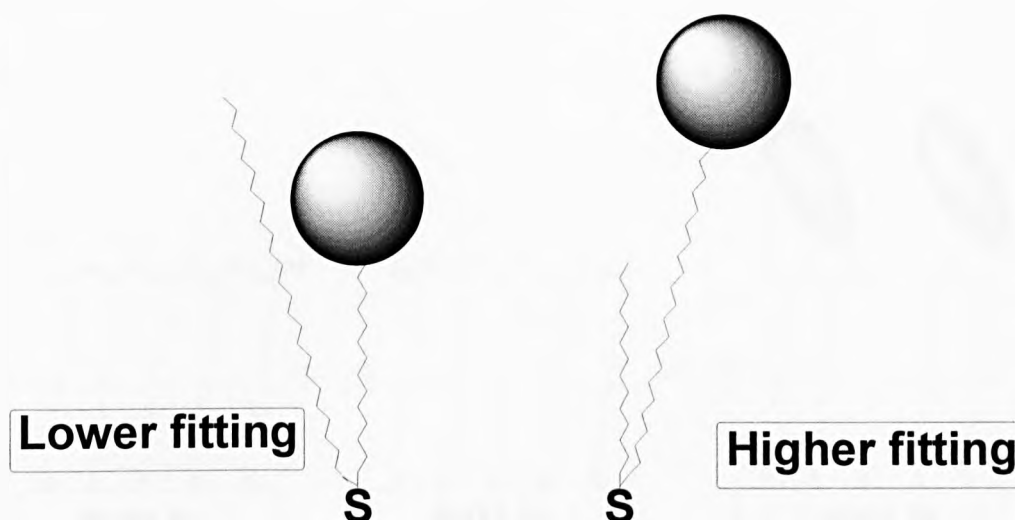


Figure 6.5

These difficulties perhaps could be explained by the instability of the thio-ether function that in the presence of air is easily oxidised to the sulphoxide or sulphone affecting its capability of being absorbed on gold.

Due to these ambiguous results a multi-step surface modification procedure that allows the specific immobilisation of a macrocycle/catenane onto a gold film was attempted. 11-Mercaptoundecanoic acid was used to preform a monolayer on gold and then in two distinct experiments macrocycle **148** and catenane **149** containing a phenyl group were covalently attached to the layer.

Specifically, the chemical modification steps were the following: **[1]** the adsorption and self-assembly of an 11-mercaptoundecanoic acid monolayer on an evaporated gold thin film; **[2]** the activation of the carboxylic group using EDCI **[3]** the reaction of the activated acid with the phenol of the macromolecule to create the desired film (Figure 6.6).

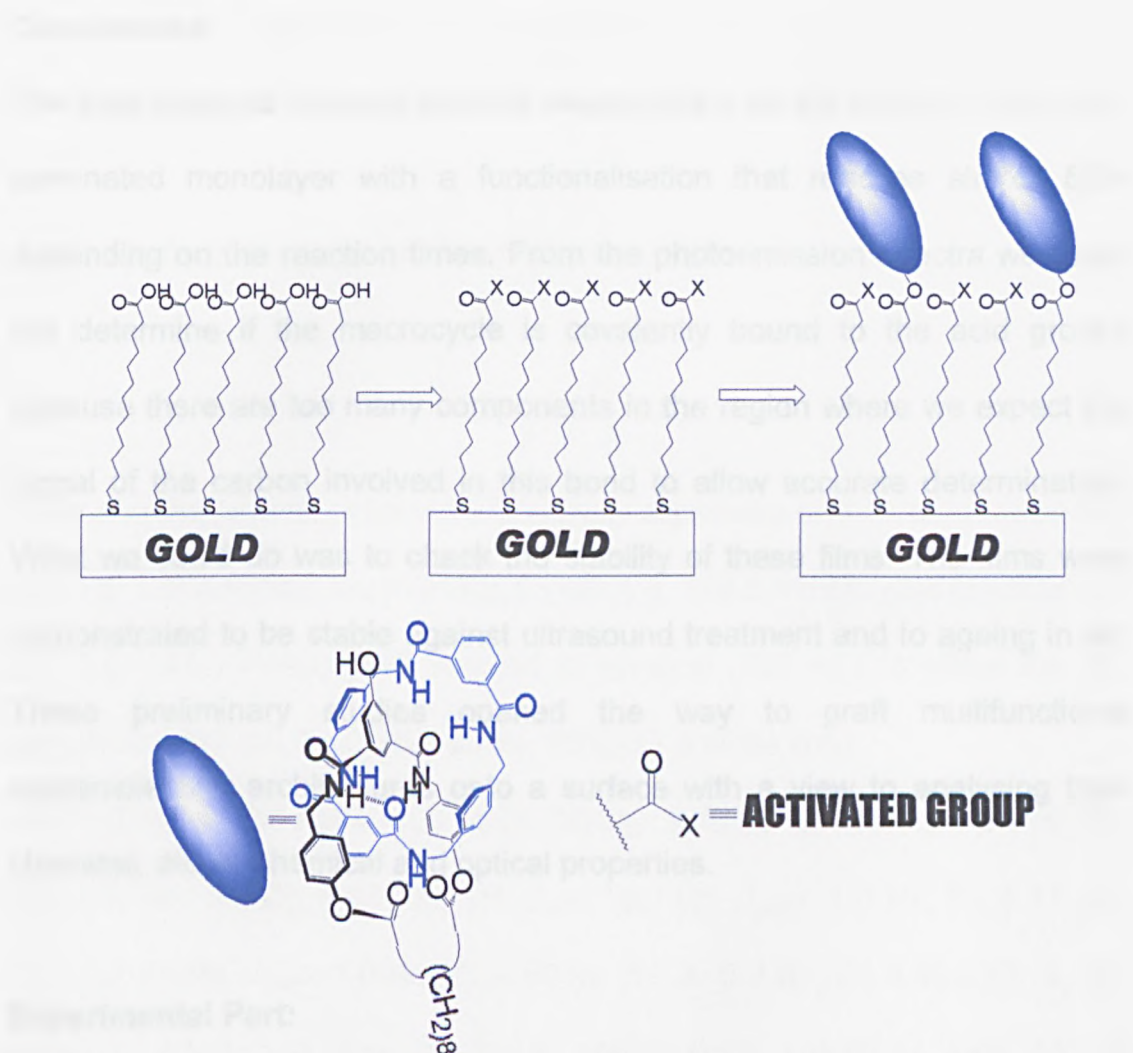


Figure 6.6

Preliminary experiments performed using both the amphiphilic macrocycle **148** and catenane **149** show incorporation of these materials on the film. The supramolecular species absorbed onto the gold film cannot be removed by heating procedures and are assumed to be covalently attached to the monolayer.

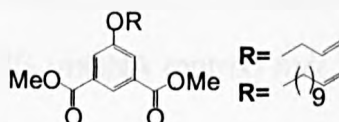
Characterisation of the modified surfaces, estimation of the surface coverage and stability of the films for macrocycle **148** were conducted by Professor Petra Rudolf and Mrs. Francesca Cecchet at the University Notre-Dame de la Paix, Namur.

Conclusions

The data obtained indicates that the macrocycle is on the surface of the acid-terminated monolayer with a functionalisation that reaches almost 50% depending on the reaction times. From the photoemission spectra we could not determine if the macrocycle is covalently bound to the acid groups because there are too many components in the region where we expect the signal of the carbon involved in this bond to allow accurate determination. What we could do was to check the stability of these films. The films were demonstrated to be stable against ultrasound treatment and to ageing in air. These preliminary studies opened the way to graft multifunctional supramolecular architectures onto a surface with a view to analysing their chemical, electrochemical and optical properties.

Experimental Part:

5-Alkoxyisophthalic acid esters

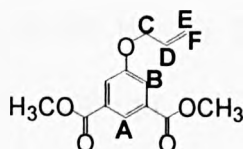


General procedure

To a stirred solution of 5-hydroxyisophthalic dimethyl ester **130** (1.0 eq) in acetone, crushed K_2CO_3 (1.3 eq) and the bromide (**131** or **133**) of the protecting group (1.2 eq) were added. The mixture was refluxed overnight (whilst being monitored by TLC) then evaporated to dryness under reduced pressure. The residue was partitioned between CHCl_3 and water and the organic layer was washed twice further with water, dried (MgSO_4) and

evaporated to give the 5-alkoxyisophthalic acid esters without need for further purification.

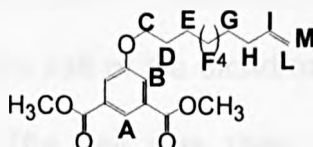
5-Allyloxyisophthalic acid dimethyl ester (**132**)



Following the general procedure 5-hydroxyisophthalic acid dimethyl ester **130** (25.8 g, 122.9 mmol), crushed K_2CO_3 (22.1 g, 159.8 mmol), allyl bromide **131** (17.8 g, 147.5 mmol) were reacted in acetone (200 mL) to afford the *title compound* **132** (30.0 g, 120.0 mmol, 98%) as a white solid.

mp 145-146°C; 1H NMR (400 MHz, $CDCl_3$): δ = 8.26 (s, 1H, **A**), 7.74 (s, 2H, **B**), 6.04 (m, 1H, **D**), 5.46 (dd, 1H, J_{vic} = 16.0 Hz, J_{gem} = 1.0 Hz, **F**), 5.31 (dd, 1H, J_{vic} =9.0 Hz, J_{gem} = 1.0 Hz, **E**), 4.60 (d, 2H, J = 6.0 Hz, **C**), 3.92-3.87 (s, 6H, CH_3); ^{13}C NMR (100 MHz, $CDCl_3$): δ = 166.42 (CO), 158.97 (q, ArC), 132.79 (CH), 132.10 (q, ArC), 123.43 (ArCH), 120.38 (ArCH), 118.51 (CH_2), 69.29 (CH_2), 52.77 (CH_3). FAB MS (*m*BNA matrix) m/z 251 $[M+H]^+$; Anal. Calcd for $C_{13}H_{14}O_5$ (250.25): C, 62.39; H, 5.64. Found: C, 62.62; H, 5.59.

5-(Undec-10-enyloxy)-isophthalic acid dimethyl ester (**134**)

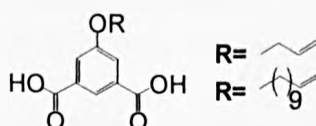


Following the general procedure 5-hydroxyisophthalic acid dimethyl ester **130** (5.0 g, 23.8 mmol), crushed K_2CO_3 (4.3 g, 30.9 mmol), 11-bromo-1-

undecene **133** (6.7 g, 28.6 mmol) were reacted in acetone (200 mL) to afford the *title compound 134* (8.1 g, 22.3 mmol, 94%) as a white solid.

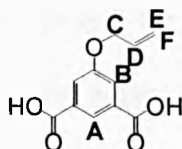
mp 142-143°C; ^1H NMR (CDCl_3): δ = 8.25 (s, 1H, **A**), 7.73 (s, 2H, **B**), 5.81 (m, 1H, **I**), 4.99 (dd, 1H, J_{vic} = 16.0 Hz J_{gem} = 1.0 Hz, **L**), 4.91 (dd, 1H, J_{vic} = 9.0 Hz J_{gem} = 1.0 Hz, **M**), 4.25 (t, 2H, J = 6.0 Hz, **C**), 3.92 (s, 6H, CH_3), 2.15 (m, 2H, **H**), 1.80 (qu, 2H, J = 6.0 Hz, **D**), 1.48 (qu, 2H, J = 6.0 Hz, **E**), 1.38 (m, 2H, **G**), 1.31 (m, 8H, **F**); ^{13}C NMR (CDCl_3): δ = 166.51 (CO), 159.61 (q, ArC), 139.50 (CH), 132.07 (q, ArC), 123.08 (ArCH), 120.15 (ArCH), 114.49 (CH_2), 68.94 (CH_2), 52.77 (CH_3), 34.18 (CH_2), 29.87 (CH_2), 29.78 (CH_2), 29.69 (CH_2), 29.61 (CH_2), 29.47 (CH_2), 29.28 (CH_2), 26.33 (CH_2). FAB MS (*m*BNA matrix) m/z 363 $[\text{M}+\text{H}]^+$. Anal. Calcd for $\text{C}_{21}\text{H}_{30}\text{O}_5$ (362.46): C 69.59; H 8.34. Found: C 69.38; H 5.3

5-Substitued isophthalic acids



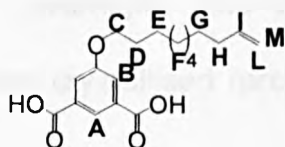
General procedure

To a stirred solution of the 5-alkoxyisophthalic acid ester in EtOH, NaOH (aq) (3.0 eq) was added and the mixture refluxed overnight. The reaction mixture was cooled and the disodium salt of the dicarboxylic acid was filtered off and washed with cold EtOH. The salt was then dissolved in water and 5M aqueous hydrochloric acid (6.0 eq) was added to precipitate the dicarboxylic acid which was filtered by suction, washed with distilled water until the filtrate was neutral and then dried *in vacuo* at 50°C.

5-Allyloxyisophthalic acid (135)

Following the general procedure 5-allyloxyisophthalic acid dimethyl ester **132** (8.0 g, 32.0 mmol) was treated with 10 M aqueous NaOH (9.6 mL, 96.0 mmol) in EtOH (150 mL) to afford the *title compound* **135** (7.1 g, 32.0 mmol, 100%) as a white solid.

mp 229-230°C; ^1H NMR (400 MHz, DMSO- d_6): δ = 8.14 (s, 1H, **A**), 7.70 (s, 2H, **B**), 6.10 (m, 1H, **D**), 5.49 (dd, 1H, J_{vic} = 16.0 Hz, J_{gem} = 1.0 Hz, **E**), 5.33 (dd, 1H, J_{vic} = 9.0 Hz, J_{gem} = 1.0 Hz, **F**), 4.73 (d, 2H, J = 6.0 Hz, **C**); ^{13}C NMR (100 MHz, DMSO- d_6): δ = 166.71 (q, CO), 158.58 (q, ArC), 133.45 (CH), 132.89 (q, ArC), 122.47 (ArCH), 119.58 (ArCH), 117.97 (CH₂), 68.95 (CH₂). FAB MS (*m*BNA matrix) m/z 223 $[\text{M}+\text{H}]^+$; Anal. Calcd for C₁₁H₁₀O₅ (222.19): C, 59.46; H, 4.54. Found: C, 59.21; H, 4.62.

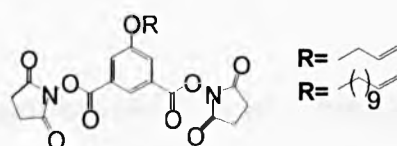
5-(Undec-10-enyloxy)-isophthalic acid (136)

Following the general procedure 5-(undec-10-enyloxy)-isophthalic acid dimethyl ester **134** (8.0 g, 22.1 mmol) was treated with 10 M aqueous NaOH (6.6 mL, 66.0 mmol) in EtOH (150 mL) to afford the *title compound* **136** (7.4 g, 22.1 mmol, 100%) as a white solid.

mp 220-221°C; ^1H NMR (400 MHz, DMSO- d_6): δ = 13.17 (bs, 2H, OH), 8.09 (s, 1H, **A**), 7.61 (s, 2H, **B**), 5.71 (m, 1H, **I**), 4.94 (dd, 1H, J_{vic} = 16.0 Hz J_{gem} =

1.0 Hz, L), 4.88 (dd, 1H, J_{vic} = 9.0 Hz J_{gem} = 1.0 Hz, M), 4.00 (t, 2H, J = 6.0 Hz, C), 1.92 (m, 2H, H), 1.70 (qu, 2H, J = 6.0 Hz, D), 1.36 (qu, 2H, J = 6.0 Hz, E), 1.25 (m, 2H, G), 1.18 (m, 8H, F); ^{13}C NMR (100 MHz, DMSO- d_6): δ = 166.76 (CO), 159.05 (q, ArC), 138.98 (CH), 133.28 (q, ArC), 122.84 (ArCH), 118.86 (ArCH), 114.63 (CH₂), 68.30 (CH₂), 33.54 (CH₂), 29.87 (CH₂), 29.35 (CH₂), 29.20 (CH₂), 29.14 (CH₂), 28.91 (CH₂), 28.66 (CH₂), 25.78 (CH₂). FAB MS (mBNA matrix) m/z 335 $[\text{M}+\text{H}]^+$. Anal. Calcd for C₁₉H₂₆O₅ (334.41): C, 68.24; H, 7.84. Found: C, 68.11; H, 7.99.

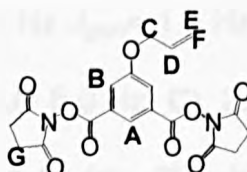
Activation of the isophthalic acids



General procedure

To a stirred solution of 5-alkoxyisophthalic acid (1.0 eq) in dry THF *N*-hydroxysuccinimide **137** (2.2 eq) and DCC (2.2 eq) were added after cooling the solution using an ice bath. After 30 mins the ice bath was removed and the solution stirred at RT overnight. The turbid solution was filtered, evaporated *in vacuo* and then crystallised (propanol) in order to afford the *title compound*.

5-Allyloxyisophthalic acid bis (2,5-dioxo-pyrrolidin-1-yl) ester (**138**)

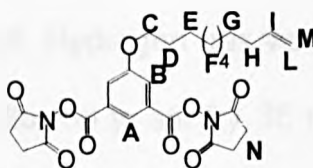


Following the general procedure 5-allyloxyisophthalic acid **135** (6.1 g, 27.4 mmol), *N*-hydroxysuccinimide (6.9 g, 60.3 mmol) and DCC (6.3 g, 54.9

mmol) were reacted in dry THF (150 mL) to afford the *title compound 138* (6.24 g, 15.0 mmol, 55%) as a white solid.

mp 198-199°C; ^1H NMR (400 MHz, CDCl_3): δ = 8.48 (s, 1H, **A**), 7.93 (s, 2H, **B**), 6.03 (m, 1H, **D**), 5.45 (dd, 1H, J_{vic} = 16.0 Hz, J_{gem} = 1.0 Hz, **E**), 5.34 (dd, 1H, J_{vic} = 9.0 Hz, J_{gem} = 1.0 Hz, **F**), 4.66 (d, 2H, J = 6.0 Hz, **C**), 2.91 (s, 8H, **G**); ^{13}C NMR (100 MHz, CDCl_3): δ = 169.43 (CO), 161.04 (CO), 159.50 (q, ArC), 132.09 (CH), 127.74 (q, ArC), 124.80 (ArCH), 122.95 (ArCH), 119.19 (CH_2), 69.93 (CH_2), 26.07 (CH_2). FAB MS (*m*BNA matrix) m/z 417 $[\text{M}+\text{H}]^+$. Anal. Calcd for $\text{C}_{19}\text{H}_{16}\text{N}_2\text{O}_9$ (416.34): C, 54.81; H, 3.87; N, 6.73. Found: C, 55.07; H, 4.26; N, 6.52.

5-(Undec-10-enyloxy)-isophthalic acid bis-(2,5-dioxo-pyrrolidin-1-yl) ester (**139**)

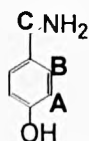


Following the general procedure 5-(undec-10-enyloxy)-isophthalic acid **136** (6.0 g, 18.0 mmol), *N*-hydroxysuccinimide (4.5 g, 39.4 mmol) and DCC (8.1 g, 39.4 mmol) were reacted in dry THF (150 mL) to afford the *title compound 139* (8.1 g, 15.3 mmol, 86%) as a white solid.

mp 190-191°C; ^1H NMR (CDCl_3): δ = 8.46 (s, 1H, **A**), 7.90 (s, 2H, **B**), 5.80 (m, 1H, **I**), 5.00 (dd, 1H, J_{vic} = 16.0 Hz J_{gem} = 1.0 Hz, **L**), 4.91 (dd, 1H, J_{vic} = 9.0 Hz J_{gem} = 1.0 Hz, **M**), 4.07 (t, 2H, J = 6.0 Hz, **C**), 2.92 (s, 8H, **N**), 2.03 (m, 2H, **H**), 1.81 (qu, 2H, J = 6.0 Hz, **D**), 1.44 (qu, 2H, J = 6.0 Hz, **E**), 1.36 (m, 2H, **G**), 1.31 (m, 8H, **F**); ^{13}C NMR (CDCl_3): δ = 170.27 (CO), 169.53 (CO), 160.15 (q,

ArC), 139.56 (CH), 127.69 (q, ArC), 124.33 (ArCH), 122.63 (ArCH), 114.49 (CH₂), 69.41 (CH₂), 37.60 (CH₂), 29.81 (CH₂), 29.73 (CH₂), 29.60 (CH₂), 29.49 (CH₂), 29.24 (CH₂), 26.05 (CH₂), 25.63 (CH₂). FAB MS (*m*BNA matrix) *m/z* 529 [M⁺]. Anal. Calcd for C₂₇H₃₂N₂O₉ (528.55): C, 61.35; H, 6.10; N, 5.30. Found: C, 61.10; H, 5.74; N, 5.02.

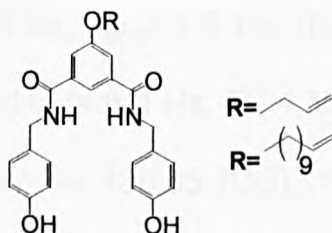
4-(Aminomethyl)phenol (**141**)¹¹



Raney[®] Nickel (50% slurry in H₂O, 18.0 g) was washed several times with anhydrous MeOH until the washings were clear and then transferred to a flask with anhydrous MeOH (250 mL). The flask was evacuated and NH₃(g) bubbled through the solution. The inlet was removed and the remaining NH₃(g) allowed to bubble off. Hydrogen gas was introduced to the flask via balloons and the solution allowed to stir for 35 mins. A solution of 4-cyanophenol **140** (25.0 g, 0.21 mol) in anhydrous MeOH (30 mL), dissolved under an atmosphere of hydrogen, was added and allowed to stir for 3 days, refilling the hydrogen balloons when required. When the uptake of hydrogen had ceased the reaction mixture was allowed to settle and the clear solution was decanted off from the solid catalyst, filtered through celite and concentrated under reduced pressure, yielding a pale green solid, which on re-crystallisation from THF yielded pale yellow-white crystals (22.85 g, 0.19 mol, 88%).

mp 148-149°C (Lit. m.p. 148-149°C.¹¹); ¹H NMR (400 MHz, DMSO-*d*₆): δ= 7.09 (AA' part of AA'BB' system, 2H, *J*= 8.5 Hz, **A**), 6.90 (BB' part of AA'BB' system, 2H, *J*= 8.5 Hz, **B**), 4.20 (bs, 2H, NH₂), 3.60 (s, 2H, **C**).

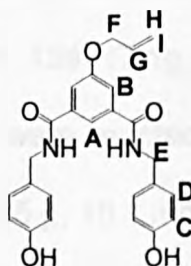
N,N'-bis-(4-Hydroxybenzyl) isophthalamides



General procedure

Under an atmosphere of argon to a stirred solution of the activated ester (1.0 eq) in dry THF 4-(aminomethyl) phenol (2.5 eq) and triethylamine (2.5 eq) were added. The solution was then stirred at RT overnight. The torpid solution was filtered, evaporated *in vacuo* and the oil dissolved in ethyl acetate and then washed twice with a 1N HCl (aq) solution, water, dried over magnesium sulphate, filtered and then concentrated to give the *title compound* as a powder.

5-Allyloxy-*N,N'*-bis-(4-hydroxy-benzyl)-isophthalamide (**142**)

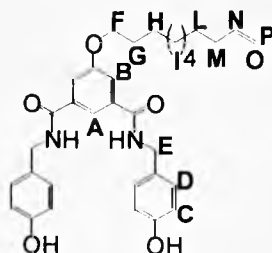


Following the general procedure 5-allyloxyisophthalic acid bis (2,5-dioxo-pyrrolidin-1-yl) ester **138** (10.0 g, 24.0 mmol), 4-(aminomethyl) phenol **141**

(7.4 g, 60.0 mmol) were reacted in anhydrous THF (200 mL) to afford the *title compound* **142** (7.19 g, 16.6 mmol, 69%) as a white solid.

mp 118-119°C; ^1H NMR (400 MHz, $\text{DMSO}-d_6$): δ = 9.29 (s, 2H, **B**), 9.00 (t, 2H, J = 6.0 Hz, NH); 7.98 (s, 1H, **A**), 7.10 (AA' part of AA'BB' system, 2H, J = 8.5 Hz, **C**), 6.71 (BB' part of AA'BB' system, 2H, J = 8.5 Hz, **D**), 6.07 (m, 1H, **G**), 5.42 (dd, 1H, J_{vic} = 16.0 Hz, J_{gem} = 1.0 Hz, **H**), 5.28 (dd, 1H, J_{vic} = 9.0 Hz, J_{gem} = 1.0 Hz, **I**), 4.66 (d, 2H, J = 6.0 Hz, **F**), 4.36 (d, 4H, J = 6.0 Hz, **E**); ^{13}C NMR (100 MHz, $\text{DMSO}-d_6$): δ = 165.65 (CO), 158.39 (q, ArC), 156.62 (q, ArC), 136.36 (q, ArC), 133.69 (CH), 130.00 (q, ArC), 129.06 (ArCH), 119.21 (CH₂), 117.95 (ArCH), 116.31 (ArCH), 115.36 (ArCH), 68.95 (CH₂), 42.65 (CH₂). FAB MS (*m*BNA matrix) m/z 433 $[\text{M}+\text{H}]^+$. Anal. Calcd for $\text{C}_{25}\text{H}_{24}\text{NO}_5$ (432.47): C, 69.43; H, 5.59; N, 6.48. Found: C, 69.22; H, 5.42; N, 6.37.

***N,N'*-bis-(4-hydroxybenzyl)-5-(undec-10-enyloxy)-isophthalamide (**143**)**

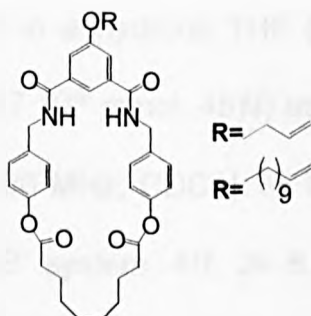


Following the general procedure 5-(undec-10-enyloxy)-isophthalic acid bis-(2,5-dioxo-pyrrolidin-1-yl) ester **139** (7.1g, 13.4 mmol), 4-(aminomethyl) phenol **141** (4.0 g, 33.7 mmol) were reacted in anhydrous THF (200 mL) to afford the *title compound* **143** (5.5 g, 10.1 mmol, 75%) as a white solid.

mp 108-110°C; ^1H NMR ($\text{DMSO}-d_6$): δ = 9.31 (s, 2H, **B**), 9.00 (t, 2H, J = 6.0 Hz, NH), 8.01 (s, 1H, **A**), 7.17 (AA' part of AA'BB' system, 4H, J = 8.5 Hz, **C**), 6.73 (BB' part of AA'BB' system, 4H, J = 8.5 Hz, **D**), 5.78 (m, 1H, **N**), 5.00 (dd,

1H, J_{vic} = 16.0 Hz J_{gem} = 1.0 Hz, O), 4.91 (dd, 1H, J_{vic} = 9.0 Hz J_{gem} = 1.0 Hz, P), 4.40 (d, 4H, J = 6.0 Hz, E), 4.07 (t, 2H, J = 6.0 Hz, F), 3.48 (m, 2H, M), 2.01 (qu, 2H, J = 6.0 Hz, G), 1.73 (qu, 2H, J = 6.0 Hz, H), 1.42 (m, 2H, L), 1.32 (m, 8H, I); ^{13}C NMR (DMSO- d_6): δ = 166.68 (CO), 159.87 (q, ArC), 157.44 (q, ArC), 140.40 (q, ArC), 137.25 (CH), 130.96 (q, ArC), 130.68 (ArCH), 120.28 (ArCH), 116.81 (CH₂), 115.94 (ArCH), 115.81 (ArCH), 69.20 (CH₂), 43.61 (CH₂), 34.80 (CH₂), 30.27 (CH₂), 30.12 (CH₂), 30.05 (CH₂), 29.93 (CH₂), 29.81 (CH₂), 29.58 (CH₂), 26.69 (CH₂). FAB MS (*m*BNA matrix) m/z 545 [M^+]. Anal. Calcd for C₃₃H₄₀N₂O₅ (544.68): C, 72.77; H, 7.40; N, 5.14. Found: C, 72.68; H, 7.45; N, 5.09.

Amphiphilic macrocycles

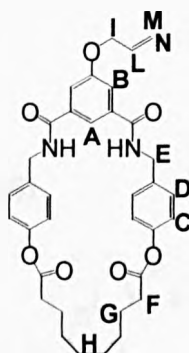


General procedure

Under an atmosphere of argon, to a stirred slurry of the 4-hydroxybenzyl isophthalamide (1.0 eq) and triethylamine (3.0 eq) in anhydrous THF at 0°C, a solution of sebacoyl chloride **144** (1.5 eq) in anhydrous THF (200 mL) was added dropwise over 2h. The reaction mixture was allowed to stir at RT overnight. The resulting brown precipitate was filtered and washed with THF, then concentrated under reduced pressure yielding a yellow oil. The viscous

oil was purified by silica gel column chromatography (CHCl₃-MeOH 99.5-0.5) to afford the desired [1+1] macrocycle.

Allyloxy-macrocycle (123)



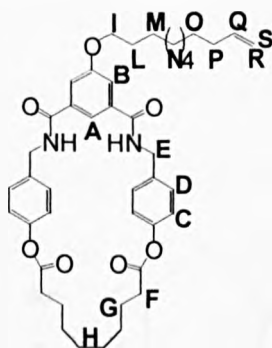
Following the general procedure 5-allyloxy-*N,N'*-bis-(4-hydroxybenzyl)-isophthalamide **142** (700.0 mg, 1.5 mmol), triethylamine (462 μ L) and a solution of sebacoyl chloride **144** (394 mg, 1.7 mmol, 352 μ L) in anhydrous THF (20 mL) were reacted in anhydrous THF (200 mL) to afford the [1+1] macrocycle **123** (367 mg, $6.7 \cdot 10^{-2}$ mmol, 45%) as a white powder.

mp 274-275°C; ¹H NMR (400 MHz, CDCl₃): δ = 7.41 (s, 2H, **B**), 7.28 (s, 1H, **A**), 7.26 (AA' part of AA'BB' system, 4H, J = 8.5 Hz, **C**); 6.95 (BB' part of AA'BB' system, 4H, J = 8.5 Hz, **D**), 6.69 (t, 2H, J = 6.0 Hz, NH), 5.98 (m, 1H, **L**), 5.32 (dd, 1H, J_{vic} = 16.0 Hz, J_{gem} = 1.0 Hz, **M**), 5.21 (1H, dd, J_{vic} = 9.0 Hz, J_{gem} = 1.0 Hz, **N**), 4.47 (d, 4H, J = 6.0 Hz, **E**), 4.41 (d, 2H, J = 6.0 Hz, **I**), 2.49 (t, 4H, J = 6.5 Hz, **F**), 1.65 (q, 4H, J = 6.5 Hz, **G**), 1.32 (8H, bs, **H**); ¹³C NMR (100 MHz, CDCl₃): δ = 172.69 (CO), 167.00 (CO), 159.59 (q, ArC), 150.60 (q, ArC), 136.49 (q, ArC), 135.73 (q, ArC), 132.85 (CH), 129.90 (ArCH), 122.39 (ArCH), 118.66 (CH₂), 117.53 (ArCH), 116.37 (ArCH), 69.44 (CH₂), 44.22 (CH₂), 34.43 (CH₂), 29.64 (CH₂), 28.83 (CH₂), 25.29 (CH₂). FAB MS (*m*BNA

matrix) m/z 599 [M^+]. Anal. Calcd for $C_{35}H_{38}N_2O_7$ (598.69): C, 70.22; H, 6.40; N, 4.68. Found: C, 68.52; H, 6.23; N, 4.09.

The incorrect value obtained for the C in the elemental analysis was due to the persistent presence of solvent in the sample even after high-vacuum treatment overnight.

Undecenyoxy macrocycle (145)

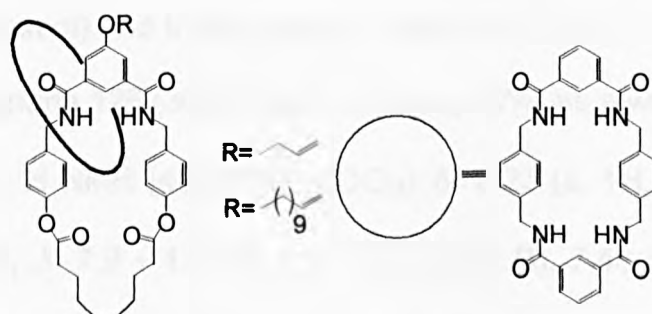


Following the general procedure *N,N'*-bis-(4-hydroxybenzyl)-5-(undec-10-enyoxy)-isophthalamide **143** (4.3 g, 7.9 mmol), triethylamine (2.5 mL) and a solution of sebacoyl chloride **144** (2.8 g, 11.9 mmol) in anhydrous THF (400 mL) were reacted in anhydrous THF (700 mL) to afford the macrocycle **145** (4.6 g, 6.5 mmol, 82%) as a white powder.

mp 183-185°C; 1H NMR (400 MHz, $CDCl_3$): δ = 7.57 (s, 1H, **A**), 7.37 (AA' part of AA'BB' system), 4H, J = 8.5 Hz, **C**), 7.31 (s, 2H, **B**), 7.04 (BB' part of AA'BB' system, 4H, J = 8.5 Hz, **D**), 6.40 (t, 2H, J = 6.0 Hz, NH), 5.83 (m, 1H, **Q**), 5.25 (dd, 1H, J_{vic} = 16.0 Hz J_{gem} = 1.0 Hz, **R**), 5.00 (dd, 1H, J_{vic} = 9.0 Hz J_{gem} = 1.0 Hz, **S**), 4.59 (d, 4H, J = 6.0 Hz, **E**), 4.07 (t, 2H, J = 6.0 Hz, **I**), 2.60 (t, 4H, J = 6.5 Hz, **F**), 2.50 (m, 2H, **P**), 2.10 (qu, 4H, J = 6.5 Hz, **G**), 1.80 - 1.50 (m, 2H, **L**), 1.80 - 1.50 (m, 2H, **O**), 1.80 - 1.50 (m, 2H, **M**), 1.40 (m, 8H, **N**), 1.32 (m, 8H, **H**); ^{13}C NMR (100 MHz, $CDCl_3$): δ = 172.09 (CO), 168.17 (CO),

159.84 (q, ArC), 151.07 (q, ArC), 135.99 (q, ArC), 135.04 (q, ArC), 133.24 (CH), 129.86 (ArCH), 121.91 (ArCH), 118.03 (CH₂), 117.09 (ArCH), 115.68 (ArCH), 68.32 (CH₂), 43.62 (CH₂), 34.21 (CH₂), 29.92 (CH₂), 29.83 (CH₂), 29.70 (CH₂), 29.64 (CH₂), 29.59 (CH₂), 29.41 (CH₂), 29.17 (CH₂), 28.83 (CH₂), 26.33 (CH₂), 25.29 (CH₂). FAB MS (*m*BNA matrix) *m/z* 711 [M⁺]. Anal. Calcd for C₄₃H₅₄N₂O₇ (710.90): C, 72.65; H, 7.66. N, 3.94. Found: C, 72.60; H, 7.76, N, 3.86.

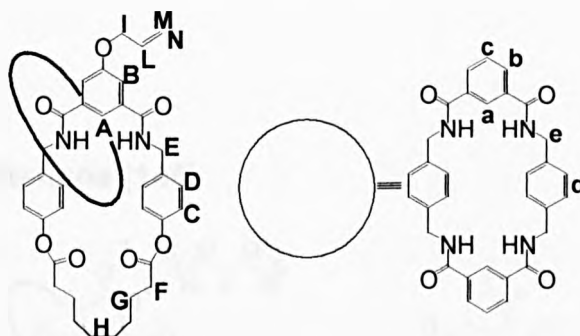
Heterocircuit [2]catenanes



General procedure

Under an atmosphere of argon, solutions of isophthaloyl dichloride **22** (12.0 eq) in CHCl₃ and *p*-xylylenediamine **26** (12.0 eq) in CHCl₃ were added, *via* syringe pumps, to a stirring solution of the [1+1] macrocycle (1.0 eq) and triethylamine (25.0 eq) in chloroform. The reaction mixture was then washed with water several times, dried over MgSO₄, filtered and concentrated under reduced pressure and finally purified by silica gel column chromatography (pure CHCl₃) to afford the heterocircuit [2]catenane.

Allyloxy Catenane (125)

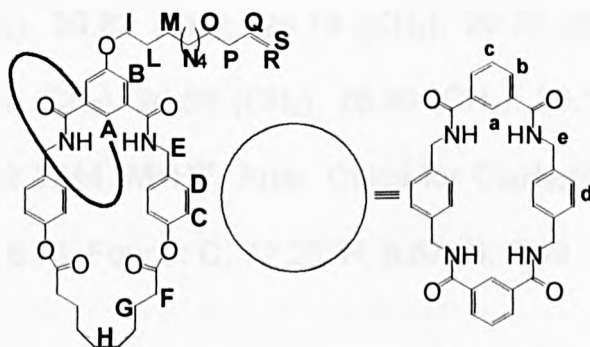


Following the general procedure isophthaloyl dichloride **22** (2.1 g, 10.0 mmol) in CHCl_3 (75 mL) and *p*-xylylenediamine **26** (1.4 g, 10.0 mmol) in CHCl_3 (75 mL) were added to a stirring solution of the [1+1] allyloxy-macrocyclic **123** (500.0 mg, 0.8 mmol) and triethylamine (1.46 mL) in CHCl_3 (500 mL) to afford the [2] allyl-catenane **125** (362.0 mg, 0.3 mmol, 40%) as a white powder.

mp 274-275°C; ^1H NMR (400 MHz, CDCl_3): δ = 8.23 (s, 1H, **A**), 7.88 (s, 2H, **a**), 7.80 (dd, 4H, J = 7.9 + 1.4 Hz, **b**), 7.72 (s, 2H, **B**), 7.48 (t, 2H, J = 6.0 Hz, $\text{NH}_{\text{amphmac}}$), 7.29 (t, 2H, J = 7.9 Hz, **c**), 7.26 (t, 4H, J = 5.0 Hz, $\text{NH}_{\text{smallmac}}$), 7.05 (s, 8H, **d**), 6.27 (AA' part of AA'BB' system, 4H, J = 8.5 Hz, **C**), 6.16 (BB' part of AA'BB' system, 4H, J = 8.5 Hz, **D**), 6.03 (m, 1H, **L**), 5.43 (dd, 1H, J_{vic} = 16.0 Hz, J_{gem} = 1.0 Hz, **M**), 5.29 (dd, 1H, J_{vic} = 9.0 Hz, J_{gem} = 1.0 Hz, **N**), 4.55 (d, 2H, J = 6.0 Hz, **I**), 4.26 (d, 8H, J = 5.0 Hz, **e**), 4.12 (d, 4H, J = 6.0 Hz, **E**), 2.50 (t, 4H, J = 6.5 Hz, **F**), 1.66 (bs, 4H, **G**), 1.48 (bs, 8H, **H**); ^{13}C NMR (100 MHz, CDCl_3): δ = 173.41 (CO), 167.25 (CO), 165.05 (CO), 159.76 (q, ArC), 149.80 (q, ArC), 138.10 (q, ArC), 136.99 (q, ArC), 135.52 (q, ArC), 134.62 (q, ArC), 134.18 (CH), 133.70 (ArCH), 133.02 (ArCH), 131.56 (ArCH), 131.18 (ArCH), 133.02 (ArCH), 131.18 (ArCH), 122.15 (CH_2), 118.55 (ArCH), 116.08 (ArCH), 69.53 (CH_2), 44.70 (CH_2), 34.18 (CH_2), 30.10 (CH_2), 28.81 (CH_2), 27.94 (CH_2), 24.65 (CH_2). FAB MS (*m*BNA matrix) m/z 1131 [M^+]. Anal. Calcd for

C₆₇H₆₆N₆O₁₁ (1131.27): C, 71.13; H, 5.88; N, 7.43. Found: C, 70.98; H, 5.72; N, 7.19.

Undecenyoxy Catenane (146)

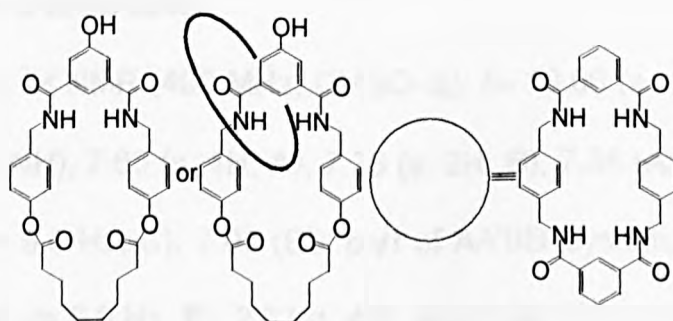


Following the general procedure isophthaloyl dichloride **22** (1.7 g, 8.3 mmol) in CHCl₃ (50 mL) and *p*-xylylenediamine **26** (1.1 g, 8.3 mmol) in CHCl₃ (50 mL) were added to a stirring solution of the [1+1] macrocycle **145** (500 mg, 0.7 mmol) and NEt₃ (1.7 g, 17.2 mmol) in CHCl₃ (500 mL) as described in the general procedure to afford the [2]catenane **146** (320.5 mg, 37%) as a white powder.

mp 265-267°C; ¹H NMR (CDCl₃): δ= 8.41 (s, 1H, **A**), 7.88 (s, 2H, **a**), 7.76 (dd, 2H, *J*= 7.9 + 1.4 Hz, **b**), 4.40 (t, 2H, *J*= 6.0 Hz, NH_{bigmac}), 7.33 (t, 4H, *J*= 5.0 Hz, NH_{smallmac}), 7.18 (s, 2H, **B**), 7.16 (t, 2H, *J*= 7.9 Hz, **c**), 7.00 (s, 8H, **d**), 6.55 (AA' part of AA'BB' system, 4H, *J*= 8.5 Hz, **C**), 6.37 (BB' part of AA'BB' system, 4H, *J*= 8.5 Hz, **D**), 5.83 (m, 1H, **Q**), 4.98 (dd, 1H, *J*_{vic}= 17.1 Hz *J*_{gem}= 1.0 Hz, **R**), 4.89 (dd, 1H, *J*_{vic}= 10.5 Hz *J*_{gem}= 1.0 Hz, **S**), 4.45 (d, 8H, *J*=5.0 Hz, **e**), 4.41 (d, 4H, *J*= 6.0 Hz, **E**), 3.90 (t, 2H, *J*= 6.0 Hz, **I**), 2.19 (t, 4H, *J*= 6.5 Hz, **F**), 1.72 (m, 2H, **P**), 1.61 (qu, 4H, *J*= 6.5 Hz, **G**), 1.60 - 1.40 (m, 2H, **L**), 1.60 - 1.40 (m, 2H, **O**), 1.60 - 1.40 (m, 2H, **M**), 1.25 (m, 8H, **N**), 1.10 (m, 8H, **H**); ¹³C NMR (CDCl₃): δ= 172.99 (CO), 168.77 (CO), 167.06 (CO), 158.99

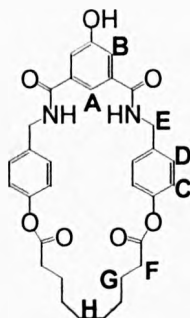
(q, ArC), 152.01 (q, ArC), 150.32 (q, ArC), 139.60 (q, ArC), 135.94 (q, ArC), 134.01 (q, ArC), 132.93 (CH), 131.77 (ArCH), 129.93 (ArCH), 129.67 (ArCH), 129.27 (ArCH), 128.16 (ArCH), 127.81 (ArCH), 122.08 (CH₂), 117.25 (ArCH), 114.55 (ArCH), 68.32 (CH₂), 43.04 (CH₂), 34.71 (CH₂), 34.67 (CH₂), 34.19 (CH₂), 29.92 (CH₂), 29.83 (CH₂), 29.76 (CH₂), 29.52 (CH₂), 29.31 (CH₂), 28.54 (CH₂), 27.12 (CH₂), 26.38 (CH₂), 26.00 (CH₂), 25.17 (CH₂). FAB MS (*m*BNA matrix) *m/z* 1244 [M+H]⁺. Anal. Calcd for C₇₅H₈₂N₆O₁₁ (1243.49): C, 72.44; H, 6.65; N, 6.76. Found: C, 72.20; H, 6.57; N, 6.49.

Deprotection of the O-allyl ethers of macrocycles and catenanes



General procedure

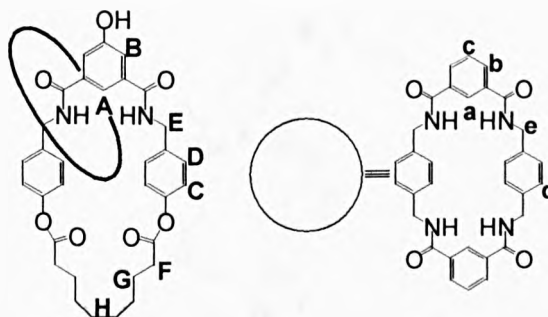
A mixture of the O-allyl ether of the macrocycle or catenane (1.0 eq.), Pd(OAc)₂ (**147**) (1.0·10⁻² eq.), PPh₃ (4.0·10⁻² eq.), formic acid (3.0 eq.) were dissolved in a solution of THF (4 parts) and EtOH (1 part) and stirred under reflux before being filtered on celite, concentrated under reduced pressure, solubilised in CH₂Cl₂ washed with water, dried over MgSO₄, filtered and concentrated under reduced pressure and finally purified by silica gel column chromatography (pure CHCl₃) to afford the final product.

Hydroxyl macrocycle (148)

Following the general procedure a solution of allyloxy macrocycle **123** (760.0 mg, 1.36 mM), Pd(OAc)₂ **147** (169.0 mg, 0.75 mM), PPh₃ (2.4 g, 9.15 mM), formic acid (17 mL) were dissolved in a solution of THF (40 mL) and EtOH (10 mL) and reacted to afford the deprotected macrocycle **148** (665.0 mg, 1.1 mmol, 94%) as a white solid.

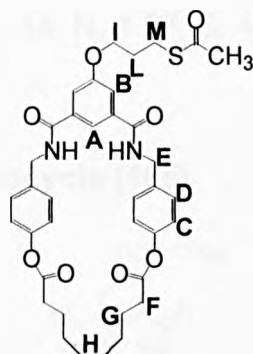
mp 201-203°C; ¹H NMR (400 MHz, DMSO-*d*₆): δ= 10.00 (s, 1H, OH), 8.82 (t, 2H, *J*= 6.0 Hz, NH), 7.63 (s, 1H, **A**), 7.36 (s, 2H, **B**), 7.35 (AA' part of AA'BB' system, 4H, *J*= 8.5 Hz, **C**), 7.03 (BB' part of AA'BB' system, 4H, *J*= 8.5 Hz, **D**), 4.43 (d, 4H, *J*= 6.0 Hz, **E**), 2.57 (t, 4H, *J*= 6.5 Hz, **F**), 1.59 (qu, 4H, *J*= 6.5 Hz, **G**), 1.31 (bs, 8H, **H**); ¹³C NMR (100 MHz, DMSO-*d*₆): δ= 172.25 (CO), 166.50 (CO), 157.79 (q, ArC), 149.75 (q, ArC), 137.13 (q, ArC), 136.62 (q, ArC), 131.68 (ArCH), 129.35 (ArCH), 122.01 (ArCH), 117.18 (ArCH), 40.5 (CH₂), 39.53 (CH₂), 39.12 (CH₂), 34.65 (CH₂), 33.41 (CH₂). FAB MS (*m*BNA matrix) *m/z* 557 [M-H]⁺. Anal. Calcd for C₃₂H₃₄N₂O₇ (558.62): C, 68.80; H, 6.13; N, 5.01. Found: C, 67.97; H, 6.20; N, 4.81.

Hydroxyl catenane (149)



Following the general procedure a solution of allyl catenane **125** (180.0 mg, 0.16 mmol), Pd(OAc)₂ **147** (40.0 mg, 0.2 mmol), PPh₃ (560.0 mg, 2.1 mmol), formic acid (4 mL) were dissolved in a solution of THF (40 mL) and EtOH (10 mL) and reacted to afford the deprotected catenane **149** (150.0 mg, 0.13 mmol, 87%) as a white powder.

mp 280-281°C; ^1H NMR (400 MHz, $\text{DMSO}-d_6$): δ = 10.07 (s, 1H, OH), 8.69 (t, 2H, J = 6.0 Hz, $\text{NH}_{\text{amphmac}}$), 8.47 (t, 4H, J = 5.0 Hz, $\text{NH}_{\text{smallmac}}$), 8.02 (s, 1H, A), 7.78 (s, 2H, a), 7.75 (dd, 4H, J = 7.9 + 1.4 Hz, b), 7.46 (s, 2H, B), 7.41 (t, 2H, J = 7.9 Hz, c), 7.08 (s, 8H, d), 6.65 (AA' part of AA'BB' system, 4H, J = 8.5 Hz, C), 6.20 (BB' part of AA'BB' system, 4H, J = 8.5 Hz, D), 4.15 (d, 8H, J = 5.0 Hz, e), 4.10 (t, 4H, J = 6.0 Hz, E), 2.19 (t, 4H, J = 6.5 Hz, F), 1.35 (bs, 4H, G), 1.17 (bs, 8H, H); ^{13}C NMR (100 MHz, $\text{DMSO}-d_6$): δ = 180.96 (CO), 172.12 (CO), 166.08 (CO), 154.59 (q, ArC), 149.00 (q, ArC), 138.19 (q, ArC), 136.52 (q, ArC), 135.68 (q, ArC), 134.85 (q, ArC), 131.79 (ArCH), 129.61 (ArCH), 129.07 (ArCH), 128.77 (ArCH), 128.66 (ArCH), 121.90 (ArCH), 122.01 (ArCH), 117.38 (ArCH), 39.05 (CH_2), 35.89 (CH_2), 34.18 (CH_2), 31.15 (CH_2), 30.08 (CH_2), 28.50 (CH_2). FAB MS (*m*BNA matrix) m/z 1091 [M^+]. Anal. Calcd for $\text{C}_{64}\text{H}_{62}\text{N}_6\text{O}_{11}$ (1091.21): C, 70.44; H, 5.73; N, 7.70. Found: C, 70.20; H, 5.64; N, 7.51.

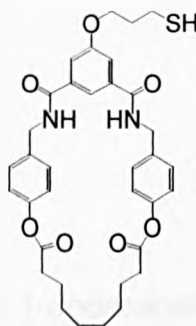
3-(Acetylsulfanyl)-propyloxy macrocycle (151)

A mixture of allyloxy macrocycle **123** (600.0 mg, 1.0 mmol) and thioacetic acid **152** (144.4 mg, 1.9 mmol) were dissolved in toluene (20 mL) previously degassed and heated to 90°C. To the solution a catalytic amount of VAZO[®] (**153**) (16.0 mg, $5.0 \cdot 10^{-2}$ mmol) was added. The reaction mixture was then stirred at 90°C over a period of 24h after which chloroform was added (80 mL) and the organic solution washed (2×100 mL) with a saturated solution of sodium bicarbonate in water, then dried over MgSO₄, filtered, concentrated under reduced pressure and dried further in *vacuo* to afford the desired product **151** (673.3 mg, 1.0 mmol, 100%) as a white powder.

mp 185-187°C; ¹H NMR (CDCl₃): δ= 7.47 (s, 1H, **A**), 7.42 (s, 2H, **B**), 7.21 (AA' part of AA'BB' system, 4H, *J*= 8.5 Hz, **C**), 7.04 (t, 2H, *J*= 6.0 Hz, NH), 6.92 (BB' part of AA'BB' system, 4H, *J*= 8.5 Hz, **D**), 4.42 (d, 4H, *J*= 6.0 Hz, **E**), 3.83 (t, 2H, *J*= 6.0 Hz, **I**), 2.79 (t, 2H, *J*= 6.0 Hz, **M**), 2.50 (t, 4H, *J*= 6.5 Hz, **F**), 2.41 (s, 3H, CH₃), 1.66 (qu, 4H, *J*= 6.5 Hz, **G**), 1.51 (qu, 2H, *J*= 6.0 Hz, **L**), 1.40 - 1.20 (bm, 8H, **H**); ¹³C NMR (CDCl₃): δ= 177.57 (CO), 172.61 (CO), 169.02 (CO), 159.97 (q, ArC), 150.44 (q, ArC), 136.30 (q, ArC), 135.86 (q, ArC), 129.60 (ArCH), 128.72 (ArCH), 120.75 (ArCH), 117.92 (ArCH), 68.56 (CH₂), 44.02 (CH₂), 34.68 (CH₂), 32.39 (CH₃), 31.25 (CH₂), 29.64 (CH₂), 28.83 (CH₂), 28.64 (CH₂), 25.29 (CH₂). FAB MS (*m*BNA matrix) *m/z*

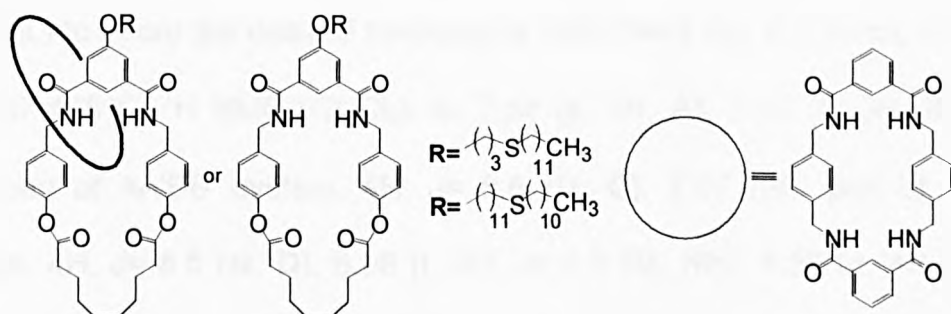
675 [M⁺]. Anal. Calcd for C₃₇H₄₂N₂O₈S (674.80): C, 65.86; H, 6.27; N, 4.15; S, 4.75. Found: C, 65.83; H, 6.14; N, 4.07; S, 4.61.

3-Mercapto-propyloxy macrocycle (155)



Under an atmosphere of argon hydrazine acetate (**154**) (30.0 mg, 0.3 mmol) was added to a stirred solution of 3-(acetylsulfanyl)-propyloxy macrocycle **151** (200.0 mg, 0.3 mmol) previously dissolved in anhydrous DMF (200 mL). The colour of the solution immediately turned brown, then orange and, finally to a dark yellow. The reaction mixture was stirred over a period of 1h after which the product was precipitated by the addition of water, filtered, dissolved in ethyl acetate (100 mL), washed with water (3×100mL), dried over MgSO₄, filtered and then dried further in *vacuo*. Unfortunately only break down products of the macrocycle were isolated (¹H-NMR).

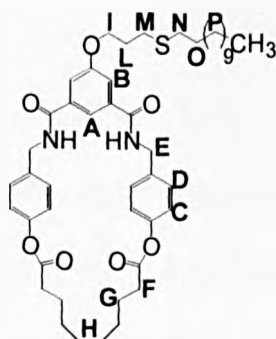
Dialkyl sulfides



General procedure

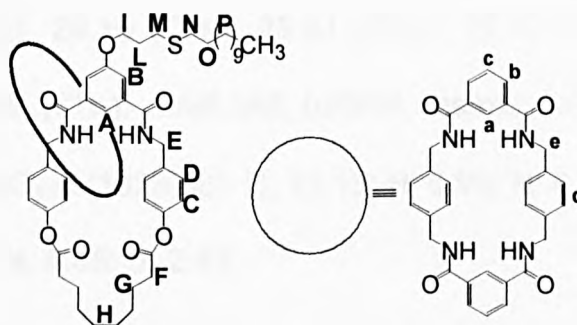
Under an atmosphere of argon, 1-dodecanethiol (**157**) (1-decanethiol for the C11 **162**) (3.0 eq) and a 0.5 M solution of 9-BBN in THF (**158**) (0.3 eq) were added to a solution of macrocycle or catenane (1.0 eq) in THF at 0°C. The mixture was then stirred over a period of 48h at RT. The solvent was then evaporated and the reaction mixture dissolved in chloroform, washed twice with water, dried over MgSO_4 , filtered and then dried further in *vacuo*. The oil was dissolved in petroleum spirit with immediate precipitation of the desired compound.

3-(Dodecylsulfanyl)-propyloxy macrocycle (**159**)



Following the general procedure allyloxy macrocycle **123** (150.0 mg, 0.3 mmol), dodecanethiol (**157**) (152.0 mg, 0.9 mmol) and a 0.5 M solution of 9-

BBN in THF (**158**) ($15\mu\text{L}$, $9.0\cdot 10^{-2}$ mmol) were reacted in anhydrous THF (100 mL) to afford the desired macrocycle **159** (244.8 mg, 0.3 mmol, 100%). mp 167-168°C; ^1H NMR (CDCl_3): δ = 7.58 (s, 1H, **A**), 7.55 (s, 2H, **B**), 7.36 (AA' part of AA'BB' system, 4H, J = 8.5 Hz, **C**), 7.07 (BB' part of AA'BB' system, 4H, J = 8.5 Hz, **D**), 6.98 (t, 2H, J = 6.0 Hz, NH), 4.58 (d, 4H, J = 6.0 Hz, **E**), 3.75 (t, 2H, J = 6.0 Hz, **I**), 2.58 (t, 4H, J = 6.5 Hz, **F**), 1.71 (qu, 4H, J = 6.5 Hz, **G**), 1.67 (t, 2H, J = 6.0 Hz, **M**), 1.64 (t, 2H, J = 6.5 Hz, **N**), 1.45 - 1.20 (m, 2H, **O**), 1.45 - 1.20 (qu, J = 6.0 Hz, 2H, **L**), 1.45 - 1.20 (bm, 18H, **P**), 1.45 - 1.20 (bm, 8H, **H**), 1.45 - 1.20 (s, 3H, CH_3); ^{13}C NMR (CDCl_3): δ = 172.68 (CO), 169.15 (CO), 159.80 (q, ArC), 150.96 (q, ArC), 136.56 (q, ArC), 135.00 (q, ArC), 130.34 (ArCH), 122.74 (ArCH), 118.63 (ArCH), 116.06 (ArCH), 68.32 (CH_2), 43.62 (CH_2), 32.23 (CH_2), 32.42 (CH_2), 30.92 (CH_2), 29.93 (CH_2), 29.89 (CH_2), 29.82 (CH_2), 29.75 (CH_2), 29.70 (CH_2), 29.65 (CH_2), 29.62 (CH_2), 29.59 (CH_2), 29.52 (CH_2), 29.41 (CH_2), 29.17 (CH_2), 28.83 (CH_2), 26.33 (CH_2), 26.12 (CH_2), 25.29 (CH_2), 25.02 (CH_3). FAB MS (*m*BNA matrix) m/z 801 [M^+]. Anal. Calcd for $\text{C}_{47}\text{H}_{64}\text{N}_2\text{O}_7\text{S}$ (801.09): C, 70.47; H, 8.05; N, 3.50; S, 4.00. Found: C, 70.50; H, 8.11; N, 3.47; S, 3.94.

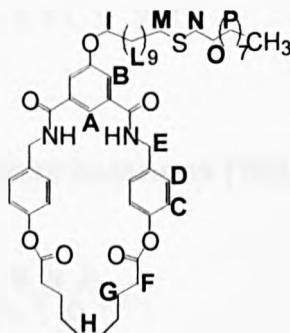
3-(Dodecylsulfanyl)-propyloxy catenane (160)

Following the general procedure allyloxy catenane **151** (60.0 mg, $5.0 \cdot 10^{-2}$ mmol), dodecanethiol (**157**) (96.7 mg, 0.15 mmol) and a 0.5 M solution of 9-BBN in THF (**158**) ($4.0 \mu\text{L}$, $2.0 \cdot 10^{-2}$ mmol) were reacted in anhydrous THF (100 mL) to afford the desired catenane **160** (67.0 mg, $5.0 \cdot 10^{-2}$ mmol, 99%) as a white solid.

mp 251-252°C; ^1H NMR (CDCl_3): δ = 7.98 (s, 1H, **A**), 7.88 (s, 2H, **a**), 7.72 (d, 2H, J = 7.9 Hz, **b**), 7.65 (t, 2H, J = 6.0 Hz, $\text{NH}_{\text{bigmac}}$), 7.33 (t, 4H, J = 5.8 Hz, $\text{NH}_{\text{smallmac}}$), 7.28 (s, 2H, **B**), 7.16 (t, 2H, J = 7.9 Hz, **c**), 7.03 (s, 8H, **d**), 6.50 (AA' part of AA'BB' system, 4H, J = 8.5 Hz, **C**), 6.27 (BB' part of AA'BB' system, 4H, J = 8.5 Hz, **D**), 4.34 (d, 8H, J = 5.8 Hz, **e**), 3.91 (d, 4H, J = 6.0 Hz, **E**), 2.96 (t, 2H, J = 6.0 Hz, **I**), 2.73 (t, 4H, J = 6.5 Hz, **F**), 1.70 - 1.50 (qu, 4H, J = 6.5 Hz, **G**), 1.70 - 1.50 (t, 2H, J = 6.0 Hz, **M**), 1.70 - 1.50 (t, 2H, J = 6.5 Hz, **N**), 1.45 - 1.20 (bm, 18H, **P**), 1.45 - 1.20 (m, 2H, **O**), 1.45 - 1.20 (qu, 2H, J = 6.0 Hz, **L**), 1.45 - 1.20 (s, 3H, CH_3), 1.45 - 1.20 (bm, 8H, **H**); ^{13}C NMR (CDCl_3): δ = 172.68 (CO), 169.77 (CO), 169.15 (CO), 159.80 (q, ArC), 150.96 (q, ArC), 136.56 (q, ArC), 135.43 (q, ArC), 135.00 (q, ArC), 134.78 (q, ArC), 131.98 (ArCH), 131.23 (ArCH), 130.07 (ArCH), 128.34 (ArCH), 126.71 (ArCH), 123.53 (ArCH), 119.17 (ArCH), 117.02 (ArCH), 64.98 (CH_2), 43.34 (CH_2), 32.34 (CH_2), 32.12 (CH_2), 31.98 (CH_2), 29.87 (CH_2), 29.80 (CH_2),

29.71 (CH₂), 29.68 (CH₂), 29.64 (CH₂), 29.59 (CH₂), 29.50 (CH₂), 29.41 (CH₂), 29.31 (CH₂), 29.10 (CH₂), 28.91 (CH₂), 27.10 (CH₂), 26.68 (CH₂), 25.39 (CH₂), 25.49 (CH₃). FAB MS (*m*BNA matrix) *m/z* 1334 [M⁺]. Anal. Calcd for C₇₉H₉₂N₆O₁₁S (1333.68): C, 71.15; H, 6.95; N, 6.30; S, 2.40. Found: C, 71.20; H, 6.70; N, 6.35; S, 2.43.

11-(Decylsulfanyl)-undecyloxy macrocycle (**162**)

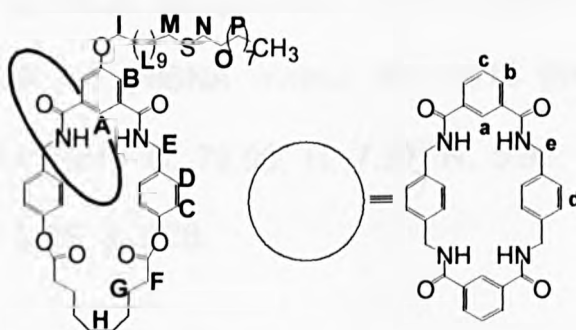


Following the general procedure undecenyloxy macrocycle **145** (75.0 mg, 0.1 mmol), 1-decanethiol (**161**) (52.3 mg, 0.3 mmol) and a 0.5 M solution of 9-BBN in THF (**158**) (6.0 μL, 3.0 · 10⁻² mmol) were reacted in anhydrous THF (75.0 mL) to afford the desired macrocycle **162** (92.1 mg, 0.1 mmol, 99%) as a white solid.

mp 145-147°C; ¹H NMR (CDCl₃): δ= 7.78 (s, 1H, **A**), 7.74 (s, 2H, **B**), 7.59 (AA' part of AA'BB' system, 4H, *J*= 8.5 Hz, **C**), 7.31 (BB' part of AA'BB' system, 4H, *J*= 8.5 Hz, **D**), 7.18 (t, 2H, *J*= 6.0 Hz, NH), 4.80 (d, 4H, *J*= 6.0 Hz, **E**), 3.78 (t, 2H, *J*= 6.0 Hz, **I**), 2.61 (t, 4H, *J*= 6.5 Hz, **F**), 1.76 (qu, 4H, *J*= 6.5 Hz, **G**), 1.69 (t, 2H, *J*= 6.0 Hz, **M**), 1.66 (t, 2H, *J*= 6.0 Hz, **N**), 1.45 - 1.30 (m, 2H, **O**), 1.45 - 1.30 (m, 18H, **L**), 1.30 - 1.10 (bm, 14H, **P**), 1.30 - 1.10 (s, 3H, CH₃), 1.30 - 1.10 (bm, 8H, **H**); ¹³C NMR (CDCl₃): δ= 172.68 (CO), 169.15 (CO), 159.80 (q, ArC), 150.96 (q, ArC), 136.56 (q, ArC), 135.00 (q, ArC),

130.34 (ArCH), 122.74 (ArCH), 118.63 (ArCH), 116.06 (ArCH), 68.32 (CH₂), 43.62 (CH₂), 32.23 (CH₂), 32.42 (CH₂), 30.92 (CH₂), 29.93 (CH₂), 29.89 (CH₂), 29.82 (CH₂), 29.80 (CH₂), 29.75 (CH₂), 29.72 (CH₂), 29.70 (CH₂), 29.65 (CH₂), 29.62 (CH₂), 29.59 (CH₂), 29.52 (CH₂), 29.48 (CH₂), 29.41 (CH₂), 29.30 (CH₂), 29.17 (CH₂), 28.86 (CH₂), 28.83 (CH₂), 26.33 (CH₂), 26.12 (CH₂), 25.29 (CH₂), 25.02 (CH₃). FAB MS (*m*BNA matrix) *m/z* 885 [M⁺]. Anal. Calcd for C₅₃H₇₆N₂O₇S (885.25): C, 71.91; H, 8.65; N, 3.16; S, 3.62. Found: C, 72.01; H, 8.57; N, 3.11; S, 3.67.

11-(Decylsulfanyl)-undecyloxy catenane (**163**)



Following the general procedure undecenyl oxy catenane **146** (60.0 mg, 0.05 mmol), 1-decanethiol (**161**) (26.2 mg, 0.15 mmol) and a 0.5 M solution of 9-BBN in THF (**158**) (3.0 μ L, 0.02 mmol) were reacted in anhydrous THF (75 mL) to afford the desired macrocycle **163** (66.3 mg, 97%) as a white solid. mp 228-230°C; ¹H NMR (CDCl₃): δ = 8.07 (s, 1H, **A**), 7.98 (s, 2H, **a**), 7.86 (dd, 2H, *J* = 7.9 + 1.4 Hz, **b**), 7.77 (t, 2H, *J* = 6.0 Hz, NH_{bigmac}), 7.42 (t, 4H, *J* = 5.0 Hz, NH_{smallmac}), 7.40 (s, 2H, **B**), 7.31 (t, 2H, *J* = 7.9 Hz, **c**), 7.12 (s, 8H, **d**), 6.62 (AA' part of AA'BB' system, 4H, *J* = 8.5 Hz, **C**), 6.44 (BB' part of AA'BB' system, 4H, *J* = 8.5 Hz, **D**), 4.38 (d, 8H, *J* = 5.0 Hz, **e**), 4.08 (d, 4H, *J* = 6.0 Hz, **E**), 3.04 (t, 2H, *J* = 6.0 Hz, **I**), 2.80 (t, 4H, *J* = 6.5 Hz, **F**), 1.68 (qu, 4H, *J* = 6.5

Hz, **G**), 1.59 (t, 2H, $J = 6.0$ Hz, **M**), 1.56 (t, 2H, $J = 6.0$ Hz, **N**), 1.55 - 1.45 (m, 18H, **L**), 1.55 - 1.45 (m, 2H, **O**), 1.45 - 1.10 (bm, 14H, **P**), 1.45 - 1.10 (bm, 8H, **H**), 1.45 - 1.10 (s, 3H, CH₃); ¹³C NMR (CDCl₃): $\delta =$ 172.68 (CO), 169.15 (CO), 168.89 (CO), 158.87 (q, ArC), 151.15 (q, ArC), 139.87 (q, ArC), 137.54 (q, ArC), 134.98 (q, ArC), 134.01 (q, ArC), 131.87 (ArCH), 130.53 (ArCH), 128.87 (ArCH), 128.07 (ArCH), 127.74 (ArCH), 125.51 (ArCH), 118.65 (ArCH), 117.00 (ArCH), 67.98 (CH₂), 43.35 (CH₂), 33.05 (CH₂), 32.76 (CH₂), 31.12 (CH₂), 30.00 (CH₂), 29.91 (CH₂), 29.88 (CH₂), 29.85 (CH₂), 29.81 (CH₂), 29.77 (CH₂), 29.72 (CH₂), 29.68 (CH₂), 29.61 (CH₂), 29.58 (CH₂), 29.50 (CH₂), 29.48 (CH₂), 29.41 (CH₂), 29.37 (CH₂), 29.31 (CH₂), 29.20 (CH₂), 29.03 (CH₂), 28.84 (CH₂), 26.31 (CH₂), 25.81 (CH₂), 25.12 (CH₂), 25.09 (CH₃). FAB MS (*m*BNA matrix) m/z 1418 [M⁺]. Anal. Calcd for C₈₅H₁₀₄N₆O₁₁S (1417.84): C, 72.00; H, 7.39; N, 5.93; S, 2.26. Found: C, 72.01; H, 7.32; N, 5.88; S, 2.28.

Preparation of the Gold Film

Macrocycle **148**, which contains a hydroxyl function, was reacted with the acid moiety localised on the tail of the SAM. To activate the acid groups on the monolayer EDCI was used as coupling agent.

The substrate used was a polycrystalline gold film deposited onto a Si wafer. The Au-covered substrates were cleaned in an ozone discharge for 15 mins, followed by sonication in ethanol for 20 mins. The SAMs were prepared by immersion of the substrate in a 1 mM chloroform solution of 11-MUA (11-mercaptoundecanoic acid) for 21h. Then were rinsed in chloroform and dried

under Argon before their characterisation by XPS (X-ray Photoelectron Spectroscopy) and CA (Contact Angle Measurements).

In order to graft the macrocycle onto the functionalised films, the acid-terminated self-assembled monolayer was immersed in a 1 mM dichloromethane solution of EDCI and macrocycle **154**, then rinsed in dichloromethane and subjected to ultrasound treatment for 10 seconds before the analysis by XPS and CA.

References:

1. (a) Johnston, A.G.; Leigh, D.A.; Pritchard, R.J.; Deegan, M.D. *Angew. Chem. Int. Ed. Engl.* **1995**, 34, 1209. (b) Johnston, A.G.; Leigh, D.A.; Nezhat, L.; Smart, J.P.; Deegan, M.D. *Angew. Chem. Int. Ed Engl.* **1995**, 34, 1212. (c) Leigh, D.A.; Moody, K.; Smart, J.P.; Watson, K.J.; Slawin, A.M.Z. *Angew. Chem. Int. Ed. Engl.* **1996**, 35, 306. (d) Craig Harris PhD thesis, University of Manchester Institute of Science and Technology (UMIST) **1997**. (e) Sheila Stichell PhD thesis, University of Manchester Institute of Science and Technology (UMIST) **1998**. (f) Harson, R.W.; Law, H.D. *J. Chem. Soc.* **1965**, 7285.
2. (a) Pérolhier, C.; Leigh, D.A. unpublished results. (b) De Nadai, C.; Whelan, C.M.; Perollier, C.; Clarkson, G.J.; Leigh, D.A.; Caudano, R.; Rudolf, P. *Surf. Sci.* **2000**, 454-456, 112. (b) Whelan, C.M.; Cecchet, F.; Clarkson, G.J.; Leigh, D.A.; Caudano, R.; Rudolf, P. *Surf. Sci.* **2001**, 474, 71. (c) Fustin, C.A.; Rudolf, P.; Taminiaux, A.F.; Zerbetto, F.; Leigh, D.A.; Caudano, R. *Thin Solid Films* **1998**, 329, 321.

3. Inaba, T.; Umezawa, I.; Yuasa, M.; Inoue, T.; Mihashi, S.; Itokawa, H.; Ogura, K. *J. Org. Chem.* **1987**, *52*, 2956.
4. Harson, R.W.; Law, H.D. *J. Chem. Soc.* **1965**, 7285.
5. (a) Huisman, B.H. PhD thesis, Universiteit Twente **1998**. (b) Flink, S. PhD thesis, Universiteit Twente **2000**.
6. Clegg, R.S.; Hutchinson, J.E. *J. Am. Chem. Soc.* **1999**, *121*, 5319.
7. (a) Schierbaum, K.D.; Weiss, T.; Thoden van Velzen, E.U.; Engbersen, J.F.J.; Reinhoudt, D.N.; Göpel, W. *Science* **1994**, *265*, 1413. (b) Huisman, B.H.; Rudkevich, D.M.; van Veggel, F.C.J.M.; Reinhoudt, D.N. *J. Am. Chem. Soc.* **1996**, *118*, 3523. (c) Friggeri, A.; van Veggel, F.C.J.M.; Reinhoudt, D.N. *Chem. Eur. J.* **1999**, *12*, 3595. (d) Beulen, M.W.J.; Huisman, B.H.; van der Heijden, P.A.; van Veggel, F.C.J.M.; Simons, M.G.; Biemond, E.M.E.F.; de Lange, P.J.; Reinhoudt, D.N. *Langmuir* **1996**, *12*, 6170. (e) Beulen, M.W.J.; Kastenbergh, M.I.; van Veggel, F.C.J.M.; Reinhoudt, D.N. *Langmuir* **1998**, *14*, 7463. (f) Huisman, B.H.; Rudkevich, D.M.; Farrán Morales, A.; Verboom, W.; van Veggel, F.C.J.M.; Reinhoudt, D.N. *Eur. J. Org. Chem.* **2000**, *2*, 269.
8. Huisman, B.H.; Schönherr, H.; Huck, W.T.S.; Friggeri, A.; van Manen, H.J.; Menozzi, E.; Vansco, G.J.; van Veggel, F.C.J.M.; Reinhoudt, D.N. *Angew. Chem. Int. Ed. Engl.* **1999**, *38*, 2248.
9. Beulen, M.W.J.; Bügler, J.; Lammerink, B.; Geurts, F.A.J.; Biemond, E.M.E.F.; van Leerdam, K.G.C.; van Veggel, F.C.J.M.; Engbersen, J.F.J.; Reinhoudt, D.N. *Langmuir* **1998**, *14*, 6424.
10. Beulen, M.W.J.; Bügler, J.; de Jong, M.R.; Lammerink, B.; Huskens, J.; Schönherr, H.; Vancso, G.J.; Boukamp, B.A.; Wieder, H.; Offenhäuser,

A.; Knoll, W.; van Veggel, F.C.J.M.; Reinhoudt, D.N. *Chem. Eur. J.* **2000**, 6, 1176.

11. Johnston, A.G.; Leigh, D.A.; Murphy, A.; Smart, J.P.; Deegan, M.D. *J. Am. Chem. Soc.* **1996**, 118, 10662.

Appendix: General Experimental Data

All melting points were determined using an Electrothermal 9100 melting point apparatus and are uncorrected.

^1H and ^{13}C NMR spectra were all performed on a Bruker DPX 400 spectrometer at Warwick University and on a Bruker AC 300 or AC 200 at UMIST with TMS as internal standard at 26°C except where stated, and referenced to the residual solvent signal as internal standards (CHCl_3 at d_{H} : 7.26, s; d_{C} : 77.00, t; $[\text{D}_5\text{H}]$ DMSO at d_{H} : 2.54, m; d_{C} : 40.45, q). Chemical shifts are reported in parts per million (ppm) from low to high field. ^1H NMR data are reported as follow: b = broad; vb = very broad, s = singlet; d = doublet; dd = doublet of doublets; t = triplet; q = quadruplet; qu = quintuplet, m = multiplet; J = coupling constant. ^{13}C NMR are reported as follows: q = quaternary.

Column chromatography was carried out using Kieselgel C60 (Merck, Germany) as a stationary phase.

TLC was performed on pre-coated silica gel plates (0.25mm thick, $\text{C}_{60}\text{F}_{254}$, Merck, Germany). Plates were observed under UV light where applicable before being stained by immersion in 10% potassium permanganate solution. Elemental analyses were performed by the UMIST (University of Manchester Institute of Science and Technology) and by the Warwick University Microanalysis service. At Warwick, the values are reported to 2 decimal places whilst at UMIST (University of Manchester Institute of Science and Technology) the values are reported to 1 decimal place.

Appendix

Mass spectra were performed by the UMIST (University of Manchester Institute of Science and Technology) and by the University of Warwick mass spectroscopy service using fast-atom bombardment (FAB).

Anhydrous solvents and reagents used for reactions were purchased from Aldrich and used without further purification. Isophthaloyl dichloride was routinely recrystallised from hexane before use. Also, *p*-xylylene diamine was distilled under reduced pressure.